DECLASSIFIED
RECORDS ADMINISTRATION
R0138656

DP - 96
Copy 39
SPECIAL DISTRIBUTION

CORROSION IN HYDROGEN SULFIDE - WATER SYSTEMS

by

J. A. Snyder and D. Warren

Development Engineering Division
Engineering Department
Wilmington, Delaware

October 1955

RECORD COPY

[redacted]

Issued by

E. I. du Pont de Nemours & Co.
Explosives Department — Atomic Energy Division
Technical Division — Savannah River Laboratory

[redacted]

DECLASSIFIED
[redacted]

253246

UNCLASSIFIED

DP - 96

SPECIAL DISTRIBUTION

[redacted] Number 39 [redacted]

CORROSION IN HYDROGEN SULFIDE - WATER SYSTEMS

by

J. A. Snyder and D. Warren
Development Engineering Division
Engineering Department
Wilmington, Delaware

October 1955

Classification Cancelled or Changed
TO Declassified
By Authority of
TID-1148 Vol. 13 No. 8 4/30/57
Name Title Date
5/6/58
NSF 3/4/59 B. L. M.

[redacted]

Issued by
E. I. du Pont de Nemours & Co.
Explosives Department - Atomic Energy Division
Technical Division - Savannah River Laboratory

Printed for
The United States Atomic Energy Commission
Contract AT(07-2)-1

UNCLASSIFIED
[redacted]
DECLASSIFIED

UNCLASSIFIED SPECIAL DISTRIBUTION

INTERNAL DISTRIBUTION

Copy No.		
1-5.	AEC, SROO	Aiken, S. C.
6.	R. M. Evans - B. H. Mackey	Wilmington AED
7.	J. E. Cole - J. B. Tinker	"
8.	H. Worthington - J. C. Woodhouse	"
9.	M. S. Bloomsburg	"
10.	V. R. Thayer	"
11.	"W" File	"
12-13.	S. I. Winde	Engineering Department
14.	C. M. Cooper - C. E. Daniels - T. H. Chilton - ERL - AE File	"
15.	ERL - AE File	"
16.	J. A. Snyder - D. Warren	"
17.	D. A. Miller - F. H. Endorf	Savannah River Plant
18.	W. P. Overbeck	"
19.	P. S. Shane	"
20.	PRD File	"
21.	M. H. Wahl - C. W. J. Wende	Savannah River Laboratory
22.	J. W. Morris - W. P. Bebbington	"
23.	P. H. Permar	"
24-38.	TIS File	"
39.	TIS File Record Copy	"
40.	R. P. Kelley	Dana
41.	W. R. Keller	Dana
42.	C. W. Reilly	AEC, Terre Haute

EXTERNAL DISTRIBUTION

43.	Armed Forces Special Weapons Project (Sandia)
44.	Armed Forces Special Weapons Project, Washington
45-47.	Atomic Energy Commission, Washington
48.	Chicago Patent Group
49.	Patent Branch, Washington
50.	USAF Headquarters
51-65.	Technical Information Service, Oak Ridge

UNCLASSIFIED

ABSTRACT

This report gives a detailed account of the corrosion test work carried out by the Engineering Research Laboratory on the behavior of materials of construction in the hydrogen sulfide-water system. Results developed during the period from October 1950 through November 1954 are included.

TABLE OF CONTENTS

		Page
I.	SUMMARY	14
	A. Purpose	14
	B. Results and Conclusions	14
II.	DISCUSSION	18
	A. Introduction	18
	B. Chronology of H_2S-H_2O Study at the Engineering Research Laboratory	19
	C. Blistering and Embrittlement	25
	1. Petroleum Industry Experience	25
	2. Procedures to Minimize Blistering	25
	3. Results of Plate Inspection	26
	4. Strip-Lining Procedures	27
	a. Laboratory Tests	27
	b. Summary of Stainless-Clad Plate Inspection	28
	5. Laboratory Investigation of Blistering	29
	6. Embrittlement	31
	a. Theory	31
	b. Tensile Tests	31
	c. Test Results	32
	7. Summary	33
	D. General Corrosion Studies	34
	1. Experimental Procedure	34
	a. Corrosion Test Conditions	34
	b. Apparatus	35
	c. Results	36
	2. Corrosion Tests of Ferrous Alloys	39
	a. Procedure	39
	3. Mechanism of Sulfide Corrosion of Steel	40
	a. Iron Sulfides	40
	b. Hydrotroilite	40
	4. Inhibitor Evaluation	41
	a. Corrosion Test Procedure	42
	b. Synergistic Effects	44
	c. Inhibitor Recycling	44
	d. Sludging Effects of Inhibitors	45
	e. Summary	47
	5. Corrosion by Liquid H_2S	48
	a. Pitting of Storage Tank	48
	b. Laboratory Tests	48
	c. Results	50
	d. Summary	51

TABLE OF CONTENTS (Continued)

		Page
6.	Repair Welding GS-Process Equipment	52
	a. Procedure	52
	b. Repair Welds at the Dana Plant	53
	c. Hydrogen-Evolution Studies	54
	d. Summary	54
7.	Behavior of O-Ring Materials	55
8.	Plug Cock Lubricants	56
9.	Iron Sulfide Precipitation	57
	a. Deposits Found in GS Units	57
	b. Mechanism of Deposition	58
	c. Laboratory Deposition Tests	59
	d. Investigation of Chemical Cleaning Procedures	60
	e. Iron Sulfide Solubility Tests	64
	f. Corrosion Tests in Sodium Hydrosulfide Solutions	65
	g. Determination of Process pH by Colorimetric Means	66
	h. Phosphate Deposits in GS Units	67
10.	High Temperature Corrosion Tests	68
11.	Erosion-Corrosion Testing	69
12.	Correspondence Between Plant Experience and Laboratory Tests	71
13.	Corrosion of Silver Solder	72
14.	Miscellaneous Corrosion Tests	74
15.	Purity of H_2S Used at the Engineering Research Laboratory	74
E.	Sulfide Corrosion Cracking	75
1.	General Theory of Stress-Corrosion Cracking	75
	a. Theories of Stress-Corrosion Mechanism	76
2.	Review of the Literature on Sulfide Corrosion Cracking	77
	a. Introduction	77
	b. Characteristics of Sulfide Corrosion Cracking	77
	c. Materials Susceptible to Sulfide Corrosion Cracking	78
	d. Effect of Environment on Sulfide Corrosion Cracking	79
	e. Factors Controlling Sulfide Corrosion Cracking	81
	f. Mechanism of Sulfide Corrosion Cracking	84
	g. Prevention of Sulfide Corrosion Cracking	86

TABLE OF CONTENTS (Continued)

		Page
	Sulfide Corrosion Cracking Tests on Bolting Materials	87
	a. Introduction	87
	b. Experimental Details	87
	c. Discussion of Results	94
	d. Summary	107
4.	Other Sulfide Corrosion Cracking Tests	109
	a. Tests Using Dead-Weight Loading	109
	b. Bubble-Cap Failures	113
	c. Miscellaneous Stress Corrosion Tests	115
	d. Summary	121
III.	BIBLIOGRAPHY	123
IV.	EXHIBITS	
A.	Derivation of Formula Used for Calculating Stresses on 3/8-Inch Allen Head Cap Screws	237
B.	Relaxation of Bolt Loads	238
C.	Acknowledgments	241

LIST OF FIGURES

Figure		Page
1	Schematic Representation of Hydrogen Blistering	125
2	Blisters in Steel Plate After Exposure to H_2S	126
3	Apparatus for Sampling Hydrogen in Blisters	127
4	Test Autoclave at Engineering Research Laboratory	128
5	Autoclaves Used for Corrosion Inhibitor Evaluation	129
6	Erosion-Corrosion Test Apparatus	130
7	Experimental Heat Exchanger Arrangement	131
8	Arrangement of Sulfide Deposition Unit	132
9	Glassware for Filtration at High H_2S-H_2O Pressures	133
10	Autoclave for Indicator pH Tests of H_2S-H_2O Systems	134
11	Effect of Time on the Corrosion of Plain Carbon Steel in the H_2S-H_2O Systems - Intermittent Exposure	135
12	Effect of Time on the Corrosion of Plain Carbon Steel in the H_2S-H_2O System - Continuous Exposure	136
13	Cross Section of Sulfide Scale on Steel	137
14	Finger Penetration of Steel Surface by Sulfide Scale	137
15	Effects of Corrosion Inhibitors on the Corrosion of Steel in H_2S-H_2O Systems	138
16	Apparatus for the Distillation of H_2S into Exposure Containers	139
17	Pitting of Weld Exposed to Liquid H_2S Containing Aqueous Chloride Solutions	140
18	Ball Bearing Grease Test Unit	141
19	Cross Section of Typical Heat-Exchanger Tube Plugged with Sulfide Scale	142
20	Erosion-Corrosion Test Specimens	143
21	Erosion-Corrosion of Type 430 Stainless Steel Pump Impeller Inserts	144
22	Erosion-Corrosion of Plain Carbon (A212) Steel	145
23	Relative Impingement Erosion-Corrosion of Types 304 and 430 Stainless Steel	146
24	Typical Attack of Sil-Fos Silver Solder near Exposed Surface	147
25	Typical Attack of Sil-Fos Silver Solder - 3/8 Inch Below Exposed Surface	147
26	Microstructure of As-Deposited Sil-Fos Silver Solder	147
27	Microstructure of As-Deposited Easy-Flo 45 Silver Solder	147
28	Physical Properties of Hardened and Drawn 3/8 Inch AISI 4140 Allen Head Cap Screws	148

LIST OF FIGURES (Continued)

Figure		Page
29	Bar-Type Jig Used for Loading 3/8-Inch Allen Head Cap Screws	149
30	Sleeve-Type Jig Used for Loading Large Stud Bolts	149
31	Sketch of Calibration Block Used for Checking the Strain Measurement Techniques Applied to 3/8-Inch Allen Head Cap Screws	150
32	Cracking Susceptibility of 3/8-Inch AISI 4140 Bolts Exposed in H_2S-H_2O System at 38°C and 250 psi	151
33	Minimum Applied Stress Required to Produce Cracking of 3/8-Inch AISI 4140 Bolts in H_2S-H_2O System at 38°C and 250 psi	152
34	Cracking Susceptibility of 3/8-Inch AISI 4140 Bolts Exposed in an H_2S-H_2O System at Room Temperature and Atmospheric Pressure	153
35	Cracking Susceptibility of Large AISI 4140 Bolts Exposed in H_2S-H_2O System Both at Room Temperature-Atmospheric Pressure and at 38°C and 250 psi	154
36	Cracking Susceptibility of 3/8-Inch AISI 4140 Bolts Exposed in an H_2S-H_2O System at 120°C and 250 psi	155
37	Effect of Plastic Prestrain on the Cracking Susceptibility of 3/8-Inch AISI 4140 Bolts Exposed in an H_2S-H_2O System at 38°C and 250 psi	156
38	Effect of Inhibitors on the Cracking Susceptibility of 3/8-Inch AISI 4140 Bolts Exposed in an H_2S-H_2O System at 38°C and 250 psi	157
39	Effect of Hardness on Time to Failure of 3/8-Inch AISI 4140 Bolts Exposed in an H_2S-H_2O System at 38°C and 250 psi	158
40	Effect of Hardness on Time to Failure of 3/8-Inch AISI 4140 Bolts Exposed in an H_2S-H_2O System at Room Temperature and Atmospheric Pressure	159
41	Effect of Applied Stress on Time to Failure of 3/8-Inch AISI 4140 Bolts Exposed in an H_2S-H_2O System at 38°C and 250 psi	160
42	Effect of Prestressing on Time to Failure of 3/8-Inch AISI 4140 Bolts Exposed in an H_2S-H_2O System at 38°C and 250 psi	161

LIST OF FIGURES (Continued)

Figure		Page
43	Typical Fractures of 3/8-Inch AISI 4140 Allen Head Cap Screws Which Failed by Sulfide Corrosion Cracking A. Gage Failure 6 X B. Nut Failure 6 X C. Shank Failure 6 X D. Head Failure 6 X	162
44	Fracture Surface of a One-Inch AISI 4140 Stud Bolt Which Displayed Ductile Fracture Characteristics at the Core and Brittle Fracture Characteristics in the Surrounding Area	163
45	Circumferential Cracking in the Fracture Surface of a 1-1/4-Inch AISI 4140 Stud Bolt Which Failed by Sulfide Corrosion Cracking	163
46	Large Sulfide Corrosion Notch in Thread Root of AISI 4140 Bolt Exposed in an H_2S-H_2O System at 38°C and 250 psi	164
47	Large Sulfide Corrosion Notches and Accompanying Crack at Thread Root of AISI 4140 Bolt Exposed in an H_2S-H_2O System at Room Temperature and Atmospheric Pressure	164
48	"Finger-Type" Pattern of Sulfide Corrosion at Thread Roots of AISI 4140 Bolts Exposed in Various H_2S-H_2O Systems A. 38°C and 250 psi System B. Room Temperature - Atmospheric Pressure System C. 120°C and 250 psi System	165
49	Sulfide Corrosion Cracks in Longitudinal Section of Failed 3/8-Inch AISI 4140 Bolt	166
50	Network of Sulfide Corrosion Cracks in Longitudinal Section of Failed 7/8-Inch AISI 4140 Bolt	166
51	Network of Sulfide Corrosion Cracks Which Originated at Fracture Surface of Failed 7/8-Inch AISI 4140 Bolt	167
52	Branching Sulfide Corrosion Cracks Which Originated at Thread Root of Failed 3/8-Inch AISI 4140 Bolt	167
53	Sulfide Corrosion Cracks Normal to Fracture Surface of Failed 3/8-Inch AISI 4140 Bolt	168
54	Fine Sulfide Corrosion Cracks Initiating at Thread Root of Failed 3/8-Inch AISI 4140 Bolt	168
55	Sulfide Corrosion Crack With Intergranular Appearance in Failed AISI 4140 Bolt Etched in 2% Nital	169

LIST OF FIGURES (Continued)

Figure		Page
56	Sulfide Corrosion Crack With Transgranular Appearance in Failed AISI 4140 Bolt Etched in 2% Nital	169
57	Intergranular Sulfide Corrosion Cracks Near the Fracture Surface of Failed 75ST Aluminum Bolt Etched in 0.5% HF	170
58	Sulfide Corrosion Cracks at Edge of Fracture of Failed Duronze Bolt Etched in NH_4OH-H_2O_2	170
59	Microstructure of 3/8-Inch AISI 4140 Cap Screws as a Function of Hardness. Etchant was 2% Nital	171
	A. Ferrite and Pearlite R_c 21	
	B. Tempered Martensite R_c 21	
	C. Tempered Martensite R_c 26	
	D. Tempered Martensite R_c 31	
	E. Tempered Martensite R_c 36	
	F. Martensite R_c 55	
60	Stress on Unfailed Large AISI 4140 Bolts After Exposure in H_2S-H_2O Systems as a Function of the Original Applied Stress	172
61	Broken End of Annealed Type 316 Stainless Steel Tensile Specimen	173
62	Intergranular Cracks in Sensitized Type 316 Stainless Steel in Tension	173
63	Intergranular and Transgranular Cracking of Sensitized Type 316 Stainless Steel Tensile Specimen	174
64	Intergranular Cracking of Sensitized Type 316 Stainless Steel Bend Specimen	174
65	Intergranular Cracking of Type 304 Stainless Steel Strongback	175
66	Intergranular Cracking of Type 304 Stainless Steel Slip Tube - Dana	175
67	Single Point Loading Jig	176
68	Cracked Type 304 Stainless Steel Bubble Cap and Blank	177

LIST OF TABLES

Table		Page
I	Charpy Impact Tests	178
II	Hydrogen Embrittlement Tests of A212 Steel Bars	179
III	Effect of Interruptions on Corrosion Rates	180
IV	Interplanar Spacings of Powder Patterns of Hydrotroilite	181
V	Inhibitors Suggested by Tests at Columbia University	182
VI	Tests of Sample Cleaning Procedure	183
VII	Inhibitors Most Effective in Tests at the Engineering Research Laboratory	184
VIII	Synergistic Effects of Inhibitor Combinations	185
IX	Sludging Effects of Inhibitors	186
X	Results of Sludging Tests in Circulating Systems	187
XI	Corrosion of Materials in Liquid H_2S	188
XII	Effect of H_2S Exposure on Steel Weldability	189
XIII	Field Repair Welds	190
XIV	Compression Tests of O-Ring Sections	191
XV	Degradation Tests of Plug Cock Lubricants	192
XVI	Stressed Ball Bearing Tests of Plug Cock Greases	193
XVII	Constitution of Sulfide Deposits from GS Units	194
XVIII	Scale Removal Treatments	196
XIX	Solubility of Iron as Iron Sulfide in H_2S-Saturated Water	201
XX	Effects of Starting pH on Iron Sulfide Solubility	202
XXI	Iron Sulfide Solubility Tests at Low H_2S Pressures	203
XXII	Corrosion by Dilute Sodium Hydrosulfide Solutions	204
XXIII	Erosion-Corrosion in Dilute NaHS Solutions	205
XXIV	High Temperature Corrosion Test Data	206
XXV	Corrosion of Silver Solders	207
XXVI	Corrosion Resistance of Materials in H_2S-H_2O at 250 psi	208
XXVII	Corrosion Resistance of Materials in H_2S-H_2O at Low Pressure	209
XXVIII	Corrosion Resistance of Metals and Nonmetals Exposed to H_2S	210
XXIX	Analyses of Gas in H_2S Cylinders	211
XXX	Chemical Composition of 3/8-Inch Allen Head Cap Screws	212
XXXI	Hardness of 3/8-Inch Allen Head Cap Screws as a Function of Tempering Temperature	212
XXXII	Typical Chemical Analyses of Two Large Stud Bolts Originally Obtained from the Dana Plant	213

LIST OF TABLES (Continued)

Table		Page
XXXIII	List of Environments Used for Sulfide Corrosion Cracking Tests on Bolting Materials	213
XXXIV	Summary of Test Data for Annealed 3/8-Inch AISI 4140 Bolts Exposed in an H_2S-H_2O System at 38°C and 250 psi	214
XXXV	Summary of Test Data for Large AISI 4140 Bolts Exposed in an H_2S-H_2O System at 120°C and 250 psi	214
XXXVI	Summary of Test Data for 3/8-Inch AISI 4140 Bolts Exposed in H_2S-H_2O Systems at 250 psi and 60, 80, 100, and 120°C	215
XXXVII	Summary of Test Data for all AISI 4140 Bolts Exposed in a Water-Saturated Mixture of 100 ppm H_2S in Air	215
XXXVIII	Summary of Test Data for all AISI 4140 Bolts Exposed in a Water-Saturated Mixture of 1% H_2S in Air	216
XXXIX	Effect of Plastic Prestrain on the Cracking Susceptibility of Quenched and Drawn 3/8-Inch AISI 4140 Bolts Exposed in an H_2S-H_2O System at 38°C and 250 psi	216
XL	Effect of Plastic Prestrain on the Cracking Susceptibility of Annealed 3/8-Inch AISI 4140 Bolts Exposed in an H_2S-H_2O System at 38°C and 250 psi	217
XLI	Effect of Metallic Coatings on Susceptibility of 3/8-Inch AISI 4140 Bolts to Sulfide Corrosion Cracking	218
XLII	Effect of Nickel Plating on the Sulfide Corrosion Cracking Susceptibility of 5/8-Inch AISI 4140 Bolts	219
XLIII	Summary of Exposure Data for Type 316 Stainless Steel Bolts Exposed in an H_2S-H_2O System at 38°C and 250 psi	219
XLIV	Summary of Exposure Data for Inconel Bolts Exposed in a Number of H_2S-H_2O Systems	220
XLV	Summary of Exposure Data for Inconel-X Bolts Exposed in a Number of H_2S-H_2O Systems	221
XLVI	Summary of Exposure Data for Monel Bolts Exposed in a Water-Saturated Mixture of 1% H_2S in Air	222
XLVII	Summary of Exposure Data for K-Monel Bolts Exposed in a Number of H_2S-H_2O Systems.	223
XLVIII	Summary of Exposure Data for Duronze (5% Aluminum Bronze) Bolts Exposed in a Number of H_2S-H_2O Systems	224
XLIX	Summary of Exposure Data for 75ST Aluminum Bolts Exposed in Two H_2S-H_2O Systems	225

LIST OF TABLES (Continued)

Table		Page
L	Summary of Corrosion Rates for AISI 4140 Steel Exposed in Various H_2S-H_2O Systems	226
LI	Qualitative Evaluation of Condition of Metallic Coated AISI 4140 Bolts after Exposure to Various H_2S-H_2O Systems	227
LII	Qualitative Evaluation of Condition of Nonferrous Bolts After Exposure to Various H_2S-H_2O Systems	228
LIII	Sulfide Stress Corrosion Tests	229
LIV	Sulfide Stress Cracking of Austenitic Stainless Steel	232
LV	Beam Deflection Tests of AISI 4140	233
LVI	Stress on Unfailed Nonferrous Bolts Before and After Exposure in H_2S-H_2O Systems	234
LVII	Stress Relaxation Data for 5/8-Inch AISI 4140 Bolts at Room Temperature and at 120°C	235
LVIII	Stress Relaxation Data for Various Nonferrous Bolting Materials at Temperatures of 20 to 30°C	236

CORROSION IN HYDROGEN SULFIDE - WATER SYSTEMS

I. SUMMARY

A. PURPOSE

This work was undertaken to develop information on materials of construction for the fabrication of process equipment for handling hydrogen sulfide - water systems. Such systems are unique with respect to the number and diversity of materials problems which they involve. General corrosion, the case of uniform metal attack, is of obvious economic importance in the choice of materials for the many types of equipment required. In addition, the factors of erosion, blistering, and sulfide stress cracking, as they apply to exposure in this environment, must be considered to the degree that they constitute materials limitations.

B. RESULTS AND CONCLUSIONS

Sufficient information on the behavior of materials of construction in the hydrogen sulfide - water system was developed to allow sound specification of new equipment and to provide adequate solutions for the maintenance problems in existing structures. Many topics of technical and scientific interest remain to be elucidated.

Special observations follow:

1. Plain carbon steels exhibit positive but tolerable corrosion rates under conditions simulating those of major vessels in the GS process for making heavy water.

a. Corrosion in these systems is controlled by the presence of gross iron sulfide scale (corrosion product) on the metal surface. While the corrosion rate in the early periods of exposure is high, it decreases exponentially with time to the level of one mil per year.

b. Under these conditions any circumstance of erosion, such as liquid or gas impingement, or mechanical abrasion, which results in film removal will contribute to high corrosion rates.

c. Hot-rolled, low-carbon steel (such as ASTM A212) was found to be resistant to sulfide stress cracking when exposed at stresses less than its yield point.

d. Blistering and fissuring were observed only in materials which were "dirty" or contained gross internal defects.

e. Corrosion of plain carbon steel in liquid hydrogen sulfide proceeded slowly in the presence of a water phase, but was accelerated by the presence of chlorides as contaminants.

f. Ultrasonic inspection techniques were found to be suitable for the nondestructive inspection of steel plate for internal defects.

2. Low-alloy steels exhibit corrosion rates essentially the same as plain carbon steels. Because they are hardenable, however, they are considerably more susceptible to sulfide stress cracking. This susceptibility to cracking is particularly important with respect to the use of hardened low-alloy steels as bolting materials.

a. Failure of ASTM A193-B7 steel (AISI 4140) by sulfide corrosion cracking occurred in the following environments:

1) Pressurized (250 psi) H_2S-H_2O systems in the temperature range of 40 to 120°C.
2) Water-saturated H_2S at ambient temperature (20 to 35°C) and atmospheric pressure.

b. The susceptibility of A193-B7 steel bolting to sulfide corrosion cracking decreased with increasing temperature over the range of 40 to 120°C.

c. In the absence of plastic deformation, no sulfide corrosion failures of A193-B7 steel bolts occurred at hardnesses less than R_c 27.

d. At higher hardness levels (R_c 27-55) the sulfide cracking susceptibility of A193-B7 steel bolts increased with increasing hardness and increasing applied stress.

e. Plastic prestraining of A193-B7 steel bolts resulted in sulfide corrosion failures at hardnesses as low as R_c22.

f. The following bolting materials were completely resistant to sulfide corrosion cracking under the conditions tested:

"Inconel"	"Monel"
"Inconel-X"	"K-Monel"

Of these materials, "Inconel-X" was observed to offer the optimum combination of load-carrying capacity and general resistance to sulfide corrosion.

3. Austenitic stainless steels generally exhibit negligible corrosion under GS-process exposure conditions.

a. Because sulfide scale is not critical in these alloys, they are essentially immune to erosion-corrosion.

b. While cold-drawn material is quite susceptible to sulfide corrosion cracking, the annealed alloys crack only when subjected to stresses above their yield strength.

c. Quench-annealing of these alloys at temperatures of 1800 to 2000°F eliminated stress-cracking of cold-drawn parts.

d. Cracking of stainless steel alloys that have been heated into the plain carbon steel stress-relieving range of 1100 to 1400°F has been observed. The "sensitization" thus suffered by the unstabilized alloys also appears to contribute to intergranular cracking of these alloys under conditions involving high stress.

4. Martensitic stainless steel alloys such as Type 410 (12% Cr) and 430 (16%) exhibit moderate corrosion rates in GS-process conditions.

a. Their general corrosion rates fall between plain carbon steel and the austenitic alloys.

b. These materials are particularly susceptible to sulfide corrosion cracking in the hardened condition.

c. These alloys are subject to erosion-corrosion attack.

5. Nonferrous metals, with some notable exceptions, are not satisfactory for GS service.

a. While aluminum is not seriously corroded in dry gas at low temperatures, it is anodic to all of the ferrous materials and to iron sulfide, so that it is unsuitable for service in aqueous exposure.

b. Copper alloys and magnesium alloys show very rapid corrosion.

c. Copper-rich silver solders exhibit selective attack of the copper primary phases.

d. Titanium, zirconium, "Hastelloy C," platinum, gold, tantalum, "Elgiloy," "Stellite," and "Inconel" all exhibit negligible corrosion in GS-process conditions.

6. Nonmetallic materials are of limited utility in this system.

a. "Teflon" tetrafluoroethylene resin, graphite, asbestos impregnated with "Teflon," "Kel-F," "Haveg," and "Duron"

exhibited no apparent degradation at temperatures as high as 120°C.

b. Conventional rubber-bonded asbestos steam sheet performed well as gasket material for laboratory vessels. This material hardens with time, however, and has limited reusability.

c. Similarly, the conventional elastomeric O-ring materials hardened with time, particularly at 120°C. Silicone rubber suffered no serious degradation at temperatures up to 100°C.

Organic coatings on plain carbon steel were generally unsatisfactory. Porosity and permeability to water vapor caused failure by under-film corrosion or blistering.

7. Corrosion inhibitors did not demonstrate sufficient advantage to justify their use.

a. While significant reductions in corrosion rate could be obtained by inhibitor additions in short exposure periods, no significant long-range reduction below that of the uninhibited system could be realized.

b. In the presence of corrosion inhibitors, sludging, or loosening of the iron sulfide scale to form particulate solids in the system constituted a serious shortcoming.

c. The cost of inhibitor removal from the waste stream or of recovery for recycling turned out to be excessive.

J. A. Snyder

D. Warren

C. M. Cooper
Development Engineering Division
Engineering Department
Wilmington, Delaware

II. DISCUSSION

A. INTRODUCTION

During 1950 the du Pont Company undertook a contract with the Atomic Energy Commission to produce certain materials, one of which was heavy water. The process adopted for making heavy water (the "GS" process) posed major problems in the selection of suitable materials of construction. A research program to deal with these and associated problems was carried out at the du Pont Engineering Research Laboratory, and is the subject of this report.

The GS process involves contacting water and H_2S in large towers operating at about 250-lb pressure and at temperatures varying from 30 to 210°C. A water solution of H_2S under these conditions is corrosive and the selection of materials of construction which are readily available and reasonably inexpensive is one of the most important phases of the development involved in successfully exploiting the process.

The GS process was originally studied by the du Pont Company in connection with the Manhattan District program in 1942. The evidence then available indicated that a plant would have to be built entirely of austenitic (nickel-chromium) stainless steel. The scarcity of this material in a war economy was one of the reasons for deciding against use of the GS process in the 1942 campaign for production of heavy water.

Renewed interest in large quantities of heavy water as a moderator prompted reconsideration of the GS process for the production program initiated by the Atomic Energy Commission in 1949-50. As before, the problems of materials of construction were of first importance. There was now available, however, some limited industrial experience to indicate that ordinary carbon steel might be suitable for some of the large-tonnage items of GS-process equipment. This experience originated in two places: (1) in the petroleum industry, which encounters H_2S as a component of "sour" crude oil and "sour" natural gas; and (2) in du Pont's sulfur dye production. Technical personnel of several oil companies were quite helpful in pointing out their various problems and evaluating the effectiveness of various corrective steps that might be taken. Experience gained in du Pont's sulfur dye production offered hope that iron sulfide formed by corrosion of carbon steel would act as a protective coating and so reduce corrosion to an acceptable level.

It is important to note that the use of such a protective coating, formed in place by a corrosion product over a relatively long period of time, is unusual in the process industries. In this situation the conventional short-term corrosion tests, although useful for scouting purposes, do not develop significant information bearing on the long-term

suitability of the material of construction being tested. Long exposures of test specimens are required to develop such information. This fact complicated the problem of selecting materials of construction without unduly delaying design and building of the plants.

Research sponsored by the Manhattan District at Columbia University in 1942 included some scouting work on corrosion and corrosion inhibitors in the H_2S-H_2O system. The work at Columbia, however, was confined to short-term tests and the conclusions drawn from it were handicapped by this feature.

Another problem that must be taken into account in the handling of H_2S in steel equipment is that of "stress corrosion cracking" which is encountered not only with ordinary carbon steels but also with various types of stainless steels. This subject is discussed in detail later in the report.

B. CHRONOLOGY OF H_2S-H_2O STUDY AT THE ENGINEERING RESEARCH LABORATORY

The study at the Engineering Research Laboratory included (a) a survey of all available industrial experience and literature references, (b) an intensive testing and research program, (c) corrosion test samples for Louisville and the Dana pilot plant, (d) assistance in evaluating results of the tests, and (e) contact with the plants during and after start-up.

In order to meet required delivery schedules, a number of major decisions had to be made on the basis of available knowledge and judgment before experience or conclusive data were available. Plant experience has indicated that most of these decisions were sound. Certain of them were conservative and in other cases changes were made in specifications as required. Some compromises in details were made in order to expedite delivery.

After a review of the materials problems in October 1950, du Pont specified silicon-killed steel (ASTM A212, Grade B) of "firebox" quality for all major items. This high-quality tonnage steel was commercially available. Plates made from this grade are of better quality with regard to internal defects that might cause blistering than rimmed steel, ASTM A285. The A212 steel is also a better steel for welding.

In most chemical operations involving H_2S the first step involves drying of the gas in order to minimize corrosion problems. However, the natural gases encountered in the oil fields must be handled as they come from the ground with from 1 to 20% H_2S and varying amounts of water. Gross blistering

has occurred when poor quality (laminated) steel plates have been exposed to gases containing H_2S. Cracking of hardened steel and cold-worked stainless steel has been another source of trouble. By selecting high-quality steels with a maximum hardness of R_c 20 (Rockwell "C" scale) the oil industry is handling sour gas at up to 5000 psi pressure.

The first problem studied at the Engineering Research Laboratory involved the inspection of a group of cracked roller bearings from a blower in the Dana pilot plant. These were of AISI-52100 steel and failure appeared to have occurred by sulfide stress cracking.

An extensive series of corrosion and stress-corrosion tests were started. Tests on horseshoe bend and dead-weight loaded specimens were first made in small pressure vessels but later in a 45-inch diameter autoclave.

The Sperry ultrasonic reflectoscope was found to be the most suitable instrument to sort out any A212 steel plate that might contain internal defects that could become blister sites. Decision was therefore made to test all plate for GS equipment with this instrument. Inspection was started on December 11, 1950.

A number of corrosion, stress-corrosion, and special test samples were prepared for field tests at the pilot plant and for tests at Louisville. A number of corroded samples and other items were evaluated after exposure to process conditions. One autoclave from Louisville was pressure tested after approximately four months' service and found to be unaffected by the service exposure.

Hydrogen-permeability tests were made to study how hydrogen generated by H_2S corrosion penetrates steel. Cathodic charging was used for preliminary tests of permeability. Because of the sensitivity of the system to minor variations in conditions, only qualitative results were obtained. Austenitic stainless steel showed no hydrogen permeability, indicating that the rates of hydrogen penetration were too low to be measured by this technique.

Although several corrosion inhibitor tests had been run at Louisville, the results were inconclusive. A series of tests was started at the Engineering Research Laboratory in cooperation with the Chemical Department. When steel is first exposed to H_2S-H_2O solutions, a rapid corrosion occurs until a layer of iron sulfide is built up. Thus, scouting corrosion tests of a few hours' duration or even of two or three hundred hours show high rates of attack. This short-term high rate of attack can be reduced by the addition of certain organic amines or, to a limited extent, by addition of ammonia.

When tests are continued for 1000 hours or, more definitively, 2000 hours, however, it is observed that corrosion in the uninhibited system drops to an acceptable value, actually lower than the rate observed when amines are present. A relatively long period of experimental work was necessary to develop these findings. This experimental work also showed that even if the inhibitors were beneficial, there is a serious practical difficulty involved in their use. This difficulty arises because the inhibitor causes such iron sulfide as is formed to be taken into suspension in the process liquid. This suspended solid then settles out in pipelines and in other parts of the system, which quickly become inoperable. The practical use of carbon steel as a material of construction in the GS process depends, therefore, upon the formation of a tight protective coating of iron sulfide built up during the initial period of exposure. This takes place in most of the equipment. Experience has shown, however, that erosion due to process flow conditions prevents formation of an iron sulfide coating at certain locations, including the heat-exchanger tubes, tower trays, bubble caps, pumps, and throttle valves; and such items must be fabricated of stainless steel.

During test runs of the pilot plant with air-water mixtures, rusting of the steel caused an appreciable amount of sludge. Tests at the Engineering Research Laboratory indicated that ammonia could be used to minimize corrosion of plant equipment during such dummy running. Addition of 200 ppm ammonia to the water phase was recommended.

Fatigue tests indicated that H_2S exposure under conditions of repeated flexing does not lead to premature failure of plain carbon steel. Stress raisers that are present in most equipment were concluded to be more detrimental than corrosion fatigue.

Short-time tests of aluminum showed low corrosion rates at low temperatures. Use of aluminum was therefore considered for heat exchangers. A series of three dummy heat exchangers was assembled using aluminum tubes with various other materials for tube sheets and ferrules. Rapid corrosion of the aluminum was observed. In order to learn more about the corrosion of aluminum, a series of electrode potential measurements was made. These measurements indicated that aluminum was cathodic to plain carbon steel at low temperatures but quite anodic to stainless steel and to carbon steel at 120°C thus eliminating it from further consideration.

A rigid practice for stress relieving was specified for field use in the assembly of process equipment in order to obtain stress relief and to minimize local hardening adjacent to welds. Since the ASME Boiler Code does not require stress relief of section 3/8 inch thick or less, there was no commercial equipment for the stress relief of welds in

pipe of 5-inch diameter and smaller. A series of small portable furnaces was developed for this purpose. These furnaces were electrically heated and designed for butt joints, elbows, and tees. They were designed for a minimum voltage of 90 v and had plug-in resistance boxes attached for voltage adjustment. At minimum voltage, they required a maximum of 90 min. to heat joints in Schedule 80 pipe to 1100°F. Units were made to order by the Industrial Heater Company of New York.

A series of corrosion tests was run to determine the effect of temperatures in the range 120 to 225°C. Tests run in a small heat exchanger designed to simulate stripper heat-exchanger (SX) conditions showed low corrosion rates for austenitic alloys and moderate rates for A212 steel. Further tests were run in an autoclave designed for high-temperature corrosion tests. These tests indicated that corrosion (short-time exposure) of Type 410 stainless steel and A212 steel increases as the temperature is increased. Austenitic stainless alloys showed low corrosion rates in all of these tests.

A series of tests was made to evaluate elastomers for O-ring service. The most critical application was a moving seal for a pump handling water at 120°C. No material was satisfactory at 120°C. Silicone rubber was satisfactory from 25 to 100°C, while neoprene and "Buna-N" were degraded above 40°C.

Paper-base phenolic resin sheets were tested for possible low-pressure rupture disks to be installed downstream from the regular rupture disks. Air at low pressure applied between the disks could be used to check the regular disks. No degradation of the phenolic resin exposed to wet H_2S could be observed.

When process difficulties interrupted start-up of the first unit at the Dana Plant, hardware in the towers of this unit was examined. A considerable number of cracked Type 410 stainless steel bubble caps were observed. Metallographic study indicated that overheating during stress relief followed by air-quenching had hardened the crowns of some caps, thus rendering them crack-sensitive. All such hardware already installed in the first units was removed and annealed to eliminate crown-cracking. A Magnetic Analysis Comparator was adapted for testing caps in place. When tests indicated that caps in the last units had been properly stress relieved, annealing was discontinued. A modified heat treatment was specified for hardware still in process of fabrication.

In order to minimize corrosion and eliminate cracking, Type 304 stainless steel hardware was specified for all the towers at the Savannah River Plant. Laboratory tests indicated that full annealing after final cold-drawing was necessary to eliminate cracking of the caps.

When H_2S storage tanks at the Dana Plant pilot plant were examined, a number of deep pits were found. Chlorides were found in the corrosion products in these tanks. Tests at the Engineering Research Laboratory, as outlined later, indicated that chlorides as contaminants in water-saturated liquid H_2S can cause deep pitting.

Stainless-clad steel was considered to be the ideal material for large equipment. Its low corrosion rate would minimize scale in the system. Since its hydrogen permeability is practically nil, blistering would be eliminated. However, stainless-clad plate was not available in sufficient quantities to meet construction schedules. Stainless-clad A212 steel plate and three types of stainless steel strip linings were used for most of the towers at the Savannah River Plant. In samples submitted to the Engineering Research Laboratory for evaluation, all showed a continuous layer of Type 316 stainless steel with good quality welds.

All bolts for this equipment were specified ASTM A193-B7 steel. This is a standard high-strength bolting material. These bolts are usually heat-treated to about R_c40 to take advantage of their superior strength. In oil industry R_c20 is set as the maximum hardness for steel to be exposed in H_2S in order to avoid sulfide stress cracking. An extensive series of tests was run in the laboratory to determine the conditions of hardness and stress that should be specified for H_2S service. Rapid failure of hardened cap screws in the blower housing at the Dana Plant served to emphasize the need for this information. Test details and results are listed in a later section.

Erosion-corrosion tests were run at the Engineering Research Laboratory in order to assess the effects of flowing solutions saturated with H_2S. These included tests of pump rotors, restricted flow in pipe sections, and jet impingement. Austenitic alloys showed good resistance to erosion-corrosion. Ferritic stainless alloys and plain carbon steels were often damaged due to the removal of their protective scales.

Certain parts of standard equipment are particularly susceptible to sulfide stress failure. One such part is the hardened steel ball used in loading Merco-Nordstrom valves. Normal installation of such balls produces high surface tensile stresses. Even though these are loaded to only a fraction of their yield point of 300,000 psi they can suffer early failure. To minimize breakage of these thrust balls, the lubricant used in the valves should be one that is impermeable to H_2S so as to blanket the balls. A series of tests indicated that several of the lubricants prevented cracking during the tests. Sintered tungsten carbide and "Stellite" balls were found to be resistant to cracking under these conditions.

After the Dana Plant had been in operation for several months, gross amounts of sulfide deposits were found in the strippers. X-ray analyses indicated these to be marcasite (FeS_2). Other deposits were found wherever the H_2S-saturated water was heated.

A series of tests was made in an effort to work out a chemical sulfide-removal procedure. Assistance was obtained from Dowell, Inc. Within the restrictions imposed by the combination of materials in the heat exchangers no satisfactory cleaning procedure could be found.

Studies made by the Atomic Energy Division indicated that there was an effective decrease in solubility of iron sulfides in H_2S-saturated water as the temperature was raised. These studies also showed that by adding sodium hydrosulfide to the feed water, the sulfide deposits could be reduced to such an extent that they no longer were a significant problem.

Samples from a defective slip tube from a primary condenser (PC) heat exchanger were received from the Dana Plant. It was made of austenitic stainless steel and had failed by sulfide stress cracking. The material was in the sensitized condition and the cracking was intergranular. A survey of slip-tube failures indicated that stresses due to differential expansion between plain carbon steel and stainless steel welded to each other were important factors in these failures.

Measurements of the pH of H_2S-H_2O systems at normal pressure were desired as an aid to understanding the corrosion mechanism in this system. No commercial electrodes were available for such measurements at high pressures. A small autoclave with two sight glasses was used for colorimetric determination of pH. Results indicated that pressure has little effect on the pH of the system.

After approximately one year of service several of the 800-hp blower motors at the Dana Plant started to vibrate under load. Several broken joints between the armature bars and the end rings were observed. Sections of the Sil-Fos joints examined at the Engineering Research Laboratory showed deep penetration from H_2S corrosion. Laboratory tests showed erratic corrosion rates for this silver solder with some as high as 600 mils/yr.

Although the sodium hydrosulfide additions eliminated the major trouble from sulfide deposits in heat exchangers, another deposit was observed to build up slowly in the stripper. X-ray diffraction showed this material to be hydroxyapatite, $Ca_5(OH)(PO_4)_3$. The rate of build-up of the apatite deposit was not great enough to be a serious problem.

C. BLISTERING AND EMBRITTLEMENT

1. Petroleum Industry Experience

In the oil industry, blistering of vessels and piping exposed to sour (H_2S-containing) gas has been a serious problem. A number of failures have occurred in which thick steel plates have developed large blisters (up to 24-inch diameter). Subsequent examination has indicated that the voids common to dirty or laminated steel serve as important blister sites. The gas in all such blisters that have been carefully investigated has been found to be essentially pure hydrogen.

Hydrogen sulfide acts as a poison or accelerator to promote penetration of the steel by a part of the hydrogen developed in the corrosion reaction. This hydrogen penetrates the steel interstitially as protons. The effect is analogous to that of hydrogen under extremely high pressure. Protons are hypothesized to diffuse through the steel until they come to another surface (i.e., leave the lattice) at which point hydrogen molecules form. Any void, inclusion, or lamination is, in effect, a potential blister site. Hydrogen gas trapped at such locations can build up pressure to cause rupture at the blister. A sketch representing this mechanism is shown in Figure 1.

2. Procedures to Minimize Blistering

Two procedures are possible in order to minimize blistering. One method is to minimize the number of blister sites by using high-quality steel with 100 per cent inspection. The second is to keep hydrogen from entering the steel by using austenitic stainless steel linings. Both methods were used for GS equipment. To date there have been no blister failures nor has any evidence of blistering or fissuring of A212 steel been seen in the process equipment.

Silicon-killed steel, ASTM Specification A212, was specified for all plates to be used for towers or heat-exchanger shells. Since it is silicon-killed, A212 steel contains a minimum of potential blister sites traceable to gas evolution on freezing from the melt. As rimmed steel freezes numerous blowholes are formed just below the ingot skin. Although most of these holes are welded during hot-rolling, traces of some do remain. These cause no trouble in most uses of the steel, but would be potential blister sites if the steel were exposed to wet H_2S. Since aluminum-killed steel is inherently dirty it was not specified for this use. When a steel is deoxidized with aluminum, a part of the aluminum oxide formed remains in the steel as inclusions. These impair the weldability and if present as large areas might also permit blistering.

It was not possible to purchase steel plate free from all laminations that might later cause blistering. The U. S. Navy purchases "marine plate" to a rigid quality specification. This specification requires a Magnaflux (magnetic particle) inspection of all cut edges of each plate. Defects larger than certain arbitrary standards result in rejection of the plates. Cost of this steel is 2-1/2 to 3 times the cost of "firebox" quality A212 steel because the ingot to plate yield is only 30 per cent, instead of a normal 60 per cent. Since the rejected plate cannot be readily sold, most steel mills prefer not to accept orders for "marine plate."

The Sperry reflectoscope used to detect blister sites is a pulse-echo type instrument that in effect measures the thickness of sound material under the probe. Thicknesses so measured that are less than the full-plate thickness are direct indications of internal voids or laminations. Any defects large enough to act as blister sites could thus be detected. The inspection was done at the various fabricating shops by the Material and Equipment Section of the Construction Division. The principal requirements of the procedure were:

(a) All plate to be fabricated into column or heat-exchanger parts subject to H_2S pressure must be scanned for laminar defects.

(b) A Sperry reflectoscope was to be used with a frequency of 2-1/4 megacycles per second, traversing the plate on 3-inch centers with a 1-inch crystal.

(c) A lamination of 4 sq. in. or less in area was acceptable without venting.

(d) Plates with laminations larger than 200 sq. in. were rejected.

(e) Venting of defects between 4 and 200 sq. in. was permitted. This was done by drilling holes to a depth of 60 per cent of the wall thickness from the outside surface.

Use of Type 316 stainless-clad steel plate was considered desirable in that corrosion would be minimized and hydrogen penetration would be eliminated. Since not enough stainless-clad plate could be obtained for this equipment, decision was made to use only as many lined towers at the Savannah River Plant as could be procured without delaying the startup schedules. About three-fourths of the towers were lined with Type 316 stainless steel strip. The remainder of the equipment was made with A212 steel plate.

3. Results of Plate Inspection

A review of the results of the ultrasonic reflecto-

scope inspection of plate for GS equipment indicated that 95 per cent of the plate passed reflectoscope examination. A total of 5714 plates were inspected before fabrication for the Dana and Savannah River Plants. Of these, 143 (2.5%) were rejected and hence downgraded. Venting was required on 130 plates (2.3%).

4. Strip-Lining Procedures

a. Laboratory Tests

Steel equipment may be lined with austenitic stainless steel by any of several techniques. These include welding of narrow strips, spot welding of wide sheet, arc welding through wide sheet to the steel plate, and conventional rolled-on cladding. All four of these methods were used by the fabricators who made the lined equipment for the Savannah River Plant.

Each of the fabricators submitted two sample plates to the Engineering Research Laboratory for check purposes. These plates were as follows:

Fabricator	Location	Lining Method
Wyatt Metal & Boiler Works	Houston, Texas	Strip 4-1/2 inches wide welded to steel plate
Wyatt Metal & Boiler Works	Dallas, Texas	Sheet overlay arc welded through to shell
Nooter Corporation	St. Louis, Missouri	Sheet overlay arc welded through to shell
A. O. Smith, Corporation	Milwaukee, Wisconsin	Sheet overlay spot welded to shell
Chicago Bridge & Iron Co.	Birmingham, Alabama	Conventional rolled-on cladding (Lukens Steel Co.)

Surface inspections were made of all specimen linings and welds using "Zyglo" equipment. No defects were found. As a further check the ammonia-phenolphthalein method was used to see if any defects penetrated the stainless steel lining. Ammonia at 20 psi was used to pressurize the space under the stainless steel lining. Single pinholes were found in each of two welds.

Bond strengths of the welds were determined by measuring the hydrostatic pressure required to rupture the stainless steel envelope. Each strip was pressurized with water using a hand pump and a conventional pressure gage.

A number of spot welds on the A. O. Smith plate were removed mechanically to determine the extent of bonding between the stainless steel lining and the carbon steel backing plate.

Cross sections from various parts of each type of weld were etched to characterize the depth of penetration. All stainless steel strip-to-steel welds were checked for evidence of underbead cracking. Hardness surveys made across all metallographic sections of welds indicated no underbead cracking. None of the heat-affected zones were harder than VHN 275 (Vickers Hardness Number).

Free-bend tests were made of all welds. Chemical analyses were made of selected weld deposits to check rod and plate composition. Spot tests indicated molybdenum (therefore, the presence of Type 316 stainless steel) in all welds and plates.

b. Summary of Stainless-Clad Plate Inspection

1. Each fabrication method represented by the test plates was apparently satisfactory for lining a heavy-wall steel vessel with an essentially continuous overlay of stainless steel.

2. No cracks were found in the cladding in any of the test plates. Single pinholes were found in welds on each Wyatt plate. A number of pinholes are likely to occur in the miles of welds required for the towers, even with good shop practice and reasonable inspection procedures.

3. Hydrostatic pressures of 950-2000 psi were necessary to rupture the envelopes formed by welding the stainless overlay to the base material.

4. Bend tests of the welds indicated adequate ductility.

5. Cross sections through the welds indicated that some of the manual welds gave very slight penetration. Automatic procedures showed as much as 3/16-inch penetration.

6. Type 316 stainless steel was used for all lining sheet. One plate was welded with Type 310 Mo stainless steel rod but all others were welded with Type 316 stainless steel rod.

7. Although underbead cracking was expected, none could be found on any of the 25 sections examined. Hardness traverses showed maxima of about 250 Brinell.

5. Laboratory Investigation of Blistering

A laboratory study on hydrogen permeability indicated that up to about 30 per cent of the hydrogen generated by the corrosion reaction penetrated A212 steel. Tests of austenitic stainless steels indicated that under process conditions hydrogen permeability would be negligible. This may have been due to the low corrosion rates and the lack of precision in the test equipment. Hydrogen transfer by cathodic charging of Type 304 stainless steel was reported by Petrovich to proceed at about 0.2 per cent of the rate observed for mild steel.

A number of samples thought to contain potential blister sites were placed in test. Most of these were too thin to be checked with the reflectoscope. The only blisters that could be found on these samples were small ones such as those developed at the laminations in rimmed steel corresponding to the subsurface blowholes. No large blisters have been reported at other laboratories where similar studies are in progress. All steel plates exposed to H_2S in the laboratory were examined for defects. Blisters were found on one of the plates used as a weight for stressing samples in the 45-inch pot. These are shown in Figure 2.

A section of strip-clad plate exposed in the 45-inch autoclave developed a definite bulge after a year of exposure. This was a sample from a Wyatt plate with a 7/64-inch thick strip of Type 316 stainless steel welded to an A212 steel base 1-1/8 inches thick. Circumferential weld beads were 4-1/2 inches apart and had been made by the automatic submerged-arc process. After approximately 2000 hr at 40°C and 4000 hr at 120°C the center of the strip had been raised 1/4 inch.

It was suspected that some hydrogen generated by corrosion of the A212 steel had penetrated through the 1-1/8 inches of A212 steel to the void under the stainless steel. The exposed surfaces of the A212 steel were badly scaled although the stainless steel was not. Another possibility was that H_2S might have entered through a pinhole in the weld and expanded the stainless steel sheet as the pressure was released at the end of the test.

By determining the pressure and volume under the bulge the approximate rate of hydrogen transfer could be determined. The sampling setup shown in Figure 3 was used to check the pressure inside the blister. By this means the original gas pressure was found to have been approximately 165 psi. This gas burned with a typical hydrogen flame and gave no H_2S odor.

Total hydrogen volume was 445 cc at standard temperature and pressure. This corresponded to less than 10 per

cent of the hydrogen generated on the steel surfaces by corrosion at 1 mil/yr. Corrosion rates on test panels and measurement of the thickness of the sulfide scale indicated a somewhat higher rate. Although some pitting was observed on the weld bead surfaces, the Type 316 stainless steel was not measurably attacked.

A similar section without the sealing welds showed no bulging. This indicated that corrosion products alone did not appreciably lift the stainless steel lining. Although the cavity under the stainless steel was filled with corrosion products, no accelerated corrosion was observed on either the steel or the stainless steel surfaces.

Because of the difficulty involved in making miles of welds in these towers it was assumed that some pinholes would occur in the welds of the Type 316 stainless steel lining. Although no practical inspection procedure would find all of these defects, the H_2S would find any that penetrated the lining.

Corrosion under the lining might then cause bulging due to one of three mechanisms:

(a) Hydrogen generated by the corrosion might cause bulging of the lining if a pinhole existed which was later blocked to prevent free escape of the gas. One volume of H_2S-saturated water would contain enough H_2S to generate 30 volumes of H_2 (STP) on reaction with steel.

(b) Some of the hydrogen might penetrate the A212 steel and recombine under an adjacent strip. This could cause bulging of a strip which had sound welds.

(c) A third possibility would occur during shutdown. If the system pressure were released quickly, any pressure built up by fluids leading through a pinhole might cause rapid bulging of the lining.

To check the possibility of hydrogen diffusing along a plate, a sandwich was made with two 4-inch square samples of Type 316 stainless steel welded to a steel plate. Welds were checked with a General Electric leak detector, Type H, and found to be leak-free. Hardened zones at the welds were softened by a 4-hr stress relief at 1100°F. Samples were then exposed at 60 and 120°C. No effect was observed after 4 weeks at 60°C. Bulging of the stainless steel overlay was evident, however, on the sample tested at 120°C after two weeks' exposure. The sharp rise in hydrogen permeability[32] over this temperature range may have been the important factor in this difference.

After a total of 2000 hr at 120°C, the centers of the Type 316 stainless steel patches had bulged a total of

0.126 inch. This indicated that appreciable hydrogen had penetrated the plain carbon steel, and collected under the stainless steel sheets. The gas from inside the synthetic blister burned like hydrogen. Since it returned to size when pressurized with 80 psi of nitrogen, a pressure of 80 psi of hydrogen was assumed. This indicated that about 60 cc of hydrogen had collected under each patch of stainless steel. This amount of hydrogen corresponded to between one per cent and 5 per cent of that generated by corrosion of the plain carbon steel surfaces.

As a check on the hydrogen permeability of austenitic stainless steels several pillow samples were tested. Pairs of 16-ga Type 316 stainless steel that had been edge-welded to form synthetic blisters exposed to the wet H_2S at 40 and 120°C for times up to 10,000 hr. No measurable bulging was observed on any of the samples. This confirmed previous indications that little hydrogen was generated by corrosion of stainless steel and that the hydrogen transfer rate was so low that it could not be measured by this type of test.

6. Embrittlement

a. Theory

Embrittlement, another type of damage that may be caused by hydrogen has been observed in steel after pickling and electroplating, as well as under conditions that might favor sulfide stress cracking. Tests in which hydrogen was charged into steel cathodically have indicated that no embrittlement is observed in low-carbon steel until the hydrogen concentration is about 3 cc/100 gm of steel[27]. As much as 15 cc H_2/100 gm of steel (approx. 17 ppm by wt) could be charged by this technique. At this level of hydrogen saturation, reduction of area as measured in the tensile test dropped from 60 to 20 per cent. Data obtained by Sieverts[28] indicated that steel at 900°C in equilibrium with 1 atm H_2 would contain 3 cc H_2/100 gm. Embrittlement of drill rod has been troublesome in sour oil well service. Aging of the embrittled rods at ambient temperatures and low hydrogen partial pressure atmospheres has been found effective as a means of restoring the ductility of embrittled drill rod.

b. Tensile Tests

A series of tests was made with A212 steel to determine if exposure to process conditions might cause hydrogen embrittlement. Initial Charpy impact tests showed no evidence of embrittlement of A212, rimmed steel, or Type 410 stainless steel after exposure to H_2S-H_2O at 120°C. Results are listed in Table I.

Two factors were considered as important in these tests:

(a) The impact test may not be critical for detecting hydrogen embrittlement. There seems to be an incubation period required that is longer than the duration of the impact test.

(b) Hydrogen in the steel may have escaped before the test was made.

Tensile tests were made with particular attention to these factors. As soon as the H_2S container pressure was released, the tensile samples were removed, washed in cold water, then quenched in liquid nitrogen. Since the diffusion rate for hydrogen in steel decreases sharply as the temperature is reduced, it was reasoned that storing at liquid nitrogen temperatures would minimize hydrogen losses during the time required to deliver the samples to the testing machine and to make the first test.

c. Test Results

Results of the series of tensile tests are shown in Table II. It was observed that the samples corroded at 120°C showed no evidence of embrittlement. However, since in the order of 30 minutes after removal from H_2S was required to complete the test, it cannot be positively concluded that no embrittlement occurred.

Samples corroded at 40°C and then cooled in liquid nitrogen to minimize escape of hydrogen showed reduced ductility. Ultimate tensile strength values were similar, but the elongation decreased 20 per cent and the reduction in area decreased 50 per cent. Since this loss of ductility was of the same order as that obtained with cathodic charging[27], no further tests were made. Cooling with liquid nitrogen had only a negligible effect on the tensile properties of unexposed A212 steel. There was no indication of embrittlement.

Although the precise conditions of the vessel walls are not known, these tests, together with plant experience, point out several things. The A212 steel vessel walls have been charged to some degree with hydrogen. At hot-tower conditions the hydrogen transfer rate may be high enough to minimize any hydrogen build-up in the steel[32]. At cold-tower conditions the build-up of the hydrogen content of the vessel walls would tend to be greater. (No direct evidence is available on this point.) The A212 steel in the cold-tower walls would be expected to show about the same yield strength and ultimate strength as the test samples from the as-rolled plates. There would, however, be a slight drop in the elongation and a moderate decrease in the reduction of area values for specimens tested in their present condition.

7. Summary

It has been indicated that one of the factors that must be considered in the corrosion of plain carbon steel in the H_2S-H_2O system is the absorption of a portion of the hydrogen generated by the displacement reaction with the plain carbon steel. Sulfur, as well as arsenic, tellurium, and other ions in solution, are specified as "poisons" to promote hydrogen absorption. One description of this process, probably oversimplified, states that the effect of the presence of these ions is that of raising the hydrogen overpotential, thus increasing the difficulty of combination of the hydrogen atoms generated to the molecular form, and thus promoting their absorption into the iron lattice.

One gross effect of this absorption is that of blistering. In this case the hydrogen, having entered the lattice, combines to the molecular form at any suitable internal site in the steel. The mechanism of recombination here is analogous to that existing at the "back" or uncorroded side of the plate. Because the driving force for recombination is great, high internal pressures can be developed and failure by "fissuring" or rupturing of the surface is widely described in the petroleum industry literature. Adequate descriptions of suitable sites for blistering are, however, not available. It is for this reason that killed steel was chosen and ultrasonic inspection was undertaken in lieu of any more conventional means for the plate material involved in GS-process vessels. Arbitrary standards of defect size for plate acceptance had to be chosen at the time, and these values appear to have been chosen adequately, perhaps conservatively, based on the fact that no blisters have been observed in the field. It is true that the difficulty in the petroleum industry equipment may be caused or aggravated by any of a number of contaminants which are not present, at least to the same degree, in GS systems. Annual inspection practices should certainly include examination for this type of difficulty.

A clear understanding, even on a descriptive basis, is not available on the effects of the dissolved hydrogen in low-carbon steel vessel walls or pressure-carrying membranes.

It can be demonstrated, as in the tests described in Table II that killed steel suffers in ductility provided that (a) the specimen is wholly enclosed in the corrosive medium, and (b) precautions are taken to break the specimen while still charged with hydrogen. Condition (a) is important, because in this case the specimen is believed to be saturated with hydrogen for each exposure condition. On the basis of current knowledge it is not possible to relate this case with that obtained in a vessel wall which is exposed to corrosive conditions on one side, and to air on the other. The concentration of hydrogen in the plate cross section may approach--or be quite low with respect to--the saturation

level if the controlling resistance to hydrogen flow is on the corroded or "back" sides of the wall, respectively. The critical resistance cannot now be located or even defined with any certainty.

Condition (b) above may represent an extreme case because the portion of the vessel wall which contains hydrogen at the saturation level is not known. Nor is information available on the effects of hydrogen at lower concentrations. The fact that steel in corroding does pass hydrogen at a finite rate is direct evidence that a concentration gradient does exist across the vessel wall cross section.

It should be noted that the tensile strength of the steel is not reduced in these tests and that, as reported by others, decrease in ductility is manifest only in tests of low deformation rate. These phenomena can be demonstrated in either conventional tensile or slow-bend tests, but not in notched-bar impact tests. The significance of reductions in elongation as measured in fracture tests is still a subject of considerable discussion.

It is apparent from this discussion that a clear description of the physical properties of vessel walls in GS-process service is not at hand. No evidence exists to indicate that (a) a real deleterious effect does exist or (b) if such an effect is real, how it is influenced by exposure time. It would appear reasonable, therefore, to make every effort to explore this possibility and to examine the structure and properties of typical sections of equipment as they are retired from service in the course of normal maintenance practice.

D. GENERAL CORROSION STUDIES

1. Experimental Procedure

a. Corrosion Test Conditions

Corrosion tests were started at the projected hot-tower conditions, 120°C with 250 psi of H_2S-H_2O. Additional tests were run at various temperatures from 25 to 250°C. H_2S concentrations varied from 100 ppm to 400 psi. Tests were run with samples both submerged in the liquid and exposed in the gas phase.

Care was taken to minimize oxygen and chlorides in the H_2S. A standard procedure was adopted of analyzing each 50-lb cylinder received. Any that showed as much as 0.1 per cent of oxygen, chlorides, and CO_2 was not used for these tests. Oxygen was minimized in the large test vessel by boiling the water and flushing twice with nitrogen before adding H_2S. Small test vessels were flushed with nitrogen and H_2S before adding H_2S to the desired pressure. When the

tests were to be run at temperatures above ambient, the autoclave to be used was brought up to temperature and pressure tested with nitrogen before H_2S was added to start the test.

b. Apparatus

1. Corrosion tests at 15-lb H_2S pressure were initially run at 100°C in an over-heated aluminum pressure cooker. Since the seal was unsatisfactory, a steam-jacketed steel autoclave with an O-ring seal was used to replace this unit.

2. Stress-corrosion tensile tests of A212 steel were started at room temperature using specimens sealed by means of O-rings in short tube sections.

3. The 45-inch diameter autoclave shown diagrammatically in Figure 4 was obtained for corrosion and stress-corrosion tests at 120°C and 250 psi.

4. Three of the autoclaves used at the Girdler Corporation were adapted for tests at the Engineering Research Laboratory at 30 to 40°C and 250 psi pressure. Two of these 10-inch diameter x 48-inch tall units were used, primarily for the bolting tests at high pressures.

5. Hydrogen-transfer tests were made with vessels fabricated from 1-1/2-inch pipe sections. These were jacketed for heating with steam or water and the ends sealed with O-ring closures so that test diaphragms could be placed in contact with gas or liquid. Test conditions were 40 to 120°C at 250 psi pressure. Electropotential tests of aluminum were run in these units by replacing the bottom test plates with special "Bakelite" holders to seal and insulate the electrodes.

6. Inhibitor tests were run in a set of 24 small (1/2 gal.) jacketed autoclaves. These had "Buna-N" O-ring seals for use at 40 to 120°C. Arrangement of these units is shown in Figure 5.

7. Corrosion fatigue tests were run on a "Sonntag" fatigue testing machine. The procedure and results have been described in another report.

8. Erosion-corrosion tests were run in the circulating systems shown in Figure 6. Each of these contained a surge tank 4 ft high made from 4-inch pipe, a pump ("Aurora G4" or "Jacuzzi" SB15HR4), a flow meter, and connecting piping.

Two types of erosion-corrosion test specimens were used. One was a stepped probe inserted in the line to restrict the cross-sectional area of the water passage. By restricting the area of the passage in three steps, the velocity of the liquid flowing along the plain carbon steel probe was varied.

The second type of sample was a disk centered under an orifice 0.2 inch in diameter.

9. Bolt tests at atmospheric pressure H_2S were conducted in a 5-gallon paint can with auxiliary tubing and bubblers so that flow rates could be checked.

10. Bolt tests at 1 to 3% H_2S and at 100 ppm H_2S were conducted in two 5-gallon stainless steel vessels. These had O-ring seals to confine the H_2S.

11. Corrosion tests in liquid H_2S were run in 4-lb H_2S cylinders. By cooling the cylinders with dry ice, H_2S could be condensed into them.

12. Conditions in stripper (SX) heat exchangers were simulated in the equipment shown in Figure 7. This unit was designed as a loop to simulate the most corrosive conditions in the GS heat exchangers. There were three seven-tube heat exchangers, each two feet long, tubed with Types 304, 316, and 329 stainless steels as well as plain carbon steel. Steam at 275 psi supplied the heat to the shell side of two exchangers. One exchanger was below the liquid level. The second was horizontal and partially filled. The third unit was water-cooled on the shell side to condense the vapor and complete the thermal cycle.

13. Static high-temperature corrosion tests were made in a sealed autoclave.

14. Sulfide deposition tests were run in the equipment shown in Figure 8. This consisted of a surge tank filled with steel rings, an exchanger for heating the H_2S saturated water, and a second one to cool the water.

15. Sulfide solubility tests were run in the equipment shown in Figure 9. The glassware was covered with "Teflon" tetrafluoroethylene fiber and placed in an autoclave that could be maintained at temperatures of from 40 to 175°C.

16. Measurement of pH by use of indicator techniques was made in a small stainless vessel which had sight glasses to form the front and back walls. A sketch of the setup is shown in Figure 10.

c. Results

Steel exposed to dry H_2S was virtually unaffected at low temperatures. The several samples tested remained bright and clean. Interiors of several H_2S cylinders were found to be clean and bright. Cylinders that corroded were found to contain a separate water phase in some cases.

1. Corrosion Rate of Plain Carbon Steel vs. Time: At 120°C corrosion was observed to be as high as 2000 mils/yr for 1-hr tests in H_2S saturated water, but it dropped off rapidly with time and tended to level off below 10 mil/yr. At 25 to 40°C the short-time corrosion rates were lower, but the film formed was softer and less protective. Hence, the decrease in corrosion rates was not so sharp as that observed for 120°C.

The results of 100 tests at 120°C and 75 at 40°C were analyzed statistically and the dependence of corrosion rates on exposure time determined. At 120°C the corrosion rate is related to time as follows:

$$C = \frac{338.5}{T^{0.7}}$$

At 40°C the relationship is:

$$C = \frac{149.4}{T^{0.512}}$$

T - total time in test (hr)
C - average corrosion rate in mil/yr

The two curves, plotted in Figure 11, show the average corrosion rates that might be expected at 40°C and at 120°C.

As a check on the effect of test interruptions, several samples were run for continuous tests and compared with tests that were interrupted once per week. Results listed in Table III show that samples exposed continuously had significantly lower rates than those whose exposures were discontinuous. This fact indicated that exposure to air damaged the protective sulfide scale. This damage was almost equivalent to complete removal of the scale so that the iron surface would then start over to build up a coating.

Test data from a series of uninterrupted tests were analyzed for comparison with those mentioned above. The curve that fit the points best had the following description:

$$C = \frac{847}{T^{0.882}}$$

This curve is shown in Figure 12 with the observed rates shown superimposed. It is evident that the over-all corrosion drops below 1 mil/yr after 2000 hr. Plant experience gained since this work has substantially confirmed this observation.

The protective effect of the sulfide film formed on steel makes use of plain-carbon steel practical for GS-plant construction. As long as care is taken to keep the sulfide

film intact, steel can be used without undue corrosion losses. Results of the first series of tests were listed in earlier reports.

2. Effects of Impurities in H_2S and H_2O: A number of minor changes were made in test conditions to determine factors that might accelerate or inhibit corrosion of steel by wet H_2S. Tests were made in which 20 per cent of the H_2S was replaced by oxygen, carbon monoxide, or carbon dioxide. Samples were immersed in distilled water in glass as were the control specimens. No acceleration or inhibition of corrosion was evident during these tests. A rapid pressure drop was observed just after H_2S was added to the oxygen. The sulfur present in the test unit indicated that the oxygen had been used up in oxidation of the H_2S. Minor differences in the water used had no appreciable effect on corrosion of steel at hot-tower conditions. Water samples included, Wilmington tap water, distilled, deionized-distilled water, Dana Plant water, and process water from the GS units.

Several short-time tests were made in which sulfuric acid was added to reduce the pH of the feed water used to 2. This required about 500 ppm of H_2SO_4. Average corrosion rates for steel in the H_2S-H_2O using pH 2 water at 120°C were from two to three times the rates observed when the initial pH of the water was 5 or more. Sodium hydroxide additions in the range of 50 to 2500 ppm did not cause consistent changes in the corrosion rates of the steel samples tested. Addition of 2500 ppm of caustic did reduce the corrosion rates somewhat, although not as much as would be expected of useful inhibitors. At lower concentrations of caustic, corrosion rates for steel samples were equal to or slightly higher than average rates for steel tested in distilled water.

3. Effect of Steel Composition: Carbon steel and several low-alloy steels showed similar corrosion rates. A212, cold-rolled rimmed steel, annealed rimmed steel, AISI-1018 steel, 5% Ni, 9% Cr, A285 steel, cast iron and AISI-4140 steel were tested at 120°C. Although these materials exhibited normal variations in corrosion rates, the rates obtained all fell within the limits of reproducibility for A212 plain carbon steel. For conditions where no erosion was involved long-time corrosion rates were in the range of 1 to 5 mils/yr. Type 410 stainless steel showed lower corrosion rates in the range of 1 to 2 mils/yr. Austenitic alloys showed corrosion rates of 0.1 to 0.5 mil/yr, with shallow pitting accounting for most of the loss. Pitting was accelerated under scale particles lodged on the stainless surfaces. This condition was more severe in laboratory tests than in plant equipment. Degradation of sulfide scale when tests were interrupted (and the test vessels opened to the air) may have formed some dilute sulfuric acid which accelerated corrosion during later laboratory tests. As might be expected, Type 316 stainless steel showed less pitting than Type 304 stainless steel during the same exposure.

4. Effect of Test Interruptions: When tests were interrupted and samples cleaned to determine weight losses, the clean steel surface on re-exposure again started to corrode over at approximately the original rates. Samples examined between runs, but not cleaned, showed intermediate rates for succeeding periods, indicating that the sulfide film was degraded by exposure to air even though no effort was made to remove it. Results listed in Table III indicate that samples exposed continuously show significantly lower corrosion rates than those whose exposures are discontinuous.

Degradation of wet sulfide films exposed to air makes oxidation possible. This oxidation occurred every time a laboratory autoclave was opened. These oxidized sulfides react to produce weak sulfuric acid much as acid mine water is produced from wet pyrite exposed to air. This dilute acid, being present as it is in the scale, is quite difficult to remove. It lowers the pH of the water, making it more corrosive than it would be with H_2S alone, as indicated above. Tests in glass can be compared with each other, since the effect of scale is eliminated. Under plant conditions the volume of water passing through is enough to dilute and minimize any effect from scale oxidation. However, laboratory tests in steel equipment result in a build-up of acidity because of the low water volume compared to the quantity of scale. This increased acidity results in higher-than-normal corrosion rates in many cases.

2. Corrosion Tests of Ferrous Alloys

a. Procedure

In order to determine the average corrosion rates for various materials that might be used in process equipment, many tests were made. The materials investigated included A212 steel and a number of plain-carbon and low-alloy steels. Most of the alloys and different types of nonmetallics that are used for chemical plant construction were also included. Testing times were varied in order to learn the corrosion rates that might be expected during long-time plant service. Most exposures were for 48 to 500 hr which were convenient times for laboratory tests. Other samples were exposed for from 1 to 2000 hr to determine changes of corrosion rate with time. Some samples were exposed continuously, others were exposed, cleaned, and re-exposed. Some were re-exposed without cleaning.

The cleaning procedure for plain carbon and low-alloy steel samples included immersion in cold 10% HCl inhibited with Barrett No. 53 inhibitor. Samples were submerged until gas evolution stopped. This procedure loosened the scale but did not remove all of it. The scale seemed to be undermined, indicating that the layer adjacent to the steel was soluble although part of the scale was not dissolved by

the acid. Samples were then cleaned with a detergent, washed in hot water, rinsed in acetone containing VPI (Vapor Phase Inhibitor) and dried. Steel samples were stored in a desiccator until they were weighed or re-exposed. Clean steel samples treated by this procedure showed weight losses due to pickling alone corresponding to less than 0.1 mil/yr. Stainless steel samples were cleaned with cold 65% HNO_3.

3. Mechanism of Sulfide Corrosion of Steel

A study of the films formed and the changes in corrosion rates indicates that the mechanism of sulfide corrosion of steel resembles that of high-temperature oxidation. The initial film or tarnish forms at an extremely high rate when clean steel is exposed to wet H_2S. Corrosion thereafter depends upon diffusion of iron or sulfur through the scale[23]. Sulfide ions may diffuse into the steel sulfide interface, or iron ions may diffuse out to the scale surface. No information is at hand which describes the rate-limiting process.

a. Iron Sulfides

As the scale grows in thickness the diffusion path becomes longer and attack of the steel decreases. The outer layers are gradually converted to the higher sulfides (sulfur-rich compounds) which are more stable. Thus, all four of the iron sulfides normally reported, troilite, pyrrhotite, marcasite, and pyrite were found in scale samples. Troilite and pyrrhotite are of the same type, Fe_nS. For troilite n = 1 and for pyrrhotite n may vary from 0.8 to 1.0. Both minerals as formed in place appear brown in color and have hexagonal crystal forms. When polished sections are examined metallographically, both are creamy white by white vertical reflected light. Polished pyrrhotite surfaces are strongly anisotropic so that they show various shades of brown when examined by plane polarized light. Troilite is gray under polarized light. Both pyrite and marcasite are disulfides with the same formula FeS_2. Both are creamy white under vertical reflected light. Pyrite is isometric and shows no color change under polarized light. Marcasite is orthorhombic and under polarized light shows various shades of green and brown. Although massive crystals of these sulfides are easily distinguished by their crystal forms, they are more difficult when present as mixtures of very small particles. X-ray diffraction was found to be a suitable method for identification.

b. Hydrotroilite

Examination of a number of cross sections of corroded carbon steel indicated that the first layer formed at the steel-scale interface was similar on all specimens. The physical contour of the scale varied widely, as shown in Figures 13 and 14. After long-time exposure the surface

appeared simply roughened in most cases and quite irregular, with fingers of sulfides originating at the surface on other specimens. Although some sulfides were deposited on austenitic stainless steel surfaces the amount formed in place by corrosion appeared to be very small. Metallographic and X-ray diffraction studies of the scales were carried out.

At low temperatures the sulfide formed next to the steel was relatively stable but its X-ray diffraction pattern did not match any of the four common iron sulfides mentioned above. Hence, it was termed sulfide X. It was later identified as hydrotroilite. Although no samples of this mineral could be obtained and no X-ray patterns are recorded in the literature the methods of preparation described involve treating iron with cold aqueous H_2S[17]. X-ray patterns of hydrotroilite were peculiar in that there appeared to be two structures, one with strong lines and one with faint lines. Although this might have indicated a mixture of two compounds, the same lines with the same relative intensities were observed for several different samples. No structure could be found that would account for all of these lines. However, a tetragonal cell having A_o = 5.20A and C = 5.03A can be assumed that would account for most of the strong lines. The interplanar spacings are listed in Table IV. Hydrogen analyses indicated that the hydrotroilite may have the formula FeS·n H_2O with n approximately 0.2. Differential thermal analysis of hydrotroilite showed evidence of phase transitions at 90°C and at 114°C, although the phases were not identified. Neither pyrrhotite nor troilite showed similar transitions.

X-ray patterns indicated that scale samples from the plant were mostly pyrite and marcasite. Samples prepared in the laboratory were usually hydrotroilite, troilite, and pyrrhotite. Since the only general difference in conditions was in the exposure times, tests were run to check the effect of additional exposure. Hydrotroilite scale made by exposure of steel to H_2S at 25°C and atmospheric pressure was exposed to H_2S at 120°C and 250 psi pressure. After one week an appreciable proportion of this scale had been converted to pyrite and marcasite. Additional tests indicated that loose scale was converted more rapidly than scale on steel. Conversion at 25 to 40°C was relatively slow. Examination of additional plant samples indicated that each of the five sulfides can be found if samples are taken from appropriate locations. Other tests indicated that hydrotroilite was converted to troilite at 120°C even though no H_2S was present.

4. Inhibitor Evaluation

Since inhibitors are widely used in the petroleum industry to minimize H_2S corrosion, a study was initiated to find inhibitors suitable for the GS process. It appeared desirable in the early part of this work not only to reduce the corrosion rate of plain carbon steel to minimize equipment

deterioration, but also to decrease the amount of sulfide scale formation. It can be shown that a corrosion rate of 10 mils/yr is equivalent to the production of a pound of scale/sq ft/yr. Scale in this quantity, if not adherent, could constitute a serious problem in equipment fouling. Present knowledge of inhibitors is not sufficient to extrapolate data determined under one set of conditions to another corrosive condition. Therefore, an Edisonian type of testing program was a virtual necessity.

Early inhibitor tests at Columbia University were run at relatively high concentrations (1000 to 5000 ppm). Seven of the inhibitors reported to be effective were rechecked at the Engineering Research Laboratory using concentrations of 500 ppm. Results are listed in Table V. Isoquinoline was the only compound that was considered to be effective as a practical inhibitor in these tests.

In the first series of inhibitor appraisal tests at the Girdler Corporation Laboratory in Louisville dimethylamine (100 ppm), tributylamine (20 ppm), diethylaniline (30 ppm) and piperidine (10 ppm) were included. Corrosion rates for steel samples were slightly reduced by these compounds, but the effects were too small to indicate that any could be considered as practical inhibitors. Additional tests with formaldehyde (200 ppm),"Kontol"120 (25 ppm), and pyridine (20 ppm) showed no marked improvements. Later tests with inhibitors suggested by the results of work at the Engineering Research Laboratory indicated that concentration of more than 100 ppm (preferably about 500 ppm) would be required for even the most potent inhibitors. Ammonia at 2,000 to 10,000 ppm also showed promise in the early tests.

Tests of a series of compounds were started in cooperation with the Chemical Department. Compounds used commercially in oil wells as well as a wide variety of other inhibitors and surface-active agents were used. A total of 700 different materials were included in these tests. About 250 of these materials showed some evidence of corrosion inhibition and were tested further. Certain of the complex amines such as tetraethylenepentamine were found to be the most effective of those tested in reducing the sulfide corrosion of mild steel.

a. Corrosion Test Procedure

Initial screening tests were run by the Chemical Department in distilled water containing 1000 ppm of the candidate inhibitor to be tested. Strips of rimmed steel were placed in test tubes containing these solutions saturated with H_2S at room temperature and atmospheric pressure. After a 48-hr test period each inhibitor was rated on the basis of blistering, solution discoloration, and sample discoloration. Approximately 250 of these inhibitors were effective in

reducing corrosion and eliminating blistering of the steel. These, together with a few ineffective compounds for check tests, were sent to the Engineering Research Laboratory for further testing.

Evaluation tests were carried out by exposing rimmed-steel specimens of approximately 100 sq cm area in beakers containing 250 ml of water at 120°C and 230 to 250 psi of H_2S. Samples cut from 22 ga cold-rolled sheet were annealed at 1500°F to develop a microstructure similar to that found in typical hot-rolled A212 steel plate. Inhibitor test units are shown in Figure 2.

Steel samples were placed in the beakers and covered with the solution to be tested. The test pots were sealed with O-rings that had to be replaced for each test. By cleaning each lid with steel wool, as it was removed, the effects of the scale on the sealing surfaces were minimized. In starting these exposures, air in the unit was displaced by pressurizing and blowing down twice with nitrogen and twice with H_2S before adding H_2S to 250 psi.

Corroded specimens were cleaned with cold 10% HCl containing 1600 ppm of Barrett No. 53 inhibitor. This concentration was obtained by adding one drop of the inhibitor per 25 ml of 10% HCl. After gas evolution stopped, samples were washed quickly with a detergent to remove the "smut" of undissolved sulfide, rinsed in acetone containing VPI, dried, and stored in a desiccator until weighed.

As a check on the cleaning procedure, a series of pickling tests was run using clean steel samples. Results of these tests are listed in Table VI. Samples being cleaned were exposed to the acid for not more than 10 minutes after H_2S evolution stopped. Vigorous scrubbing with the detergent was found to remove about 4 mg per specimen. A weight loss of 4 mg corresponds with a corrosion rate of 0.1 mil/yr for a 160-hr test. These tests indicated that the cleaning procedure had less effect upon the corrosion rate than normal variations between consecutive tests.

To assist in inhibitor evaluation a series of blank runs was conducted as the work progressed. These were run in the same manner as the inhibitor tests but with no inhibitor added. While some were run before the inhibitor tests were started most of them were check runs inserted to assure that subsequent tests would not be affected by the carry-over of volatile components from one exposure to the next in the same vessel. No such cross contamination was observed.

The first screening was done with inhibitor concentrations of 50 ppm. Corrosion tests of 48-hr duration were run to check each inhibitor. An arbitrary rate of 10 mils/yr was set as the acceptable maximum. This criterion reduced the

number of likely inhibitors to 55. All of these were then tested at concentrations of 50 ppm for periods of 1, 2, and 3 weeks.

Additional tests were made of the most promising inhibitors at concentrations varying from 10 to 10,000 ppm. Results of these tests indicated that an inhibitor concentration of 500 ppm would be necessary in order to get consistent inhibition results from the most effective inhibitors. Results for the seven best inhibitors are shown in Table VII. All of these inhibitors reduced the corrosion of steel by 80 to 95% during one-week tests. Essentially the same corrosion rates were observed in 1-, 2-, and 3-week tests. These results indicated that the films which inhibit H_2S corrosion were effective from the start of the exposure. Still longer tests did not show any lower corrosion rates, which indicated that the corrosion barrier did not improve with time.

X-ray studies of the corrosion products formed in the presence of inhibitors indicated that there was little or no conversion to the harder sulfides, pyrite and marcasite. This was true even for loose scale that had been detached from the steel. After the scale had been washed to remove the inhibitor and exposed to H_2S a second time, it was then converted to pyrite in a short time, indicating that the inhibitor was not tightly adherent to the sulfide.

All of the available data on the inhibitors listed in Table VII have been plotted in Figure 15 to show the effect of time on corrosion rates of steel with and without inhibitors. Inhibitor concentrations were 500 ppm.

b. Synergistic Effects

Since "once through" use of inhibitors at 500 ppm would require excessive amounts of material, several alternate procedures were studied. A number of combinations were tried using low concentrations of the most effective inhibitors. Various addition agents were included. Results of these tests are shown in Table VIII. None of these combinations showed consistent reduction of the short-time corrosion rate to the order of 1 mil/yr. Although some improvements were indicated, it appeared that this effect would not make it possible to use inhibitors on a "once through" basis. Some means of inhibitor recovery would still be needed to minimize stream pollution and reduce the need for appreciable make-up.

c. Inhibitor Recycling

At the same time that the efficiencies of inhibitors were being determined other resultant and concomitant problems were also considered. Recycling appeared desirable for two reasons: (a) it would reduce the make-up inhibitor cost; (b) it would reduce the loss of H_2S in the waste stream.

Since most of the good inhibitors were alkaline they combined to form stable sulfides. These might not be completely decomposed by the H_2S stripper which was designed for a maximum temperature of 210°C. Thus, inhibitors would tend to cause stream pollution by increasing the sulfide content of the waste water. An arbitrary limit of 20 ppm of sulfides was set as the maximum tolerable amount. Oxidation in the holdup pond was expected to correct for quantities less than this amount. Procedures for continuously extracting the inhibitor and combined sulfur were desired.

Preliminary tests indicated that amines such as TEPA (tetraethylenepentamine) could be recovered by ion-exchange techniques. Several ion-exchange resins were tested and order-of-magnitude estimates were made of the equipment requirements. These estimates indicated that a plant costing about 2 million dollars would be required for recycling TEPA at 500 ppm. This procedure would involve continuing expenses for ion-exchange resin, sulfuric acid, caustic, and inhibitor make-up to compensate for losses.

Use of volatile inhibitors was also considered. Since these compounds tend to concentrate in the hot tower they might be recycled by making certain piping alterations in the present equipment. Order-of-magnitude cost estimates indicated that these changes would cost in the order of $500,000.

Results of corrosion tests in solutions containing volatile inhibitors indicated that these were much less effective than inhibitors with high boiling points.

d. Sludging Effects of Inhibitors

Since ammonia had been an effective inhibitor for oil industry applications involving sour gas, it was tried at the Dana pilot plant. Soon after ammonia additions were started the system stopped operating. Inspection indicated that sludge had plugged the constrictions such as the slots of the bubble caps. Since the pilot plant had operated for a series of short periods on air and water and with H_2S-H_2O, there had been a considerable scale build-up. The ammonia solution seemed to dislodge this scale. It then settled out on the trays and in various pipelines and instrument tubing.

Since amines are similar to ammonia, it was considered possible that amine inhibitors might have a similar effect if introduced into a system that had been corroded. During routine testing of inhibitors at the Engineering Research Laboratory high concentrations, 10,000 to 20,000 ppm, of certain amine inhibitors were observed to remove large areas of scale from the autoclave walls. Other methods of scale removal had been tried with little success. Wire-brushing and scraping removed only a part of the scale.

To evaluate the amines being considered for plant service, static and dynamic tests were run to check sludging effects.

Static tests were conducted under both hot-tower and cold-tower conditions. Test samples, roughly 3/4 inch by 9 inches were cut from corroded plates of 1/8-inch thick steel. These plates had been exposed to process conditions for approximately a year and were heavily scaled. Since the large autoclave had been opened a number of times during the year, the sulfide scale was thicker than would be expected in plant service.

Two inhibitors were used and two controls included. Trimethylamine (TMA) and tetraethylenepentamine (TEPA) were considered typical of the low- and high-molecular-weight amines, respectively. An uninhibited test was run to determine the amount of scale that would normally be loosened. A solution (3000 ppm) of ammonia (2700 to 3500 in practice) was also used as a control, since at this concentration considerable amounts of scale had been loosened in the pilot plant.

A glass beaker containing two samples was placed in an inhibitor pot with enough test solution to cover the scaled steel samples. The pot was then closed and pressurized with H_2S to 250 psi. After a 4-day exposure, the pots were opened and the samples carefully washed to remove any loose scale. Solutions were filtered and the filter paper and residue dried at 105 to 110°C. After drying, all samples were cooled in a desiccator. Each set of filter paper and sample was exposed outside the desiccator for about the same period of elapsed time (30 to 40 sec) to minimize errors due to water adsorption during weighing.

Five separate runs were made. Fresh solutions were used for each run and after the fifth run the samples were pickled in inhibited 10% HCl to remove the remaining scale. From these data the total weight of scale on each sample was computed. Weight of scale that sloughed off each sample was computed as a percentage of the total sulfide scale on that particular sample.

A summary of the data from the static tests is shown in Table IX. Ammonia, tetraethylenepentamine (TEPA), and trimethylamine (TMA) all loosened considerable quantities of scale. TMA at 500 ppm showed little effect at 120°C. However, this concentration was too low for effective corrosion inhibition. Clean steel rings, as tower packing, were placed in each of the surge tanks. These added 16 sq ft of surface per unit.

Tests were run with a series of inhibitors to check the sludging due to loosening of scale in the system. The units had been used for erosion-corrosion tests in H_2S-H_2O

and contained appreciable scale.

Tests were run with TMA, TEPA, and a blank to check the effect of these inhibitors on the scale present in the system. Subsequent tests were made with various inhibitor combinations to determine whether the scale formed was adherent or formed a sludge that was readily sloughed off during the test. Test units were filled with the solution to be tested and operated at 120°C with 100 to 150 psi of H_2S pressure. The first runs were interrupted because of loss of solution through the pump shaft seals. Make-up tanks were then installed so that additional solution could be added to compensate for losses.

After each run the H_2S was released and all the loose sludge in the surge tank and piping washed out. All the rings were removed and the loose scale washed from them. This scale was then dried and weighed to determine weight losses and compute corrosion rates.

After each run, scale was removed from the surge tanks and piping by pickling. Since the pump impellers and housings were cast iron they would have been rapidly attacked by the inhibited acid. Therefore, the pumps were not cleaned between runs. In any case, the surface area of each pump was only a small proportion of the total area in each unit.

Results of these tests are listed in Table X. During the tests with inhibited solutions much larger fractions of the sulfide scale were removed than for the uninhibited solutions. During the inhibited runs starting with pickled steel surfaces, sludge was formed at the rate of 2 to 5 gm/wk/10 sq ft (0.02 to 0.05 psf/yr).

These results indicate that the use of inhibitors would not solve the sludging problem. Although appreciably less sludge would be formed if there was no sulfide scale present when inhibitor additions were started, there appears to be no assurance against rapid plugging of the system.

e. Summary

Although short-time tests indicated that inhibitors might help minimize H_2S corrosion, long-time tests showed little advantage. The curves of over-all corrosion rates tend to come together so that after 2000 hr of exposure there would be little or no improvement to be gained by using an inhibitor. Most equipment in GS units was designed for continuous operation. The disadvantages of higher operating costs, more complex waste disposal, and sludging were much greater than any gain indicated for inhibitors. Hence, consideration of inhibitors was dropped and tests terminated.

5. Corrosion by Liquid H_2S

a. Pitting of Storage Tank

During a routine examination of the H_2S storage tank at the Dana pilot plant, severe pitting was observed. Most of the attack was at the bottom of this tank in the vicinity of the nozzle and girth-joint welds near the external heating coil. A 2-inch steel line carrying process gas from the manifold to the tank also failed by gross pitting. The tank had been in service for 11 months, the pipe for 5 months. Field observers noted that the corrosion was always associated with a heavy, black, oily sludge and occurred preferentially on welds. Analysis of the sludge indicated the presence of oil, iron oxide, iron sulfide, reaction products of oil and H_2S, water and approximately 5% chlorides. The pitting of the tanks and the piping was postulated to be the result of either water, sulfide scale, or chlorides, or a combination of these, in the H_2S.

Commercial H_2S is water-scrubbed and then dried by passing over $CaCl_2$ during manufacture. The dried H_2S is then compressed in regular cylinders for transporting to the point of use. Most cylinders contain no water. However, some cylinders have been found to be wet on the inside. This indicated that the drying procedure had been ineffective. As such water entered the cylinders it might have contained some calcium chloride by entrainment. This was considered as the most likely source of chlorides in the H_2S storage tank at the Dana pilot plant. The H_2S cylinders were emptied by inverting them so that the liquid H_2S could be drained through the lines to the storage tank. This simplified the transfer procedure but made possible the transfer of any water from the bottoms of the H_2S cylinders. Normally, only H_2S gas is boiled off from the cylinder. In this case any nonvolatile salts such as calcium chloride remain in the cylinder as the H_2S is removed.

b. Laboratory Tests

A series of tests was set up at the Engineering Research Laboratory to investigate the effect of these variables on the corrosion resistance of materials of construction in liquid H_2S.

Specifically, seven autoclaves were charged with liquid H_2S under the following conditions.

Test	Condition
1	Liquid H_2S + H_2O
2	Liquid H_2S + H_2O
3	Liquid H_2S + H_2O +"Duomeen T"(saturated)
4	Liquid H_2S + H_2O + FeS scale
5	Liquid H_2S + H_2O + 5% NaCl
6	Liquid H_2S + H_2O
7	Liquid H_2S minus H_2O (0.059% H_2O max.)

All samples were individually contained in test tubes into which water plus the scale, inhibitor, or chlorides were placed in such a way as to cover approximately one-half the sample. The test tubes were then located in the autoclave and H_2S distilled into it until the tubes were completely submerged in liquid H_2S, Figure 16. The choice of distillation over mechanical transfer of the liquid H_2S as a means of submerging the samples in liquid H_2S was to reduce the possibility of carry-over of contaminants entrained in the liquid. The commercial cylinders of H_2S were found to contain yellowish green crystals analyzing in part S - 82.49%, Fe 2.04%, Ba less than 0.10% and SiO_2 4.87%. In all autoclaves excepting No. 7, distillation took place with the source vessel at atmospheric temperature and the receiving vessel or condenser at 9°C. The vapor pressure of H_2S is approximately 20 atmospheres at 25.5°C and 10 atmospheres at 0°C.

In autoclave No. 7, no water was added and an effort was made to reduce the water content of commercial H_2S to as low a figure as possible. No absorption medium such as P_2O_5 or $Mg(ClO_4)_2 \cdot 3H_2O$ could be found which was specific for water in the presence of H_2S. To attain dehydration of the H_2S, a low-temperature distillation was used, the source held at 0°C and the condenser at -78°C. Lacking information pertaining to the partial pressures of H_2S and H_2O, respectively, over the hydrate $H_2S \cdot 6H_2O$ at the temperatures involved, the assumption was made that they did not differ from those of pure H_2S and H_2O at those temperatures. The partial pressure of water with respect to that of H_2S at 0°C is 4.5 mm to 760 mm Hg, respectively (0.059%).

The depth of liquid H_2S inside the autoclave in all distillations was determined by measuring the frost line which occurred upon the endothermic expansion of the gas from the liquid. Weight measurements were made periodically to check on leakage from the system.

During exposure, all autoclaves were housed in a chamber equipped with electric light bulbs to keep the temperature approximately 38°C. The materials tested in this condition were as follows:

A212 steel
A212 steel welded with "Fleetweld" No. 5
Type 410 stainless steel
Type 304 stainless steel
Type 316 stainless steel
Zinc-sprayed steel 0.006 inch thick - 1 coat vinyl paint
Zinc-sprayed steel 0.006 inch thick - 2 coats vinyl paint
Aluminum-sprayed steel 0.006 inch thick - 1 coat vinyl paint
Aluminum-sprayed steel 0.006 inch thick - 2 coats vinyl paint
Stainless steel 0.006 inch
"Heresite"-coated steel

The welds were exposed in the "as welded" condition. The sample size restriction imposed by the autoclave neck made it necessary to use samples approximately 4 inches x 1/2 inch x 1/8 inch. The welded samples had a longitudinal bead covering the greater part of one surface providing a high weld-metal-to-parent-metal ratio.

c. Results

1) Type A212 Steel: Results of these tests are shown in Table XI. For A212 steel, it was evident that an over-all corrosion rate for 5000 hr would be in the order of 2 to 3 mils/yr, as shown in tests No. 1 and 6. Rates for 1000 hr in Test No. 2 were approximately 7-9 mils/yr. The addition to the liquid $H_2S + H_2O$ of iron sulfide scale taken from an H_2S-H_2O system at 120°C and 250 psi increased the 5000 hr corrosion rate of A212 steel to a rate as high as that associated with a 1000-hr exposure. The major damage, however, was located at the end covered by the scale. Attack was general and not by gross pitting as in the storage tank condition previously mentioned. It was noted that the foreign scale added to the system became securely attached to the samples, making it very difficult to remove.

In test No. 5, a 5% aqueous solution of NaCl was used; equivalent to 3% chloride in the system. After a continuous exposure to the 3% chlorides for 4944 hr the A212 steel samples were covered with a thick, black, oily sludge which appears to be similar to that observed at the Dana Plant in the process gas storage tank. Corrosion rates were increased to 8 to 14.5 mils/yr but do not reflect the extent of the deterioration involved. Attack was similar to that described in the report on conditions in the storage tank, in that the attack was not general but confined to certain areas located in the mid-section of samples. The weld samples are of particular interest, in that attack was preferential to the weld metal itself, as shown in Figure 17. The cross-sectional view illustrates the extent and distribution of corrosion.

It is believed that these tests have isolated the chloride ion as a cause of the serious pitting problem in the

gas storage tank.

Test results indicate that the corrosion rates for liquid H_2S and water are nominal. It was of academic interest, however, to note that the use of an inhibitor of the fatty diamine type such as "Duomeen T"* reduced corrosion to less than 0.5 mil/yr. Corrosion rates with Duomeen T were 1/5 to 1/10 of the standard rate for 5000 hr in liquid H_2S and H_2O. For purposes of the tests, "Duomeen T" which is virtually insoluble in cold water, was mixed in equal quantities with cold water.

Another angle of attack that was successful in reducing general corrosion in liquid H_2S was that of drying the H_2S as described above. The corrosion rates in this instance were also below 1 mil/yr; these were less than one-fifth of the standard rates in liquid H_2S and H_2O.

2) Stainless Steels: The behavior of austenitic steel was generally good with the exception of the chloride-bearing environments. Three per cent chloride ion as NaCl in water produced corrosion rates of approximately 1 mil/yr.

Ferritic stainless steel was satisfactory in liquid H_2S-H_2O but had high rates in scale in the chloride-bearing environments.

3) Sprayed Coatings: Sprayed coatings of zinc, 0.006 inch thickness, sealed with 1 and 2 coats of vinyl paint were generally unsatisfactory, except in the anhydrous liquid H_2S.

The 0.006-inch aluminum-sprayed coatings with 1 or 2 coats of vinyl paint are apparently more resistant than those of zinc, although all exposures tested with the exception of the anhydrous H_2S brought about some blistering and exfoliation of the coatings.

The stainless steel sprayed samples (Type 304) were entirely void of coating after exposure in the liquid H_2S and H_2O as well as the chloride-ion environments. The coating was contiguous and bright in the anhydrous H_2S exposure.

Heresite blistered in the liquid H_2S-H_2O with scale but was in good condition after 6000 hr in the inhibited test.

d. Summary

1. Tests have shown that the chloride ion, known to be present in the storage tanks, is probably the cause of gross pitting.

* Armour Company

2. It has been established that corrosion by liquid H_2S-H_2O produces only nominal rates in the order of 2 to 3 mils/yr. The type of deterioration in this instance is general and not localized in nature.

3. The hypothesized reduction in general corrosion rate by the expedients of using amine inhibitor or drying the liquid H_2S were substantiated.

4. The behavior of stainless steel in liquid H_2S and H_2O has been shown to be excellent, with the exception of the chloride-bearing environments. The latter behavior is not unusual.

5. Sprayed coatings of zinc, aluminum, and stainless steel proved to be unsatisfactory for wet, liquid H_2S service.

6. Repair Welding GS-Process Equipment

Since repair welding is necessary during normal maintenance of plant equipment, a study of repair welding problems was undertaken to determine the effect of H_2S exposure on subsequent welding of carbon steel plate. Welding of used GS equipment is complicated by the presence of dissolved hydrogen in the steel and a heavy sulfide scale on any surfaces exposed to process fluids.

Tests were conducted to study these factors and to provide a basis for a procedure for producing sound welds. A series of test welds made at the Dana Plant were also evaluated for comparison.

Initial work was done to evaluate welds made on steel that had been exposed to GS-process conditions. Test welds were made on corroded steel plates with and without surface preparation. Hydrogen-evolution measurements were made on steel samples exposed with the plates.

a. Procedure

Weld test bars were machined with a 37-1/2° bevel along the edges to be butt welded. New hot-rolled 1/2-inch plate was used for some specimens and 5/8-inch steel plate weights exposed for 7000 hr in the 45-inch diameter autoclave were used for others. Backup strips were made from 1/2-inch plate for all welds. Some were clean and others were exposed with the weld plates. H_2S-H_2O exposures were made at 40°C and 250 psi for two weeks. Plates were removed from test, dried, and quickly ground and preheated as desired before welding. Machine welding was done to reproduce conditions as closely as possible on successive welds.

Welding Conditions Used for Test Welds:

1. 1/8-inch dried electrodes - ASTM-A233-48T - E6010 - Hobart No. 10
2. 120 amp, direct current, reverse polarity, burn-off rate 7.5 inch/min
3. Stick feeder - GE Automatic Arc Welding Head Type WFS
4. Arc voltage - 8 v
5. Plate traverse speed - 6 inches/min
6. Weld 2-1/2 inches long on a 4-1/2-inch sample

Plate treatments were varied to check the effects of different cleaning procedures, preheating, and different intervals between H_2S exposure and welding. One set of butt welds was made on clean 1/2-inch plate sections. These were control samples that had not been exposed to H_2S. Data on these and other test welds and results of the bend tests are given in Table XII.

One set of samples was ground and welded promptly after removal from the H_2S. These showed poor results in the bend test. A second set was preheated before welding. Longitudinal bend tests made with the guided-bend-test jig showed a consistent decrease in quality from the control to the preheated test to the nonpreheated one. These two tests were made using backup plates that had also been exposed.

Backup plates for the 5/8-inch plate were not exposed to H_2S before the test. This condition resulted in the production of better welds in the second series. Bend tests indicated that these welds were all of good quality as seen in Table XII.

Bead-on-plate weld tests showed very strikingly the need for thorough cleaning by grinding. Scale on the uncleaned plate tended to form a lumpy slag with the weld rod coating. This left the weld deposit bare, with gross porosity and cracking. Wire-brushing was of only slight value because enough of the sulfide scale remained to spoil the weld.

b. Repair Welds at Dana

These welds were made as plant tests to help determine the minimum precautions needed for repair welds. Tensile and bend tests were made on welded 6-inch pipe samples from the Dana Plant. These were prepared and tested as indicated in the ASME Boiler and Pressure Vessel Code, Section 9, Welder Qualification Test using 6-inch pipe with 3/8-inch wall. Results of the tests are listed in Table XIII. These results were in general agreement with the tests at the Engineering Research Laboratory. Ultimate strengths of even the poorest of these welds were quite high. A comparison of samples C, D, and E indicates that grinding and preheating contributed

to improvement of the elongation and bend properties. There were, however, numerous "fisheyes" on the broken welds, indicating that the preheating had removed only part of the hydrogen. This confirmed the importance of a 30-minute preheat.

c. Hydrogen-Evolution Studies

At the same time that the welding experiments were conducted, other samples of the same steels exposed in the same vessel were checked for hydrogen evolution. These were exposed to cold-process conditions for two weeks, removed, and then allowed to outgas at room temperature. The gas was collected over mercury.

Two samples removed from the H_2S atmosphere and quickly placed in collecting cells evolved 9.3 and 10.7 cc/100 gm of steel, respectively. A third sample was heated to 1200°F for 5 minutes and water-quenched after removal from the H_2S-H_2O atmosphere. This sample yielded 2.8 cc of gas/100 gm of steel, indicating that a reduction of about 75% of the hydrogen present might be expected by torch preheating. Since this treatment would leave sufficient hydrogen to cause measurable embrittlement of most steels as reported by others[27], a longer preheating time would be desirable. Therefore, a 30-minute preheat at 1200°F and a 30-minute stress relief at 1200°F were recommended for repair welding.

d. Summary

1. Results of these tests indicated that acceptable repair welds could be made of steel equipment that had been exposed to GS-process conditions.

2. All sulfide scale must be removed from the edges to be welded. This requires careful grinding.

3. A preheat is needed to remove hydrogen from the corroded steel.

4. Preheating to 1200°F for 5 minutes removed most but not all of the hydrogen in a test sample. Therefore, 30-minute heating time would be preferable.

5. Welds should be made with standard welding procedures. The joint may cool to room temperature after welding without adverse effects.

6. Postheating to 1200°F for stress relief is recommended. Allow at least 5 minutes at temperature, and 30 minutes if possible.

7. Behavior of O-Ring Materials

O-ring compounds, particularly those intended for moving seals must be practically unaffected by (a) the gas or liquid retained by the seal, and (b) the outside atmosphere at the temperature of the seal. Since it is difficult to predetermine the service conditions for an O-ring seal, laboratory tests must be regarded only as guides. An attempt to bracket the total range of possible conditions might correspondingly require an excessive number of tests.

Several types of tests were run in evaluating the different compounds for possible GS service. All of the small pressure vessels made for corrosion and stress-corrosion tests were sealed with O-rings. All of the "Buna-N" and neoprene-based compounds were found to be satisfactory for 100 to 500 hr at temperatures in the range of 25 to 40°C. Rings used at 100 to 120°C showed evidence of embrittlement. This apparent embrittlement occurred within the first few hours of exposure and appeared to be due to oxidation. These O-rings still retained enough resilience to seal the test vessels until each test was complete frequently for periods measured in weeks. O-rings were used for only one exposure at these temperatures. Since 100°C is above the normal operating temperature for neoprene and "Buna" rubber compounds, the gradual hardening at these temperatures may have been due to over-vulcanization, rather than degradation from H_2S exposure. Tests of "Teflon" tetrafluoroethylene fiber and "Kel-F" indicated that these materials were not visibly affected by exposure to H_2S-H_2O at 120°C. Since these materials are expensive and not sufficiently resilient for use on moving seals, only a few "Kel-F rings" were tested. "Teflon" tetrafluorethylene fiber O-rings became available after most of the tests were complete, and were not included in these tests.

For the initial tests, samples of various O-ring materials were exposed to H_2S-H_2O at 120°C. Details of these results are listed in a previous report. "Buna" and neoprene rubber compounds were hardened and the silicones crumbled during one exposure period of 24 hr.

Another series of tests was made at 40, 80, 100, and 120°C. Short O-ring sections 3/16-inch nominal diameter were clamped between stainless steel bars. The restrained portion of each ring was compressed 0.030 inch, and the remainder left unrestrained to check for swelling. These specimens were examined at one week intervals to check for swelling, permanent set, and changes in Durometer hardness.

Results are listed in Table XIV. After two periods at 120°C all of the elastomers were seriously degraded. The silicone material appeared to be only slightly affected after 1500 hours at 100°C and virtually unaffected at 40°C. It was the best of the eight materials included in the tests. Linear

KCC-70, an O-ring of neoprene-W, showed good resilience and a minimum of permanent set at all temperatures. However, the free end showed swelling at temperatures of 80°C and above. At 40°C both of the "Buna-N" O-rings tested showed appreciable permanent set indicating that they would be inferior to the neoprene compounds for moving seals at this temperature.

8. Plug Cock Lubricants

A series of tests was run on 9 lubricants to determine the ones most suitable for use in Merco-Nordstrom plug cocks in H_2S service. These plug cocks are designed with a hardened ball bearing through which the thrust load is applied to keep the plug tight in its seat. Grease is forced into the opening between the mating surfaces of the plug and seat. Thus, the grease serves to lubricate these steel surfaces of the plug cock and to isolate the ball from the fluid being controlled. For H_2S-H_2O service the grease must be protective to prevent stress-corrosion cracking of the ball.

A screening test was made to determine which of the greases were impermeable to H_2S. In order to be usable for H_2S service, it appeared that the grease would need to be sufficiently protective to prevent corrosion of a ball bearing imbedded in it. A small steel ball bearing of polished AISI-52100 steel was placed in the bottom of a test tube and covered with the sample grease. By heating to 200°F and centrifuging, each grease was packed firmly around a ball bearing with approximately 1 inch of grease in each tube. Samples were then exposed at hot-tower (HT) and cold-tower (CT) conditions for two 1-week periods. Results as shown in Table XV indicate that all but the "Halocarbon" stopcock grease showed color changes, indicating some degradation after exposure to H_2S-H_2O at 40°C. All of the greases seemed to have been degraded by exposure at 120°C. While corrosion of the ball bearings occurred in most cases, there were a few of the greases that appeared to prevent corrosion of the polished steel ball bearings during the exposures.

Additional tests to simulate service conditions were made on the 5 greases that gave good protection to the ball bearings. Three check tests were run, one with no grease and two with greases that gave poor protection for H_2S corrosion.

A unit for exposing balls under compressive loading, similar to that sketched in Figure 18, was made from a high-pressure fitting. The space around the two 3/4-inch diameter ball bearings was filled with the grease to be tested. By means of a torque wrench, a compressive load of 8000 lb was applied. This load was sufficient to cause a slight flattening of each ball in the area of contact. Average compressive stresses at the area of contact were estimated to

be 290,000 psi based on the area of the "flat" between balls. Calculation of the maximum surface tensile stresses adjacent to the area of contact indicated that they were approximately the same. This was of the order of the yield point for the hardened AISI-52100 ball bearing steel and in any case high enough to cause rapid ball failure if the grease in test were not protective. This loading was believed to be of the same magnitude as that on a thrust ball in a Merco-Nordstrom hyperseal plug cock. After the first check test with no grease present, one ball was shattered into four pieces, although apparent corrosion was very slight. The polished ball surfaces were only lightly stained.

The results of the tests are listed in Table XVI. From the standpoint of H_2S corrosion there were four satisfactory greases. These were impermeable to H_2S-H_2O and were not hardened by the H_2S-H_2O exposure. Service tests run at the Dana Plant at the same time as these tests indicated that Dow Corning No. 11 grease gave most satisfactory service.

Comparison tests of "Stellite" and tungsten carbide balls indicated that these are not likely to fail by sulfide stress cracking. Thus, tungsten carbide balls should be recommended for critical service. These are cheaper and more readily available than "Stellite."

9. Iron Sulfide Precipitation

a. Deposits Found in GS Units

After the GS plant had been in operation for several months, liquid flow through the strippers was found to be impeded. Bubble caps and trays were found to be covered by a mossy deposit consisting of numerous tiny slender crystals which bridged the slots of the caps and almost stopped the flow. Samples submitted to the Engineering Research Laboratory were shown by X-ray diffraction to be marcasite with small amounts of pyrite. By cutting out alternate ligaments on the caps, the slot width was approximately tripled. Although it did not correct the difficulty, this change in the bubble caps extended the time between stripper shutdowns to about one year.

Another type of deposit was observed in the liquor-heater (LH) heat exchangers. It consisted of dense brown crystals that tended to be hexagonal in shape. Other deposits in the system were finer grained and resembled pyrite in color.

It was observed that these deposits occurred in the equipment at points where the H_2S-saturated water was being heated, thus, exhibiting an apparent inverse solubility effect. X-ray analyses were made of a number of deposits. Since conditions in the process change during service, it was not

possible to determine the precise thermal history for all parts of each heat exchanger. This information would be needed to accurately determine the temperature at which each of the various sulfides was deposited.

From reviewing the results in Table XVII, it was observed that pyrrhotite started depositing at approximately 85°C. Pyrite was first observed at about 120°C and marcasite at 150 to 210°C. Since most of the deposits were mixtures, it was not possible to determine whether part of the pyrite or marcasite in a mixed deposit might have been deposited as pyrrhotite and converted to the higher sulfides after deposition. No appreciable pyrrhotite deposits have been found in the liquor heater (LH) heat exchanger cold end where the temperatures are below 85°C. In some cases, such as Samples 27 and 28, the deposit was found beyond the heat exchanger, indicating either that the deposition process possessed a high degree of hysteresis, or that some of the particles were dislodged by the flowing liquid and swept downstream to collect in the outlet piping. In the strippers and the hot ends of the stripper heat exchangers (SX), marcasite was usually the principal deposit with incidental amounts of other sulfides. Troilite and hydrotroilite were found in samples from several low-temperature locations.

b. Mechanism of Deposition

An intensive study of FeS solubility was undertaken by the Technical Section at the Dana Plant. Results of a theoretical study indicated that the amount of iron in solution under process conditions was controlled by pH and H_2S concentration. As the temperature of the process stream was raised in the heat exchangers the H_2S and the FeS solubilities decreased.

Acid additions might be used to lower the pH of the feed water. Although this would increase the total iron in solution there would be less change in solubility with temperature. This, in turn, would reduce the amounts deposited. However, lower pH would tend to increase the equipment corrosion rate in the system.

Caustic additions to increase the pH would reduce the total iron in solution and also reduce the differential solubility across the GS process. There would, thus, be less iron sulfide to precipitate out. By using NaHS as the caustic addition, a portion of the normal gas make-up requirement would be met.

Samples of process streams for analysis had to be carefully taken in order to avoid errors due to precipitation, flushing of sample lines, etc. Iron content of the stream at cold-tower conditions was 3 to 7 ppm and at hot-tower conditions 0.5 to 1 ppm. After sampling and analytical

procedures had been worked out, several series of 18 to 24 consecutive samples at the same point showed good reproducibility.

After caustic injection was started to adjust the feed-water pH, the total iron content of the process streams was reduced. Since the maximum iron content of the streams was below 1 ppm there was much less iron sulfide to deposit. Subsequent plant experience confirmed the validity of the theoretical study.

c. Laboratory Deposition Tests

In order to confirm the solubility calculations made by the Technical Section at the Dana Plant a sulfide deposition unit was assembled at the Engineering Research Laboratory. A sketch of the arrangement is shown in Figure 8. This unit was arranged to circulate the water by acting as a thermal syphon. Cold water saturated with H_2S entered the lower heat exchanger through line C. An orifice plate with a 1/2-inch diameter hole near the bottom was located at the cold end of this exchanger. On the hot end the orifice plate had a hole near the top so that any H_2S gas coming out of solution as the temperature was raised could pass on up to the surge tank without causing a vapor lock.

As the heated water passed through the upper exchanger it was cooled. It then flowed to the surge tank, which was filled with steel rings. The lower part of the surge tank was cooled by passing cold water through the jacketed portion.

It was intended that the H_2S-saturated water in the surge tank would pick up some iron from the steel rings and approach equilibrium at about 40°C. As this liquid was heated by the steam on the shell side of the heat exchanger, some of this iron would come out of solution to be precipitated as pyrrhotite.

After the 300-hr run a number of small hexagonal crystals were found on the orifice plate at the hot end of the lower exchanger. These were brown and magnetic. X-ray diffraction patterns confirmed the indications that they were pyrrhotite.

This test was repeated using water to which 200 ppm of NaOH had been added. Under these conditions no pyrrhotite deposit was observed. Water from the Dana Plant was used for both of these tests.

Small tube-like deposits of iron sulfides were observed on steel surfaces in a laboratory autoclave after tests at 150°C. The diameters of these tubes were about the same as those of the condensate droplets. X-ray diffraction analyses indicated that these were marcasite deposits. These

deposits contained a number of steps or growth rings, indicating a cyclic growth process. A check of the temperature control indicated that the temperature varied from 145 to 155°C. These temperature cycles required about one hour. By changing the thermocouple placement the temperature variation was reduced to ± 1°C. Thereafter no more marcasite deposits were observed.

From the above the following are evident:

1) Laboratory tests confirmed the mechanism of iron sulfide deposition from H_2S-H_2O solutions as they were heated.
2) Caustic additions of 200 ppm NaOH virtually eliminated this deposition.
3) Pyrrhotite was deposited in the temperature range of 40 to 110°C.
4) Marcasite was deposited when the temperature fluctuated between 145 and 155°C.

d. Investigation of Chemical Cleaning Procedures

A program was established to investigate the possibility of removing deposited sulfides from the heat exchangers by chemical cleaning. Such a technique could have been used to replace the mechanical cleaning operation then in use which was both costly and time consuming.

The liquor heater (LH) heat exchangers at the Dana Plant were designed with the process water stream passing through the tubes and stripped waste water passing through the shell. The heated stream and sulfide precipitation were therefore inside the tubes. The tubes were of Type 304 stainless steel. Tube sheets, heads, baffles, and shells were of plain carbon steel. Heat exchangers at the Savannah River Plant were similar in construction but were operated with the process stream passing through the shell and the stripped waste water through the tubes.

To be fully acceptable, a chemical cleaning technique had to meet the following requirements: (a) the solution had to be capable of removing deposits of marcasite, pyrite, pyrrhotite, and troilite, (b) the solution could not be excessively corrosive to either steel or stainless steel, (c) the cleaning had to take place below 211°C, the maximum steam temperature available at the plant, (d) the reaction pressure should not exceed 450 psi, the maximum pressure at which the heat exchangers had been tested, and (e) the operation should preferably be complete in one day, and certainly in four days.

Dowell, Inc., a chemical plant and oil refinery cleaning subsidiary of Dow Chemical Company was contracted to simultaneously investigate chemical cleaning. In general, no

satisfactory solution was found. They felt that a solution containing an oxidizing agent (i.e., chromic acid) to oxidize the sulfide to sulfate and a mineral acid to dissolve the sulfate would be required. None of the combinations tried gave sufficient scale removal.

The tests at the Engineering Research Laboratory also did not uncover any practical treatment. Nearly 200 tests were run without finding a solution which would rapidly attack the scale and not be highly corrosive to the heat-exchanger materials.

A survey of the literature was made to investigate means of taking into solution pyrite, pyrrhotite, etc. Reactions used in analytical chemistry involved solutions highly corrosive to heat-exchanger materials (e.g., Br-HNO_3-HCL) or temperatures excessively high (i.e., at red heat). The main commercial use of pyrite involves oxidation of FeS_2 that is partially or fully oxidized "roasted" in air to form SO_2 in specially constructed ovens at minimum temperatures of 700°F. Attempts to simulate this reaction at a lower temperature, even with oxygen, were unsuccessful. The Sulfide Ore Company of New York has patented a process[19] for obtaining high-purity iron from pyrrhotite (but not pyrite or marcasite) by reacting it with $FeCl_3$ to form $FeCl_2$ and sulphur and extracting the iron from the $FeCl_2$ by electrolytically forming Fe and $FeCl_3$, the latter of which is recirculated. It was not possible to use iron chloride, for fear of promoting stress corrosion cracking and pitting in the stainless steel tubes and other ferric salts were ineffective. The Sulfide Ore Process (which was duplicated, the reaction being complete in two hours) required finely divided pyrrhotite, an advantage not available here. The oxidation of pyrite by caustic solutions has been reported[29] by the University of British Columbia. Again, finely divided ore is required. A hydrometallurgical process for the production of pure metal from sulfides known as the Forward Process has been reported[9]. The metal sulfides are reacted with NH_3 to form soluble metal amines. The only iron sulfide susceptible to this, by test, was troilite (FeS).

A search of the files of the U.S. Patent Office in Washington, D. C. did not produce any significant leads to the solution of this problem.

All tests were made either on sulfides broken from heat exchangers or on 1-inch to 3-inch lengths of actually plugged tubes, (both from the Dana Plant) usually the latter. A cross section of a plugged tube is shown in Figure 19. The crosspiece is a Type 304 stainless steel turbulence promoter. While the plugging shown was typical, some tubes were completely closed.

The tests were run according to one of the four following procedures:

1) Constant-Temperature and Boiling-Flask Tests: Samples were exposed in solutions in 1-liter flasks at room temperature at 50°, 65°, and 80°C in constant temperature baths, and at the boiling point. Solutions were changed frequently where depletion of components present in small quantities was possible. Many of the tests were run with gas purges; for example, oxygen was used to promote oxidation of the sulfides to sulfates.

2) Gas-Phase Exposures: Samples were placed in a tube furnace, usually at 200° or 250°C and exposed to various gases which were passed through the tube over the samples, and then vented. Many of these treatments were followed by boiling the samples in sulfuric acid to obtain solution in case the gas phase reaction converted the sulfides to more soluble forms.

3) Autoclave Exposure Tests: Samples were exposed to candidate scale solvents in autoclaves at pressures from 50 to 450 psi and up to 250°C. Most of these samples were also exposed to boiling sulfuric acid after autoclave exposure.

4) Forced Circulation Tests: Samples of actually plugged tubes were placed in the exhaust tube of a submerged pump and hot test solutions forced through the tubes. Usually, the erosive action of the solvent increased its attack on the stainless steel tube or steel corrosion test coupon far more than on the scale.

Various cleaning solutions tested were selected on the basis that they would either (a) oxidize the sulfides to sulfates or to oxides which would then be soluble in dilute mineral acids, (b) reduce the sulfides by forming H_2S and free iron which would be soluble, (c) chelate the ferric ion in the sulfides, or (d) dissolve the sulfides.

The results of the testing program fell into three categories which follow:

a) Treatments Too Severe for the Equipment:

1) Room temperature 65% HNO_3 readily attacks the scale and not stainless steel. However, the carbon steel in the heat exchangers and piping is strongly attacked.

2) Heat-transfer salt (eutectic mixture of 53% KNO_3, 40% $NaNO_2$, and 7% $NaNO_3$) when heated above its melting point of about 220°C will attack the scale. In some cases it eventually caused the sulfides to ignite and burn violently at red heat. Any diluents added raise the melting point of salt to above 250°C. Removal of the salt after reaction would be extremely difficult.

b) Borderline Treatments:

1) Oxygen bubbled through a 30% solution of NH_4OH and then passed over scale samples in a tube furnace at 250°C reacted with the scale so that it fell free from the tube when later boiled in 10% H_2SO_4. Reducing the tube furnace temperature to 200°C still allowed complete but slower scale removal. However, boiling 10% H_2SO_4, even when inhibited, attacked the stainless steel and carbon steel severely. Inhibition of H_2SO_4 is not effective above 80°C and at this temperature scale removal was not achieved. Lowering the gas phase reaction to 186°C did not permit removal of the scale, even in boiling acid.

2) Certain samples of scale removed from the tube sheet fell apart in boiling 10% sulfamic acid. Exposed scale samples from tubes and actual partially plugged sections of tubes were not affected by this treatment. The acid is extremely corrosive to steel.

3) A boiling 10% oxalic acid solution containing 1% $Fe(NO_3)_3$ was also effective in one test on tube sheet scale but not to scale from tubes or to actual tube samples.

4) An agitated 30% $FE(NO_3)_3$ solution heated to 90°C partially attacked the scale so that it fell free from the tube but a steel corrosion coupon was nearly dissolved in this 20 hr test.

5) Pyrrhotite was dissolved by boiling samples in 10% K_2S + 1% NaOH followed by boiling 5% H_2SO_4. The corrosiveness of the H_2SO_4 to both steel and stainless steel was too great and the other sulfides were not attacked.

c) Treatments of No Promise: Over 150 tests were run with solutions which showed no promise as scale solvents. The solutions and the conditions of exposure are given in Table XVIII. An evaluation was made of the most promising solution reported by Dowell, Inc. This was 10% chromic acid, 3% nitric acid "properly" inhibited at 180°F. Thirteen separate experiments were run to verify this observation and the results were, in every case, negative. The most severe exposure was run for 30 hr at 180°F, with the acid solution being continuously pumped through a partially plugged tube. The acid was changed every three hours to avoid depletion of the nitric acid.

Consideration was given to the possibility of a mechanical cleaning action. Two significant but unfruitful tests are reported here:

1) Scale could not be broken from the tube by soaking in water containing a wetting agent and then freezing by plunging in liquid nitrogen.

2) An effort was made to break up scale by soaking first in a $NaHCO_3$ solution and then in a H_2SO_4 solution to cause gas evolution but with no success.

e. Iron Sulfide Solubility Tests

A series of solubility tests was made to check the amounts of iron in solution in the H_2S-H_2O system. For these tests a small autoclave was prepared in which two pairs of filtration bottles, as shown in Figure 9, could be inserted.

To make a run, approximately 110 ml of water and 1 to 2 gm of steel or sulfide were placed in the filter bottle. The autoclave was then assembled and pressurized with nitrogen to flush out oxygen and then pressurized with H_2S. After the desired time at temperature, it was assumed that the iron content of the solution had reached equilibrium. The pot was then tilted so that the solution passed through the pencil filter into the receiving bottle without otherwise changing exposure conditions. These bottles were covered with "Teflon" tetrafluoroethylene fiber sheet to keep scale from dropping into the filtered solution.

Filtered solutions were boiled to remove H_2S and submitted for analysis. Results of these analyses were in the same range as those made at the plant and showed some wide variations for duplicate runs, Table XIX. Several of the factors that might have caused these variations were studied. Because iron sulfides are so nearly insoluble, it was considered likely that only a few of these samples reached equilibrium. Small variations in conditions may have caused these differences. These tests were discontinued before the reproducibility problem was worked out.

Results of tests with altered feed water are shown in Table XX. These indicate that acid additions might markedly increase the iron in solution at low temperatures. Such solutions showed even wider differences between low and high temperature than had been observed for feed water with a pH of 6 to 8. Caustic additions seemed to cause considerable reductions in the iron in solution at low temperatures. Raising the temperature had little effect upon solubility.

Most of the solutions showed low pH values after test. Analysis of the solutions indicated that this was due to sulphate ion in the solutions. Appreciable sulfate ion was found in each of the samples analyzed-ranging from 0.76% for crushed natural pyrrhotite to 3.11% for the pyrrhotite deposit from LH301A. Although these amounts of sulfate are damaging in solubility tests, the oxidation process is too slow to help in scale removal. No sulfate interference would be anticipated in plant service.

As a precaution all 50-lb H_2S cylinders used in the laboratory were analyzed for H_2S, CO_2, O_2, Cl^-, and inerts. Most of the cylinders were found to have 99.0 to 99.8% H_2S, with 0.2 to 1.0% of inert gases. Chlorides have usually been below 0.01%. Only one cylinder was discarded because 0.3% (CO_2 plus O_2) were found.

As a further check on the low pH values obtained in the solubility tests, sulfates and chloride analyses were made on several water solutions prepared by leaching sulfide specimens. Results were as follows:

Sulfide in Contact with Water at 40°C and 250 psi H_2S	pH of water after test	SO_4^{--} (extracted from 1 gm. sulfide by 100 ml H_2O), ppm	SO_4^{--} in dry sulfide	Cl^- ppm
C.P. Troilite	3.5	47	-	0.7
Natural Pyrite	2.8	86	-	1.0
Natural Pyrrhotite	2.5	162	0.76%	-
Scale in 45 inch pot	3.3	217	1.12%	-
Pyrrhotite from LH301A	-	-	3.11%	-

Although the chloride analyses are too low to account for the low pH values, the sulfate concentrations are of the order that would be expected for these pH values if all the sulfate ion were present as sulfuric acid.

Although reduced pressure was the only change made in the conditions, all the solutions tested at 1 atm H_2S returned to approximately the original pH, as shown in Table XXI. While the data show considerable scatter, no consistent differences were observed between low- and high-temperature tests.

This work indicated the following:

1) Results of the laboratory solubility tests re-emphasized the difficulties involved in precisely duplicating plant conditions.
2) It appeared that equilibrium was not always obtained at the low iron concentrations involved (0.2 to 10 ppm).
3) Changes in the various sulfide minerals during air exposure were other factors that affected the tests.

f. Corrosion Tests in Sodium Hydrosulfide Solutions

Since substantial amounts of sodium hydrosulfide are used to generate the H_2S for make-up, it is a natural material for making caustic additions. It appeared that the amount of sodium hydrosulfide required to adjust the feed water pH would be

a large fraction of that needed for make-up gas. Although steel was expected to have adequate corrosion resistance, the effect of small hydrosulfide concentrations on bronze pump parts was not known.

A stock solution of 7% NaHS was made by bubbling hydrogen sulfide into a 5% solution of C.P. sodium hydroxide. Tests were made at NaHS concentrations from 0 to 500 ppm using Dana Plant water which had been vacuum deaerated. Some tests were also run in aerated solutions with 360 ppm of NaOH added. Results are listed in Table XXII. They indicate that steel and 90-10 bronze samples are but little affected by NaHS at concentrations that might be used to minimize sulfide deposition at the Dana Plant. Corrosion of the samples used for these tests appeared to proceed by the formation of thin black sulfide films. However, these films built up very slowly, with consequent low corrosion rates. Horseshoe-bend specimens of A212 steel were included in each test, but none of these showed any cracks. Aeration of the solutions seemed to have no effect upon corrosion rates. Corrosion rates in the sodium hydroxide were only a little lower than for the hydrosulfide.

Erosion-corrosion tests were made on samples placed 6 inches below a jet with a liquid velocity of 40 ft/sec. Check samples were placed so that the flowing liquid would cover the specimens without direct impingement. Results listed in Table XXIII indicate that corrosion was not accelerated by the erosion.

g. Determination of Process pH by Colorimetric Means

There has been no direct means of checking the pH of GS-process liquids under normal operating conditions. Standard pH electrodes are not designed to operate at these pressures. Laboratory tests were planned using colorimetric techniques for determination of process pH. By matching the color of a solution in an external beaker with an indicator solution under process conditions, the pH of the solution under H_2S pressure might be approximated.

Indicators reported to show color changes in the pH range of 3 to 5 were used for these tests. A small autoclave make of Type 316 stainless steel with 1-3/4-inch diameter sight glasses on opposite sides was used. Stainless steel piping was arranged as shown in Figure IO. The trap was required to separate any iron sulfides that might be present in the plain carbon steel piping. Even small amounts of these sulfides might cloud up the test solutions and obscure color changes. The steam coil supplied heat to the clear oil in the bath so that the test temperature could be raised. A reference cell was made from a square bottle, duplicate sight glasses, and a stainless steel pipe. This cell had essentially the same optical characteristics as the test vessel.

Tests were made by adding indicator solutions to a liter of deionized distilled water to develop the characteristic color. Part of the solution was placed in the autoclave and another portion added to the reference cell. Hydrogen sulfide was added to the test cell through the bottom to promote rapid solution and to agitate the sample. After the H_2S pressure reached 250 psi the colors in the two cells were compared. In order to match colors, dilute sulfuric acid or dilute sodium hydroxide was added dropwise to the reference cell. After a color match had been obtained, the pH of the reference solution was checked with a Beckman pH meter. The solutions in the test cells were then heated to determine if temperature increase affected the pH appreciably. Heating was discontinued when the colors could not be matched. Of the indicators tested, bromphenol blue, congo red, and alizarin red S were found to be satisfactory at 30 to 60°C. These three indicators show distinctive color changes in the pH range of 3 to 5. Results of tests at cold-tower (CT) conditions indicated process pH values of 3.9 to 4.1. Cycling the H_2S pressure from 50 to 250 psi had no appreciable effect on the pH. The colors did not change appreciably when the temperature was increased from 30 to 50°C. Both congo red and bromphenol blue indicated a peak of about 4.6 in the pH value of the H_2S-H_2O system at approximately 60°C. At 80°C the pH values returned to about 4 and the colors started to fade. Calculated pH values have indicated the pH under these conditions to be 3.6. Methyl orange and cresol red were degraded by the H_2S so that the colors could not be matched.

Two tests were made to check the buffering tendency of H_2S at cold-tower temperature and pressure. Using caustic with a pH of 11 as a starting solution, the pH under 250 psi H_2S at 30°C was 5.6. Under similar conditions using dilute sulfuric acid of approximately 0.001N at a pH of 3, a resultant pH of 3.5 was obtained.

h. Phosphate Deposits in GS Units

After sodium hydrosulfide additions were made a regular part of the GS process, analyses of plant process streams indicated an appreciable reduction in iron content. However, a different type of scale build-up was observed in the stripper and shell-side stripper heat exchanger (SX) units. The deposits were brittle and could not be readily dissolved.

Qualitative tests at the Dana Plant indicated that they were phosphate deposits. The Calgon (sodium hexameta phosphate) used in the water-treatment plant was considered to be the source of the phosphate.

Samples received at the Engineering Research Laboratory were analyzed spectrographically to determine the metallic elements present. Calcium, manganese, and magnesium lines were observed. Quantitative analyses for these elements

were made and the amounts of the phosphates that might include these metallic elements were calculated. Analyses of these scales were as follows:

	Sample V302	Sample SC-601-H
Ca	27.71% 27.78	24.38% 24.57
Mg	4.24 4.28	6.44 6.24
Mn	1.96	1.55

	Calculated Compositions	
Hydroxyapatite $Ca_5(OH)(PO_4)_3$ as indicated by per cent Ca	70%	62%
Magnesium Orthophosphate $Mg_3(PO_4)_2 \cdot 4H_2O$ from % Mg	20	30
Manganous Orthophosphate $Mn_3(PO_4)_2 \cdot 3H_2O$ from % Mn	5	4

This material balance accounted for almost all of each deposit. It was assumed that sulfide scale might make up the remainder.

X-ray diffraction patterns indicated that these deposits were mostly hydroxyapatite, $Ca_5(OH)(PO_4)_3$, with minor amounts of marcasite. Lines from the manganese and magnesium compounds were not intense enough for positive identification.

Chemical analyses of Dana Plant water indicate that the average calcium content was about one part per million. The Dana Plant water sample used for tests at the Engineering Research Laboratory was found to contain only 0.02 ppm of manganese.

Preliminary tests indicated that the hydroxyapatite was quite insoluble in the mineral acids. No investigation was made to attempt to develop a cleaning procedure for this material.

10. High-Temperature Corrosion Tests

Since relatively high corrosion rates of stainless steel samples had been observed in the stripper (SX) heat exchangers in the Dana pilot plant, laboratory tests were initiated to study the factors involved. A unit was set up at the Engineering Research Laboratory to simulate these factors. Small 7-tube heat exchangers 2 ft long were equipped with plain carbon steel, Types 304, 316, and 329 stainless steel tubes. Steam at 300 psi gage supplied the heat so that

the maximum temperature in the exchangers was 200°C.

After a 2300-hr test, no pitting or appreciable corrosion was observed in the stainless steel tubes. Corrosion of the plain carbon steel was not excessive. Corrosion rates for the test coupons were as follows:

	Corrosion Rate, mils/yr
Plain Carbon Steel - A212	5
Type 304 stainless steel	0.5
Type 316 stainless steel	0.03
Type 329 stainless steel	0.02

These rates were much lower than those observed at the pilot plant, indicating that some factor in addition to the H_2S-H_2O at 200°C may have been responsible for the high corrosion rates.

As another check of the effect of temperature on H_2S corrosion a series of static high-temperature corrosion tests was run in laboratory autoclaves. Total pressure of H_2S-H_2O was adjusted for each run to maintain about the same concentration of H_2S in the solution, 0.5 moles/l. All runs were for 168 hr, which is a relatively short time.

Results of these tests are listed in Table XXIV. The austenitic stainless steels showed relatively low corrosion rates, with only a small amount of pitting, at 120°C. The corrosion rates did increase from about 0.1 mil/yr at 120°C to 5 mils/yr at 250°C. Type 329 stainless steel showed only a moderate increase in corrosion rate with temperature. Type 410 stainless steel showed appreciably higher corrosion rates at the higher temperatures. Since all of these tests were for short, single runs, the rates were all higher than would be expected for long-time tests. The corrosion rates for A212 steel showed only a moderate increase at the higher temperatures.

11. Erosion-Corrosion Testing

After it had been established that plain carbon steel such as ASTM A212 had satisfactory corrosion resistance for exposure to H_2S-H_2O under GS-process conditions, the effect of the combination of erosion and corrosion was considered. Although all chemical process systems are designed for relatively low liquid velocities, there are certain vulnerable areas. Usually the tips of pump impellers have quite high velocities and there may be areas characterized by high Reynold's numbers denoting severe turbulence or impingement. Conditions of this type are particularly important in systems such as the present one in which the scale on metal surfaces is the controlling factor in corrosion resistance.

In order to check the effects of liquid flow at different velocities on corrosion rates a section of the 1/2-inch Schedule 80 pipe used for the circulating system on the 45-inch autoclave was reamed to 0.516-inch diameter. As a safety precaution, a section of 1-inch pipe was welded over the test portion of pipe. A valve and gage were fitted to this pipe to check hydrogen build-up. The accumulation of hydrogen in the void was expected to be indicative of corrosion of the inner steel pipe.

By inserting a long, stepped probe into the 1/2-inch line the resulting annular spaces contained reduced cross-sectional areas, thus causing increases in velocity of liquid flowing through the line. Parts of one such plug are shown in Figure 20. These were threaded together and inserted into the line through a tee.

Three additional erosion-corrosion test units were set up as shown in Figure 6. They consisted of a pump, test section, surge tank, flow meter, and auxiliary equipment. Tests were run with and without inhibitors at velocities from 10 ft/sec to 60 ft/sec.

It was assumed that the flow in the system would be reduced because of pump wear. All of the pumps had been used for H_2S service in the Girdler tests at Louisville or at the Dana pilot plant. A flow rate about one-third of normal was assumed and the test probes sized to give velocities of 60, 40, and 20 ft/sec.

Erosion-corrosion attack tended to occur in certain preferred areas at rather high rates. Usually one side of the largest diameter section of the probe was eroded. Several parts of the test piping at which there were abrupt changes in diameter, also failed by erosion. Maximum penetration rates of from 500 to 3000 mils/yr were observed at liquid flow rates of from 35 to 60 ft/sec. At the smaller portions of the test probes with lower velocities, corrosion was only slightly accelerated (about 50 mils/yr).

These high erosion-corrosion rates were of the same order as the rates observed for static corrosion of one hour or less. It was considered likely that erosion caused the removal of the sulfide scale so that it could not build up to a hard, protective layer.

Inhibitor tests showed "Duomeen T" at 500 ppm to be quite effective in reducing the corrosion rate. Three tests showed rates of 3.5 mils/yr for 35-hr exposures.

Hydrogen-penetration measurements indicated that hydrogen build-up proceeded at a rapid, uniform rate in the double-walled section of the test pipe. This indicated that corrosion of the pipe interior was continuing. Stainless

steel was then used for the test section to minimize erosion-corrosion of the pipe wall. Hydrogen build-up decreased sharply; after 15,000 hr in service, the accumulation was only 15 psi of hydrogen. This contrasted with a rate of 1 psi/hr that had been observed with a plain carbon steel pipe. This observation indicates that stainless steel does have a positive, but low, permeability for hydrogen under this type of exposure.

A second type of test was an impingement test. This was made in the same equipment by placing a nozzle with a 0.2-inch diameter opening at the inlet into the surge tank. The circular test specimen, as shown in Figure 20, was centered under the nozzle. Although only short-time tests were run with this arrangement, erosion-corrosion was very sharply reduced by the addition of 500 ppm of "Duomeen T" inhibitor. The velocity of this jet was 40 ft/sec.

After plant start-up, impingement by condensate was found to cause considerable erosion-corrosion in GS-process equipment. Use of stainless steel liners was suggested. This recommendation was based on the excellent service that had been obtained with a Type 302 stainless steel impeller in an Aurora G-40 centrifugal pump. After a full year of service the rotor was still bright with a few scattered pits. Because Type 430 stainless steel sheet was much more readily available than Type 304 at that time, due to government restrictions on nickel, its use was considered for this purpose. Tests were made to determine whether Type 430 stainless steel might be as satisfactory as Types 302 or 304 stainless steel under erosive conditions. A Type 302 stainless steel impeller for an Aurora G-40 pump was modified by inserting two pie-shaped sections of Type 430 stainless steel. These were welded into place with Type 310 stainless steel electrodes and the impeller remachined to the correct contours. After a 330-hr run with cold H_2S-H_2O at 250 psi the inserts were seriously corroded as shown in Figure 21.

Another test was run in the 45-inch pot by placing stainless steel strips over certain areas that showed deep erosion damage as seen in Figure 22. In this test Type 304 stainless steel showed no damage but the Type 430 stainless steel was deeply pitted as shown in Figure 23. Thus, it appeared that Type 430 stainless steel would be unsatisfactory as an erosion-resistant material.

12. Correspondence Between Plant Experience and Laboratory Tests

Because the differences observed in corrosion rates for laboratory, pilot-plant, and GS-plant tests sometimes were erratic, the causes of the differences should be considered. In an H_2S-H_2O system with clean steel samples and no sulfides present at the start, corrosion test results show a normal

spread. Tests in scaled steel equipment, such as the 45-inch autoclave, show rather high corrosion rates on new steel samples. Two conditions are present that tend to accelerate the corrosion: (a) the iron sulfide surface is cathodic to the steel, thus accelerating corrosion of clean steel in contact with the corroded steel or sulfide scale; (b) during inspection of the unit between runs the iron sulfide scale tends to oxidize slightly to the sulfate which is acid in its reaction. It was not possible to eliminate this acidity even by repeated rinses with hot water under a nitrogen atmosphere.

From the evidence at hand it appears that during exposure to air the various sulfides are partially oxidized to both ferric sulfate and ferric oxide. Appreciable rust is observed on the scale. When H_2S is again added, some of these oxides react with it to form more sulfate ions. Thus, the addition of H_2S has the effect of increasing the acidity of the water in a manner that is not reversible. Since the same water is recycled in the laboratory equipment, this acidity tends to build up during the run. In the plant equipment shutdowns are less frequent and there is a continuous input of water low in sulfate content. Since the feed is continuous, the sulfate formed has a negligible effect on the acidity of the system. Thus, corrosion rates for steel in process equipment would tend to approach those for tests made in glass and to be lower than rates obtained in laboratory tests using corroded steel equipment.

Average rates for similar conditions, whether in plant or laboratory tests, would be expected to approximate a curve similar to that shown in Figure 11. However, the variables in scale formation and growth will cause rather large differences between individual test results.

13. Corrosion of Silver Solder

After more than a year of plant operation several of the 800-hp Elliott blower motors at the Dana Plant developed excessive vibration. In order to correct the vibration, rebuilding of the defective motors was required.

Examination of these units indicated that breaks had occurred between the rotor bars (conductors) and the end (distribution) rings. These joints had been silver-soldered with Sil-Fos (Handy and Harman), containing 80% Cu, 15% Ag, and 5% P.

Metallographic examination of a Sil-Fos section from one of these joints indicated that there had been selective degradation of the silver solder matrix. Deep corrosion of the copper-rich primary dendrites had occurred as shown in Figure 24. This corrosion had occurred without appreciably affecting the ternary eutectic matrix of the solder. Thus, the solder examined was degraded to a depth of 3/8 inch,

although only a small amount of corrosion was evident at the surface of the Sil-Fos joints. Figure 25 shows a typical section at a depth of about 3/8 inch. X-ray diffraction patterns indicated that Cu, Ag, and Cu_2S were present in this sample.

On the basis of previous test results at hot-tower (HT) conditions, Easy-Flo 45 was recommended as superior to Sil-Fos for this application. Short-time tests indicated corrosion rates of 2 mils/yr for Easy-Flo and 100 mils/yr for Sil-Fos. All of the copper alloys tested that contained more than 70% copper had shown relatively high corrosion rates when exposed to H_2S.

In order to confirm these observations and to check the mechanism of the attack, an effort was made to reproduce the corrosion of the two silver solders. Initial tests at 40 and 80°C showed corrosion rates below 5 mils/yr for Sil-Fos and below 0.5 mil/yr for Easy-Flo 45. Since similar rates were observed at 1 and at 17 atm pressure, the corrosion rate did not appear to be significantly affected by the pressure in the system. Further tests were made at 120°C using 1 atm of H_2S plus 1 atm of air. This condition caused deep penetration of the Sil-Fos and was observed to be accelerated with time. Thus, some samples showed only moderate attack during the first period, but deep penetration was observed after additional exposure. Penetration of the Sil-Fos indicated that the corrosion rate was more than 500 mils/yr in the presence of air. A cross section of Sil-Fos in the as-cast form is shown in Figure 26. The sections through the primary dentrites appear as circles and irregular shapes. These areas are high in copper, with small percentages of silver and phosphorus.

Figure 27 shows a typical cross section of Easy-Flo 45. This alloy is of such constitution that it has no primary dendrites of copper that could corrode as did the Sil-Fos. The scale formed on the higher silver alloys was harder and more adherent than the soft black scale formed on the high-copper alloys.

Additional corrosion tests were made on a number of typical silver-solder alloys and on samples of the metallic elements used in most of them. Results are listed in Table XXV. All of these tests were run in glass so that the individual samples were isolated and no water was present except as vapor. Weight gains were determined and the proportional amounts of the various sulfides computed so that the average rates of attack could be calculated. Since there was no single cleaning procedure that could be used for all these alloys the use of the weight gains made cleaning unnecessary.

Copper and the high-copper alloys all showed high corrosion rates. The copper alloy with 7% silver showed the

highest rate. This alloy corroded slowly during the first two periods, and was completely consumed during a 500-hr exposure. These tests indicate that extremely rapid corrosion of the dendrites in Sil-Fos can occur with not more than 1 atm of H_2S present.

It follows that corrosion of the Sil-Fos joints increases their electrical resistance on a volume basis. At constant potential the temperature of the joint then rises with further acceleration of the attack. Since the blower motors run for long times at constant speed, the joints might remain intact although weakened. As these electric motors are stopped and restarted the current in the rotor bars goes much above the normal running amperage. Stresses incident to start-up might break one of the brazed joints in the motor. Such a break would alter the electrical and dynamic characteristics of the rotor and hence cause an abnormal vibration.

14. Miscellaneous Corrosion Tests

Results of the corrosion tests on a wide variety of metallic and nonmetallic materials are given in Tables XXVI to XXVIII. The tests indicate that plain carbon and alloy steels show moderate to high corrosion rates when exposed for relatively short times. In spite of its high alloy content 18% W, 4% Cr, 1% V, high-speed steel, corrodes at about the same rate as plain carbon steel. The austenitic stainless steel alloys are much more resistant; however, there is some pitting attack; hence average corrosion rates based on purely weight loss measurements, may be misleading. Type 316 stainless steel samples have shown less pitting than Type 304 stainless steel. Carpenter 20 stainless steel and "Stellite" show low corrosion rates. Chromium carbide, tantalum, and zirconium are virtually unaffected by exposure to H_2S.

Of the nonmetallics, "Orlon" acrylic fiber showed little change after a 160-hr exposure but had degraded after 1000-hr total exposure time. An epoxy resin coating on steel was badly blistered after a 2-day exposure at 40°C. Natural rubber and rubber-bonded asbestos (steam sheet) were both resilient after exposure to H_2S. The gasket for the 45-inch diameter autoclave was made from steam sheet. Such a typical gasket has operated for 25 runs without replacement. "Teflon" tetrafluoroethylene resin enamel on Type 316 stainless steel was checked as a "non-sticky" coating to minimize scale deposition. Exposure to H_2S caused no visible change in the "Teflon" coating. Although the coating was soft and hence was damaged at the corners, undercutting and consequent peeling did not occur.

15. Purity of H_2S Used at the Engineering Research Laboratory

Analyses were made of the H_2S in a series of the cylinders used to check for possible causes of the observed

variations in corrosion rates. Chloride contamination from the cylinders was suspected in view of the results recorded in Section 4. No correlation was observed between contaminants identified in the H_2S and the corrosion rates observed for plain carbon steel. Residual gases such as nitrogen were the principal impurities.

Nominal compositions were:

	Typical	Range Observed
H_2S	99.2%	(95.5 - 99.8%)
CO_2	<0.01%	(Nil - 1.7%)
O_2	<0.01%	(Nil - 0.16%)
Cl	<0.01%	Nil
Residual		(0.1 - 4.5%)

No chlorides were detected in any of the gas samples analyzed. These were all reported as less than 0.01% by wt. Only a few cylinders contained detectable amounts of CO_2 or oxygen.

A review of corrosion rates of test samples indicated that the H_2S with the highest CO_2 content, 1.7% was not appreciably more aggressive than gas from other cylinders Intentional additions of 20% CO_2 in one case and 20% O_2 in another did not accelerate corrosion of steel exposed to wet H_2S.

Impurities were determined by a modified Orsat procedure. Hydrogen sulfide plus other acid gases were determined by absorption in 40% KOH solution. Oxygen was absorbed by alkaline pyrogallol, The remaining gas was reported as residual. Carbon dioxide was determined by an infrared-absorption technique. Hydrogen chloride was determined by water scrubbing a known weight of H_2S. The water was then boiled to remove the H_2S and the chlorides determined by titration with silver nitrate. They were then reported as HCl in the H_2S. Results of these analyses are listed in Table XXIX.

E. SULFIDE CORROSION CRACKING

1. General Theory of Stress-Corrosion Cracking

Metals stressed in corrosive environments sometimes fail by cracking in relatively short times. This type of failure is known as stress-corrosion cracking and appears to be dependent upon the coexistence of stress and corrosive environments. The result is much more severe than would occur in the presence of either of these components alone. In most cases the corrosive environment is mild and does not attack the metal rapidly. It may be one that causes pitting, although the average corrosion rate is usually quite low. Stresses may be in the yield-point range although in instances they are

much lower. Tensile stresses, residual or applied, are almost invariably involved.

For most of the common metals and alloys there are specific environments in which a particular alloy or type of alloy is susceptible to stress-corrosion cracking. Brass and other copper alloys are thus affected by ammonia. Stainless steels are susceptible to stress corrosion cracking in hot chloride solutions, and plain carbon steels are so affected by hot caustic and strong ammonium nitrate solutions.

a. Theories of Stress-Corrosion Mechanisms

1) Electrochemical Theory: Dix and his associates found that at high constant stresses corrosion of aluminum is accelerated in certain media[6][21]. Two conditions were necessary for this acceleration of corrosion: (a) there must be a relatively high surface tensile stress, and (b) there must exist a susceptibility to corrosion that can progress at approximately 90° to the stress. The continuous corrosion paths may follow grain boundaries which are generally anodic to the rest of the grain. Selective precipitation at the boundaries may be a factor. Thus, a galvanic cell is set up consisting of a large cathode (the grain) and a small anode (the boundary), and the current flow from the anodic zones is accompanied by accelerated local corrosion. With the stress tending to distort the metal, the rate of corrosion is further accelerated as the attack progresses.

2) Film Theories of Stress Corrosion: It has been suggested by Chaston and Champion that the passive film covering a metal surface may be less protective at grain boundaries than over crystal faces[4][5]. Under the influence of tensile stresses, the film would tend to break at these weak points, allowing corrosion to proceed. As intergranular corrosion proceeds, notches are formed that cause local stress concentrations. If in the corrosive environment the film is self-healing, corrosion will stop and rapid crack propagation will be prevented. If corrosion continues in the presence of the hypothesized stresses, a sufficiently high stress concentration at the bottom of the crack will result in plastic deformation and rapid crack propagation.

3) Mechanical Theory of Stress Corrosion: Keating[18] has postulated that in stress-corrosion the function of the stress is purely mechanical, i.e., it tears open the metal under the surface crevice, thus propagating the crack. Corrosion by an electrochemical mechanism proceeds meanwhile. Cracking continues until the advancing crack reaches an obstacle such as an inclusion or an unfavorably oriented grain boundary. Lateral corrosion may then occur along anodic material at the sides of the crack.

This may help to explain the branching or "chevron" nature of some stress-corrosion cracks.

4) Strain-Accelerated Matrix Decomposition Theory: The above-mentioned electrochemical theories are based on the pre-existence of a pattern of anodic areas that render the material susceptible to stress-accelerated corrosion. These theories are not adequate to explain stress-corrosion of homogenous alloys such as alpha brass or stainless steel. Transgranular cracking of sensitized austenitic stainless alloys in acid chloride solutions would not be expected from the above theories. To help overcome these gaps in prior theory, Waber[35] has extended the "depleted zone" electrochemical theory. In his "Generalized Theory of Stress-Corrosion," it is suggested that one of the major functions of stress is to generate precipitation reactions, phase transformations, and order-disorder reactions which can produce the necessary localized anodic paths for corrosion.

2. Review of the Literature on Sulfide Corrosion Cracking

a. Introduction

Sulfide corrosion cracking is the term that has been used[10] to describe the spontaneous cracking of relatively high-strength ferrous materials under the combined influence of tensile stresses and corrosion resulting from exposure in aqueous hydrogen sulfide solutions.

In the past, failures due to sulfide corrosion cracking have been most commonly encountered in the handling of sour crudes in the petroleum industry. Field failures of such equipment as sucker rods, valve springs and plates, pump springs, bolting, wire filters, and tubing in hydrogen-sulfide-bearing environments have been reported[1][13][25][33]. Not all failures due to hydrogen sulfide environments have occurred within the petroleum industry, however. For example, the rupture of low-alloy steel cylinders charged with coal gas or hydrogen containing about 0.01% H_2S have been attributed to sulfide corrosion cracking[11][25].

b. Characteristics of Sulfide Corrosion Cracking

1) Time to Failure: The time required for sulfide corrosion cracking to occur in the field varies over a wide range. Such cracking has occurred after periods as short as three hours in the case of 12% Cr steel valve springs exposed to H_2S-saturated water at 40 to 100°F[1] or as little as six days in the case of 9% Ni tubing carrying well-gases containing 10% H_2S at pressures of 1350 to 3200 psig and temperatures of 96 to 100°F[33]. In the case of alloy steel gas

cylinders[11], the time to failure ranged from 24 hr after the initial filling to as long as five years of service.

2) Fracture Characteristics: The sulfide corrosion cracks found in failed steel gas cylinders[11] were generally of a branching nature and were filled with corrosion product. Cracks of a similar nature were observed in failed flapper valve plates of 12 to 14% Cr steel[25]. Fraser[10] noted that failure by sulfide corrosion cracking generally occurred via a single macroscopic crack, although there were usually microscopic cracks present. Gifkins and Rees[11] also observed that their failed test specimens all had cracks present in addition to those by which failure occurred. On many of his test specimens, Vollmer[33] found numerous fine cracks starting at the fracture surface and running parallel to the length of the specimen.

Sulfide corrosion cracking has been reported as being (a) largely intergranular[15], (b) almost completely transgranular[10], and (c) as being sometimes intergranular and sometimes transgranular[2]. Some tests by Vollmer[33] on specimens cut from a 9% nickel steel tube suggest that residual stresses can influence the type of cracking that occurs. He found that test specimens from areas of the tube containing residual fabrication stresses failed by transgranular cracking, while specimens which were stress-relief annealed failed by intergranular cracking.

3) Degree of Corrosion Accompanying Cracking: Many of the field failures resulting from sulfide corrosion cracking were accompanied by little or no general corrosion[11][25][33]. Fraser[10] concluded from laboratory tests that there was no general correlation between corrosion rate and the tendency toward sulfide corrosion cracking. However, his data indicated that there was a certain minimum amount of corrosion required before cracking occurred in H_2S environments. This is in line with his observation that corrosion pits on the surfaces of test specimens were the initiation points for microscopic cracks. Vollmer[33], however, noted little or no evidence of pitting in conjunction with many of the sulfide corrosion failures he observed.

c. Materials Susceptible to Sulfide Corrosion Cracking

Ferrous materials of a wide variety have been found to be susceptible to sulfide corrosion cracking. These are listed below:

A. Plain carbon steel[13][15]

B. Cold-drawn, high-carbon steel wire[25]

C. Medium-carbon steel bolting[1]

D. Ordinary tubing steels[10][33]
API J-55 (0.40% - 0.70% Mn)
API N-80 (0.40 C - 1.60% Mn - 0.20% Mo)

E. Low-alloy steels
AISI Type 4340[10]
2.25% Ni - 0.75% Cr - 0.65% Mo steel[11]
Mn - Mo steel[11]
Cr - Mo steel[15]

F. Higher-alloy steels
5, 7, 9, and 12% Cr steels[1][10]
9% Ni steel[33]
5% Ni - 1% Cr steel[33]
5% Ni - 0.25% Mo steel[33]
Types 322 and 410 stainless steel[10][33]

Among those materials which have been found to be resistant to sulfide corrosion cracking are the following: nonferrous metals and alloys: "Monel"[3][10], "K-Monel"[3][10], "Inconel"[3], "Stellite" No. 1 and No. 6[10], nickel[25], and brass[25]. While apparently resistant in the annealed condition[10], austenitic stainless steel (18% Cr - 8% Ni) is susceptible to failure by sulfide cracking in the cold-drawn condition[25].

d. Effect of Environment on Sulfide Corrosion Cracking

1) Service Environments: Field failures due to sulfide corrosion cracking have occurred in gaseous H_2S environments varying in H_2S concentration from 0.1%[11] to 18%[15]. Herzog[14] has stated that if the H_2S concentration in oil-well atmospheres exceeds 10%, rapid failure of susceptible materials can occur. This statement is borne out by the reported failures in the petroleum industry of relief valve springs in 8 to 10% H_2S[13] and of oil-well tubing in 19% H_2S[33]. Sulfide corrosion failures have also been observed in aqueous environments such as water saturated with H_2S[1].

2) Laboratory Environments: Laboratory experiments have produced sulfide corrosion cracking in both

aqueous and gaseous H_2S environments. Among the aqueous environments were distilled water through which H_2S was bubbled[10] and tap water saturated with H_2S and CO_2 room temperature and atmospheric pressure[33]. Fraser and Treseder[10] found that water from a sour-gas condensate well and field gas from the same type of well gave results similar to tap water and commercial H_2S. The same investigators showed that H_2S and H_2O were both required before cracking of the type observed in the field could occur. No cracking occurred in aqueous carbon dioxide solutions or in solutions of H_2S in kerosene. It was also shown[10] that while additions of O_2 and CO_2 to H_2S-H_2O systems had little effect on the cracking tendencies, increasing the acidity of the system increased the severity of the cracking.

For gaseous laboratory tests, most investigators[2][11][25] used H_2S concentrations of 50 or 100 per cent. There was disagreement among investigators as to whether the water in system had to be present as a liquid or not. Fraser and Treseder[10] concluded that the presence of liquid water was essential to sulfide corrosion cracking, because a 9% Ni steel exposed to water-saturated H_2S failed to crack. The early experiments of Gifkins and Rees[11] led them to a similar conclusion, but later modification of their equipment showed that incomplete saturation of the H_2S atmosphere with water vapor was responsible for their failure to obtain cracking. However, they did find that the presence of a wet wick on the tension side of the test specimen accelerated failure. The same investigators showed that when a 50% H_2S atmosphere was not saturated at room temperature, i.e., when the water vapor content was less than 0.5% (dew point of 0°C) no cracking occurred. This was true even though sufficient corrosion had occurred to produce a slight blackening of the specimens. They concluded that visible deposition of water on the test specimens was not necessary as long as the H_2S atmosphere was saturated with water vapor. This conclusion is supported by Herzog[15] who obtained sulfide corrosion cracking in a "moist H_2S atmosphere" and Rees[25] who obtained cracking in a 50% H_2S atmosphere saturated with moisture but not in a 50% H_2S atmosphere dried with $CaCl_2$.

3) Effect of Temperature: Service failures by sulfide corrosion cracking have occurred at temperatures varying from 20 to 80°C. Laboratory failures have also been recorded over a similar range of temperatures[3][10][33]. Fraser and Treseder[10] found that, in general, the severity

of sulfide corrosion cracking increased with decreasing temperature. For example, a 5% Ni steel which failed at 0°C in an H_2S-H_2O system did not fail at 20 to 25°C, all other conditions of the exposure being the same.

4) Effect of Pressure: Results reported in the literature[3][10][33] indicate that pressure has very little effect on sulfide corrosion cracking. According to Vollmer[33], cracking occurred at a pressure of 5000 psi in a fashion similar to that at atmospheric pressure.

e. Factors Controlling Sulfide Corrosion Cracking

1) Applied Stress and Type of Loading: Fraser and Treseder[10] have shown that the probability of failure by sulfide corrosion cracking is related to the magnitude of the applied stress. They found that the percentage of specimens of 9% Ni steel that failed in an H_2S-H_2O system increased with increasing applied stress; e.g., while none out of four specimens failed at 48,000 psi, 21 out of 21 failed at 121,000 psi. Bowers, McGuire, and Wiehe[3] applied the concept of a critical stress level to sulfide corrosion cracking; that is, a critical or threshold stress below which failure of susceptible steels will not occur. They emphasized that the values for critical stress are only relative and that they will vary with the steel being tested, the degree of plastic prestrain, and the specific H_2S environment. To these three factors can also be added the hardness and microstructure of the steel being evaluated. The influence of all these factors on the critical or minimum stress level required for sulfide corrosion cracking will be discussed in the sections to follow.

The relationship between applied stress and the time for either cracking to be observed or for failure to occur in an H_2S environment was studied by Gifkins and Rees[11]. Their data showed a poor correlation between applied stress and the time required for actual fracture. However, the same data showed that the time necessary for the formation of cracks, as determined by a magnetic crack detector, clearly increased with a decrease in the applied stress.

Not only the magnitude of the applied stress is important in determining the probability of sulfide corrosion cracking, but also the presence of stress raisers and the method used in applying the stress. It has been shown[10] that small holes drilled in test specimens at the point of maximum stress have increased the effective applied stress and thereby increased the chances of failure due to sulfide cracking. It has also been demonstrated[10] that constant-

load testing is a more severe criterion for susceptibility to sulfide corrosion cracking than constant-deformation testing. It was found that failure occurred at much lower stress levels when specimens were stressed by means of a constant applied load than when they were stressed by means of constant deflection.

2) Effect of Hardness: Sulfide corrosion cracking failures have been reported in the field at hardnesses varying from R_c 24 for 9% Ni steel tubing[33] to R_c 41-45 for 12 to 14% Cr steel valve plates[25]. Bolting failures[1] have occurred at a hardness of R_c 32 or less, while alloy steel gas cylinders[11] have failed at a hardness level of R_c 32-38. Some investigators[3] learned from laboratory tests that the hardness level of a steel was not a precise criterion of the susceptibility to sulfide corrosion cracking. They found, for example, that most low-alloy steels were susceptible to failure at hardnesses of R_c 25-30 when subjected to high applied stresses and severe prestrain. However, the higher alloy steels, such as the 9% Ni and 5% Ni - 1% Cr steels, were found to undergo failure at low hardnesses, R_c 20-23, under the same conditions of testing. The difference in the critical hardness levels for cracking of the low- and the high-alloy steels was attributed to microstructural differences between the steels. These will be discussed later.

Others[10] have observed a rough correlation between the hardness and the cracking susceptibility of a steel, but have cautioned against the use of hardness alone as a criterion. Still others[22], probably because of the severity of their test conditions, did not find any hardness level below which sulfide corrosion cracking would not occur. The above observations serve to point out that the susceptibility of a steel to sulfide corrosion cracking is determined by no single factor alone, but instead is dependent upon the combined effects of applied stress, hardness level, plastic prestrain, and microstructure.

3) Effect of Plastic Deformation: The effect of plastic deformation, or residual stresses resulting therefrom, on sulfide corrosion cracking was observed by Vollmer[33] when test specimens cut from 9% Ni steel tubing failed at locations other than the point of maximum applied stress. This behavior was attributed to plastic deformation resulting from straightening operations performed on the tubing. The influence of plastic deformation on sulfide corrosion cracking has been demonstrated elsewhere by the service performance of cold-drawn austenitic stainless steel and cold-drawn high-carbon steel wires. Such wires have been reported[25] as failing in H_2S environments when stressed to only 40% of

their normal breaking load.

The conclusions of Bowers, McGuire, and Wiehe[3] in regard to the effect of plastic deformation on sulfide corrosion cracking are of particular interest. They prestressed both low- and high-alloy steels at various hardness levels to 1000 psi above their yield strengths, to midway between their yield and ultimate strengths, and to their ultimate strengths. These steels were then tested in H_2S environments at applied stresses of 70 to 80% of their respective yield strengths. It was learned that (a) although plastic deformation was not required for the failure of susceptible steels, the presence of such deformation accelerated the failure process, (b) even after steels have been plastically deformed they did not fail unless the applied stress was above a critical amount; and (c) steels having a microstructure completely free of martensite were not affected by prestrain of the degree studied.

4) Effect of Microstructure: In one investigation[3] of sulfide corrosion cracking, all of the steels that failed had martensite, in some degree or temper, present in their microstructure. However, not all of the steels which contained martensite failed, but only those steels in which the martensite was in the form of a continuous phase or network. It was postulated by Vollmer[33] and others[3] that the sulfide corrosion failures of 9% Ni steels were due to the presence of a network of untempered martensite. They demonstrated that a double normalizing heat treatment which eliminated the martensite network also made the steel resistant to cracking. Herzog[14] found that plain carbon and low-alloy steels which had a martensitic microstructure tempered at 300 to 500°C underwent very rapid cracking in H_2S environments. Microstructures which consisted of bainite and other intermediate transformation products were also found to be very sensitive to sulfide corrosion cracking at stresses equal to or greater than the "elastic limit." The same investigator[14] stated that severely tempered martensitic microstructures ("sorbitic" microstructures) were resistant to cracking to a certain degree but became susceptible upon being cold-worked or plastically deformed. It has been reported by others[10] that a quenched and tempered microstructure is superior in resistance to sulfide corrosion cracking to a normalized microstructure at the same level of strength and ductility.*

* It is the authors' opinion that the data cited were insufficient to support this conclusion because the effect of varying degrees of plastic prestrain was neglected.

5) Effect of Surface Condition: It has been reported[3][33] that a film of corrosion products affords at least partial protection against sulfide corrosion cracking, but that such protection is quite unreliable. At the same time, it was observed that after corrosion-product films were removed from test specimens it was possible for failure of these specimens to occur quite rapidly. For example, a specimen which had been on test in an H_2S environment for 66 days without failure was removed from test and mechanically cleaned of a tightly adherent film of corrosion product. When the sample was replaced on test, failure occurred within 24 hours.

Others[11] have reported that the presence of heat-treatment scale provided some initial protection but did not completely prevent sulfide corrosion cracking. Machining of the test specimens to remove the surface scale led to accelerated failure upon exposure to H_2S.

f. Mechanism of Sulfide Corrosion Cracking

Throughout this review the term "sulfide corrosion cracking" has been used to describe the type of failures which occur in H_2S-H_2O environments. This term arose out of the lack of clear-cut evidence as to whether sulfide corrosion failures were the result of stress-corrosion cracking or hydrogen embrittlement[10]. Such uncertainty has stemmed from the very manner in which ferrous materials corrode in aqueous hydrogen sulfide.

1) Sulfide Corrosion Reaction: When hydrogen sulfide dissolves in water, it forms a weak acid which can attack steel surfaces and thereby release hydrogen according to the equation below:

$$Fe + H_2S \rightarrow FeS + 2H \rightarrow FeS + H_2$$

In addition to being the corroding agent, the H_2S also acts as a promoter for the entry of atomic hydrogen into the steel (or as a poison for the recombination of atomic hydrogen into molecular hydrogen)[1]. That the sulfide corrosion reaction is capable of charging hydrogen into steel is evident from the blisters found in soft steels exposed to sulfide environments[1]. The gas contained in such blisters has been analyzed and found to be 99.5% hydrogen[1].

2) Mechanism of Stress-Corrosion Cracking: Since the characteristics of stress-corrosion cracking have been described elsewhere in this report, it is sufficient to say here that the phenomenon of sulfide corrosion cracking has present all of the elements required for stress-corrosion

cracking. Those elements consist of an applied stress and a corrosive environment acting together to produce failure of a susceptible material in a more-or-less spontaneous fashion.

3) Mechanism of Hydrogen Embrittlement: Numerous mechanisms have been put forward to explain the manner in which steel is embrittled by hydrogen. Two typical hypotheses are outlined below. Zapffe and Sims[36] have postulated that atomic hydrogen present in the steel combines within submicroscopic faults to form molecular hydrogen. As the pressure within these faults increases, severe triaxial stress systems are created which prevent flow of the metal under load. When an external stress is then applied to the metal, brittle failure results. Evans[7] has pictured hydrogen embrittlement as resulting from the diffusion of hydrogen from the metal lattice into "rifts" in the metal during deformation or straining of the metal. The pressure of the hydrogen is sufficient to extend the rifts into cracks. Additional deformation at the root of the crack causes more hydrogen to diffuse into the crack, with the result that the crack continues to propagate.

4) Hydrogen Embrittlement as the Cause of Sulfide Corrosion Cracking: Several investigators[1][13][14][24] have attributed sulfide corrosion cracking directly to hydrogen embrittlement. Hafsten[13], for example, was able to show a good correlation between the degree of embrittlement due to hydrogen and the cracking of carbon steel springs in an 8 to 10% H_2S atmosphere. One such spring which had failed in service was quickly sectioned into three parts. One part was immediately subjected to a simple bend test and failed in a completely brittle fashion. The other two sections, one of which was baked for four hours at 400°F and one of which was aged for three weeks at room temperature, failed in a ductile fashion after undergoing appreciable plastic deformation. Herzog[14] felt that the rate of absorption of atomic hydrogen was a determinant factor in H_2S cracking. He presented data to show that a steel which was susceptible to sulfide cracking absorbed hydrogen rapidly, while a steel which was not susceptible to cracking absorbed hydrogen slowly.

5) Combined Theory of Sulfide Corrosion Cracking: Some of the people in the field[3][10][33] have considered both stress-corrosion cracking and hydrogen embrittlement as possible explanations for sulfide corrosion cracking. One group[3][33] concluded that while hydrogen embrittlement was not considered the primary cause of sulfide corrosion failures, it might have been an important contributing factor. Another group[10] presented a combined theory of sulfide corrosion cracking which embraces features of both the stress-corrosion

cracking and hydrogen-embrittlement theories. The combined theory provides for (a) the initiation of a very small crack at some point of high tensile test, e.g., a pit or notch; (b) the stressing of the metal at the base of the notch leading to the precipitation of hydrogen; and (c) the propagation of the crack by the additional stress resulting from the precipitated hydrogen.

6) Summary: The theory of Fraser and Treseder[10] serves to explain the formation and propagation of cracks from corrosion pits on the surfaces of steels exposed to sulfide environments. However, the more rapid sulfide corrosion failures which occur with little or no evidence of related corrosion may perhaps be better explained on the basis of hydrogen embrittlement.

g. Prevention of Sulfide Corrosion Cracking

The problem of preventing sulfide corrosion cracking can be approached from a consideration of the factors involved in this type of failure; that is, stress level, corrosive environment, and susceptible materials. As far as stress level is concerned, practical considerations often limit the degree to which the applied stresses can be decreased through reduced loads or redesign of the load-carrying part. The same considerations often prevent the elimination of residual or internal stresses by means of stress-relieving heat-treatments.

Perhaps the most successful method used for combatting sulfide corrosion cracking has been the modification of susceptible materials or the substitution of materials that are not susceptible to this type of failure. For susceptible materials, it has been recommended[3][33] that the maximum mechanical properties should be defined so as to insure against the presence of "damaging" martensite in the steel. One way in which this was accomplished was the use of a heat treatment that either sufficiently tempered or completely eliminated any martensite network that was present. Materials, such as "Monel", "K-Monel", "Inconel", "Stellite" No. 1 and 6, nickel, brass, and annealed austenitic stainless steel, which have been reported as resistant to sulfide corrosion cracking[10][25][33] can be substituted for susceptible ferrous materials. For example, the fabrication of Bourdon tubes and relief-valve springs from Type 316 stainless steel instead of carbon steel was successful in eliminating sulfide corrosion failures[1].

Both metallic and nonmetallic coatings have been applied to susceptible materials in an attempt to stop corrosive attack in sulfide environments. Such coatings were found to be effective in preventing sulfide cracking only if there were no uncovered spots present, particularly at

critical areas[10]. Sprayed aluminum coatings were found to be capable of protecting carbon steel springs against sulfide corrosion cracking[1][13]. It has also been reported[22] that nickel plating prevented the cracking of steel laboratory specimens in an H_2S-H_2O environment.

Inhibitor additions and cathodic protection are two methods that have been applied in an attempt to minimize sulfide corrosion cracking through control of the sulfide corrosion reaction. Morton[22] learned that a formaldehyde inhibitor decreased the corrosion of a 9% Ni and an API N-80 steel and thereby kept them from cracking. However, the same inhibitor was ineffective in the case of 5% and 9% Cr steels. Another investigator[10] stated that their tests showed that sulfide corrosion cracking could be inhibited with a commercial oil field corrosion inhibitor but gave no other details. Cathodic protection was found in one case[22] to accelerate sulfide corrosion cracking rather than prevent it. In another case[10], it was observed that cathodic protection stopped sulfide cracking in a distilled-water solution of H_2S at moderate current densities, but was unable to do so in acidified solutions of H_2S.

3. Sulfide Corrosion Cracking Tests on Bolting Materials

a. Introduction

Because of the large number of bolts that were to be exposed to H_2S-H_2O environments at the Dana and Savannah River Plants, an investigation was undertaken to determine the cracking susceptibility of various bolting materials in such environments. Early failures of hardened AISI Type 4140 steel bolts in H_2S blowers at the Dana Plant emphasized the need for design information to prevent the recurrence of similar types of field failures. In order to develop this information, the incidence of cracking in a number of H_2S-H_2O environments was studied as a function of bolting material, hardness level, magnitude of applied stress, and degree of plastic prestrain. The effect of other factors, such as metallic coatings and corrosion inhibitors, on the sulfide-corrosion-cracking susceptibility was also evaluated. Out of these studies came a specification for hardness and stress level of AISI type 4140 steel bolting material that was designed to minimize sulfide corrosion cracking in the field.

b. Experimental Details

1) Test Specimens and Bolting Materials:

a) Type of Test Specimen: Since threaded parts have unique stress patterns which are difficult to simulate

with other types of laboratory specimens, actual bolts were used for test specimens. The majority of the bolts tested in this study conformed to ASTM specification A193-B7 (AISI Type 4140-4145 steel), which was the specification designated for plant bolting material. While the Type 4140 steel bolting specimens varied in size from 3/8 to 1-1/2 inches in diameter, the greatest number of tests were run on Allen head cap screws which were 3/8 inch in diameter by 1-1/2 inches long with 6 tpi. This size bolt was chosen for two reasons: (a) bolts of a similar type had failed in blowers at the Dana Plant and (b) the large number of required test specimens limited the bolt size from the standpoint of economy, ease of procurement, and test space.

b) Allen Head Cap Screws: The 3/8-inch cap screws were purchased in one lot of 2000 bolts, all of which had been fabricated from a single heat of steel in as uniform a manner as possible. The chemical analysis for this lot of bolts is given in Table XXX. The hardness of the 3/8-inch cap screws varied from R_c 10-20 for bolts in the annealed condition and from R_c 20-55 for bolts in the hardened-and-drawn condition. Table XXXI gives the hardness of these bolts as a function of tempering temperature as determined from laboratory heat treatments. Figure 28 shows how the ultimate tensile strength and yield strength of hardened-and-drawn 3/8-inch cap screws varies with the hardness level.

c) Large Type 4140 Steel Bolts: AISI Type 4140 steel bolts larger than 3/8 inch in diameter were also tested but in smaller quantities. These larger bolts were in the form of studs which varied in size from 1/2 to 1-1/2 inch in diameter. They were obtained from existing stock at the Dana Plant. The chemical analyses for two of the large bolts indicated that such bolts did not always meet the composition specifications set up for AISI Type 4140 steel (see Table XXXII). All of the large bolts were received in the hardened-and-drawn condition, with the hardness generally ranging from R_c 25-35. Many of these bolts were quite nonuniform so far as hardness was concerned. Some of the very large sizes had soft cores, while others occasionally showed hard spots that were 10-12 R_c points above the average hardness.

d) Bolting Materials Other Than Type 4140 Steel: Type 316 stainless steel was another ferrous material which was tested, in this case in the form of 3/8- by 1-1/2 inch hex head bolts. In addition, the resistance to sulfide corrosion cracking of the following nonferrous materials was studied: "Inconel", "Inconel-X", "Monel", "K-Monel", "Duronze", and 75ST aluminum. The nonferrous materials were tested in the form of studs either 3/8 or 1/2 inch in diameter. The physical properties of these materials have been included in the discussion of results.

2) Method of Stressing Bolts:

a) Description of Loading Jigs: Two types of jigs were used for loading or applying stress to the bolts. Both types were of sufficient cross-sectional area to be relatively rigid compared to the bolts being loaded. The 3/8-inch Allen head cap screws, the 3/8-inch hex head stainless steel bolts, and some of the shorter 3/8-inch nonferrous stud bolts were loaded on bars of the type shown in Figure 29. The larger sizes of stud bolts were loaded in individual sleeves of the type shown in Figure 30. In the case of both bars and sleeves, holes were drilled in the sides to permit free circulation of the corrosive environment around all of the bolting surfaces. Certain precautions were taken to minimize misalignment of the bolts during loading on the test jigs. These precautions included (a) the machining of parallel flats on the contacting surfaces of all bars, sleeves, and washers; (b) the machining of all nut faces to align them perpendicularly to the thread axis; and (c) the chasing of all threaded surfaces prior to engagement. In order to reduce friction, powdered "Molykote"* was brushed over all of the mating surfaces of the 3/8-inch cap screws and accompanying washers and nuts. By plant request, a graphitic grease, "Gredag" No. 51, was applied to all of the larger stud bolts which were sleeve-loaded.

b) Possible Methods of Loading Bolts: The principal problem arising from the use of bolts as test specimens is that of applying to the bolts accurately known values of stress. The determination of stress in a loaded bolt can be based on either torque or strain relationships. The torque method of bolt loading was the first to be applied in this study. It was later discarded when the strain method of measuring bolting stress proved to be more accurate. Both of these methods will be discussed below.

c) Torque-Loading Technique: Lenzen[20] has discussed the accuracy with which the clamping force or load on a bolt can be related to the applied torque. He concluded that there is a linear relationship between torque and load up to the yield point of the bolt. This relationship was expressed by the following empirical formula:

Torque (lb-inch) = 0.2 bolt diameter (inch) x clamping force (lb)

According to Lenzen, individual values of the clamping force as calculated from the applied torque using this formula were occasionally in error by as much as 30%. However, the average deviation obtained by using this formula was only 6 to 7%.

* MoS_2 supplied by Alpha Corporation, Greenwich, Conn.

In order to apply the torque method of loading in this study, it was first necessary to obtain curves of torque versus load for bolts of various hardnesses. This was done by fixing one end of the bolt between the platens of a hydraulic testing machine in such a way that a load was registered on the machine whenever a torque was applied to a nut on the other end of the bolt. The values of applied torque were read directly from a calibrated torque wrench. The curves obtained in this fashion showed a linear relationship between load and torque up to the point where further increases in torque produced no increase in load, i.e., up to the yield point of the bolt.

Bolts were prepared for testing in H_2S environments by tightening them on bars or in sleeves to a known value of torque. The load corresponding to the applied torque was then read from a torque-load curve for bolts of that hardness level. Finally, the stress level was calculated by dividing the load by the minimum cross-sectional area of the bolt. The accuracy of this type of loading was found to vary considerably with the amount of friction between the mating surfaces. That is, for any given value of applied torque, the resulting load decreased as the amount of friction increased. The maximum errors in bolting stress obtained using the torque method of loading were of the same order as those reported by Lenzen[20], about 30%.

d) Strain-Measurement Technique: The strain-measurement method of applying a known stress to a bolt is based upon Hooke's law, which states that stress is proportional to strain within the elastic limit. Expressed mathematically:

$$E = \frac{\text{Stress}}{\text{Strain}}$$

where E is the modulus of elasticity of the material being stressed. For a test specimen being elongated in tension, Hooke's law can be translated into the following expression:

$$E = \frac{P/A}{e/l}$$

where P is the load on the specimen, A is the cross-sectional area of the specimen, and e is the elongation of the specimen measured over a certain gage length, l.

The stresses present in the longer stud bolts were easily determined from the above formula once the values of e and l were known. The elongation or change in length of the bolt, e, was measured directly with a micrometer. Hemispherical tips were machined on the ends of each bolt to improve the accuracy of the measurements. The gage length, l, was assumed to be the length of the sleeve plus the thickness of the two washers plus half the total thickness of the two nuts. The reason for including only half of the total nut

thickness will be discussed later.

In the case of the 3/8-inch Allen head cap screws it was necessary to use special techniques to measure the elongation under applied loads. A Graham-Mantell strain indicator, which operates on the microformer principle, provided the means of measuring the elongation of the cap screws with an estimated accuracy of 0.00005 inch.

The translation of measured elongations into bolting stresses is complicated in the case of short bolts, less than 2 inches in length, by the question of effective gage length. For these shorter bolts, the effective gage length is significantly affected by the number of mating threads that are shared with the nut. Stoeckly and Macke[30] have studied the distribution of load over the threads of nuts and bolts. They reported that the maximum load for those bolt threads mated with the nut was carried by the first thread engaged in the nut. The thread load varied from a maximum of three times the average thread load at the first thread engaged to 0.3 of the average thread load at the last thread engaged in the nut. It was also stated that this distribution of thread load was affected only slightly by the bolt diameter, the number of threads per inch, or the bolt load within the elastic limit. Similar findings were reported by Hetenyi[16], who studied the distribution of stress in threaded connections using photoelastic stress analysis methods.

The results described above indicated that about 70 to 75% of the bolt load was carried by the first half of the threads engaged in the nut. Consequently, in this study only half of the nut thickness was used in determining the effective gage length of the bolt. The largest error that could be expected to result from this procedure would be in the case of the Allen head cap screws which were only 1-1/2 inches long. Even here, however, the maximum error that could possibly arise in the calculated stress values would be about 15% at a stress of 125,000 psi. This is, for the worst case, only half of the maximum error of 30% that is possible with the torque method of determining stress. Moreover, the validity of the gage-length assumption was borne out by the check method of strain measurement to be described later. A complete derivation of the formula used for calculating the stresses in the 3/8-inch cap screws is given in Exhibit A of the Appendix.

e) Check on Strain-Measurement Method: The method of determining bolting stress by means of strain measurement as described above involved two principal assumptions: (a) that the modulus of elasticity of the bolting material was a known constant and (b) that the effective gage length of the bolt included only half of the nut thickness. In order to ascertain the accuracy of the strain-measurement method, a

technique was developed to measure the bolting stress independently of the two assumptions normally involved. The check method centered around the device shown in Figure 31. This device consisted of a cubical block on whose four side faces resistance-type strain gages were mounted parallel to the axis of the hole in the block. The block was calibrated by loading it in compression between the platens of a hydraulic testing machine and measuring the strain as indicated by the strain gages as a function of load on the testing machine. The adapters shown in Figure 31 insured a loading area equal in size to the standard washers used with the 3/8-inch cap screws and provided for single-point loading as well.

The next step in the procedure was to load the calibrated block by tightening a 3/8-inch cap screw in place through the hole in the block. As the bolt was tightened, its elongation was measured with the Graham-Mantell strain indicator while, at the same time, the strain in the block was determined by means of the resistance strain gages. The bolting stress was then calculated, both from the elongation in the bolt and the load on the block, as provided by the calibration curve. The difference between the values of bolting stress obtained by the two methods of measurement averaged about 7% for the three bolts that were checked. It was therefore concluded that the strain measurement method of determining bolting stress was sufficiently accurate for the purpose of this study.

3) Method of Prestraining Bolts:

a) Prestraining of 3/8-Inch Cap Screws: For most of the prestrain studies 3/8-inch Allen head cap screws were used as test specimens. These bolts were plastically prestrained in tension in a hydraulic testing machine. As each bolt was prestrained, its stress-strain curve was automatically recorded using a separable extensometer operating over a 2-inch gage length. The prestraining operation was stopped when the total deformation reached a predetermined amount. The total plastic deformation was then calculated from the stress-strain curve and translated into plastic strain in inches per inch over a 3/4-inch gage length on the threaded region of the bolt. The amount of plastic prestrain was also determined from reduction in area measurements made with a micrometer and from measurements of the extension between the threads made with an eyepiece comparator. All three methods of measuring plastic prestrain were in fair agreement up to stress values near the ultimate tensile strength of the bolts. The values for plastic prestrain subsequently included in this report were all taken from stress-strain diagrams.

b) Prestraining of 5/8-Inch Stud Bolts: One series of 5/8-inch stud bolts was plastically prestrained by loading

them in sleeve-type jigs. The amount of plastic deformation was determined by measuring with a micrometer the permanent set in the bolts after they were unloaded. By successively loading and unloading the bolts and measuring their change in length, the desired amount of prestrain was obtained. The effective gage length over which the bolts had been deformed was determined from measurements of the thread spacings. The plastic prestrain was then calculated in inches of plastic deformation per inch of effective gage length.

4) Method of Measuring Bolt Hardness: Special precautions were taken to obtain accurate hardness measurements on the bolts tested in this study because of the importance assigned to this property in the literature as a criterion of susceptibility to sulfide corrosion cracking. Parallel flats were carefully machined on the ends of all bolts and the faces of all bolt cross sections before hardness readings were taken.

5) Sulfide Corrosion Test Environments:

a) Types of Test Environments: The nine different environments that were used to evaluate the sulfide corrosion cracking susceptibility of the various bolting materials are listed in Table XXXIII. Most of these environments were chosen to simulate certain operating conditions within the plants. For example, the 120°C - 250 psi and the 38°C - 250 psi systems were chosen to represent hot- and cold-tower conditions, respectively. Environments "B" through "E" were used to duplicate the conditions that might arise from an H_2S gas leak in a confined area.

b) Method of Producing Test Environments: Various types of test vessels were used for producing the environments listed in Table XXXIII. These varied from simple sealed metal containers to larger and more complex autoclaves. The five pressurized H_2S-H_2O systems were prepared by first purging the test pots with H_2S, then pressurizing the systems to 250 psi, and finally sealing the systems off at that pressure. In the four environments operated at temperatures from 60 to 120°C, care was taken to avoid charging H_2S into the systems before the bolts had reached the testing temperature and also to remove the H_2S before cooling the bolts to room temperature at the end of the test period. This was accomplished by charging the systems with nitrogen during the heating and cooling cycles.

The room temperature - atmospheric pressure environment was obtained by purging a test pot with H_2S and then sealing it off at atmospheric pressure. The system was maintained by repurging the container with H_2S at periodic intervals. The 100 ppm 1% and 3% H_2S systems were produced by passing a continuous stream of gas of the desired composition through the test vessel. A premixed, 3% H_2S-in-

nitrogen mixture was blended with the proper amount of air to provide the 100 ppm and 1% H_2S environments. For the 3% H_2S system, the mixture of 3% H_2S in nitrogen was used directly from the cylinder.

The components of the systems discussed above which are essential for sulfide corrosion cracking are H_2S and H_2O. In all but the 120°C - 250 psi environment, the bolts were exposed in the vapor rather than the liquid part of the system. The results reported in the literature indicated that if sulfide corrosion cracking was to occur in H_2S vapor, the vapor must be saturated with water. Care was taken, therefore, to see that in the case of every test environment the gaseous phase was saturated with water vapor. This was accomplished by placing a container of water in each of the test pots. Moreover, in those environments where a constant gas flow was maintained (100 ppm, 1% and 3% H_2S), the gas was bubbled through water prior to entering the test vessel. In the 120°C - 250 psi system, bolts were exposed in both the liquid and vapor phases, as well as a combination of the two. As far as could be determined, there was no difference in the cracking susceptibility of bolts exposed in the liquid and in the vapor phase under the 120°C - 250 psi conditions.

6) Method of Exposing Bolts and Checking for Failures: The length of the period for which loaded bolts were exposed to the test environments depended upon the stage of the testing. During the early stages of testing, the bolts were checked for failures after periods as short as one day. Later in the course of testing, the exposure periods were often as long as three months. An attempt was made to expose all bolts for a minimum of 3000 hr before discontinuing the test.

At the end of each test period, the bolts were checked for failures by torquing each bolt to 75% of the original torque used in loading it. The principal limitation to this procedure was that occasionally, where bolts had undergone extensive corrosion, the formation of scale mechanically locked the bolts in place. Consequently, 75% of the original torque was then insufficient to detect whether or not the bolt had failed. For this reason, at the end of the test all unfailed bolts were dried out, subjected to hard blows to dislodge the scale, and then torqued to their yield points to see whether or not they had actually undergone failure during test. It is believed that this procedure was sufficient to reveal all of the bolting failures that had occurred.

c. Discussion of Results

1) Effect of Environment on Sulfide Corrosion Cracking Susceptibility of AISI Type 4140 Bolting Material: The sulfide corrosion cracking characteristics of AISI Type 4140 steel bolting material are discussed below as a function

of bolt hardness and applied stress level for each of the six H_2S-H_2O environments listed in Table XXXIII. Unless otherwise indicated, all data are for quenched-and-drawn bolts having a microstructure of tempered martensite.

a) 3/8-Inch Cap Screws Exposed at 38°C - 250 psi: The largest amount of sulfide corrosion cracking data was obtained for 3/8-inch Allen head cap screws exposed in a pressurized (250 psi) H_2S-H_2O system at 38°C. In Figure 32 the cracking susceptibility in this system is treated as a "go or no-go" proposition. That is, all of the bolts tested are shown as either failing or not failing. Total exposure time was never less than one year. Two curves have been drawn to divide the plot into three regions: (a) a no-failure region, (b) a region of possible bolt failure, and (c) a 100%-failure region. The testing region has been confined to that area below the yield-strength curve for the bolts. This was done to minimize the amount of plastic deformation introduced into the bolts by the applied stress.*

The data in Figure 32 show clearly that the susceptibility to sulfide corrosion cracking increased with increasing hardness. This is in accord with the results of other investigators[3][10]. It is important to note that no bolting failures were observed below a hardness level of R_C 27, even under applied stresses approaching the yield point. This observation is of practical importance because it demonstrates that higher bolt loads can be maintained without failure by bolts heat-treated to lower hardness and strength levels, i.e., to hardnesses below R_C 27. This is in marked contrast to the usual procedure where, in the absence of any embrittling phenomena, the hardness and strength levels are increased in order to provide for higher clamping forces.

It is also evident from Figure 32 that the level of applied stress** necessary to produce failure by sulfide corrosion cracking decreased as the hardness increased. This is

* Because of the stress-concentration factor at the thread roots, some localized yielding will occur at these points even at applied stress values which are nominally well below the yield point.

** The stress level as used here refers to the stress initially applied to the bolts before exposure to the test environments. The relaxation of this stress as a function of exposure time and temperature is discussed in Exhibit B.

even more evident in Figure 33 where the minimum bolting stress required for failure, as determined from Figure 32, has been plotted as a function of bolt hardness. The concept of a minimum stress level necessary to produce sulfide corrosion cracking has been introduced by Bowers, McGuire, and Wiehe[3]. If one assumes that their concept of a critical or threshold stress necessary to produce sulfide corrosion cracking is a valid one, then the data in Figure 33 show that such a stress is, in large measure, a function of hardness.

In addition to the above tests on quenched-and-drawn bolts, a smaller number of tests were run in the 38°C - 250 psi environment on annealed 3/8-inch cap screws having a ferritic-pearlitic microstructure and a hardness of R_c 15-21. As shown in Table XXXIV, none of the annealed bolts failed even when stressed at values approaching their yield strengths.* From these results, it can be concluded that for a given hardness level ferritic-pearlitic microstructures are no more susceptible to sulfide corrosion cracking than tempered martensitic microstructures.

b) 3/8-Inch Cap Screws Exposed at Room Temperature - Atmospheric Pressure: The cracking data for 3/8-inch Allen head cap screws exposed in an H_2S-H_2O system at room temperature and atmospheric pressure are plotted in Figure 34. For a basis of comparison the cracking curves for the 38°C - 250 psi environment from Figure 32 have been included.** On this basis there appears to be little difference in the susceptibility to sulfide corrosion cracking in the two environments. It can therefore be concluded that pressure has a negligible effect on the cracking tendency in the range of 1 to 17 atmospheres. Others[3][10][33] have drawn similar conclusions regarding the effect of pressure and over a much broader range (1 - 300 atmospheres).

c) Large Stud Bolts Exposed at (1) Room Temperature - Atmospheric Pressure and (2) 38°C - 250 psi: The test data for the larger AISI Type 4140 steel stud bolts (1/2 - 1-1/2 inch in diameter) exposed in both the room temperature - atmospheric pressure and 38°C - 250 psi H_2S-H_2O systems have been combined in Figure 35. Such a combination is believed to be warranted on the basis of the similarity in the cracking behavior of 3/8-inch cap screws exposed in these two

* As a given hardness level, the yield strength of annealed bolts was appreciably lower than the yield strength of quenched-and-drawn bolts.

** The data for the room temperature - atmospheric pressure system were believed insufficient to warrant the drawing of new cracking curves for this system.

environments. No attempt was made to define individual bolt sizes on this plot because there was no clear-cut relationship between bolt size and cracking susceptibility. The cracking curves for the 3/8-inch cap screws exposed at 38°C - 250 psi (Figure 32) have been included in Figure 35 as guideposts. It will be noted that the no-failure and 100%-failure regions defined by these curves hold very well for the larger stud bolts, with the exception of two unfailed bolts lying slightly within the 100%-failure region for the smaller bolts. This is believed to constitute good agreement when the non-uniform hardness and the varying chemical composition of the larger bolts are considered. Table XXXII shows the spread in chemical composition for two of the larger-size bolts. Hardness variations within individual bolts of 5 - 10 R_c points were observed for about 25% of the large bolts. Moreover, the 1-1/8 to 1-1/2 inch bolts were 2 - 10 R_c points softer at the center than at the edges, because the hardenability of AISI Type 4140 steel was insufficient for through-hardening of this size cross section. Despite these variations, the results shown in Figure 35 indicate that the test data obtained for the 3/8-inch cap screws can be safely used to predict the cracking behavior of larger bolts.

d) 3/8-Inch Cap Screws Exposed at 120°C - 250 psi: The 3/8-inch AISI Type 4140 steel cap screws proved to be much less susceptible to sulfide corrosion cracking when exposed to a pressurized (250 psi) H_2S-H_2O system at 120°C than when tested in a similar system at 38°C. In Figure 36 the cracking data for the 120°C - 250 psi system are plotted with the cracking curves for the 38°C and 250 psi system dotted in as a reference. The large number of unfailed bolts exposed at 120°C that fell within the 100%-failure region for the 38°C environment is striking. Moreover, there was a complete absence of bolt failures at 120°C in that region between the dotted curves where failure could and did occur at 38°C. Thus, it becomes quite obvious that there is a sharp decrease in cracking susceptibility with an increase in test temperature from 38 to 120°C. However, it was not possible to draw new cracking curves for the 120°C environment because of insufficient data.

e) Large Stud Bolts Exposed at 120°C - 250 psi: None of the fifteen larger (1/2-to 1-1/2-inch diameter) AISI Type 4140 steel stud bolts exposed in the 120°C - 250 psi H_2S-H_2O environment failed by sulfide corrosion cracking. The test data for these bolts are summarized in Table XXXV. All but one of these bolts were exposed at applied stress and hardness levels which placed them in a borderline region of possible failure as defined for the 38°C environment in Figure 32. While under these borderline conditions of hardness and stress none of the large bolts exposed at 120°C failed, Figure 35 shows that 13 out of 38 large bolts exposed at either room temperature or 38°C failed.

The above results show that the reduced cracking susceptibility of AISI Type 4140 steel bolting material at the higher testing temperature holds true for large as well as small bolts. The same relationship between temperature and the susceptibility to sulfide corrosion cracking has been observed by other investigators[10] but over a lower and more narrow range of temperature (0 to 25°C).

f) 3/8-Inch Cap Screws Exposed in Pressurized Systems at 60°, 80°, 100°, and 120°C: A brief study was made of the effect of temperature in the range of 60 to 120°C upon the cracking susceptibility of 3/8-inch Allen head cap screws. Bolts were exposed in pressurized (250 psi) H_2S-H_2O systems at 60, 80, 100, and 120°C at those conditions of hardness and stress level known to produce failure at 38°C. The results of this study are summarized in Table XXXVI. The cracking behavior at 80°C appeared to be slightly out of line with that of the other three test temperatures, since none of the five R_C 40 bolts stressed at 100,000 psi failed during the 80°C exposure. However, too small a number of bolts were tested in this study to warrant drawing any conclusions about the relative cracking severity at any of the four temperatures. It is sufficient to say that these results demonstrate that sulfide corrosion cracking can occur over the entire temperature range from room temperature to 120°C. This is in line with the results of others[3][10][33] who have reported failures in H_2S environments at temperatures ranging from 0 to 80°C.

g) Cap Screws and Stud Bolts Exposed in Low Concentrations of H_2S: No bolting failures were experienced in any of the three environments which were low in H_2S concentration, i.e., the water-saturated mixtures of 100 ppm H_2S in air, 1% H_2S in air, and 3% H_2S in nitrogen. Only those combinations of hardness and stress level known to result in sulfide corrosion failures in the 38°C - 250 psi environment were used to evaluate the cracking susceptibility of 3/8-inch AISI Type 4140 steel cap screws in the H_2S-H_2O systems just listed. Tables XXXVII and XXXVIII summarize the test data for the 100 ppm H_2S and the 1% H_2S environments, respectively. All of the bolts listed in Table XXXVIII were transferred at the end of their nine months' exposure in the 1% H_2S system to the 3% H_2S system where they were exposed for an additional period of five months. At the time of their transfer into the 3% H_2S environment, the bolts were quite heavily covered with sulfide scale and rust from their previous exposure in the 1% H_2S environment. For this reason, too much emphasis should not be placed on the negative cracking results obtained in the 3% H_2S system.

2) Effect of Plastic Deformation on the Sulfide Corrosion Cracking Susceptibility of AISI Type 4140 Steel Bolting Material:

a) Plastically Prestrained Cap Screws Exposed at 38°C - 250 psi: A series of 3/8-inch AISI Type 4140 steel cap screws ranging in hardness from R_c 24 - 33 were plastically prestrained in tension from 0.010 to 0.130 inch/inch. The results of exposing these bolts to an H_2S-H_2O system at 38°C and 250 psi are shown in Figure 37, along with the cracking curves for nonprestrained bolts exposed to the same environment. The introduction of relatively large amounts of plastic deformation into those bolts stressed at 100,000 psi and above was sufficient to produce sulfide corrosion failures at hardness levels as low as R_c 24. This compares with a minimum hardness of R_c 27 for sulfide corrosion failures of nonprestrained bolts.

In addition to causing bolt failures at hardness levels below R_c 27, plastic prestraining increased the number of failures which occurred when bolts of R_c 27 - 33 were stressed to 100,000 psi and above. This is shown by the data in Table XXXIX where the bolts have been grouped according to whether they were prestressed (or prestrained) to stress levels which were (a) below, (b) at, or (c) beyond their ultimate tensile strengths. In cases where the bolts were stressed to 100,000 psi or higher, the percentage of bolt failures increased as plastic deformation was introduced into the bolts in increasing amounts. At stress levels of 35,000 - 70,000 psi plastic prestraining had no great effect on the percentage of bolt failures.

Included in the prestrain studies were two annealed bolts having a ferritic-pearlitic microstructure instead of the usual tempered martensitic microstructure. As shown by the data in Table XL, severe plastic prestraining can even lead to failure of annealed bolts as soft as R_c 22. Ordinarily, annealed bolts were not susceptible to sulfide corrosion cracking at stress levels up to and including their yield strengths (see Table XXXIV).

b) Plastically Prestrained 5/8-Inch Bolts Exposed at 120°C - 250 psi: As discussed earlier, the susceptibility of AISI Type 4140 steel bolting material to sulfide corrosion cracking was much less in the 120°C environment than in the 38°C system. A brief attempt was made to determine whether plastic prestraining increased appreciably the cracking tendency at 120°C. Five 5/8-inch stud bolts having a hardness of approximately R_c 30 were plastically prestrained in tension from 0.055 - 0.085 inch/inch. These bolts were stressed at 95,000 - 115,000 psi and then exposed in an H_2S-H_2O system at 120°C and 250 psi. None of the prestrained bolts failed after a total exposure time of six months. It therefore appears that plastic prestrain of the degree studied has little

effect on the cracking susceptibility of R_c 30 bolts exposed in the 120°C system.

3) Effect of Metallic Coatings on the Sulfide Corrosion Cracking Susceptibility of AISI Type 4140 Steel Bolting Material: A number of different types of metallic coatings were applied to 3/8-inch AISI 4140 steel cap screws in order to evaluate their effectiveness in preventing sulfide corrosion cracking. For this study, conditions of bolt hardness and stress level were chosen that were sufficient to guarantee 100% failure of uncoated 3/8-inch bolts in the 38°C - 250 psi environment. The results of the exposure of plated bolts in both the room temperature - atmospheric pressure and the 38°C - 250 psi systems are listed in Table XLI. These data demonstrate that although most of the coatings tested were effective in increasing bolt life by a factor of 2 to 3 or more, they did not afford consistent or reliable protection against sulfide corrosion cracking. One exception to this general statement was the protection provided by a relatively heavy nickel plating (0.005 inch thick). This is shown by the data in Table XLII. Others[22] have similarly found that electroplated nickel coatings were capable of preventing sulfide corrosion cracking.

When metallic coatings are being considered as a practical means of minimizing sulfide corrosion cracking, it is well to remember that the effectiveness of any metallic coating is only as good as its freedom from defects. This word of caution is particularly pertinent in the case of bolts where threaded connections greatly increased the danger of mechanical rupture of the coating.

4) Effect of Inhibitors on the Sulfide Corrosion Cracking Susceptibility of AISI Type 4140 Steel Bolting Material: A small number of tests were run to determine whether inhibitors could be used to prevent or even minimize the sulfide corrosion cracking of AISI Type 4140 steel bolting material. On the basis of corrosion data obtained in the inhibitor screening program (discussed earlier in this report), two promising inhibitors were chosen for the cracking study. These were "Duomeen T" and TEPA (tetraethylenepentamine), two low-vapor pressure amines. All tests were carried out on 3/8-inch cap screws exposed in the liquid phase of an H_2S-H_2O system at 38°C - 250 psi. Inhibitor additions of about 500 ppm were made to the liquid phase, which was initially distilled water. Tests were run at those conditions of hardness and stress level known to produce 100% failure in the absence of any inhibitor.

The results of the inhibitor study are presented in Figure 38. The accumulative per cent of those bolts tested which failed has been plotted versus time to failure for the uninhibited and the two inhibited test systems. The TEPA proved to be the more effective of the two inhibitors in that it reduced the percentage of bolt failures from 100% to 40%.

Not too much practical significance can be attached to these results for two reasons: (a) only five bolts were tested in each inhibited system, and (b) neither inhibitor was 100% effective in the elimination of sulfide corrosion failures. However, the data do reflect the findings of two other investigators[10][22] who encountered varying degrees of success in checking sulfide corrosion cracking by means of inhibitors.

5) Susceptibility to Sulfide Corrosion Cracking of Bolting Materials Other Than AISI Type 4140 Steel: As the data summarized in Tables XLIII - XLIX show, "Duronze" and 75ST aluminum were the only two nonferrous bolting materials which showed any susceptibility to sulfide corrosion cracking. Even here, only one bolt of each material failed and then only after extremely long exposure times (1 to 1-1/2 yr). Type 316 stainless steel, "Monel", "K-Monel", "Inconel", and "Inconel-X" proved to be completely resistant to cracking in the H_2S-H_2O systems investigated. "K-Monel" and "Inconel-X" displayed an immunity to sulfide corrosion cracking even at hardness levels as high as R_c 32 - 36 and at stress levels ranging from 100,000 - 125,000 psi. The above results confirm the excellent resistance to sulfide corrosion cracking that has been reported in the literature[1][10][25][33] for Type 316 stainless steel, "Monel", "K-Monel", and "Inconel".

6) Factors Affecting the Time to Failure by Sulfide Corrosion Cracking of 3/8-Inch AISI Type 4140 Steel Cap Screws: A study of the cracking data for 3/8-inch AISI Type 4140 steel cap screws established that the time to failure of these bolts was primarily a function of hardness and secondarily a function of stress level and degree of prestressing.

a) Effect of Bolt Hardness on Time to Failure: Figures 39 and 40 show the effect of bolt hardness on the time to failure for the two H_2S-H_2O environments in which sulfide corrosion cracking was most prevalent. For each hardness level, the number of bolt failures occurring within a given exposure time has been plotted as a percentage of the total number of bolts of that hardness which failed. In the case of both test environments, the curves show that there is a marked reduction in the time to failure as the hardness level is increased. This effect is probably related to the easier initiation and the more rapid propagation of cracks in the harder, and therefore less ductile, bolts.

b) Effect of Stress Level on Time to Failure: The effect of applied stress on the time to failure of 3/8-inch cap screws exposed in the 38°C - 250 psi H_2S-H_2O environment is shown in Figure 41. These data reveal that the applied stress level had little effect on the time to failure except at the higher hardness level of R_c 39 - 43. In this upper hardness range, the time to failure was less for the

75,000 - 125,000 psi stress level than for the 15,000 - 75,000 psi stress level. It is not too surprising that the applied stress level did not affect the time to failure as markedly as the hardness, for the following reason. The effect of applied stress is minimized by the relaxation in bolt load that occurs as a crack propagates through a bolt. This hypothesis is substantiated by Gifkins and Rees[11] who found a poor correlation between applied stress and the time to actual fracture but good agreement between applied stress and the time to initiate cracking.

c) Effect of Prestressing on Time to Failure: Prestressing of 3/8-inch AISI Type 4140 steel cap screws to their ultimate tensile strength or below had little effect on their time to failure in a 38°C - 250 psi H_2S-H_2O environment. This is shown by the data in Figure 42. However, prestressing to beyond the ultimate tensile strength (total plastic prestrain of 0.070 - 0.120 inch/inch) caused a majority of the bolts to undergo failure in much shorter lengths of time. This is in line with a statement by Bowers, McGuire, and Wiehe[3] "that the presence of plastic deformation accelerated the failure process for steels susceptible to sulfide corrosion cracking." In the case of the present work, the decreased time to failure of bolts prestressed beyond their ultimate tensile strengths could not be attributed to a reduction in cross-sectional area since this was only of the order of 10%. Moreover, other data showed that there was little effect of bolt size in the range of 3/8 to 1-1/2 inches on the time to failure.

7) Fracture Studies on AISI Type 4140 Bolting Failures: A study of the fractures of 3/8-inch AISI Type 4140 steel cap screws exposed in H_2S-H_2O systems showed that the fractures occurred at four principal locations: (a) in the threaded region between the nut and the unthreaded shank (gage failure), (b) in the threaded region engaged in the nut (nut failure), (c) in the unthreaded shank (shank failure), and (d) in the minimum cross section immediately below the head (head failure). Representative macrographs of these four types of fractures are shown in Figure 43. The typical gage failure of a 3/8-inch cap screw began near the root of a thread and propagated through the cross section of the bolt in a direction that was nearly normal to the bolt axis. The result (see Figure 43A) was an almost flat fracture with a slight projection of torn metal to mark the fracture completion. Nut failures occurred in a similar fashion, except that restraint by the nut thread caused multiple cracking to occur before the fracture could be completed. This is brought out in Figure 43B where cracking has proceeded along three separate paths to fracture. The shank failures were quite brittle in appearance due to irregular fracture contours (see Figure 43C). The appearance of the head failures suggests that a number of cracks propagated simultaneously

through the minimum cross section resulting from the socket in the bolt head (see Figure 43D).

Fractures of the larger steel bolts (1/2 to 1-1/2 inches) were not nearly as uniform as those of the 3/8-inch cap screws. For example, gage failures of the larger bolts often displayed a ductile fracture at the core surrounded by an area of completely brittle appearance (see Figure 44). Sometimes a pattern of circumferential cracking was observed in the bolting fractures (see Figure 45).

A review of the fracture data for 3/8-inch AISI Type 4140 steel cap screws established that there was no apparent correlation between fracture location and any of the following factors: bolt hardness, applied stress level, degree of plastic prestrain, type of H_2S-H_2O environment, and time to failure. Upon first consideration, one might have expected that most of the prestrained bolts would have failed in the gage. However, the fact that the plastically deformed region of the bolt was partially engaged in the nut during testing contributed to failures in the nut. Even in ordinary failures of bolting material where sulfide corrosion cracking is not involved, the fracture location varies depending upon the stress concentration factors inherent in bolt design[16]. Thus, the lack of any consistent relationship between fracture location and any of the other variables in the present study is not surprising.

8) Corrosion in H_2S-H_2O Systems:

a) Corrosion of AISI 4140 Steel: Cylindrical corrosion specimens of AISI 4140 steel, 3/4 inch in diameter by 3/4 inch long, were exposed in all of the test environments listed in Table XXXIII, with the exeption of the 120°C - 250 psi environment. The corrosion rates for these H_2S-H_2O environments are summarized in Table L. In general, the corrosion rates for long-time exposures were lower than those for short-time exposures because of the formation of sulfide scale on the sample surface. The rates for the 38°C - 250 psi and the room temperature - atmospheric pressure systems were almost identical. The corrosion rates for these two systems were significantly higher than the liquid and vapor-phase rates for the 100 ppm H_2S and 3% H_2S environments and the liquid-phase rates of the 1% H_2S environment. The high-vapor-phase rates of the 1% H_2S system are believed to have resulted from the accelerating effect of air on the sulfide corrosion process. This appears to be the case, since the vapor-phase rates for the 3% H_2S in nitrogen system were more in line with the vapor-phase rates in the other four systems. While no corrosion rates are listed for the 120°C - 250 psi environment, the corrosion data discussed in another part of this report show the following. Initial corrosion in the liquid phase of the 120°C - 250 psi system was high (15-30 mils/yr for exposure periods of 100-400 hr) but rapid-scale

build-up led to much lower corrosion rates (1-2 mils/yr for exposure periods of 800-1800 hr). Finally, as far as inhibitors are concerned, they were able to reduce the corrosion rate for short periods of exposure (100-400 hr) in the 38°C - 250 psi environment by a factor of 5 or 6.

b) Corrosion of Metallic Coated AISI 4140 Steel Bolts: The corrosion behavior of the various types of metallic coatings applied to AISI 4140 steel bolts is qualitatively described in Table LI. All of the coatings were attacked to varying degrees in each of the environments. In many cases it proved very difficult to judge the extent of the corrosive attack on the underlying metal from the appearance of the plating. Because the nickel plating was the only metallic coating that was effective in preventing sulfide corrosion cracking, the condition of the nickel-plated bolts was examined more carefully than that of the others. When the light coating of sulfide scale on the nickel-plated bolts was carefully scraped away, the underlying nickel plate was found to be still intact.

c) Corrosion of Stainless Steel and Nonferrous Bolts: Qualitative observations regarding the corrosion of stainless steel and nonferrous bolts in the various H_2S-H_2O environments are listed in Table LII. "Inconel", "Inconel-X," and Type 316 stainless steel proved to have excellent resistance to sulfide corrosion in all of the environments tested. "Duronze", on the other hand, was severely corroded in all but the 100 ppm H_2S system. The other copper-bearing alloys, "Monel" and "K-Monel", were slightly to moderately corroded in the various H_2S-H_2O environments. The poor corrosion resistance of the 75ST aluminum bolts is believed to be due to the presence of iron sulfide scale in the corroding system.

9) Metallographic Studies of Sulfide Corrosion Attack, Sulfide Corrosion Cracking, and Microstructure of AISI 4140 Bolts:

a) Pattern of Sulfide Corrosion Attack in Various Environments: The microscopic pattern of corrosive attack on AISI 4140 steel bolts was found to be quite similar in the three main environments in which sulfide corrosion failures had occurred, i.e., the room temperature - atmospheric pressure system and the pressurized (250 psi) systems at 38°C and at 120°C. In general, the sulfide corrosion pattern in the three systems mentioned above consisted of rounded pitting, blunt corrosion notches, and sharp "finger-type" corrosion notches. Examples of the more blunt type of corrosion notches are shown in Figures 46 and 47. Figure 47 also illustrates how one such notch served as the origin of a severe sulfide corrosion crack. The sharper finger-type corrosion notches are pictured in Figures 48A, B, and C. The hair-like portions at the very root of these notches might

even be considered microcracks. It is easy to conceive how such extremely fine cracks or notches could develop under the influence of stress into severe macrocracks.

Such factors as bolt hardness, applied stress, and degree of plastic prestrain were found to have had very little effect on the type and extent of corrosion observed on AISI 4140 steel bolts. As would be expected, the severity and extensiveness of the corrosive attack increased as the time to failure or total exposure time increased. However, a 65-hr exposure was generally sufficient to develop a small amount of pitting and occasionally even a finger-type pattern of attack.

Although exposure in the 100 ppm-H_2S-in-air environment resulted in the formation of a very thin black coating of sulfide scale, microexamination of sectioned bolts from this environment revealed little evidence of any sulfide attack. There were no rounded pits, corrosion notches, or hairline cracks present on the threaded surfaces of any of the bolts. The corrosive attack in the 1% H_2S in air environment was quite heavy; it consisted of large rounded pits and occasional blunt corrosion notches. However, there were no fine "finger-type" corrosion notches or hairline cracks present after exposure to this environment. The corrosion observations made on the bolts exposed in the 3% H_2S in nitrogen system were obscured by the prior exposure of these bolts in the 1% H_2S in air system. Nevertheless, it was possible to conclude that fine corrosion notches and hairline cracks did not result from exposure to the 3%-H_2S-in-nitrogen system. The absence of any fine corrosion notches or hairline cracks in the bolts exposed to the 1% H_2S and 3% H_2S environments may explain the fact that no sulfide corrosion failures occurred in these two environments.

Two generalizations can be drawn regarding the corrosion behavior of AISI 4140 steel bolts exposed in an inhibited H_2S-H_2O system at 38°C and 250 psi. First, in those cases where bolt failures occurred in the inhibited system there was definite evidence of generalized pitting coupled with localized finger-type attack at the thread roots. This indicated that the inhibitor in the system had failed to provide sufficient protection against sulfide corrosion. Secondly, in the case of unfailed bolts exposed in the same inhibited system most of the threaded surfaces were largely free of corrosion pits and notches. However, some extremely fine localized attack was always present.

The microscopic pattern of the sulfide corrosion attack on the failed 75ST aluminum and failed "Duronze" bolts was similar to that on the AISI 4140 steel bolts exposed to the same environment. However, the 75ST aluminum bolt showed fewer of the finger-type corrosion notches than the AISI 4140 steel bolts.

b) Pattern of Macro- and Microcracking in Sulfide Corrosion Failures: The manner in which AISI 4140 steel bolts failed by sulfide corrosion cracking is depicted macroscopically in Figures 49 and 50. The fact that both of these bolting failures occurred in the nut could account for the multiple-cracking patterns. Such is not necessarily the case, however, since multiple cracking was also observed in bolting failures at other locations. Note that the sulfide corrosion cracks initiated in both failures at points slightly removed from the thread roots. These points of crack initiation correspond roughly to the point of maximum stress concentration for loaded bolt threads engaged in a nut[16]. In the case of bolt failures in the gage, the cracks generally originated at the very root of the threads.

Microscopic cracks, which are typical of sulfide corrosion cracks in AISI 4140 steel bolts, are illustrated in Figures 51-54. These microcracks usually initiated at either the thread roots (see Figure 54) or the fracture surface (see Figure 53). Quite often the cracks were of a branching nature (see Figures 51 and 52), and in many cases they were filled with corrosion products (see Figure 51). As well as could be determined, the number and location of the microcracks in AISI 4140 steel bolts were not influenced by such factors as hardness, stress level, and degree of plastic prestrain. The classification of the sulfide corrosion cracks as either intergranular or transgranular proved to be impossible because the grain size of the tempered martensitic microstructure was so small and poorly defined. Some cracks, such as the ones shown in Figures 55 and 56 did give the appearance of being either intergranular or transgranular. In those cases where the cracking was tentatively classified as intergranular or transgranular, no correlation could be drawn between the nature of the cracking and any of the test variables.

The only microcracks observed in the failed 75ST aluminum and "Duronze" bolts were located in those areas adjacent to the fracture surfaces. The cracking in the 75ST aluminum bolt was clearly intergranular, as illustrated by Figure 57. In the "Duronze" bolt the cracking appeared to be at least partly intergranular. (See Figure 58).

c) Microstructure of AISI 4140 Steel Bolts as a Function of Hardness: The basic microstructure of 3/8-inch AISI 4140 steel cap screws ranging in hardness from R_c 21-55 was examined. This examination revealed that there was little in the way of microstructural change from a hardness of R_c 25 to R_c 35 that would account for the sharp increase in sulfide corrosion cracking that occurred over this range of hardness. This is borne out by the series of photomicrographs in Figure 59. The only microstructural change evident in Figures 59B through 59F is the increased spheroidization of

carbides that occurs as the hardness of quenched and drawn bolts is decreased from R_c 55 to R_c 21. No traces of any untempered martensite resulting from decomposition of retained austenite were found in any of the bolts. A comparison of Figures 59A and B illustrates the marked difference between the ferritic - pearlitic microstructure of an annealed bolt at a hardness of R_c 21 and the tempered martensitic microstructure of a quenched-and-drawn bolt of the same hardness.

d. Summary

A study of the behavior of AISI 4140 steel bolting material in various H_2S-H_2O environments resulted in the following conclusions:

1. Failure by sulfide corrosion cracking occurred in the following environments:
   a. Pressurized (250 psi) H_2S-H_2O systems at temperatures ranging from 40 to 120°C.
   b. Atmospheric pressure H_2S-H_2O systems at ambient temperatures (20 to 35°C)

2. Sulfide corrosion failures did not occur in those environments involving low H_2S concentrations. These environments were water-saturated mixtures of:
   a. 100 ppm H_2S in air
   b. 1% H_2S in air
   c. 3% H_2S in nitrogen

3. The susceptibility to sulfide corrosion cracking decreased with increasing temperature over the range of 40 to 120°C.

4. Pressure of the H_2S-H_2O system within the range of 1 to 15 atmospheres had very little influence on the cracking tendency.

5. In the absence of plastic deformation, no failures occurred in any environment at hardnesses less than R_c 27 even under stresses approaching the yield strength of the material.

6. In the hardness range of R_c 27-55, the cracking susceptibility increased with increasing hardness and increasing applied stress. There was a rough relationship between these two variables which showed that as the hardness level increased, the minimum applied stress necessary to produce sulfide corrosion cracking decreased.

7. Plastic prestraining of the bolts resulted in sulfide corrosion failures at hardnesses as low as R_c 22. The percentage of bolt failures at hardness levels of R_c 24-33 and stresses of 100,000 psi or more increased with increasing

amounts of plastic prestrain.

8. The cracking curves developed for 3/8-inch Allen head cap screws were shown to be an accurate guide to the cracking behavior of the larger stud bolts.

9. Annealed bolts of R_c 15-21 in hardness were immune to sulfide corrosion cracking in the absence of severe plastic prestrain.

10. The time to failure decreased markedly with increasing hardness and decreased to a much lesser degree with increasing applied stress and increasing amounts of plastic prestrain.

11. A 0.005-inch thick electroplated nickel coating prevented the failure of bolts by sulfide corrosion cracking. Coatings of electroplated Cd, Zn, Pb, Cr, and brass and of sprayed aluminum paint did not provide reliable or consistent protection against sulfide corrosion cracking.

12. Addition of inhibitors to the liquid phase of a pressurized H_2S-H_2O system at 40°C reduced, but did not eliminate, the cracking of bolts exposed in the liquid phase of the system. Of the two inhibitors tested, TEPA (tetraethylenepentamine) proved to be more effective than "Duomeen-T."

In contrast to the AISI 4140 steel, the nonferrous and stainless steel bolting materials exhibited the following behavior upon exposure to the same H_2S-H_2O environments:

1. The following bolting materials were completely resistant to sulfide corrosion cracking under those conditions tested:

a. Type 316 stainless steel
b. "Inconel"
c. "Inconel-X"
d. "Monel"
e. "K-Monel"

2. Of those materials listed above "Inconel-X" and "K-Monel" were able to provide the maximum load-carrying capacity: bolting stresses of 100,000 - 125,000 psi at hardnesses of R_c 32-36.

3. "Duronze" and 75ST aluminum were two nonferrous bolting materials which were susceptible to a minor degree to stress corrosion cracking in H_2S-H_2O systems.

4. From the standpoint of general resistance to corrosion in H_2S-H_2O environments Type 316 stainless steel, "Inconel," and "Inconel-X" were superior to the other bolting materials tested.

4. Other Sulfide Corrosion Cracking Tests

Several types of stress-corrosion tests were used in the Laboratory. These included horseshoe-bend tests, bolt tests (discussed on pages 85-107), dead-weight loaded specimens, bubble caps, beam deflection, and several miscellaneous tests.

Initial tests were made with restrained horseshoe-bend specimens. These were steel strips 5 inches long, 1/2 inch wide, and 1/8 inch thick bent in a U shape. The ends were drilled so that they might be pulled together by means of bolts acting as chords. Thus, indeterminate tensile stresses of minimum yield strength value were present in the outer fibers of the nose of the bend. Stresses in these specimens were maintained by tightening the bolts before each exposure period.

Results of the bend tests indicated that hardened steels are most susceptible to sulfide stress cracking. Austenitic alloys did crack but required stresses well above the yield-point range. Soft steels such as A212 steel showed good resistance to cracking.

a. Tests Using Dead-Weight Loading

Although the horseshoe bends were convenient for qualitative tests of the stress cracking, and for determining the susceptibility of materials to cracking, they were not precise. Stresses in the outer fibers were always of approximately the yield strength for the materials in test and not uniform across the specimen cross section.

In order to enlarge the testing program a 45-inch diameter autoclave was fabricated with a 10-station test unit, as shown in Figure 4. Tensile stresses up to 100,000 psi were obtained in 1/8-inch diameter specimens by applying loads through lever systems. For higher stresses the specimen diameter had to be reduced because of the space limitations for weights. Several precautions were taken to minimize the effects of corrosion on these tests. "Bakelite" pins were installed initially at the joints of the loading arms to isolate the specimen electrically from the rest of the apparatus. Since these pins expanded during exposure, they were replaced with loose-fitting stainless steel pins equipped with "Teflon" tetrafluoroethylene fiber sleeves. "Teflon" washers were placed on both sides of each specimen to minimize binding due to build-up of corrosion products. A shield of Type 316 stainless steel was placed over the specimens during each run to eliminate direct impingement of liquid from the sparger, thus minimizing erosion-corrosion.

Loading was checked by using a dummy specimen on which four strain gages were mounted. This specimen was

calibrated by applying known loads with a hydraulic testing machine. A curve of load vs. strain was thus obtained. The dummy specimen was installed at a particular test station and weights were applied until the desired load was indicated. The weights were then removed and the dummy replaced with the specimen of interest. After the specimen broke or the test was discontinued, the load was again checked. In some cases there was a gain and in other cases a weight loss due to the corrosion of the weights and lack of precision in the weighing technique. The average variation was ± 5%.

1) Tests of A212 Steel: ASTM A212 steel had been specified for the walls of all the large pressure vessels needed for GS-process equipment. Although it was assumed that this steel was soft enough to be resistant to sulfide stress cracking, it was considered the most important material in the stress-cracking tests. Experience in the petroleum industry indicated that steels softer than R_c 20 were not likely to show sulfide stress cracking. As usually fabricated, Type A212 steel is well below R_c 20 in hardness.

Results of the tests indicated that A212 steel was resistant to sulfide stress cracking and are shown in Table LIII. Results of individual tests for each material are grouped together. Samples that failed are listed first and are arranged in order of decreasing applied stress. Samples that remained unbroken were also arranged in the same order.

The notched specimens had sharp 60° notches machined into them and were of the same root diameter as the unnotched specimens. The radius of the root of the notch was 0.0005 inch. For the square-notched specimens the cross-sectional area at the reduced section was only slightly greater than for the round specimens.

The samples of A212 steel that were tested showed yield points from 45,000 to 50,000 psi and ultimate strengths of 73,000 - 76,000 psi. None of the sample stressed below the yield point failed. The sample that failed at 50,000 psi did so after almost 10,000 hr of exposure. During this time corrosion of the steel reduced the cross-sectional area of the specimen with consequent increase in unit stress. Since this corrosion was irregular, final stress at the time of failure could not be accurately determined, but is known to be of the order of 50% greater.

2) Type ASTM-193-49T-B7 Steel: This is a chromium-molybdenum alloy steel used for bolting materials in high-temperature service. The ASTM and ASME Boiler Code specifications for Grade 193-B7 steel are wide enough to include AISI 4140, 4142, and 4145 steels under the B7 designations. These designations denote the same chromium-molybdenum base steel with carbon varying from 0.40 to 0.45 respectively.

The bolting material specified for the GS process was important, because these components must be of relatively high strength. In addition to the bolt tests described earlier, dead-weight loaded tests were made on a number of specimens. Some of these were cut from large bolts and others were machined from AISI 4140 steel plate. Most of these tests were on unnotched specimens.

Results as listed in Table LIII are in general agreement with the bolt tests. There was no marked improvement that could be attributed to the fact that the threads were not present to act as stress raisers. This may have been due to the fact that the notches machined into the bolts or notched tensile specimens are quite coarse as compared to the ones that are important in sulfide stress cracking.

Prestrained specimens were loaded in the Baldwin hydraulic tensile testing machine until a reduction in cross section could be observed. This corresponded to approximately 10% elongation of the gage length. Tensile loading was computed using the minimum cross section in the necked region. Although only a few tests were made, the results were in line with what might be expected from the hardness values. The amount of cold-work incident to the prestraining did not cause acceleration of cracking of the specimens softer than R_c 30. All of the specimens that were harder than R_c 38 (VHN 375) and stressed to 30,000 psi or higher failed during the first few hours after the start of the test. Failures occurred at both 35-40°C and at 120°C.

Specimens with hardness values from R_c 29 to 38 showed wide variations in time to failure. Therefore, those specimens in this hardness range that had not failed could not be regarded as safe and immune from cracking. Since no failures were observed for specimens softer than R_c 29, this was indicated as the maximum useful hardness. Because these tests included only a relatively small number of samples, the fact that some bolt samples had failed at slightly lower hardness values was not unusual. It should be noted that the precision of the Rockwell hardness test is ± 2 points.

3) Stainless Steel Specimens: As a check on the material used for tower internal parts, Type 410 stainless steels were tested. Since bend tests of hardened Type 410 stainless steel had shown this material to be quite sensitive to sulfide stress cracking, fully hardened specimens were not included. The annealed unnotched specimens broke at stresses of 70,000 to 80,000 psi, but did not break at lower stresses. Thus it was indicated that annealed Type 410 stainless steel was not likely to fail by sulfide stress cracking at stresses below its yield point.

Two other hardenable grades of stainless steel were tested in the hardened condition. These were Type 329

stainless steel (28 Cr, 4 Ni, 1.5 Mo) and precipitation hardened 17-4 steel (17 Cr, 4 Ni, 4 Cu). Both failed at stresses of 70,000 psi which is well below their corresponding yield points. Hence these alloys could not be recommended for use in the hardened condition.

Tests of austenitic stainless steels, Types 304 and 316, indicated that these alloys are resistant to sulfide stress cracking unless stressed well above their yield strengths. Annealed austenitic alloys are in a metastable condition at room temperature. Cold-working tends to transform these alloys to a magnetic phase, martensite or ferrite[8][31]. It has been suggested by Bowers[3] that martensite is an important factor in sulfide stress cracking. Although the martensite formed in the stainless alloys is soft, hydrogen dissolved in the lattice, together with transformation stresses, may be important in this respect. Although all austenitic samples that failed had been cold-worked, there were also a number of cold-worked samples that did not fail.

Most of the failures observed were transgranular, as shown in Figure 61. However, there was some evidence of shallow intergranular attack on some of the sensitized specimens, as shown in Figure 62. The time to failure for these alloys varied widely as had been observed for other steels. Most of the rapid failures showed transgranular cracking. The pair of Type 316 stainless steel specimens stressed to 70,000 psi and exposed for 5000 hr did show marked differences. At the end of 5000 hr there was some reduction in stress because of the excessive scaling of the loading device which tended to wedge the weight arms in place for both samples. Although the annealed sample showed only shallow transverse cracking, the sensitized specimen loaded to the same stress showed shallow intergranular cracking and several areas of deep penetration, Figure 63. Although the specimen appeared intact, it broke as it was removed.

Other types of test samples, as well as certain plant items, have shown this same deep intergranular penetration. Bend tests, bubble caps, cold-drawn tubing, heat-exchanger slip tubes, and stressed strongbacks have shown this type of failure. Typical examples of these cracks are shown in Figure 64-66. Although some of the grains were encircled, there was none of the grain dropping that is observed at surfaces of sensitized samples exposed to nitric acid. All of the samples that have shown this deep intergranular penetration have been severely sensitized. Sections cut from near the cracks have shown corrosion rates of from 0.002 to 0.05 inch/month in the nitric acid test. Results of the metallographic examination of various stainless steel specimens used in the sulfide stress cracking tests are shown in Table LIV.

This cracking was irregular, so that the minimum conditions for intergranular cracking were not precisely determined. Rather extensive tests would be needed to determine the relative effects of applied stress, cold-work, and sensitization.

4) Other Materials: A few high-spot tests were made of several other alloys. These are listed at the end of Table LIII. Both "Inconel-X" and "K-Monel" withstood cracking under loads of 100,000 psi. "K-Monel" showed evidence of corrosion but the "Inconel-X" was only slightly tarnished after 4400 hr. These results are in agreement with the bolt tests.

b. Bubble-Cap Failures

After startup difficulties were encountered in the first unit at the Dana Plant, the equipment was opened for inspection. Examination of the Type 410 stainless-steel tower hardware indicated that 20% of the caps had cracked at the skirt. Approximately one per cent of the caps had fragmented, cracked at the shoulder and crown, thus dropping the attached chimneys from the caps, leaving open holes in the plates. Since these open holes would drastically reduce tower efficiency, it was important that all crown-cracking be prevented.

Several aspects of this problem were attacked:

a) Metallography of the failed caps was undertaken to determine the nature of the cracking and heat treatment required to prevent future cracking.
b) A magnetic inspection procedure was worked out to check the effectiveness of the heat treatment mentioned above.
c) Cracking tests were made under simulated hot-tower (HT) and cold-tower (CT) conditions, using caps which were the hardest ones that could be found in subsequent units.

1. Metallographic Study: Metallographic studies indicated that heat treatment of Type 410 stainless steel for this application was the critical factor. Type 410 stainless steel is very sensitive to sulfide stress cracking. Any parts of the caps harder than R_C 20 are likely to fail when stressed and exposed to wet H_2S. For adequate stress relief of the formed caps, they must be heated into the range 1250°F to 1400°F. Air cooling is satisfactory on cooling from temperatures in this range. If any part of the caps are heated to 1450°F or higher, however, air hardening may occur. Any hardened caps must be heated to at least 1450°F (preferably 1500°F) and cooled slowly to 1200°F to reduce the hardness and minimize cracking susceptibility.

Since all of the fragmented caps were found to be harder than R_c 20, it appeared that the stress-relief heat treatment had been responsible. An investigation of the heat-treating facilities at the supplier's plant showed that the control of flame adjustment and the thermocouple location were such that local cap over-heating might have occurred.

All of the Type 410 stainless steel hardware was removed from the first four units and heat-treated as required. Sample caps from each heat-treatment batch were selected and tested for Rockwell hardness. These test samples were all shipped to the Engineering Research Laboratory and held for reference until the towers were functioning properly. No subsequent cracking has been observed.

2. Magnetic Comparator Testing: In order to minimize the time required for hardness checking at the plant, a "magnetic comparator" was obtained from the Magnetic Analysis Corporation.

The Magnetic Comparator is an electronic device which utilizes magnetic properties as a means of distinguishing between materials. It depends for its operation on the fact that small changes in microstructure and of hardness of magnetic materials cause major changes in magnetic susceptibility. In practice the instrument does not measure magnetic susceptibility in absolute terms but compares the response between two geometrically and electrically similar coils into which are inserted the standard and the unknown parts respectively. The coils are opposed to each other electrically. Because the magnetic susceptibility of the specimens determines the deterioration of the magnetic field, and hence the current in the coils, it is possible to compare the specimens nondestructively by means of a current measurement. Characterization of the instrument indicated that it was possible to appraise the hardness of Type 410 stainless steel bubble caps to $\pm$ 3 units R_b.

By using a coil designed for testing bubble caps, it was possible to check unknown caps in place at a rate of more than ten per minute. Thus it was possible to test a sufficiently large sample of the caps to make a statistically sound estimate of the number of hard caps to be expected.

No hard caps were found among those heat-treated and sent back to the plant. In subsequent plant units no caps harder than R_b 95 were found. Thus the hardest caps in these units were softer than any of the fragmented caps that had been examined, indicating that originally the stress-relief treatment had been adequate on these caps. Further heat-treatment of these caps was considered unnecessary. Costs of removing, heat-treating, and replacing the caps in these units were therefore saved.

3. Laboratory Cracking Tests: Twelve of the hardest caps found among the 10,000 tested in the last units to be erected were received at the Engineering Research Laboratory for evaluation. These were loaded by bolting them to small plates to simulate service conditions. Loads applied were high enough to depress the centers of the caps, 0, 1/32, 1/16, and 3/32 inch. This was intended to bracket the hold-down stresses that might be encountered in service. Other caps included in the tests were ones that had been fully hardened and others that had been spot hardened at the shoulder. All of the hardened caps cracked. None of the caps from the fifth and sixth units showed any cracks during the year they were in test. Corrosion rates were relatively high on the caps exposed to cold-tower (CT) conditions. These tests were interrupted thirty times during the year for inspection of the bubble caps and testing of the bolts included in the same autoclave.

4. Summary:

a) All Type 410 stainless steel bubble caps that showed crown cracking had maximum hardness values of R_c 21 (R_b 99) or higher.
b) Stress relief of Type 410 stainless steel bubble caps should be done at 1250 to 1400°F with rigid inspection to eliminate any hardened ones. By stress relief at 1200°F drawn caps were softened to hardness values of less than R_b 90.
c) By using R_b 90 as a maximum acceptable hardness crown cracking should be eliminated.

c. Miscellaneous Stress Corrosion Tests

In addition to the bolts and the dead-weight-loaded specimens several other types of stress-corrosion tests were made. Various components were checked to determine whether certain defects observed might result in early failure. Tests useful in petroleum applications were checked to see how both materials and tests were affected by GS-process conditions.

1. Beam-Deflection Tests: Beam-deflection tests have been used to study stress-corrosion in other systems. Scheil[26] mentioned their use for austenitic alloys. They were also used by Fraser and Treseder[10] and Vollmer[34] for tests in various sour-gas installations. The jigs used thin strip samples and provided means for controlled bending as cantilever beams to apply known stresses. With the jig shown in Figure 67 a specimen 2 inches long was supported on glass-covered pins 1.750 inches apart. Loads were applied to the center of the sample through a glass bead that could be placed with a screw. Deflections were measured with a dial gage and the maximum fiber stress computed.

Types 304, 316, and 410 stainless steel and A212 carbon steel were included in the first set of tests. Each set included three samples stressed to 20,000, 30,000, and 40,000 psi. Stressed specimens were exposed to H_2S-H_2O at 15 psi and 100°C. No cracks were observed on any of these after a total of 4300 hr. Tests were then discontinued.

A series of hardened AISI 4140 steel samples were also run. Results of these tests are listed in Table LV. These tests indicated that AISI 4140 steel hardened to R_c 54 would crack when stressed to 50,000 psi and tested at 30°C. At lower stresses, no cracks were observed. At 120°C, duplicate samples did not crack. Hardened bolts broke at 120°C. Since the results indicated this test to be less drastic and representative than the bolt tests, the beam tests were discontinued. Bolt tests appeared to be more severe, and a closer approximation to direct service tests.

2. Cracked Chimneys: Examination of the Type 410 stainless-steel bubble-cap chimneys at the Dana Plant indicated that some were cracked at the sharp bends on receipt. Several of these were sent to the Engineering Research Laboratory to determine if exposure to H_2S would extend the forming cracks and render the chimney defective. One chimney was exposed for 4,000 hr to H_2S at 100°C and 15 psi and for 2,000 hr to H_2S at 120°C and 250 psi. Although there was some general corrosion, no increase in the crack size was observed.

3. Tray Clamps: Forming cracks were found in a number of Type 410 stainless-steel L-shaped clamps which are used in the trays for the towers at the Dana Plant. A dozen of the clamps were subjected to cracking tests. They were bolted together in pairs, loaded so that they were deformed in the direction of loading, and exposed to simulated hot-tower and cold-tower conditions. Although the loading tended to open up the corner cracks, no further cracking was observed. Total exposure times were over 2,000 hr at both hot- and cold-tower conditions. Shallow pitting and general corrosion were evident although the cracks did not increase appreciably in size.

4. Strongback Tests: Strongbacks, or spreaders, were a part of the bubble-cap assembly considered vulnerable to stress cracking. These were the "T"-shaped clamps used to attach the bubble caps to the chimneys, or risers. The strongbacks used at the Savannah River Plant consisted of two strips of Type 304 stainless steel sheet spot welded together after being formed around the head of a bolt. There were several sharp corners at which stress concentrations might occur.

Annealing at 1900°F was specified to minimize residual stresses in the fabricated strongbacks. This treatment was satisfactory when both the crossbar and the bolt were

austenitic stainless steel. However, some of the bolts in the first shipments of strongbacks were Type 410 stainless steel. To avoid hardening these bolts, stress relief at 1400°F was specified. This compromise heat treatment minimized hardening of the bolts, but sensitized the Type 304 stainless steel without fully relieving the stresses due to cold work. The four strongbacks tested which contained Type 410 stainless steel bolts broke during tests at about 40°C. Nitric acid corrosion tests of the sheet stock away from the welds indicated that all four had been sensitized. Test data were listed in Table LIV. Cracking in all of these samples was intergranular, as shown in Figure 65.

Four strongbacks made from Type 304 stainless steel only were also tested. Two were annealed, and two were tested in the as-welded condition. These were designed with more generous radii and thicker sections so that less cold work was needed for forming. All were stressed to a deflection of about 10 mils at the center. No cracking was observed on any of these specimens after 3,000 hr exposume to H_2S-H_2O at 250 psi and 40°C. Tests were then discontinued. Annealing was indicated as the best procedure to eliminate the apparently adverse effects of cold-work and sensitization on sulfide stress cracking of austenitic stainless steel.

5. Hardened-Steel Specimens: Several types of hardened-steel specimens cracked during tests in simulated GS conditions. Unstressed specimens of relatively high hardness such as an AISI-52100 steel ball bearing, steel spring, molybdenum hack-saw blade, and a file did not crack during a 160 hr exposure to 15 psi H_2S-H_2O at 100°C. AISI-52100 steel is a 1% carbon 1.5% chromium steel with high hardness (R_c 60-65) and good wear resistance. The steel spring was a high-carbon steel hardened to R_c 50. The hack-saw blade was made from molybdenum high-speed steel (a typical analysis for which is 8% molybdenum, 4% chromium, 2% vanadium, and 0.85% carbon) hardened to R_c 60. The file used was of high-carbon steel of approximate R_c 65 hardness. However, the spring and the saw blade both cracked during the first period when they were strained. In other tests one of a pair of loaded ball bearings broke although they were only lightly stained by the corrosion.

During exposure tests of high-speed steel, cracking was observed around the impressions from Rockwell hardness tests. The samples were quite hard, R_c 62. It thus appeared that there were appreciable residual stresses in the deformed metal that formed a slight ridge around the impression. During exposure at 25°C and 250 psi the particles spalled from the specimens were of such shapes that they seemed to include all of the deformed metal under the conical hardness impressions.

"Stellite," sintered tungsten carbide, sintered chromium carbide, and "Elgiloy" were the only hard alloys that did not show any evidence of sulfide stress cracking.

6. Hard-Drawn Stainless Steel: Several different types of hard-drawn stainless steel cracked during tests in wet H_2S. In most cases they were so severely cold-worked that the hardness was above R_c 30. They included cold-drawn tubing of Type 316 stainless steel and cold-drawn screen wire.

This observation confirms oil-field experience in which cold-drawn austenitic stainless steel wire is often used for lowering test instruments into oil wells. To minimize cracking in sour wells, the wires are discarded after 24-hr total exposure.

7. Slip-Tube Failures: In heat exchangers with floating tube sheets, "slip tubes" are used to carry the tube-side medium through a packed gland in the head. In this process stainless steel was specified for tubes or overlays because its surface would remain smooth and not damage the packing due to its movement. Several stainless steel slip-tube failures were encountered at the Savannah River and Dana Plants.

In typical failed slip tubes received at the Engineering Research Laboratory for examination, imposed stress and sensitization appeared to be important factors. Most of the cracks were intergranular in all of the specimens examined. All of the steels were severely sensitized as a result of the stress-relief heat treatment used for the carbon steel components. Consideration of the geometry of the different designs indicated that the cracks were approximately perpendicular to the tensile stresses.

This type of cracking is difficult to predict because many of the slip tubes in other heat exchangers were of the same design and received similar treatment but did not fail. The apparently erratic behavior was probably due to slight differences in conditions that were not readily apparent.

a) Joint Details: Six defective slip tubes found at the Dana Plant were composed of stainless steel sleeves that were slipped over relatively thick steel tubes and welded at both ends. Four of these had been fabricated by American Locomotive Company (ALCO) and two by the M. W. Kellogg Company. Stress relief for 2 hr at 1150°F was specified by both suppliers.

Check analyses of the two Kellogg tubes indicated that they were of AISI Type 304 stainless steel rather than Type 316 stainless steel.

Six defective slip tubes reported by the Savannah River Plant were made by C. F. Braun Company. They consisted of 16-1/2-inch diameter tubes of Type 304 stainless steel that were welded into the plain carbon-steel floating heads of the primary-condenser (PC) heat exchangers. The steel in the floating heads was 1-3/4 inch thick and the tubes were specified as 5/8 inch in thickness. However, the two specimens received from the Savannah River Plant had been made from 3/4-inch plate. After forming the plates into tubes, the tops had been bored in order to obtain good fit-up to the floating heads. This procedure assisted in fabrication of the units but introduced additional sharp changes in cross section. Stress relief of 2 hr at 1050°F was reported by Braun.

b) Weld Metal: Weld-metal samples from the two joints from the Savannah River Plant were both 25 Cr - 20 Ni stainless steel as required by the specifications. The high-alloy rod was used to weld the stainless steel to plain carbon steel in order to minimize dilution and hardenability effects.

The cracked specimens from the Dana Plant did not include any of the weld deposit.

c) Dilution Effects: In welds used to join plain carbon steel to stainless steel it is obvious that a concentration gradient must exist. The weld deposit composition must be an average of the fused portions of the two plates and of the filler rod used. By using high-alloy welding rod, austenitic weld beads must be deposited. The most desirable structure for such welds is austenitic with a small amount of ferrite. Such a structure has good high-temperature ductility and hot strength thus avoiding cracks in the weld. It will not harden during cooling.

In order to check the condition of the joints above, a series of hardness traverses was made across the welds and heat-affected zones. The highest hardness encountered was R_b 91 which is very close to the hardness of 25-20 weld metal. In order to check the possibility that the weld might have contained a hardenable zone that was drawn back by stress relieving, another section was heated to 1600°F and air-cooled. Again the highest hardness encountered was R_b 91 indicating this effect to be unimportant in the present case.

d) Crack Detail: In all the failed slip tubes examined, the main cracks were in the stainless steel approximately parallel to the circumferential weld. In most cases there were other branching cracks perpendicular to the main ones. Only a few of these extended into the weld zones.

A typical crack is shown in Figure 66. Almost all of the cracking was intergranular, with considerable grain

encirclement. The cracks did not form the straight lines with "chevron" branching that is often observed for chloride stress-corrosion cracking.

e) Stress Relief: As a check on the heat treatments used during fabrication of the slip tubes, nitric-acid tests were made of the three samples examined at the Engineering Research Laboratory. Corrosion rates of 0.080, 0.035, and 0.045 inch/mo were observed. These relatively high rates indicated that the stainless steel had been severely sensitized. Corrosion-testing experience with various 18-8 alloys indicates that heat treatment for 1 to 4 hr at 1000-1100°F produces only mild sensitization and that corrosion rates in the range of 0.001 to 0.003 inch/mo might be expected. Severe sensitization usually occurs when 18-8 stainless steels are heated in excess of 1100°F. These tubes may have been so heated during stress-relief heat treatment.

Heating for hot forming might have caused this sensitization. Although no information was available on this point the tubes may have been heated into the sensitizing temperature range to facilitate fabrication. Such hot forming would not be detrimental if the welded tube were subsequently annealed.

f) Discussion: The geometry of these particular joints appears to have been important in the cracking of the slip tubes mentioned above. In both types, the A212 steel section near the weld was more massive than the stainless steel. Hence differential shrinkage during cooling from stress-relief temperatures would develop higher unit stresses in the stainless steel than in the plain carbon steel.

When steel parts containing residual stresses are heated, these stresses tend to be relieved by local yielding. These stresses often result from the extremely sharp temperature gradients that occur during welding. Such stresses may approach the yield point at room temperature. As a welded vessel is heated to 1100-1400°F the metal tends to distort to relieve these residual stresses. Since the yield point for steel drops to 10 or 20% of its room-temperature value in the stress-relieving temperature range, the residual stresses would usually be reduced to rather low values.

With a duplex structure containing both plain carbon steel and stainless steel, stress relief would be expected at the elevated temperatures. However, during cooling, the stainless steel, with its higher coefficient of thermal expansion, would shrink more than the ferritic steel. Thus a differential shrinkage of 0.002 inch/inch would be expected to exist between these materials on cooling from 1200°F to room temperature. Based on a modulus of elasticity of 30×10^6 this strain would correspond to a residual stress of 60,000 psi to be absorbed across the joint. Although this figure is only an

approximation, it does indicate that significant stresses can be generated in the stainless steel during cooling. In the Braun design the plain carbon-steel head was rather massive, so that the stresses in the plain carbon steel would be lower than in the stainless steel.

In the ALCO and Kellogg joints that failed at the Dana Plant, the stainless steel formed a relatively thin shell that was placed over the plain carbon-steel tube and welded at both ends. Differential contraction during cooling caused longitudinal stresses to be set up in the stainless steel.

After four of the Braun slip tubes had failed at the Savannah River Plant, a decision was made to alter all 32 of this design. Small longitudinal cracks extending from the weld into the stainless-steel base metal were reported for all of the first 16 slip tubes that were arbitrarily rebuilt. This indicated that these might have failed later; thus, the decision to repair these units was sound.

It was believed that the differential expansion between these materials would be much less important in a butt joint between tubes of similar cross sections. In this case the resultant strain would be distributed between the two materials. Such a design was incorporated into the Savannah River Plant repair.

Although the role of sensitization is not clear, sulfide stress cracking of sensitized austenitic alloys tends to be intergranular. Several other test specimens that showed intergranular cracking were checked and found to be severely sensitized. None of the specimens showed the "sugaring" that is associated with intergranular corrosion of unstressed corrosion samples in other media such as boiling nitric acid. Some samples that were sensitized and severely cold-worked did not show cracking after exposure to H_2S-H_2O. This lack of reproducibility has been reported by Scheil[26] for other stress-corrosion tests of stainless steels.

Additional study would be required to develop a better test for sulfide stress cracking of stainless steel and place more accurate limits on the stresses and heat treatments that can be tolerated without cracking.

d. Summary

1. Results of these tests indicated that GS-process conditions are less severe than conditions in the more troublesome sour crude wells. Corrosion, stress-corrosion, and blistering tend to be minimized by the adherent scale that is built up as corrosion proceeds. The continuity of this scale seems to be a result of the relative purity of the system. Oil-well fluids contain various mixtures of water, scale,

CO_2, H_2S, cyanides, and organic acids. Thus, certain combinations may be mild and others quite severe as regards sulfide stress cracking.

2. Hardened Type 410 stainless steel was quite vulnerable to sulfide corrosion cracking.

3. Forming cracks in annealed Type 410 stainless steel were not extended by exposure to H_2S.

4. Annealing of austenitic alloys minimized sulfide stress-cracking susceptibility.

5. Hardened low-alloy steels did not crack unless an external stress was applied.

6. Cold-drawn austenitic stainless steels were quite vulnerable to sulfide stress cracking.

7. "Stellite," sintered tungsten carbide, sintered chromium carbide, and "Elgiloy" showed no evidence of susceptibility to sulfide stress cracking.

8. Both "Inconel-X" and "K-Monel" resisted sulfide stress cracking at 100,000 psi.

III. BIBLIOGRAPHY

1. Bartz, M. H. and Rawlins, C. E., Corrosion, 4, No. 5, pp. 187-206 (1948).

2. Bastien, P., and Amiot, P., Academie des Sciences, Comptes Rendus, 235, No. 18, pp. 1031-1033 (1952).

3. Bowers, C. N., McGuire, W. J., and Wiehe, A. E., Corrosion, 8, No. 10, pp. 333-341 (1952).

4. Champion, F. A., "Symposium on Internal Stresses in Metal and Alloys," London, Institute of Metals, 468 (1948).

5. Chaston, J. C., "Symposium on Internal Stresses in Metals," London, Institute of Metals, 416 (1948).

6. Dix, E. H., Jr., Trans. AIME, 137, 11 (1940).

7. Evans, U. R., "Metallic Corrosion, Passivity, and Protection," New York, Longmans Green and Co., p. 216 (1946).

8. Fiedler, H. C., Averbach, B. L., and Cohen, M., "The Effect of Deformation on the Martensitic Transformation in Austenitic Stainless Steels, ASM Preprint No. 30, Cleveland, Ohio (1954).

9. Forward, F. A., J. Metals, 5, No. 6, pp. 775-779 (1953).

10. Fraser, J. P., and Treseder, R. S., Corrosion, 8, No. 10, pp. 342-350 (1952).

11. Gifkins, R. C., and Rees, W. P., Metal Treatment and Drop Forging, pp. 109-122, 131, Autumn 1948.

12. Gunnert, R., Welding J., 32, No. 6, pp. 292s-301s (1953).

13. Hafsten, R. J., Proc. Am. Petroleum Inst., 30M (III), pp. 81-87, Refining (1950).

14. Herzog, E., J. Iron Steel Inst., 174, Part 2, pp. 140-142 (1953).

15. Herzog, E., J. Iron Steel Inst., 174, Part 4, 317 (1953).

16. Hetenyi, M., Proc. Soc. for Exp. Stress Anal., 1, No. 1, pp. 147-156 (1943).

17. Jordis, E., and Schweitzer, E. Z., Angew Chem. 23, 583-7 (1910).

18. Keating, F. H., "Symposium on Internal Stresses in Metals and Alloys," London, Institute of Metals, 311 (1948).

III. BIBLIOGRAPHY (Continued)

19. Konrad, E., Chem. Engr. 60, 189 (1953).

20. Lenzen, K. H., Product Eng., 18, No. 12, pp. 130-33 (1947).

21. Mears, R. B., Brown, R. H., and Dix, E. H., Jr., "Symposium on Stress-Corrosion Cracking of Metals," Philadelphia, Pennsylvania, ASTM-AIME, pp. 323-344 (1944).

22. Morton, B. B., Corrosion, 8, No. 10, 358 (1952).

23. Pilling, N. B.; and Bedworth, R. E., J. Inst. Metals, 29, 577 (1923).

24. Prange, F. A., Corrosion, 8, No. 10, pp. 355-357 (1952).

25. Rees, W. P., "Symposium on Internal Stresses in Metals and Alloys," London, Institute of Metals, pp. 333-335 (1948).

26. Scheil, M. A., "Symposium on Stress-Corrosion Cracking of Metals," Philadelphia, Pennsylvania, ASTM-AIME, pp. 395-410 (1944).

27. Seabrook, J. B., Grant, J. N., Carney, D. J., J. Metals, 188, pp. 1317-1321 (1950).

28. Sieverts, A., Z. Electrochem., 16, pp. 707-13 (1910).

29. Stenhouse, J. F., and Armstrong, W. M., Can. Mining Met. Bull. 45, No. 477, pp. 49-53 (1952).

30. Stoeckly, E. E. and Macke, H. J., Trans. ASME, 74, pp. 103-112 (1952).

31. Storcheim, S., Iron Age, 161, No. 7, 140 (1953).

32. Sykes, C., Burton, H. H., and Gegg, C. C., J. Iron Steel Inst., 156, pp. 155-180 (1947).

33. Vollmer, L. W., Corrosion, 8, No. 10, pp. 326-332 (1952).

34. Vollmer. L. W., Can. Mining Met. Trans., 55, pp. 88-95 (1952).

35. Waber, J. R., and McDonald, H. J., Trans. Electrochem. 87, 439-451 (1945).

36. Zapffe, C. A., and Sims, C. E., Trans. AIME, 145, 225 (1941).

FIGURE 1

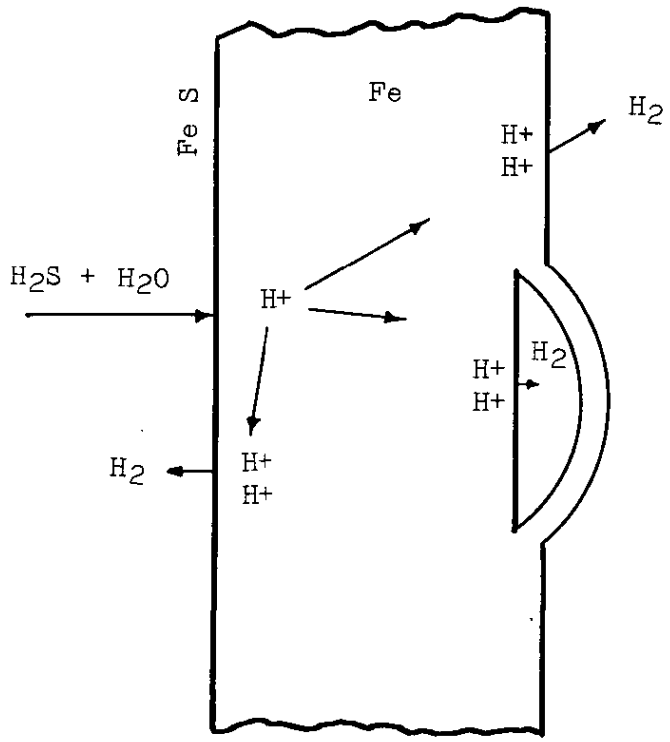

SCHEMATIC REPRESENTATION OF HYDROGEN BLISTERING RESULTING FROM SULFIDE CORROSION OF A LAMINATED STEEL PLATE

FIGURE 2

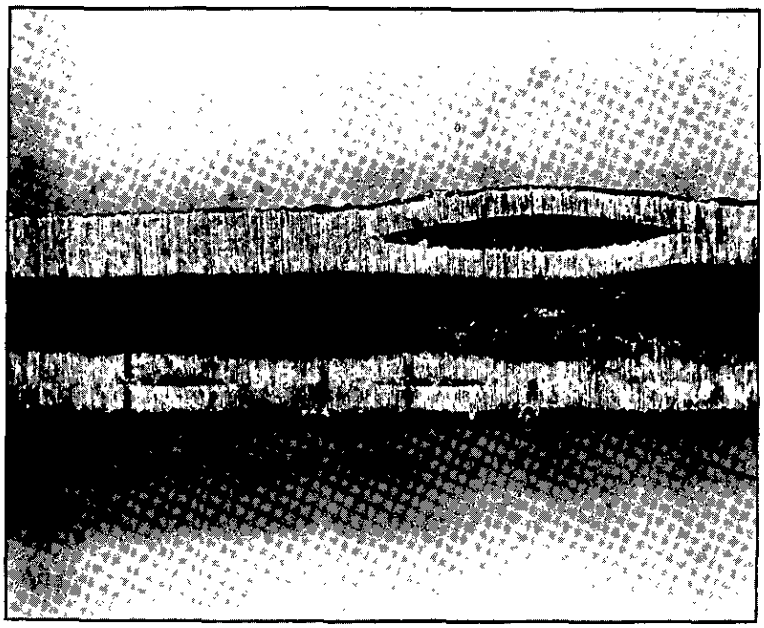

BLISTERS IN STEEL PLATE

AFTER EXPOSURE TO H_2S

FIGURE 3

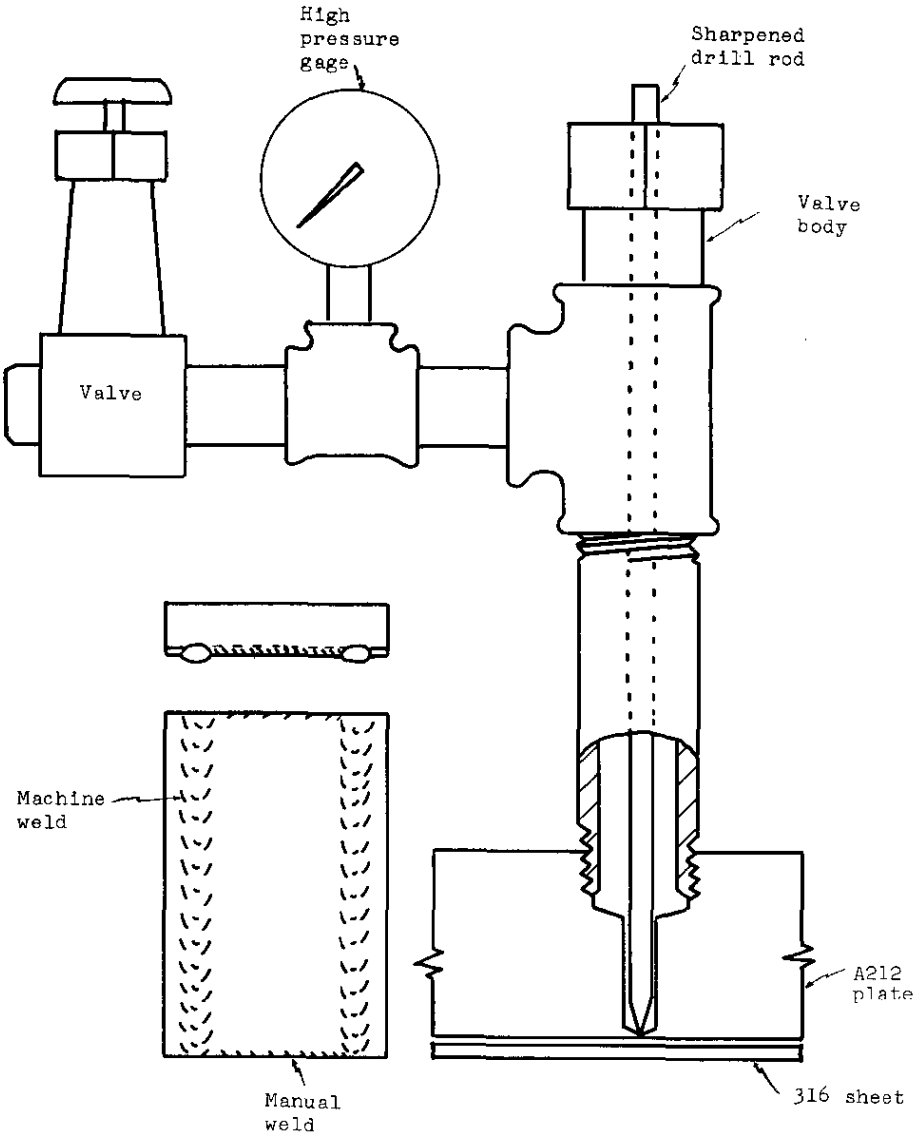

APPARATUS FOR SAMPLING HYDROGEN IN BLISTERS

FIGURE 4

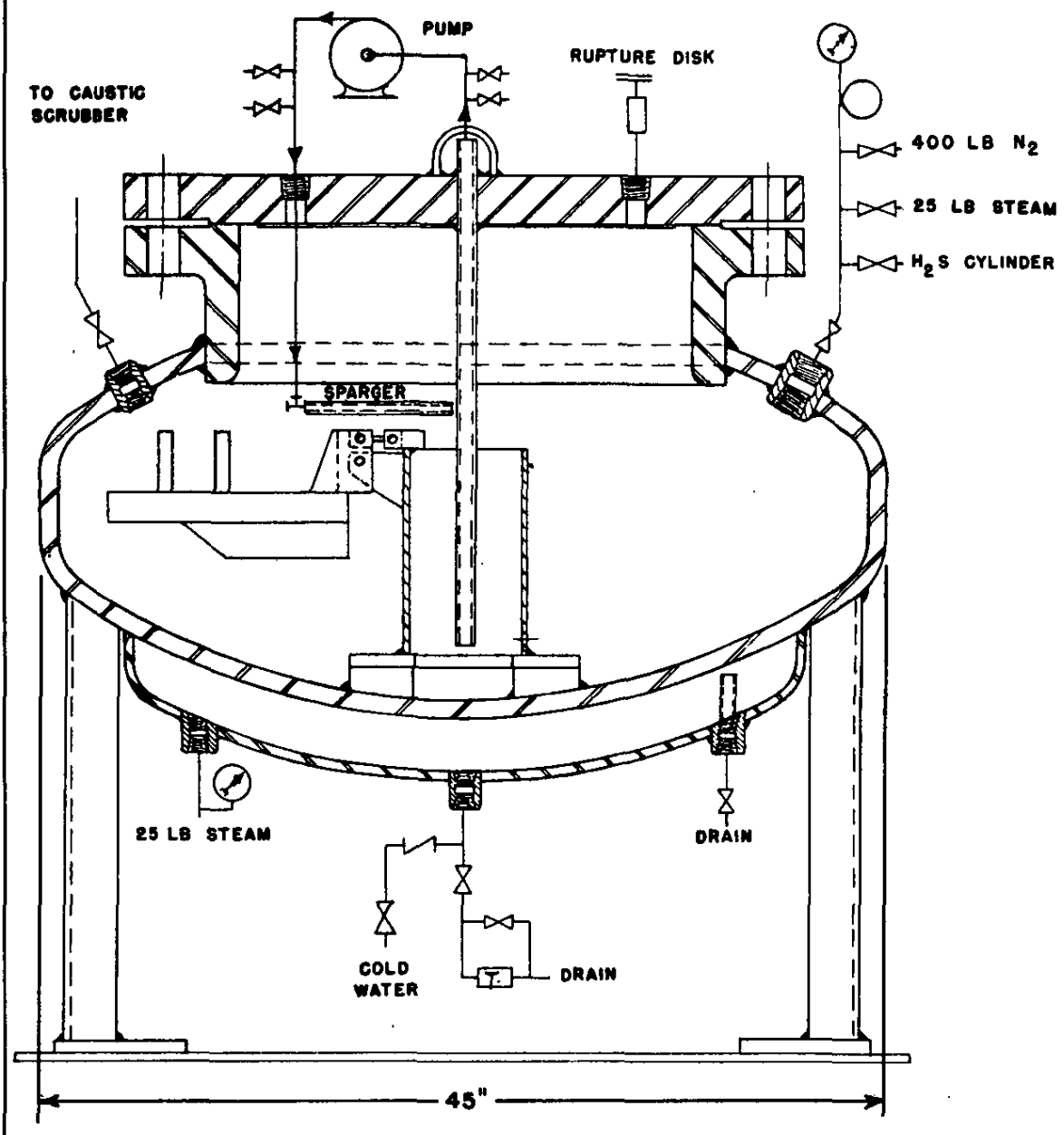

TEST AUTOCLAVE AT THE

ENGINEERING RESEARCH LABORATORY

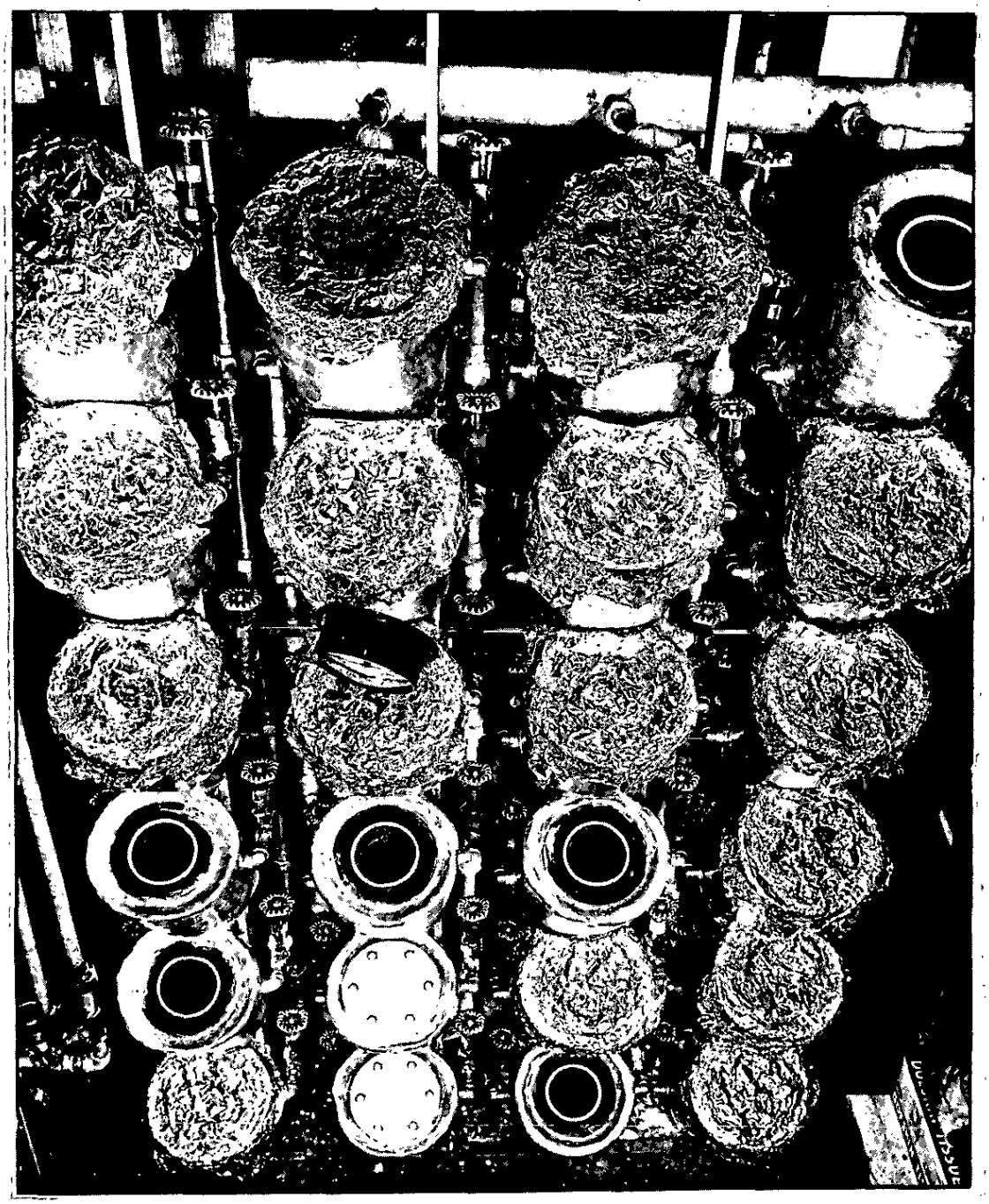

AUTOCLAVES USED FOR CORROSION

INHIBITOR EVALUATION

FIGURE 6

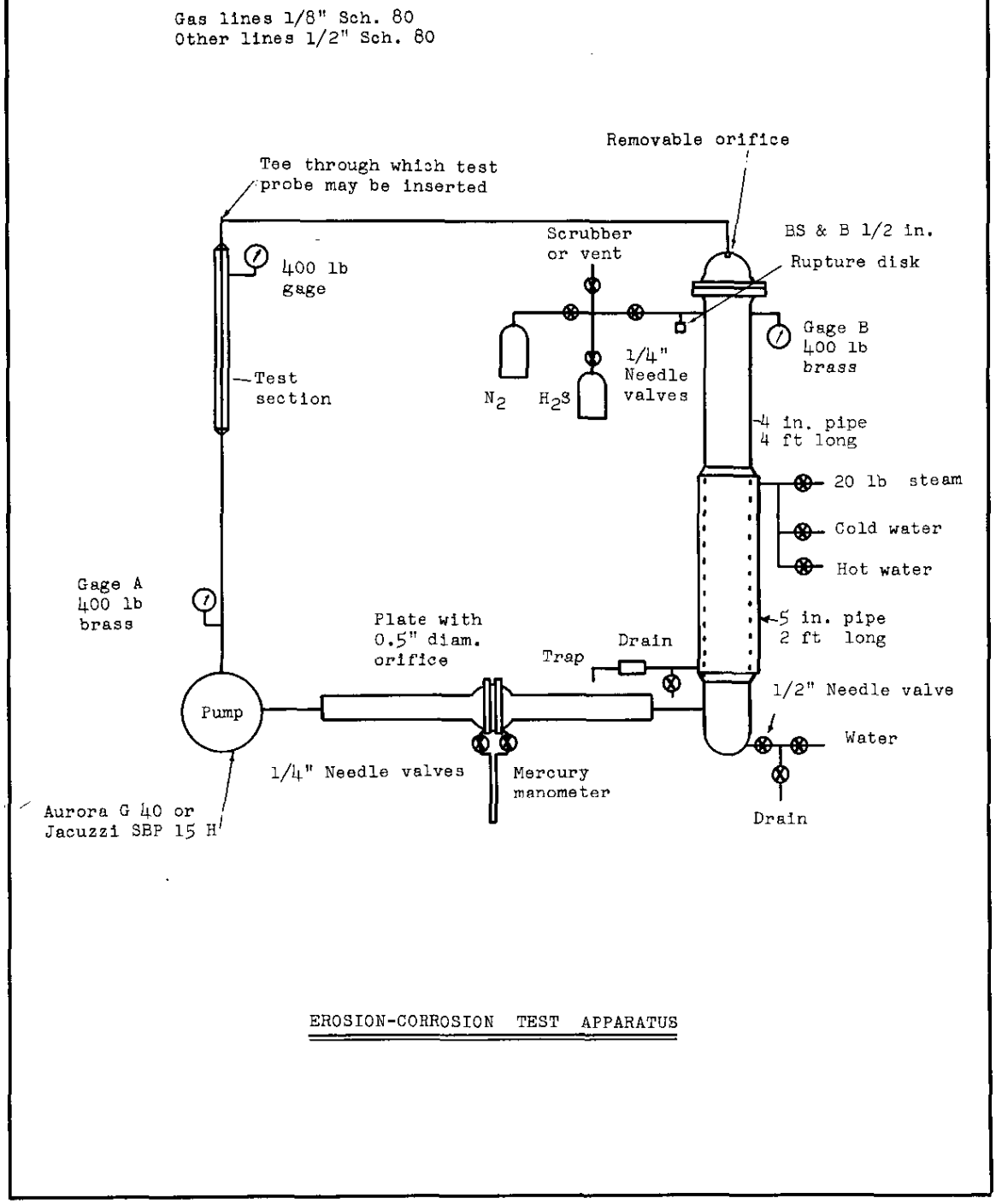

EROSION-CORROSION TEST APPARATUS

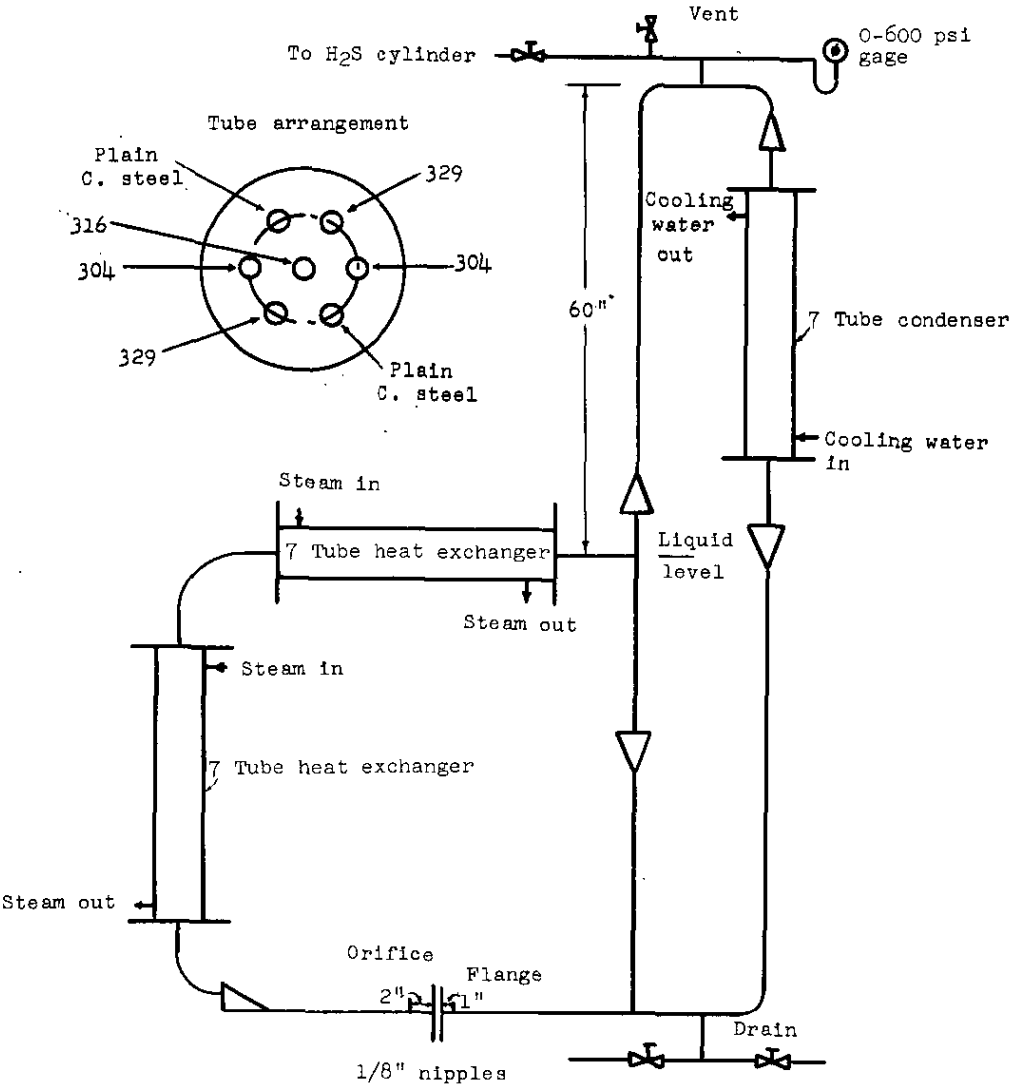

EXPERIMENTAL HEAT EXCHANGER ARRANGEMENT

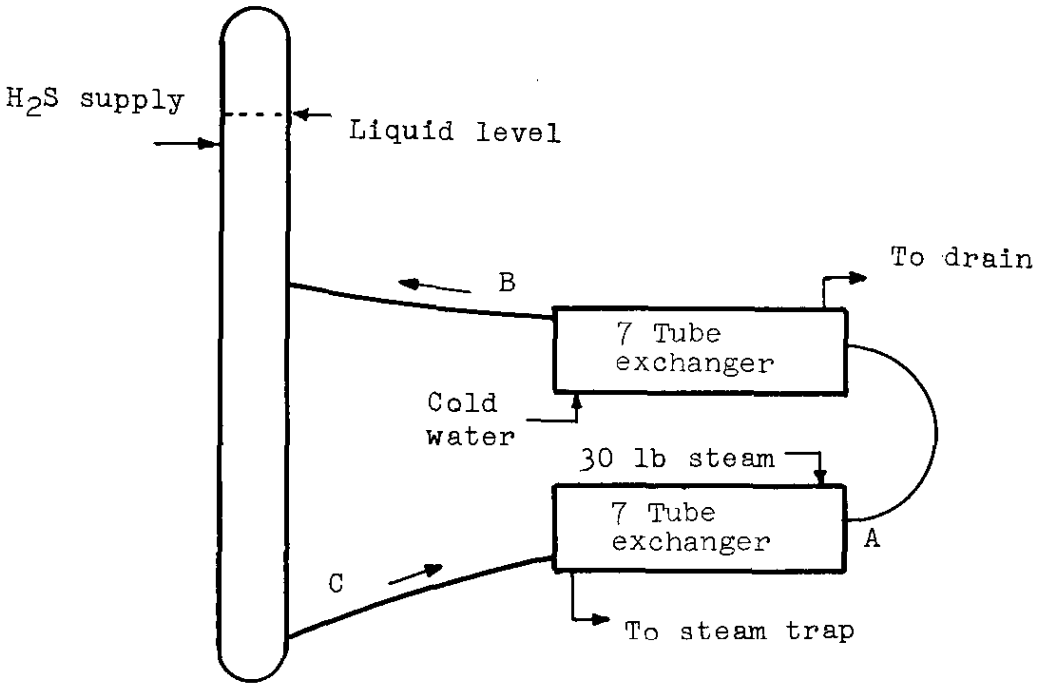

ARRANGEMENT OF SULFIDE DEPOSITION UNIT

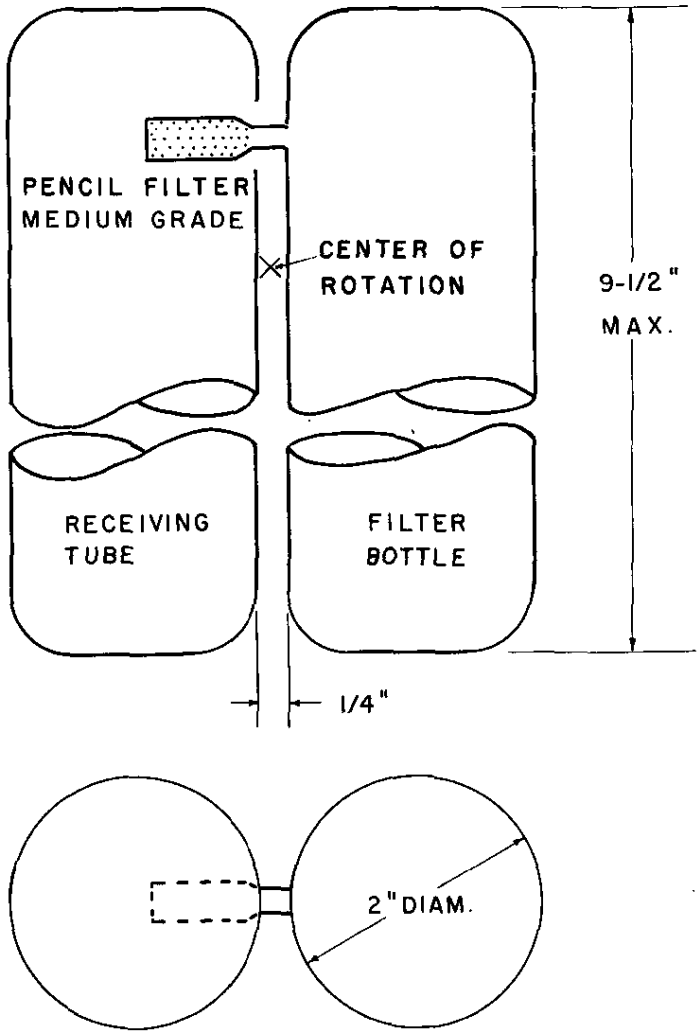

GLASSWARE FOR FILTRATION AT HIGH H_2S-H_2O PRESSURES

FIGURE 9

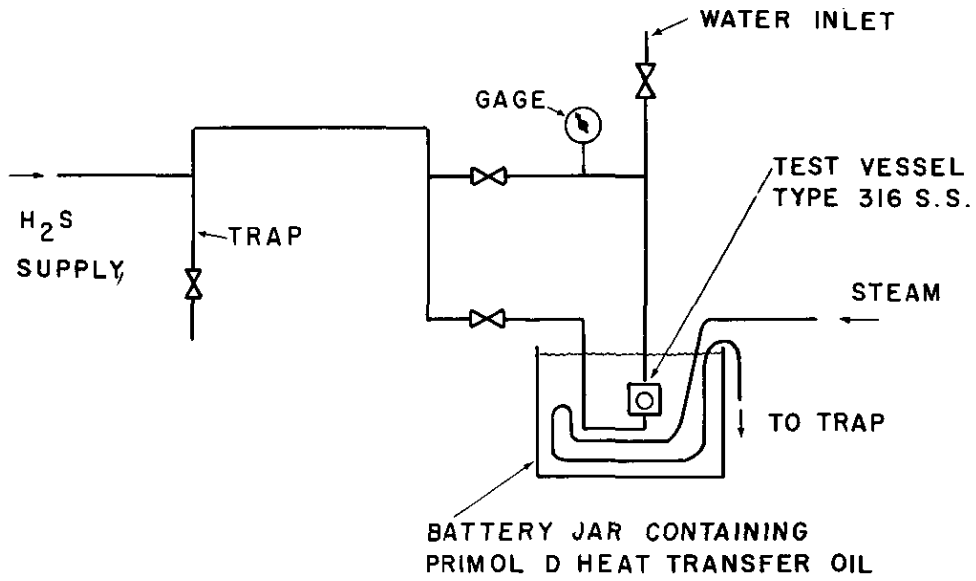

ALL LINES AND VALVES: TYPE 316 STAINLESS STEEL

FIGURE 10

AUTOCLAVE FOR INDICATOR pH TESTS OF H_2S-H_2O SYSTEMS

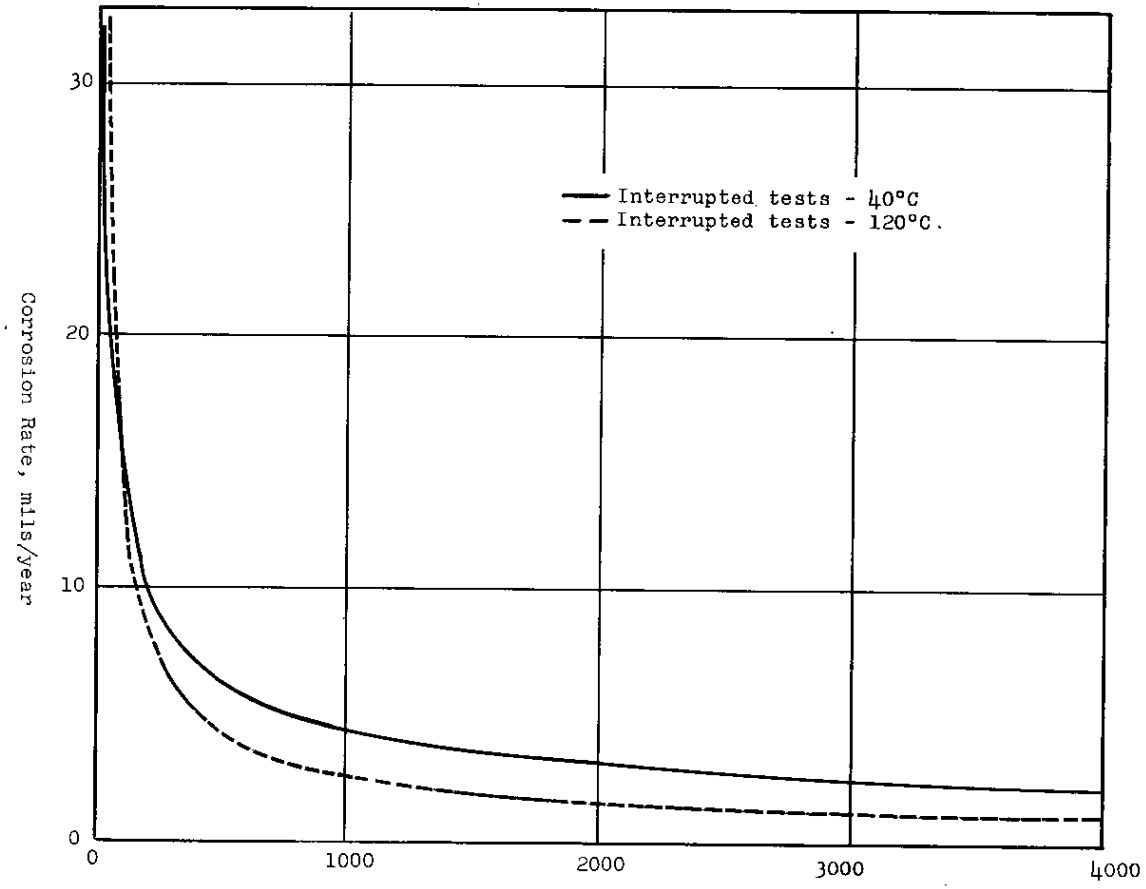

FIGURE 11

EFFECT OF TIME ON THE CORROSION OF PLAIN CARBON STEEL IN THE $H_2S - H_2O$ SYSTEM - INTERMITTENT EXPOSURE

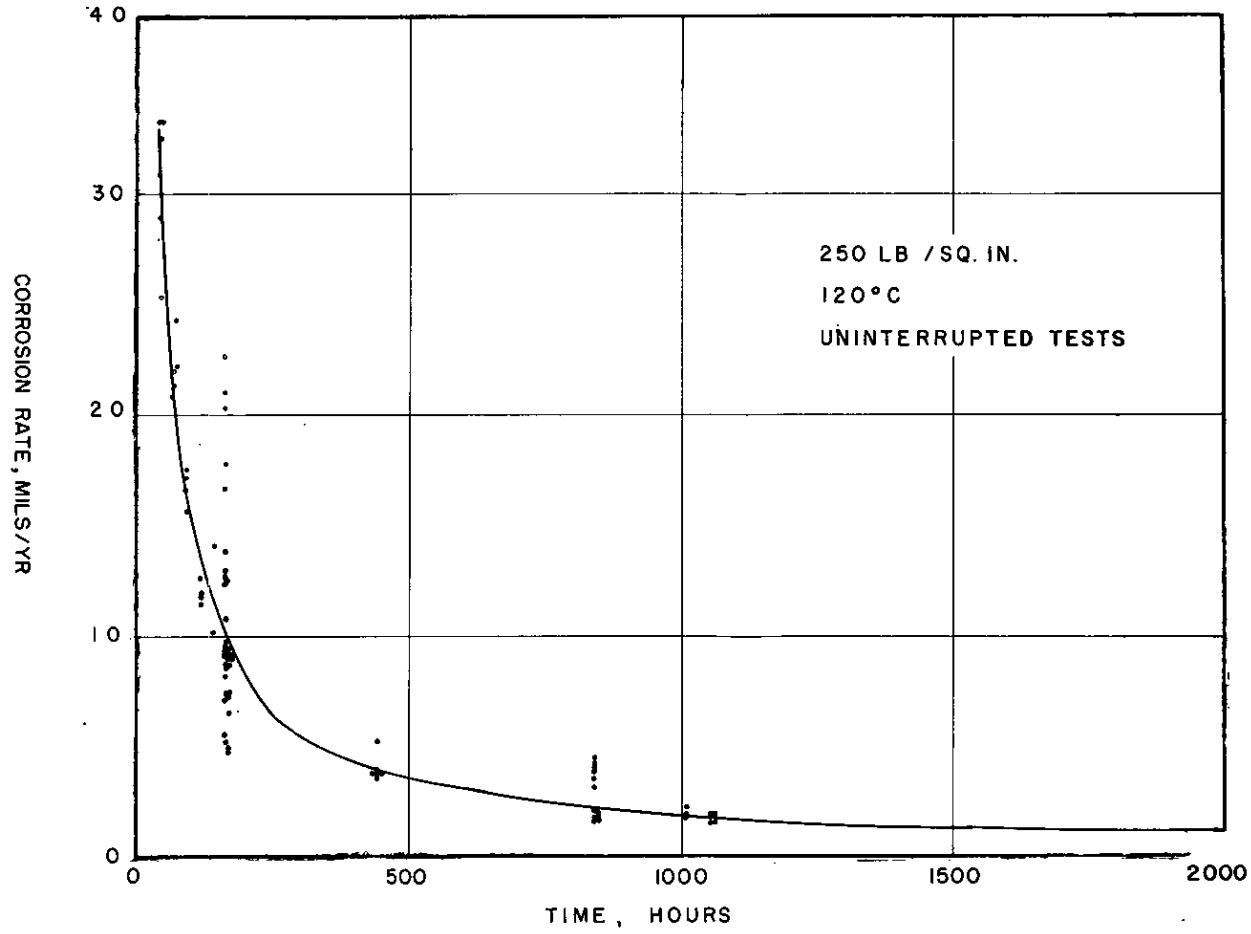

FIGURE 12

EFFECT OF TIME ON THE CORROSION OF PLAIN CARBON STEEL IN THE $H_2S - H_2O$ SYSTEM – CONTINUOUS EXPOSURE

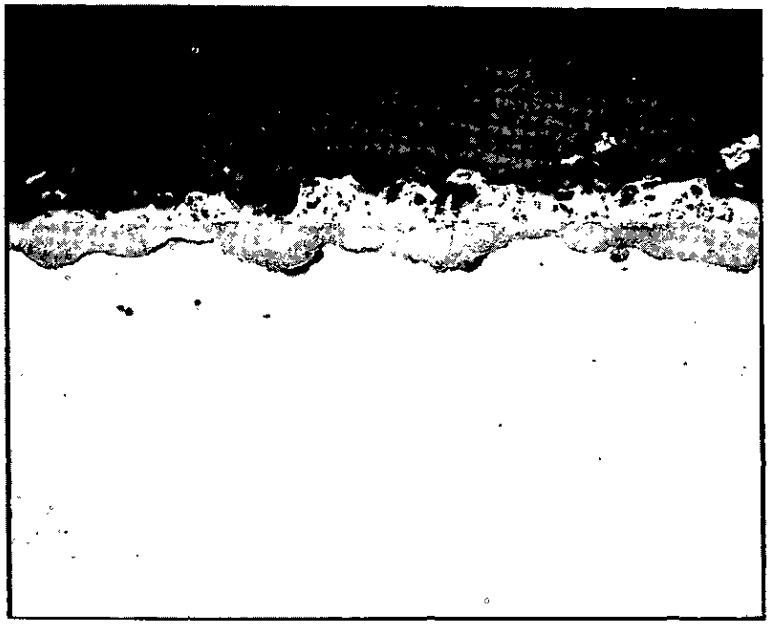

Unetched 100X

FIGURE 13 Cross section of sulfide scale on AISI 4140 steel. Exposed for 330 hr to H_2S-H_2O at 250 psi and 120°C. Stressed at 30,000 psi.

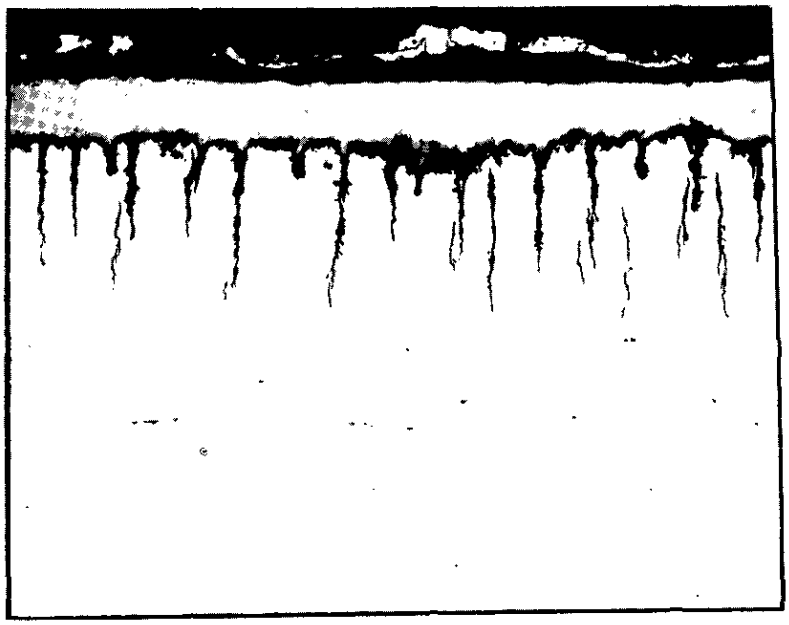

Unetched 100X

FIGURE 14 Finger penetration of steel surface by sulfide scale. AISI 4140 exposed for 1800 hr to H_2S-H_2O at 250 psi and 120°C. Stressed at 79,000 psi.

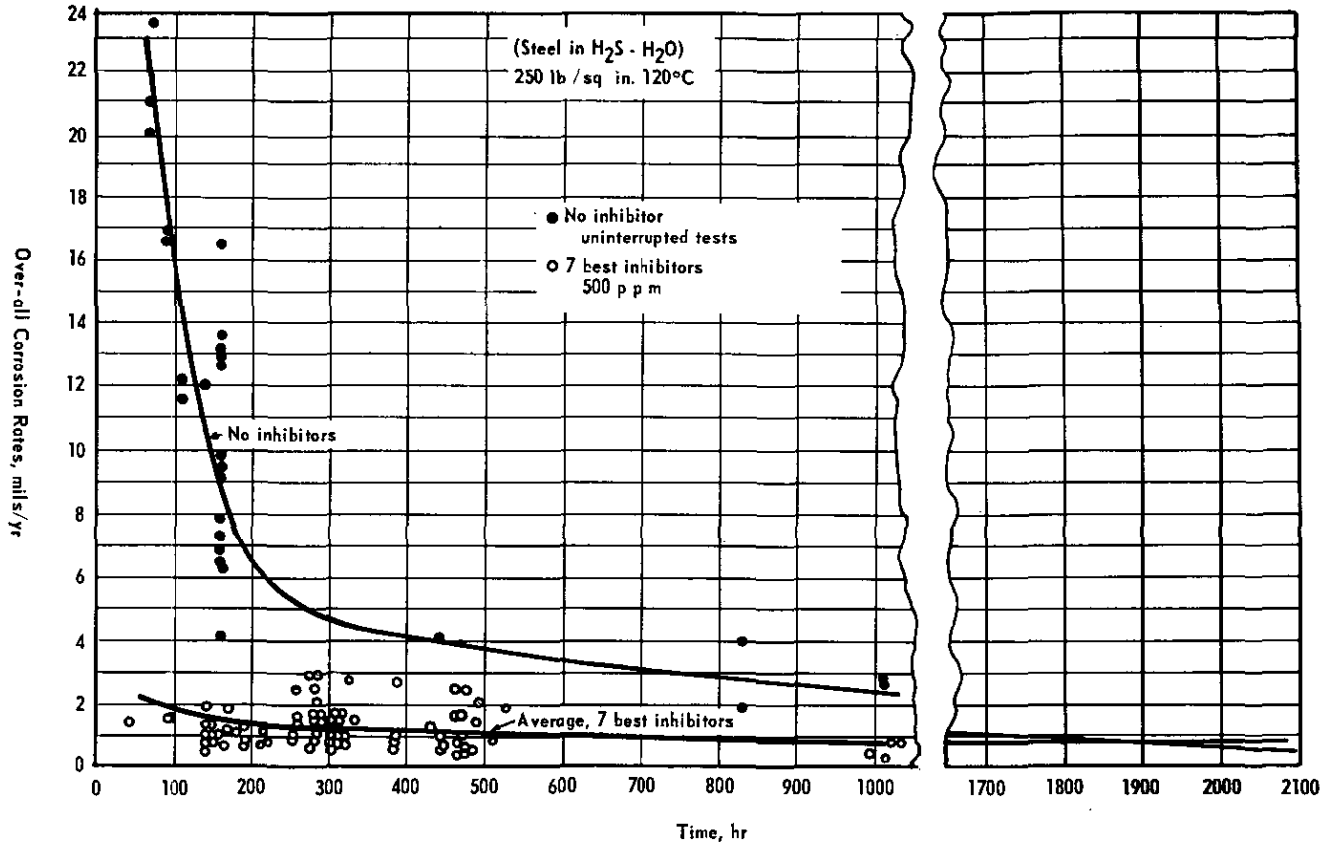

FIGURE 15

EFFECTS OF CORROSION INHIBITORS ON THE CORROSION OF STEEL IN H_2S - H_2O SYSTEMS

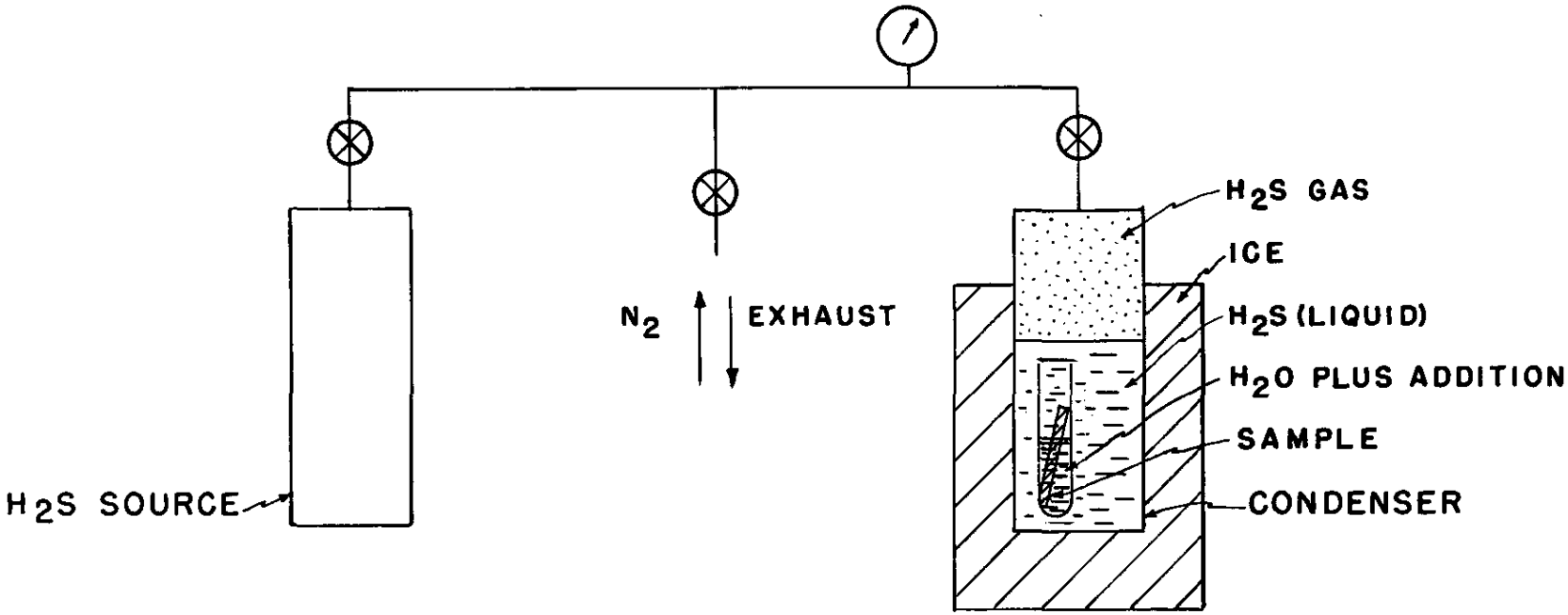

APPARATUS FOR THE DISTILLATION OF H_2S INTO EXPOSURE CONTAINERS

FIGURE 16

FIGURE 17

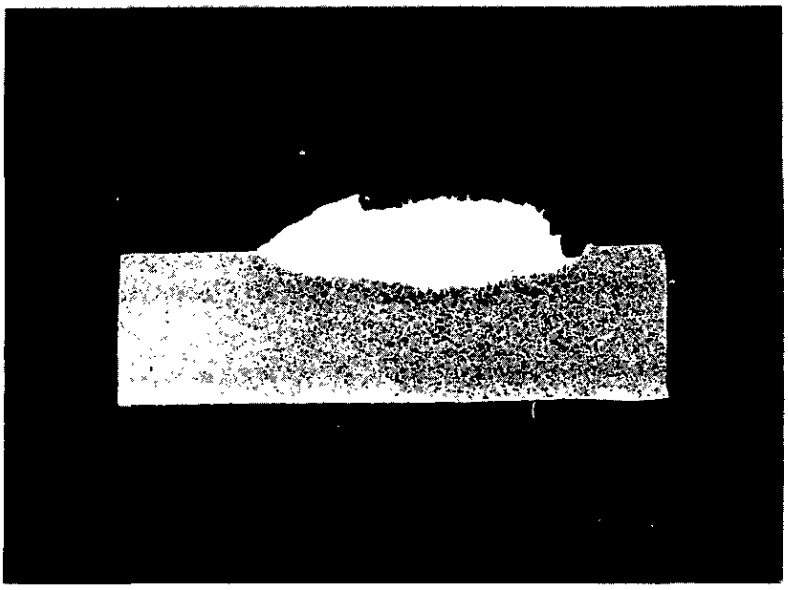

2X

Pitting of weld exposed to liquid H_2S containing aqueous chloride solutions. Fleetweld No. 5 bead on A212 plate. Exposure 5000 hr at 38°C.

FIGURE 18

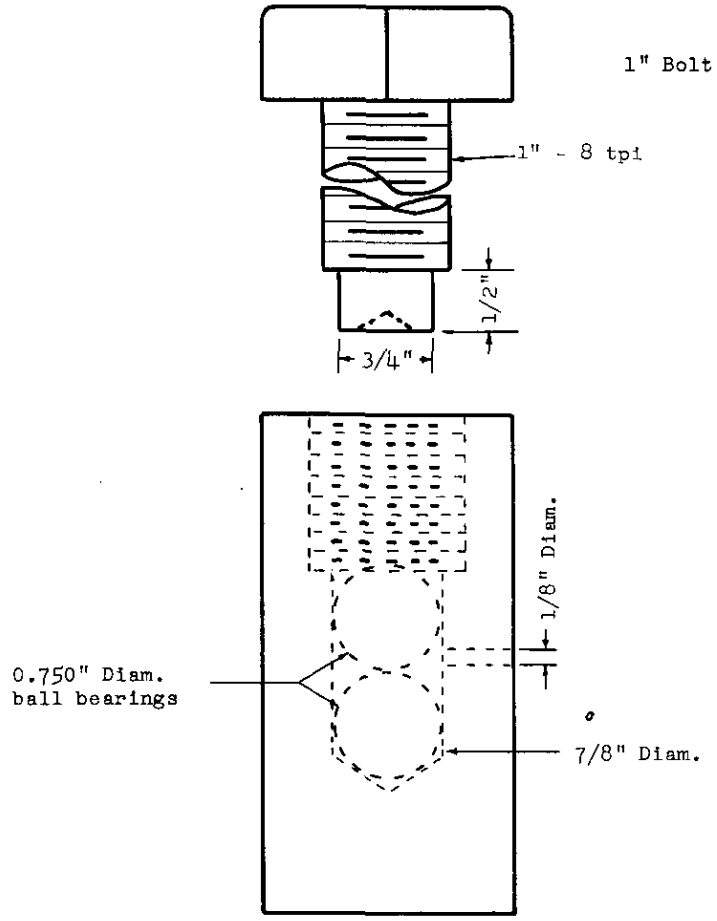

BALL BEARING GREASE TEST UNIT

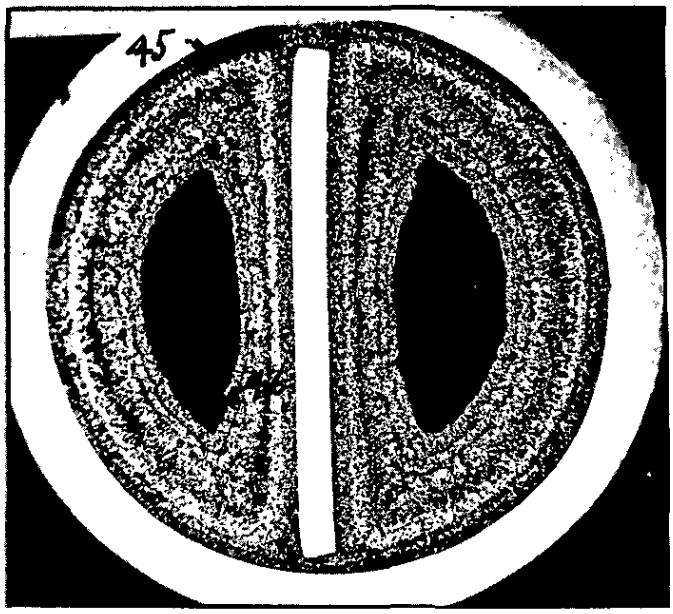

5X

Cross section of typical heat-exchanger tube plugged with sulfide scale. Stainless steel tube from LH 103. Turbulence promoter is shown at the center. Location of Samples 45 and 46 in Table XVIII are indicated.

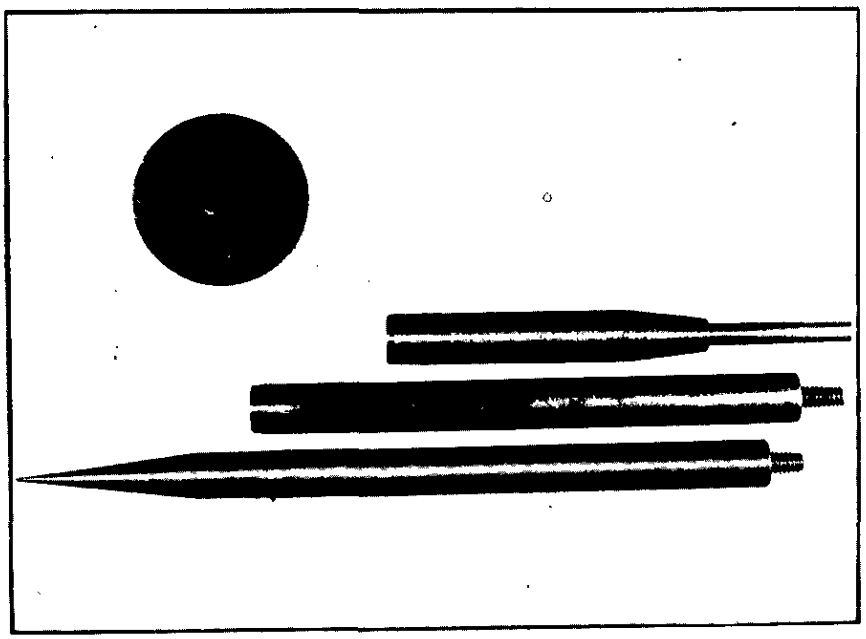

EROSION-CORROSION TEST SPECIMENS

- FIGURE 21

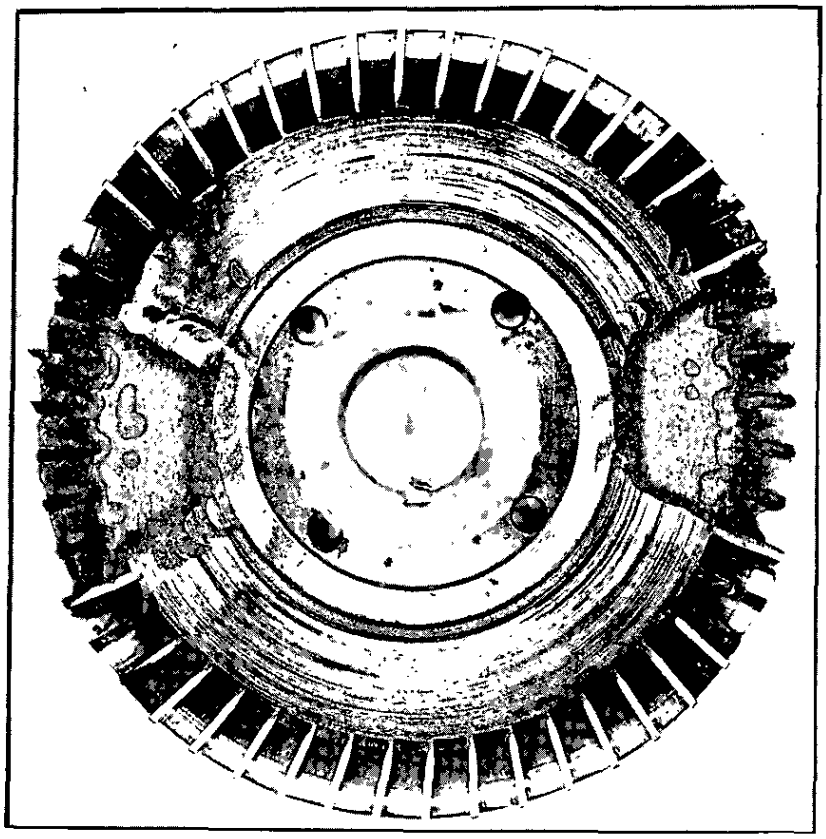

Full Size
Erosion-corrosion of Type 430 stainless steel pump impeller inserts. Type 302 impeller operated at 1750 rpm. Exposed 330 hr to H_2S-H_2O at 250 psi and 40°C.

FIGURE 22

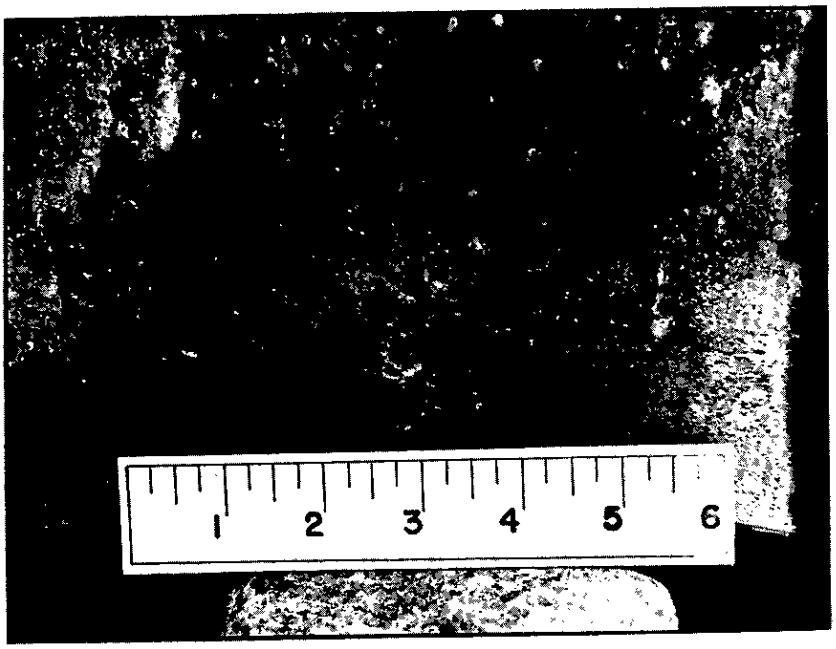

EROSION-CORROSION OF PLAIN CARBON (A212) STEEL

FIGURE 23

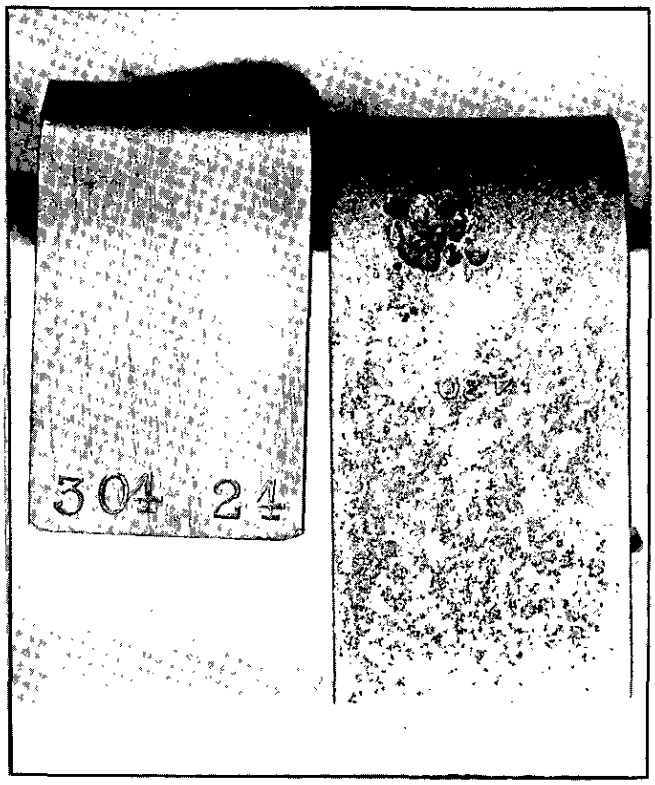

2X

Relative impingement erosion-corrosion of Types 304 and 430 stainless steels. These samples were used to protect the eroded areas shown in Figure 22. Exposed to impingement by H_2S saturated water for 330 hr at 40°C. Pressure - 255 psi.

FIGURE 24

500X

Typical attack of Sil-Fos silver solder near exposed surface

FIGURE 25

500X

Typical attack of Sil-Fos silver solder - 3/8 in. below exposed surface

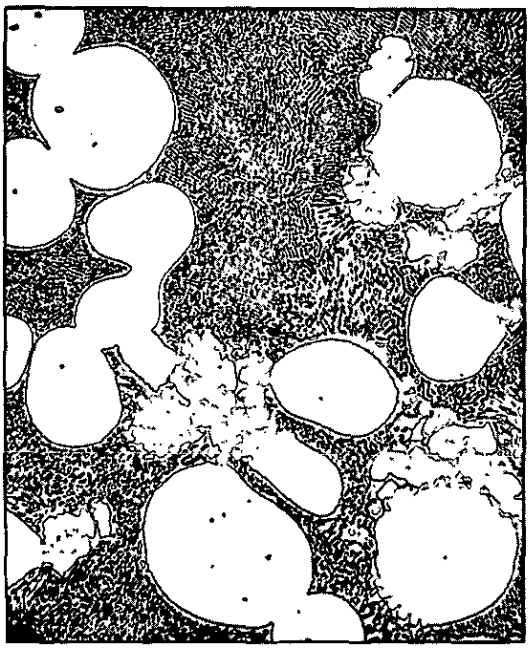

FIGURE 26

500X

Microstructure of as-deposited Sil-Fos silver solder

FIGURE 27

500X

Microstructure of as-deposited Easy-Flo 45 silver solder

FIGURE 28

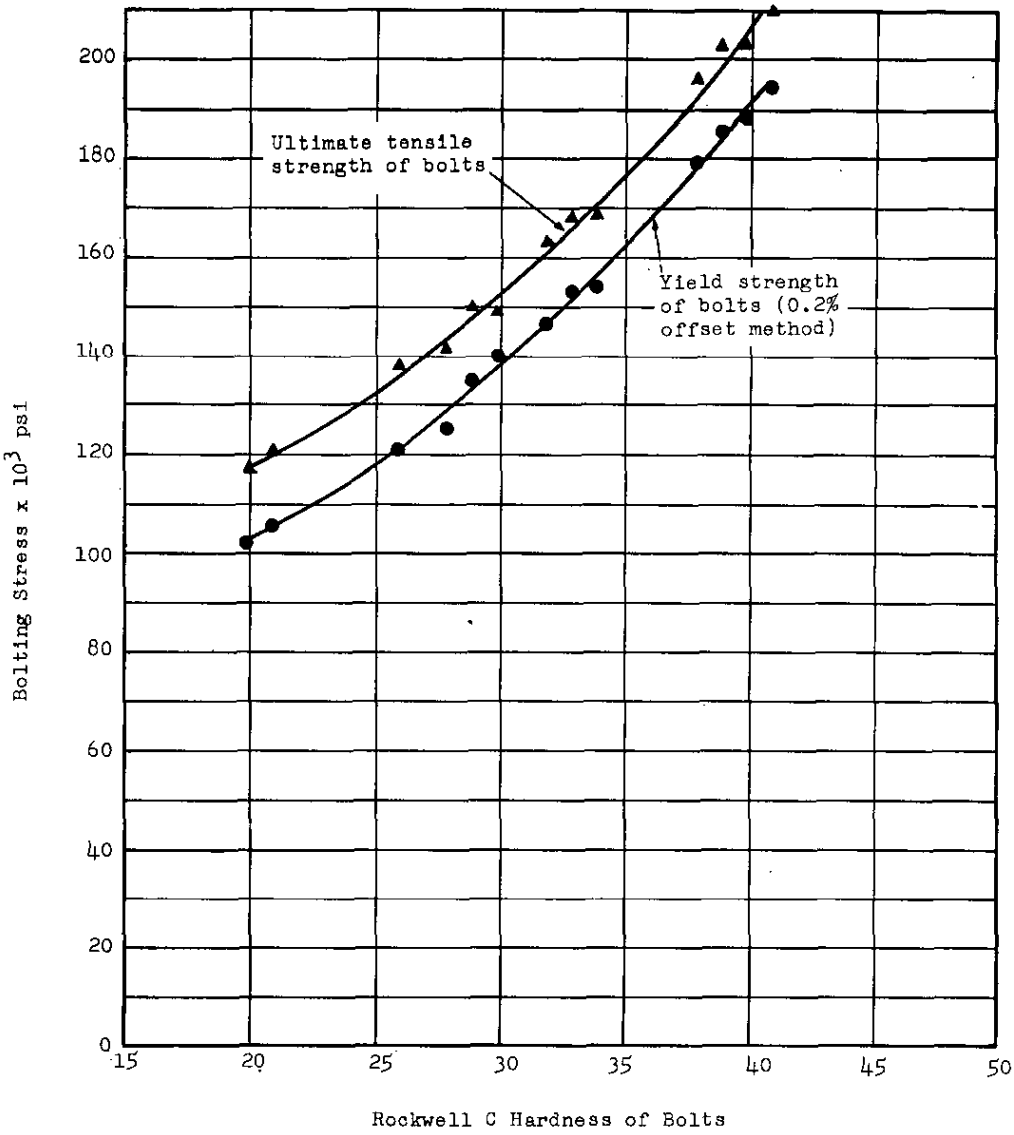

PHYSICAL PROPERTIES OF HARDENED AND DRAWN 3/8-IN. AISI TYPE 4140 ALLEN HEAD CAP SCREWS

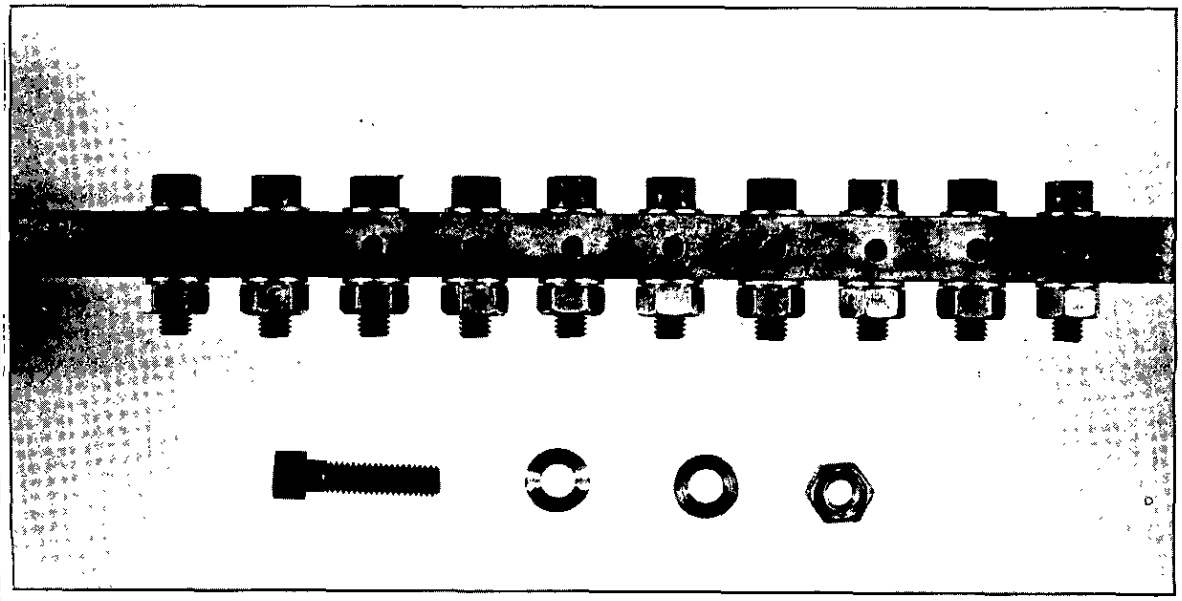

FIG. 29. BAR - TYPE JIG USED FOR LOADING 3/8-IN. ALLEN HEAD CAP SCREWS

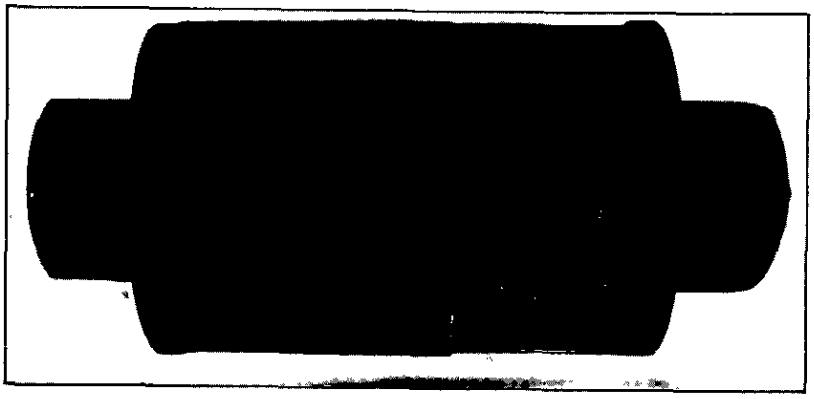

FIG. 30. SLEEVE - TYPE JIG USED FOR LOADING LARGE STUD BOLTS

FIGURE 31

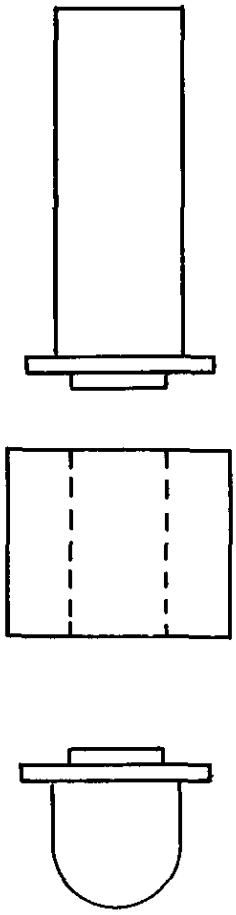

Block Shown with
Adapters for Calibration
in Tensile Machine

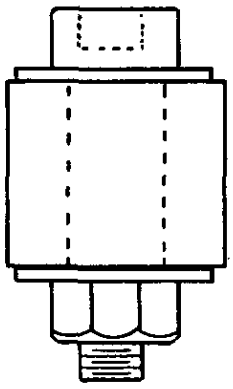

Block Shown with
3/8-Inch Allen Head Cap
Screw Loaded in Place

SKETCH OF CALIBRATION BLOCK USED FOR CHECKING THE STRAIN MEASUREMENT TECHNIQUES APPLIED TO 3/8 -IN. ALLEN HEAD CAP SCREWS

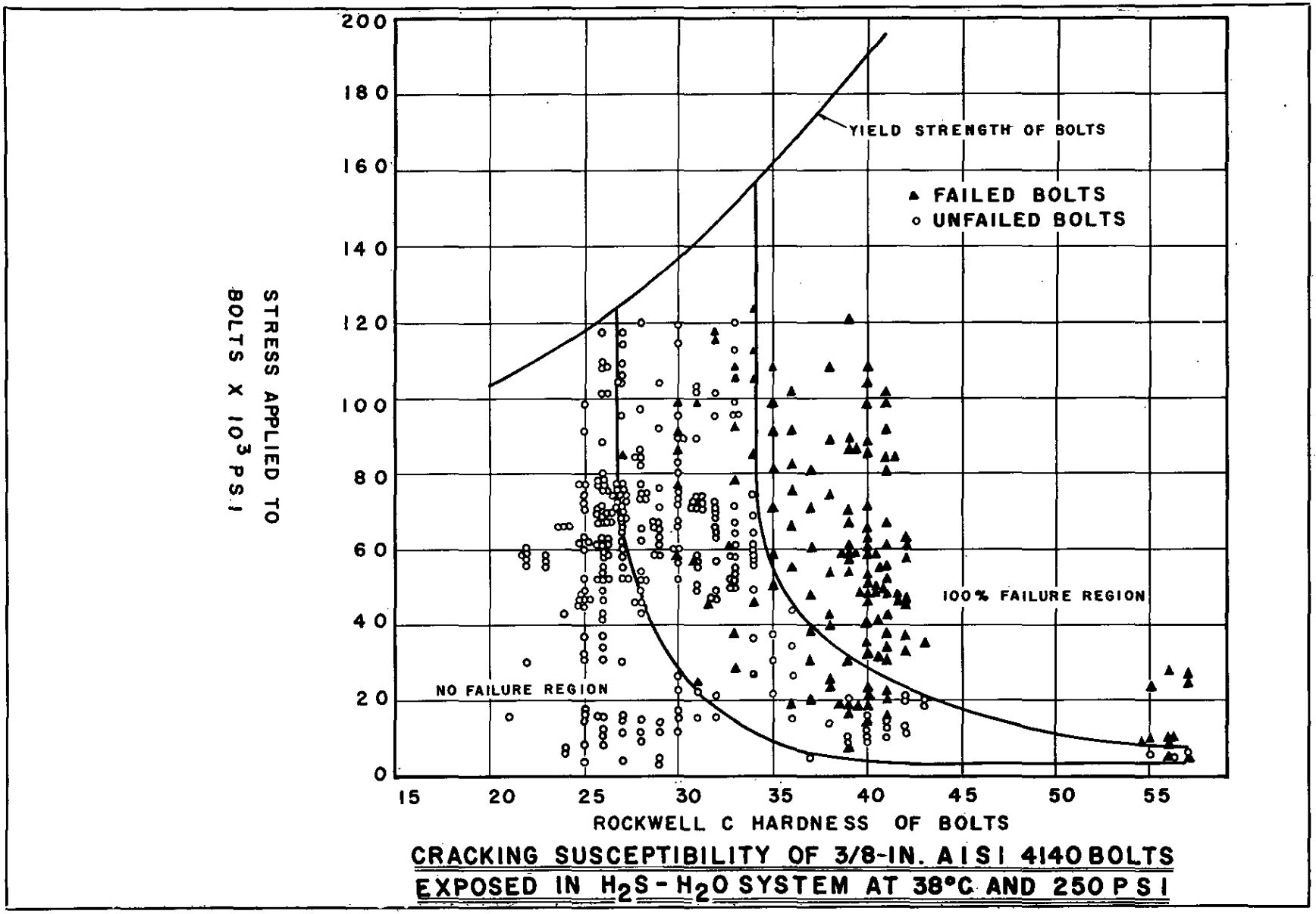

CRACKING SUSCEPTIBILITY OF 3/8-IN. AISI 4140 BOLTS EXPOSED IN H_2S - H_2O SYSTEM AT 38°C AND 250 PSI

FIGURE 32

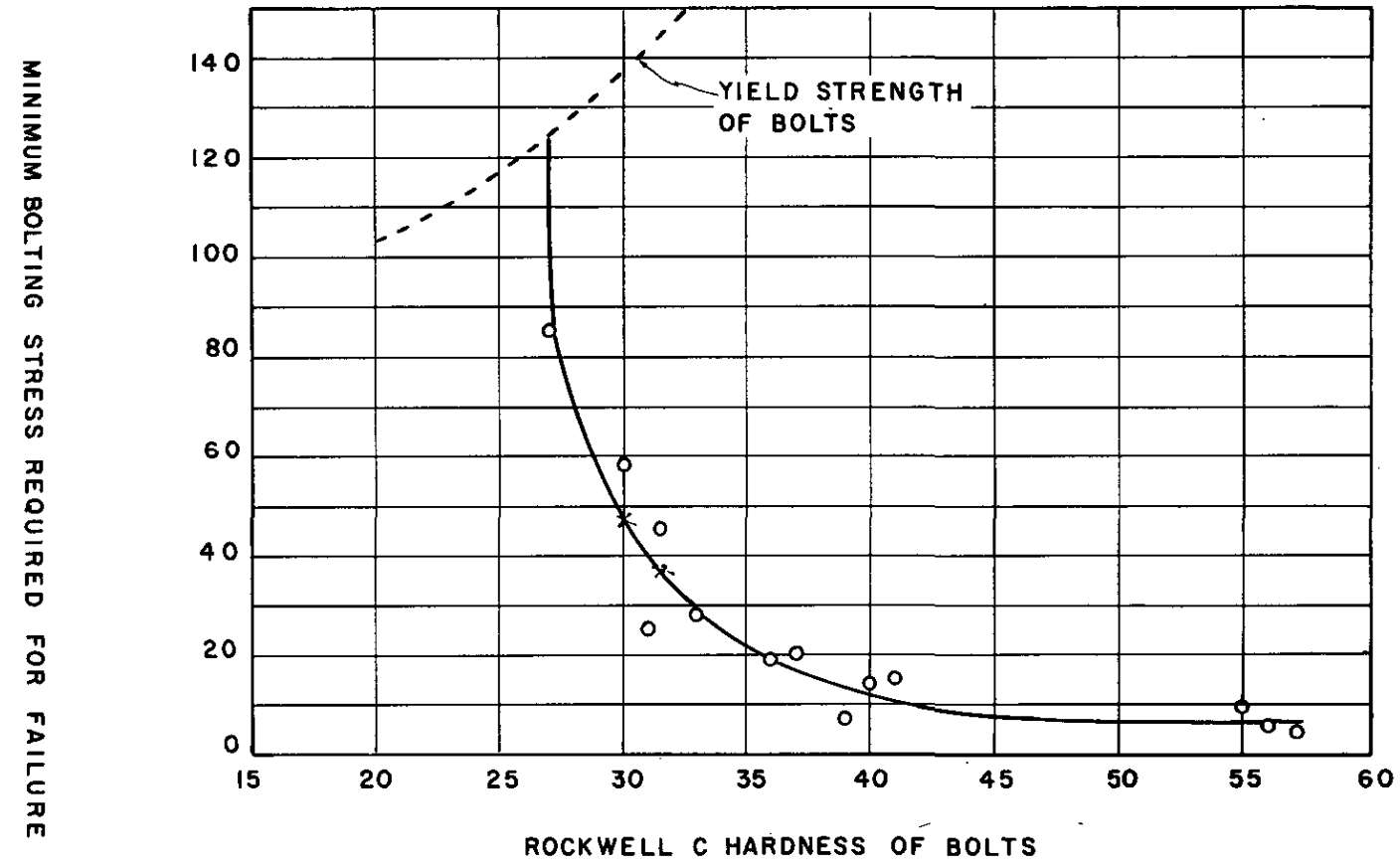

FIGURE 33

MINIMUM APPLIED STRESS REQUIRED TO PRODUCE CRACKING OF 3/8-IN. AISI 4140 BOLTS IN H_2S-H_2O SYSTEM AT 38°C AND 250 PSI

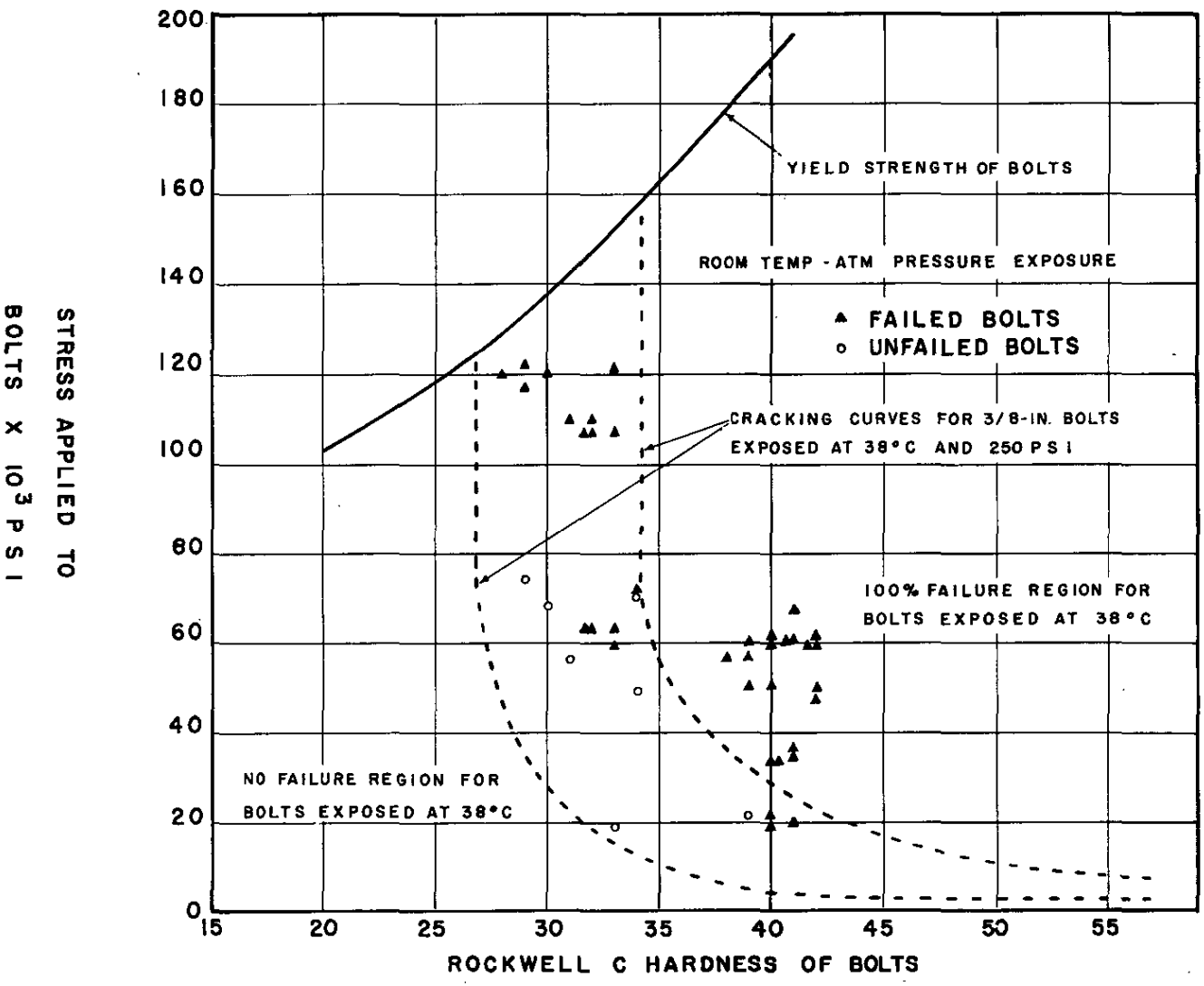

FIGURE 34

CRACKING SUSCEPTIBILITY OF 3/8-IN. AISI 4140 BOLTS EXPOSED IN H_2S-H_2O SYSTEM AT ROOM TEMPERATURE AND ATMOSPHERIC PRESSURE

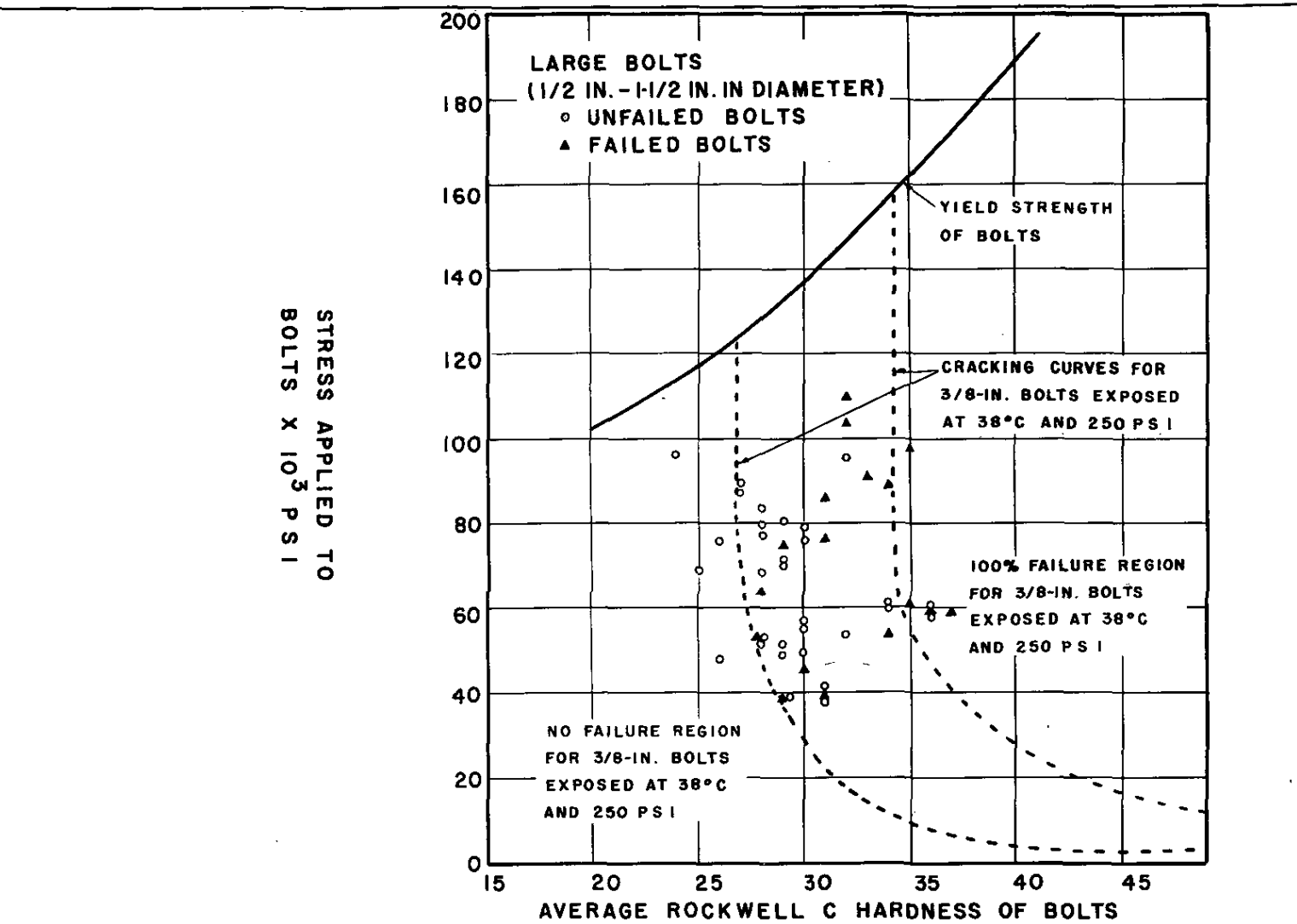

FIGURE 35

CRACKING SUSCEPTIBILITY OF LARGE AISI 4140 BOLTS EXPOSED IN H_2S-H_2O SYSTEMS BOTH AT 38°C AND 250 PSI AND AT ROOM TEMPERATURE-ATMOSPHERIC PRESSURE

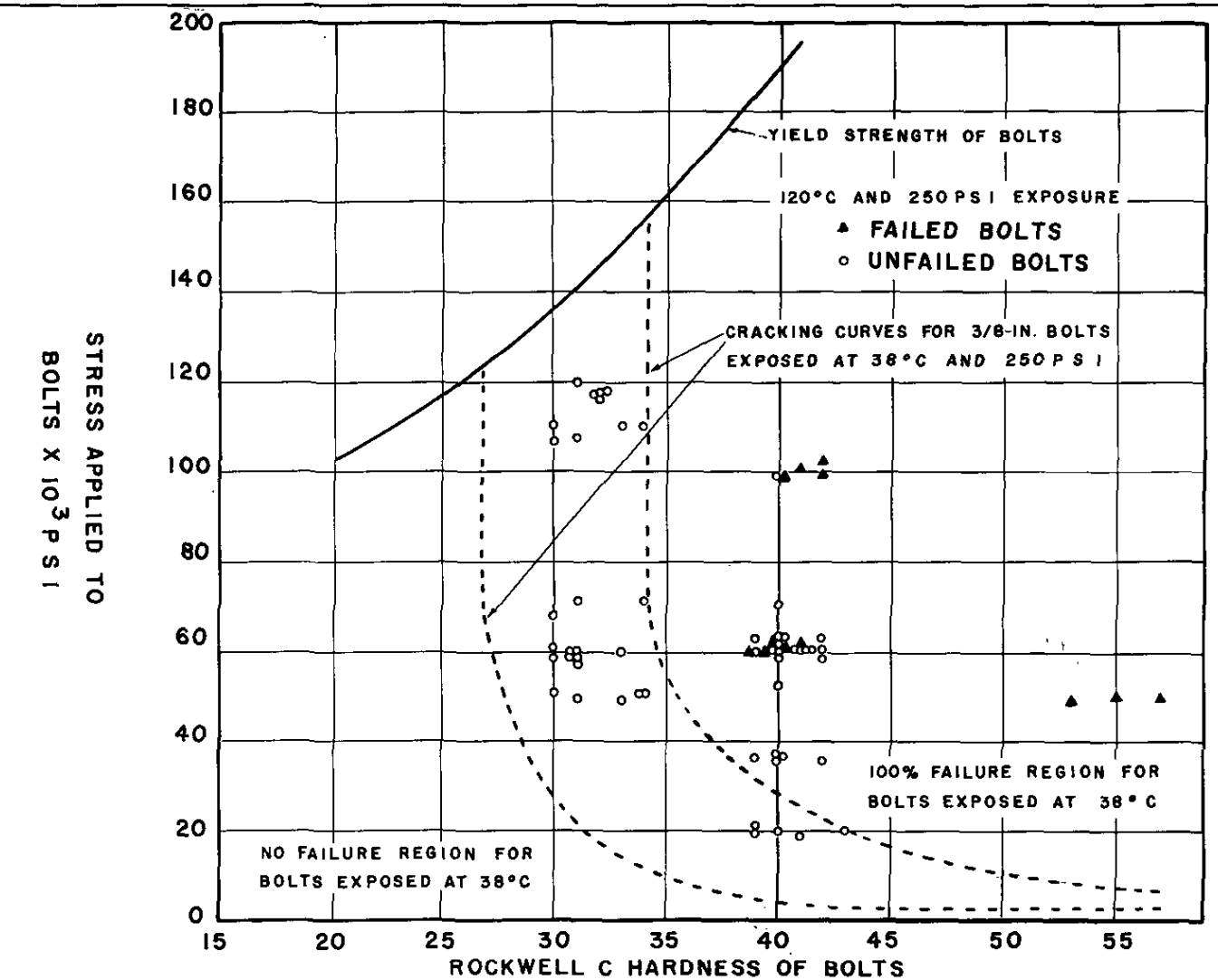

FIGURE 36

CRACKING SUSCEPTIBILITY OF 3/8-IN. AISI 4140 BOLTS EXPOSED IN H_2S-H_2O SYSTEM AT 120°C AND 250 PSI

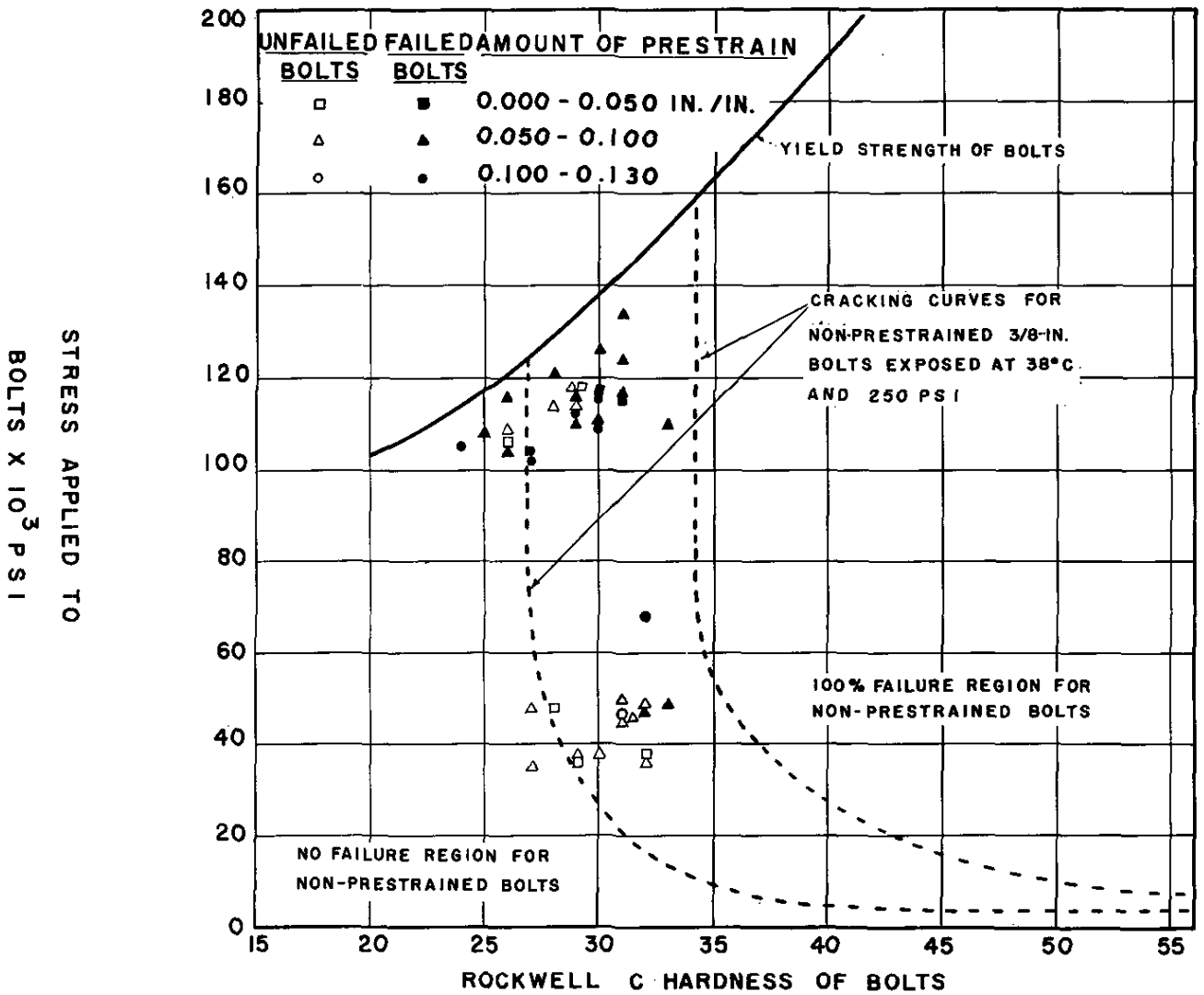

FIGURE 37

EFFECT OF PRESTRAIN ON CRACKING SUSCEPTIBILITY OF 3/8-IN. AISI 4140 BOLTS EXPOSED IN H_2S - H_2O SYSTEM AT 38°C AND 250 PSI

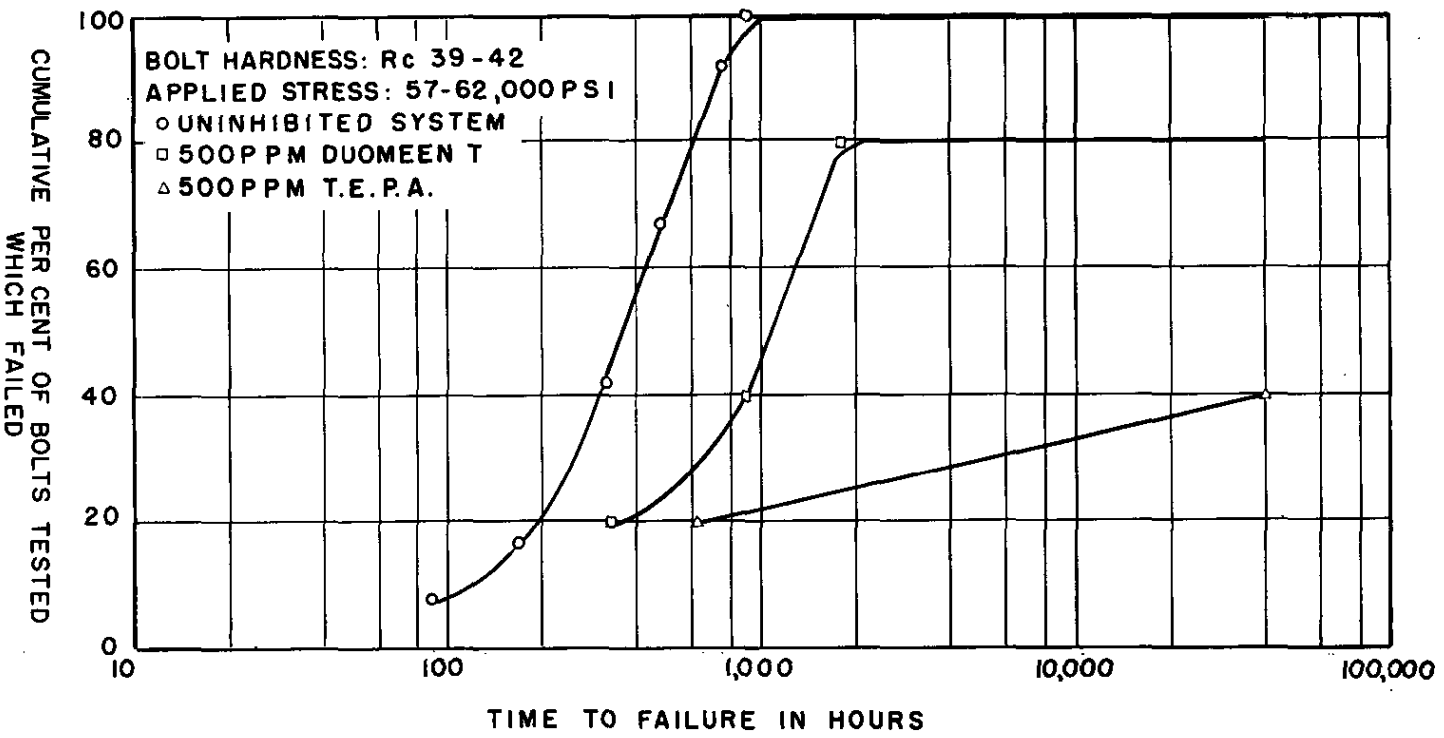

FIGURE 38

EFFECT OF INHIBITORS ON CRACKING SUSCEPTIBILITY OF 3/8-IN. AISI 4140 BOLTS EXPOSED IN H_2S-H_2O SYSTEM AT 38° C AND 250 PSI

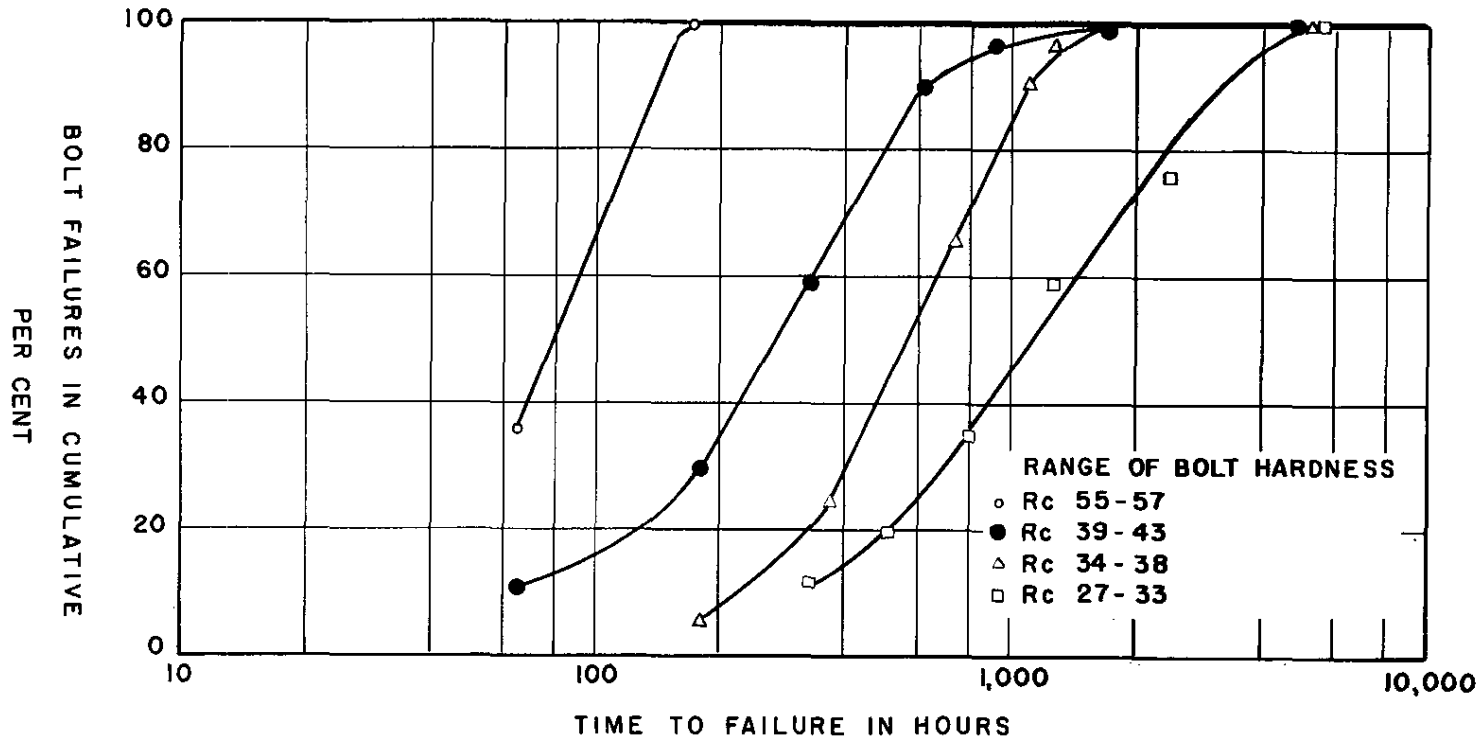

FIGURE 39

EFFECT OF HARDNESS ON TIME TO FAILURE OF 3/8 IN. AISI 4140 BOLTS EXPOSED IN H_2S-H_2O SYSTEM AT 38°C AND 250 PSI

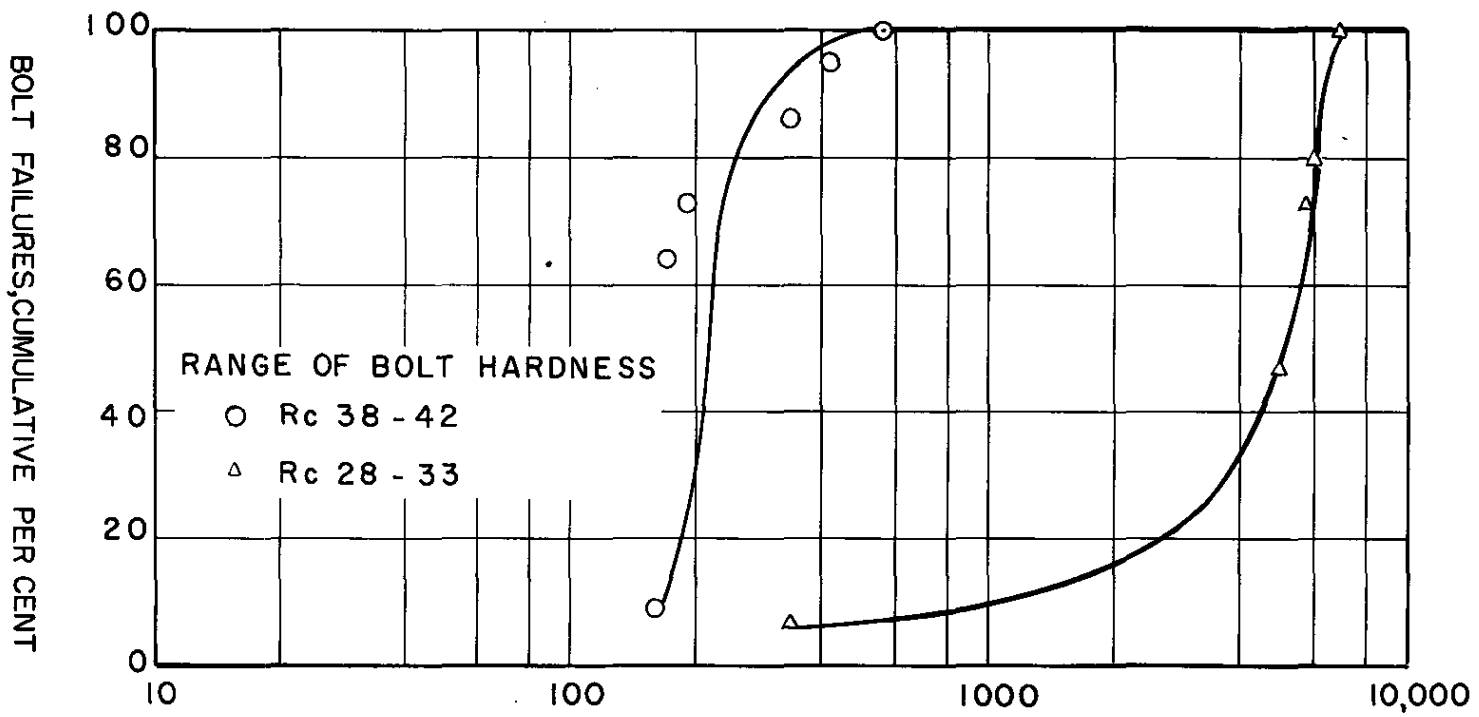

FIGURE 40

EFFECT OF HARDNESS ON TIME TO FAILURE OF 3/8-IN. AISI 4140 BOLTS EXPOSED IN AN H_2S-H_2O SYSTEM AT ROOM TEMPERATURE AND ATMOSPHERIC PRESSURE

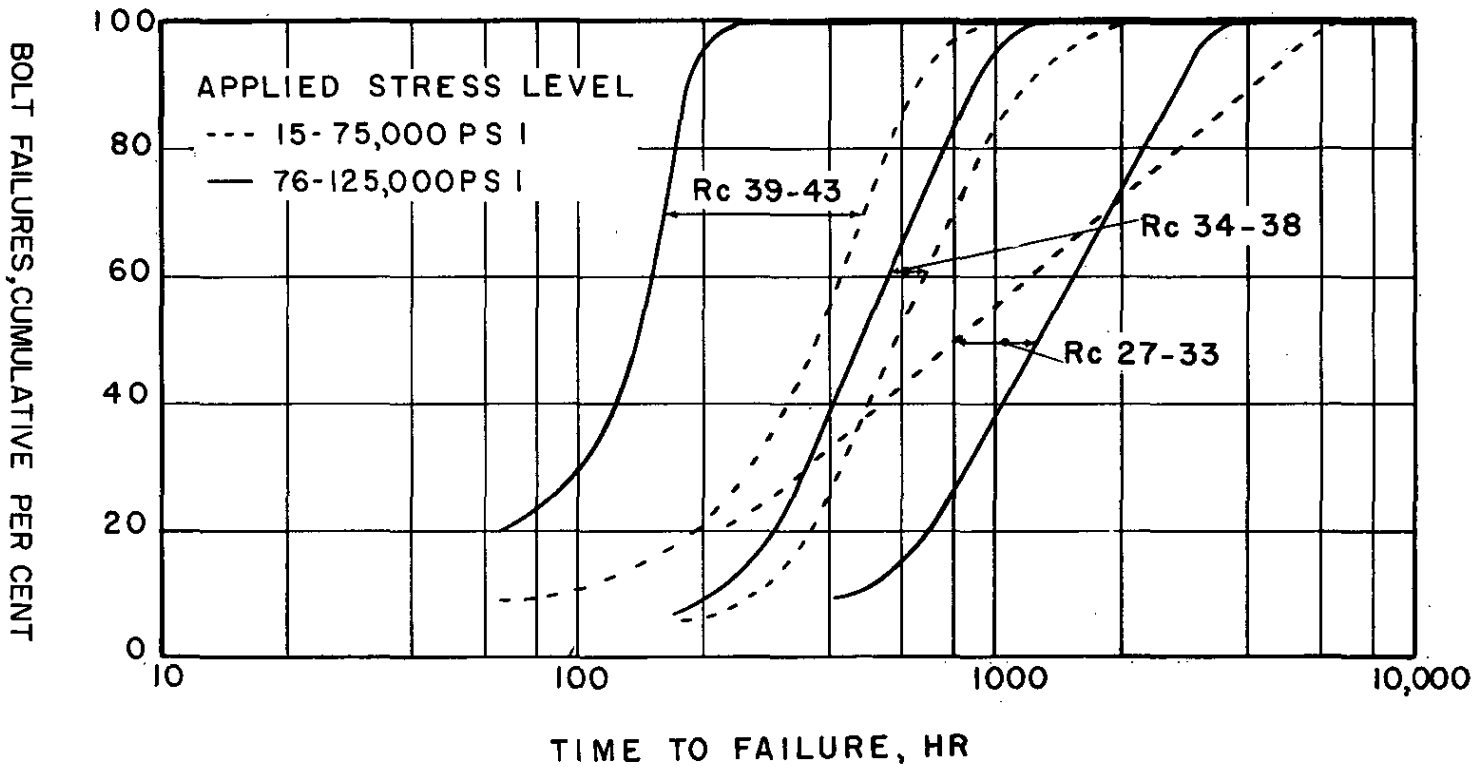

FIGURE 41

EFFECT OF APPLIED STRESS ON TIME TO FAILURE OF 3/8-IN. AISI 4140 BOLTS EXPOSED IN H_2S - H_2O SYSTEM AT 38°C AND 250 PSI

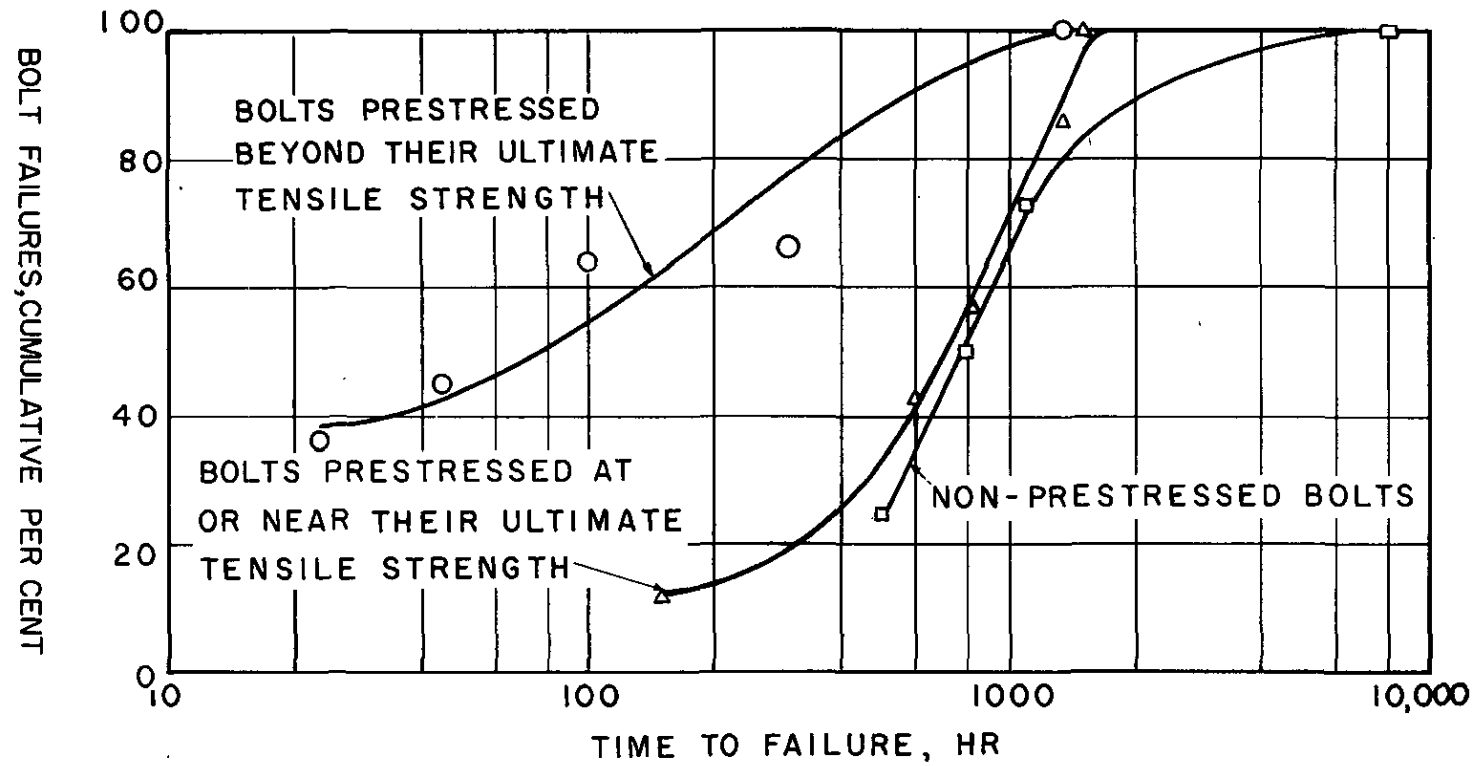

TEST PARAMETERS

APPLIED STRESS: 100,000 PSI - YIELD STRENGTH
BOLT HARDNESS: Rc 24-33

EFFECT OF PRESTRESSING ON TIME TO FAILURE OF 3/8-IN. AISI 4140 BOLTS EXPOSED IN AN H_2S-H_2O SYSTEM AT 38°C AND 250 PSI

FIGURE 42

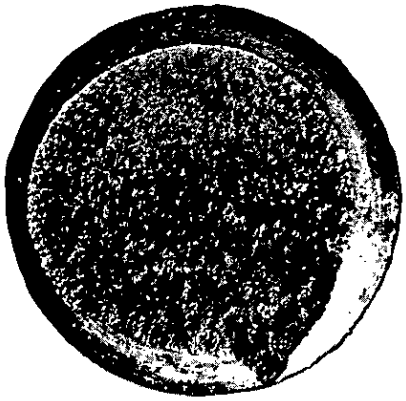

(A) Gage Failure 6X

(B) Nut Failure 6X

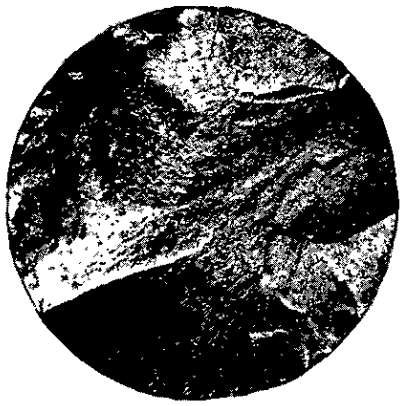

(C) Shank Failure 6X

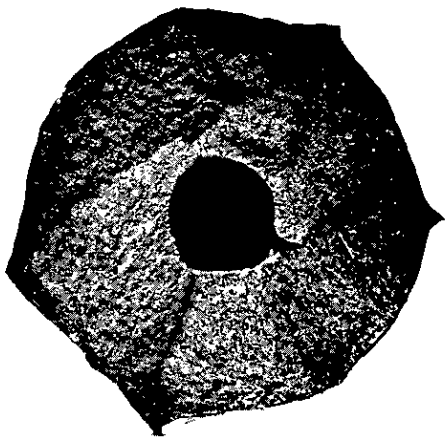

(D) Head Failure 6X

TYPICAL FRACTURES OF 3/8 - IN. AISI 4140 ALLEN HEAD CAP SCREWS WHICH FAILED BY SULFIDE CORROSION CRACKING

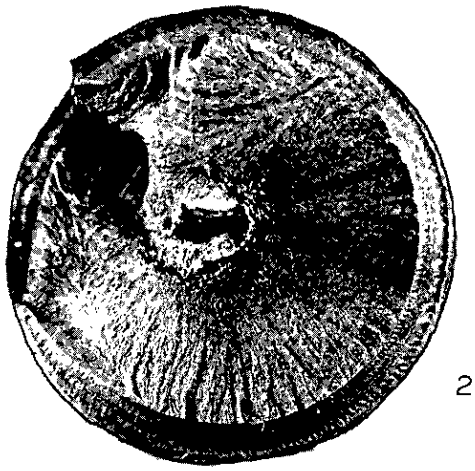

2.5 X

FIG. 44. FRACTURE SURFACE OF A 1-IN. AISI 4140 STUD BOLT WHICH DISPLAYED DUCTILE FRACTURE CHARACTERISTICS AT THE CORE AND BRITTLE FRACTURE CHARACTERISTICS IN THE SURROUNDING AREA

2 X

FIG. 45. CIRCUMFERENTIAL CRACKING IN THE FRACTURE SURFACE OF A 1-1/4-IN. AISI 4140 STUD BOLT WHICH FAILED BY SULFIDE CORROSION CRACKING

150 X

FIG. 46. LARGE SULFIDE CORROSION NOTCH IN THREAD ROOT OF AISI 4140 BOLT EXPOSED IN AN H_2S - H_2O SYSTEM AT 38°C AND 250 P S I

100 X

FIG. 47. LARGE SULFIDE CORROSION NOTCHES AND ACCOMPANYING CRACK AT THREAD ROOT OF AISI 4140 BOLT EXPOSED IN AN H_2S - H_2O SYSTEM AT ROOM TEMPERATURE AND ATMOSPHERIC PRESSURE

FIGURE 48

250 X

(A) 38°C - 250 psi System

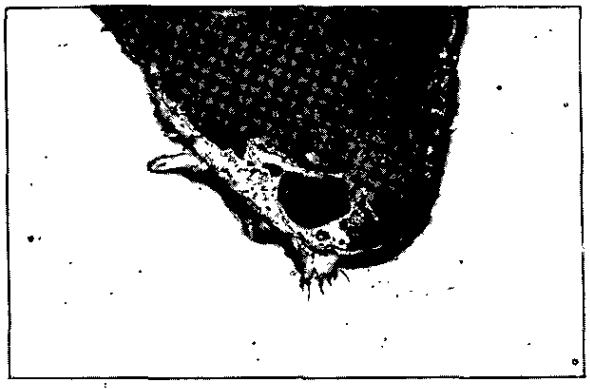

100 X

(B) Room Temperature - Atmospheric Pressure System

150 X

(C) 120°C - 250 psi System

"FINGER-TYPE" PATTERN OF SULFIDE CORROSION AT THREAD ROOTS OF AISI 4140 BOLTS EXPOSED IN VARIOUS H_2S - H_2O SYSTEMS

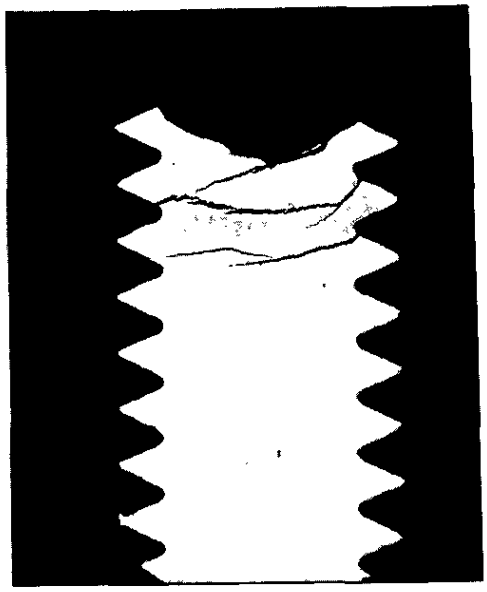

3.5 X

FIG. 49. SULFIDE CORROSION CRACKS IN LONGITUDINAL SECTION OF FAILED 3/8-IN. AISI 4140 BOLT

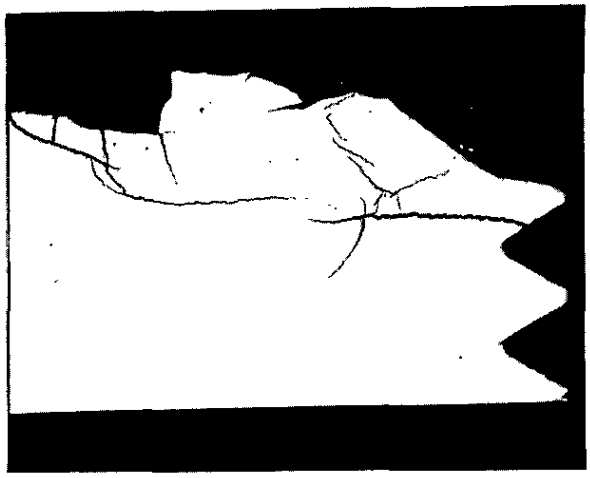

3.5 X

FIG. 50. NETWORK OF SULFIDE CORROSION CRACKS IN LONGITUDINAL SECTION OF FAILED 7/8-IN. AISI 4140 BOLT

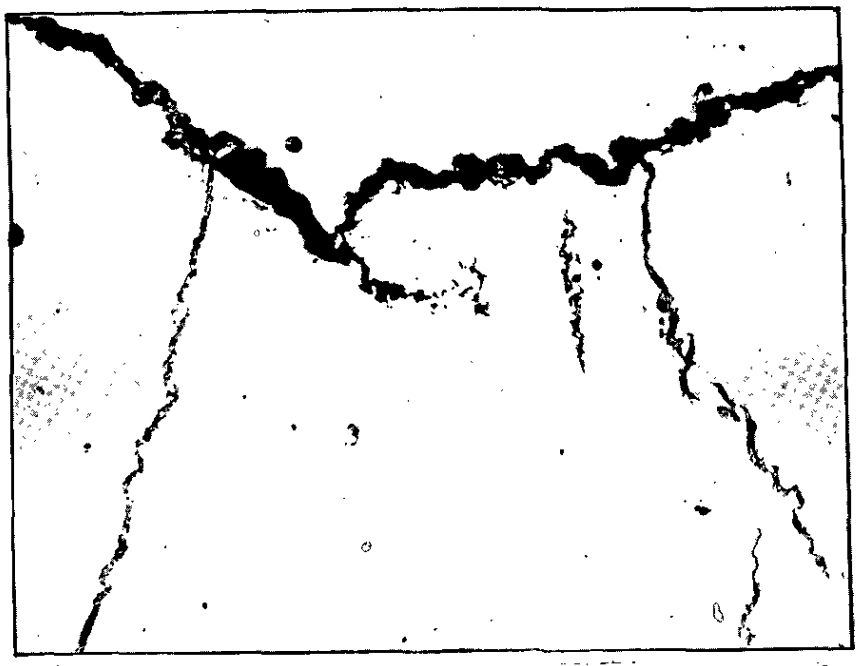

FIG. 51. NETWORK OF SULFIDE CORROSION CRACKS WHICH ORIGINATED AT FRACTURE SURFACE OF FAILED 7/8-IN. AISI 4140 BOLT 150X

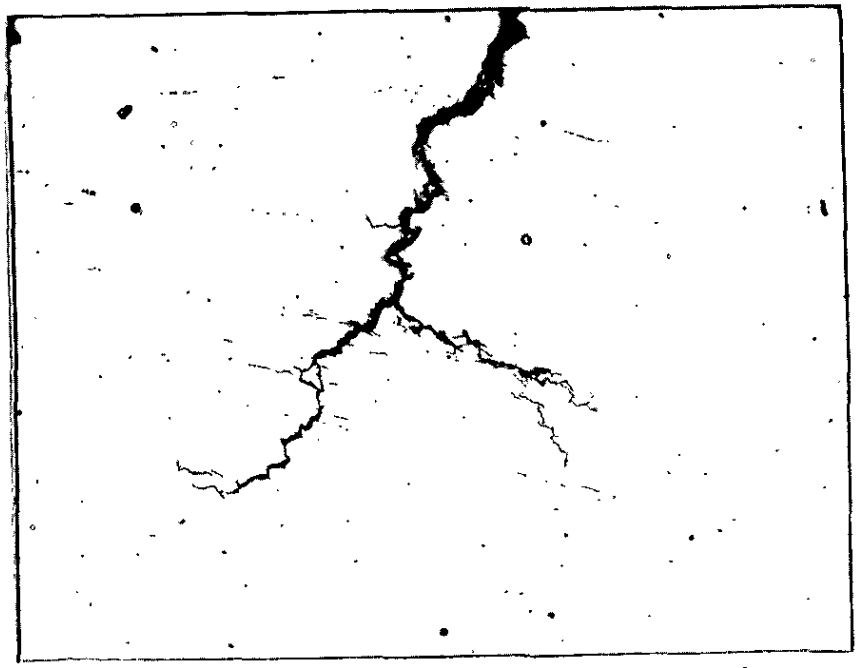

FIG. 52. BRANCHING SULFIDE CORROSION CRACKS WHICH ORIGINATED AT THREAD ROOT OF FAILED 3/8-IN. AISI 4140 BOLT 100X

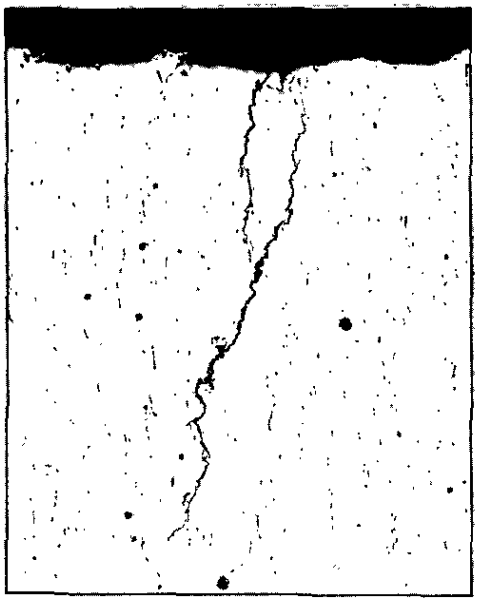

100 X

FIG. 53. SULFIDE CORROSION CRACKS NORMAL TO FRACTURE SURFACE OF FAILED 3/8-IN. AISI 4140 BOLT

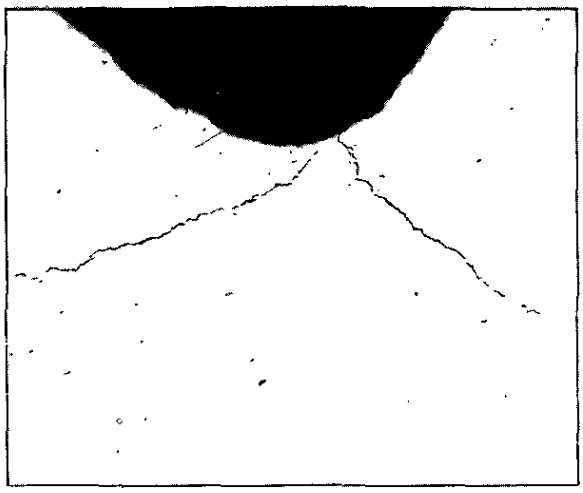

250 X

FIG. 54. FINE SULFIDE CORROSION CRACKS INITIATING AT THREAD ROOT OF FAILED 3/8-IN. AISI 4140 BOLT

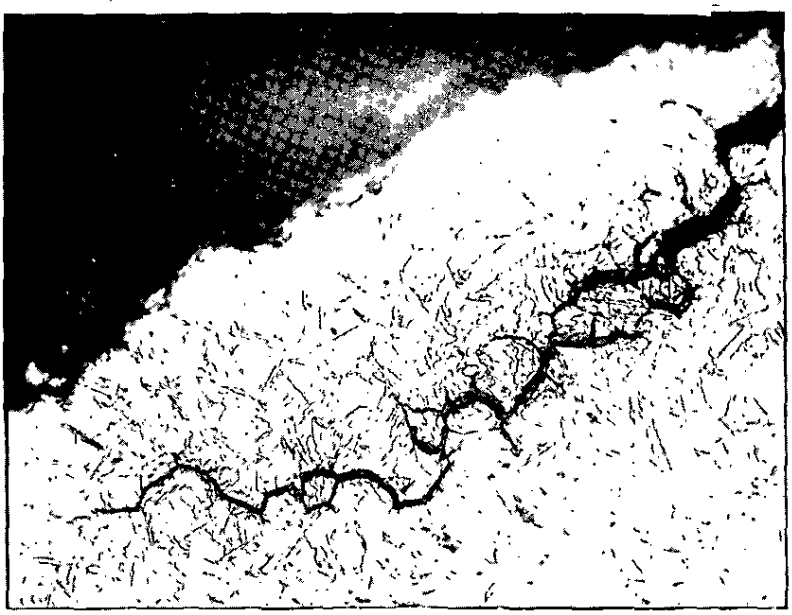

FIG. 55. SULFIDE CORROSION CRACK WITH INTERGRANULAR APPEARANCE IN FAILED AISI 4140 BOLT ETCHED IN 2% NITAL 500X

FIG. 56. SULFIDE CORROSION CRACK WITH TRANSGRANULAR APPEARANCE IN FAILED AISI 4140 BOLT ETCHED IN 2% NITAL 500X

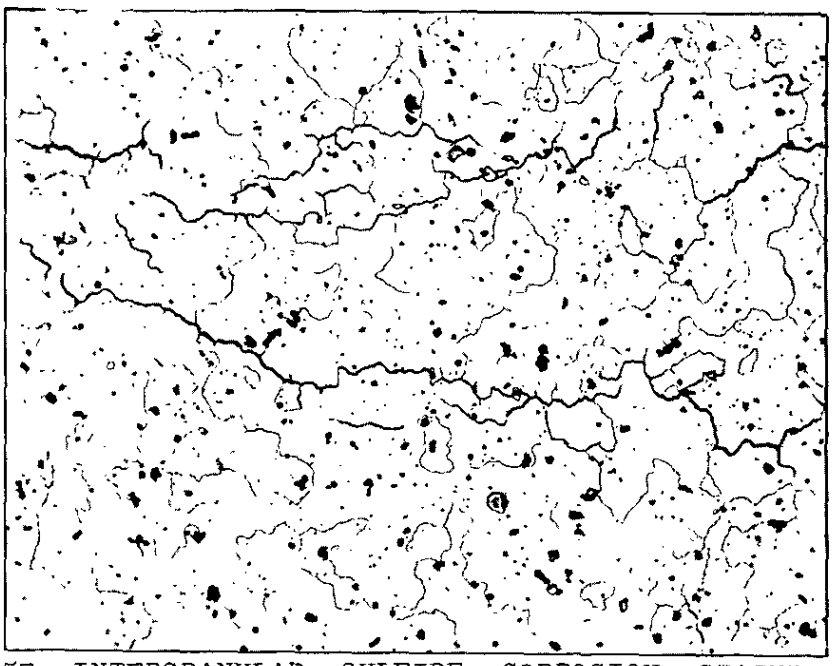

FIG. 57. INTERGRANULAR SULFIDE CORROSION CRACKS NEAR THE FRACTURE SURFACE OF FAILED 75ST ALUMINUM BOLT ETCHED IN 0.5% HF 250X

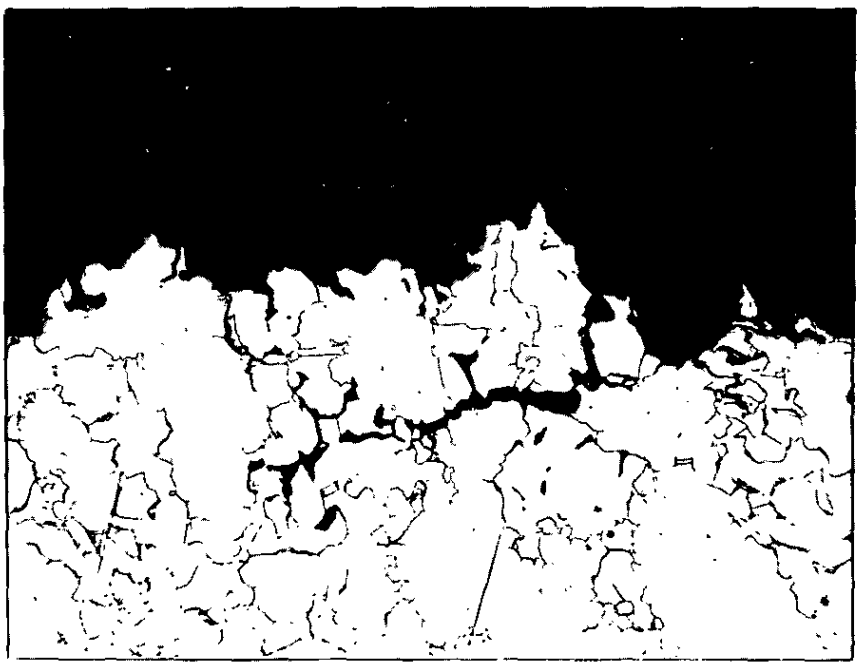

FIG. 58. SULFIDE CORROSION CRACKS AT EDGE OF FRACTURE OF FAILED DURONZE BOLT ETCHED IN $NH_4OH - H_2O_2$ 250X

FIGURE 59

(A) Ferrite and Pearlite Rc 21

(B) Tempered Martensite Rc 21

(C) Tempered Martensite Rc 26

(D) Tempered Martensite Rc 31

(E) Tempered Martensite Rc 36

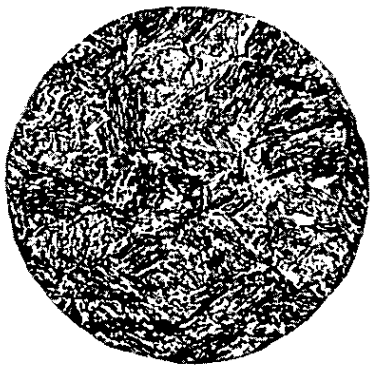

(F) Martensite Rc 55

MICROSTRUCTURE OF 3/8-IN. AISI 4140 CAP SCREWS AS A FUNCTION OF HARDNESS, ETCHANT WAS 2% NITAL 1000X

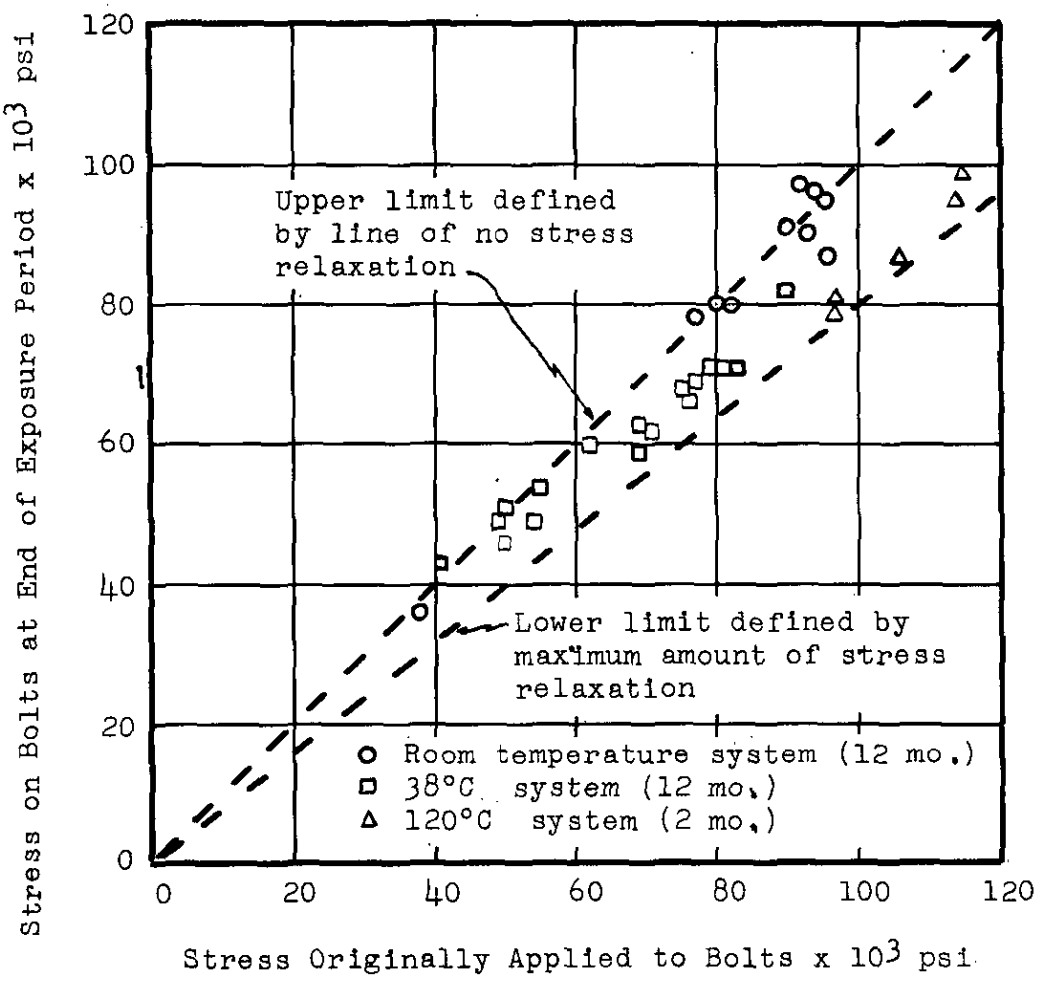

STRESS ON UNFAILED LARGE AISI 4140 STUD BOLTS AFTER EXPOSURE IN H_2S - H_2O SYSTEMS AS A FUNCTION OF THE ORIGINAL APPLIED STRESS

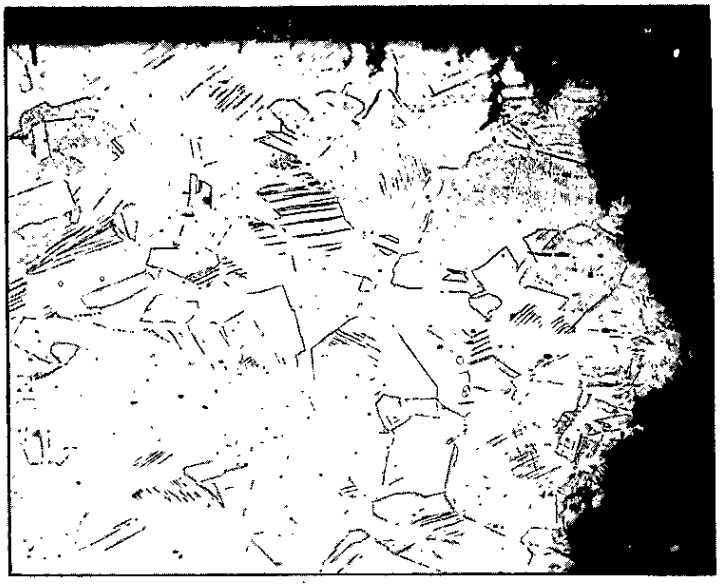

FIGURE 61 Oxalic Acid 100X
Broken end of annealed Type 316 stainless steel tensile specimen. Note shallow transverse cracks. Exposed to H_2S-H_2O at 250 psi and 120°C. Tensile stress 70,000 psi. Broke after 524 hr.

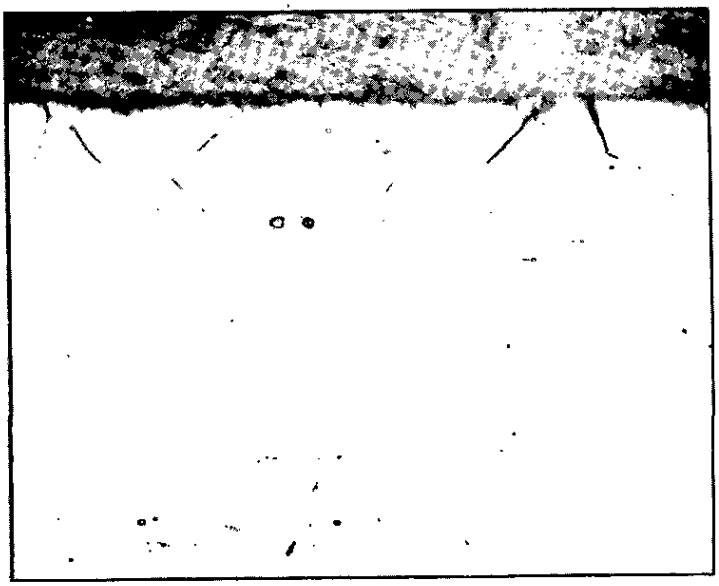

FIGURE 62 Oxalic Acid 100X
Intergranular cracks in sensitized Type 316 stainless steel in tension. Exposed to 250 psi H_2S-H_2O for 2000 hr.

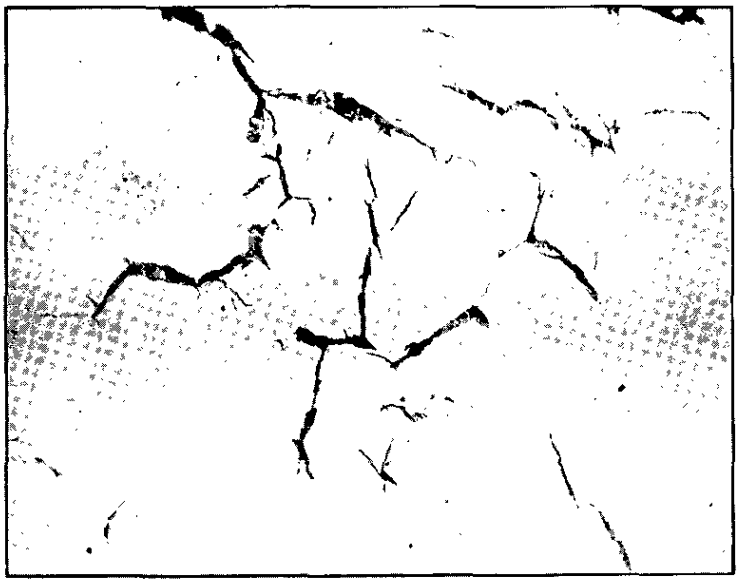

Unetched 250X

FIGURE 63 Intergranular and transgranular cracking of sensitized Type 316 stainless steel tensile specimen. Exposed 5000 hr to H_2S-H_2O at 250 psi. Stressed at 70,000 psi.

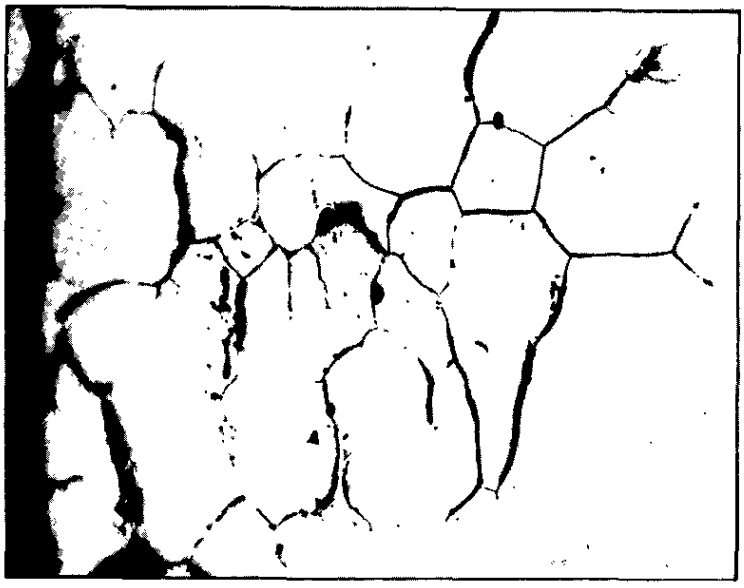

Unetched 100X

FIGURE 64 Intergranular cracking of sensitized Type 316 stainless steel bend specimen. Exposed 7000 hr to H_2S-H_2O at 250 psi.

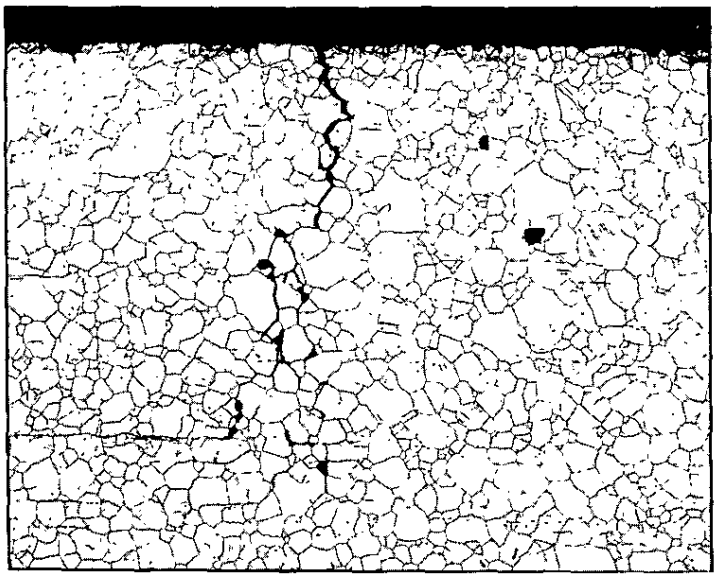

Oxalic Acid 100X

FIGURE 65 Intergranular cracking of Type 304 stainless steel strongback. Exposed to H_2S-H_2O at 250 psi for 570 hr.

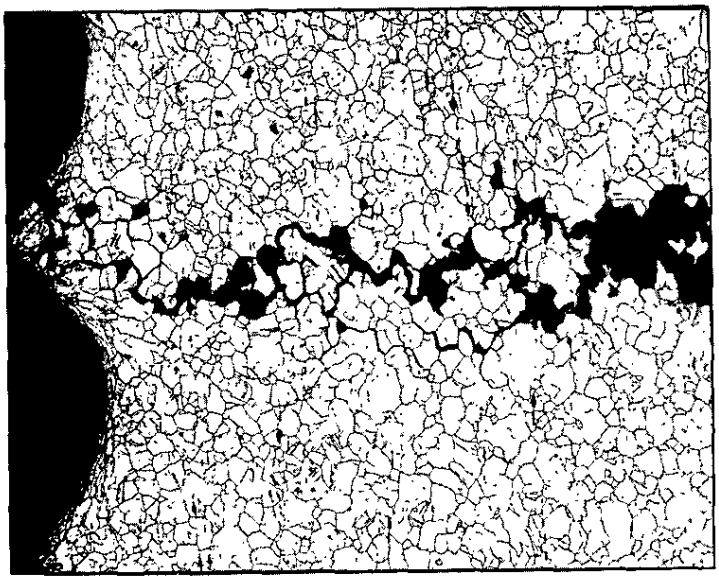

Oxalic Acid 100X

FIGURE 66 Intergranular cracking of Type 304 stainless steel slip tube - Dana

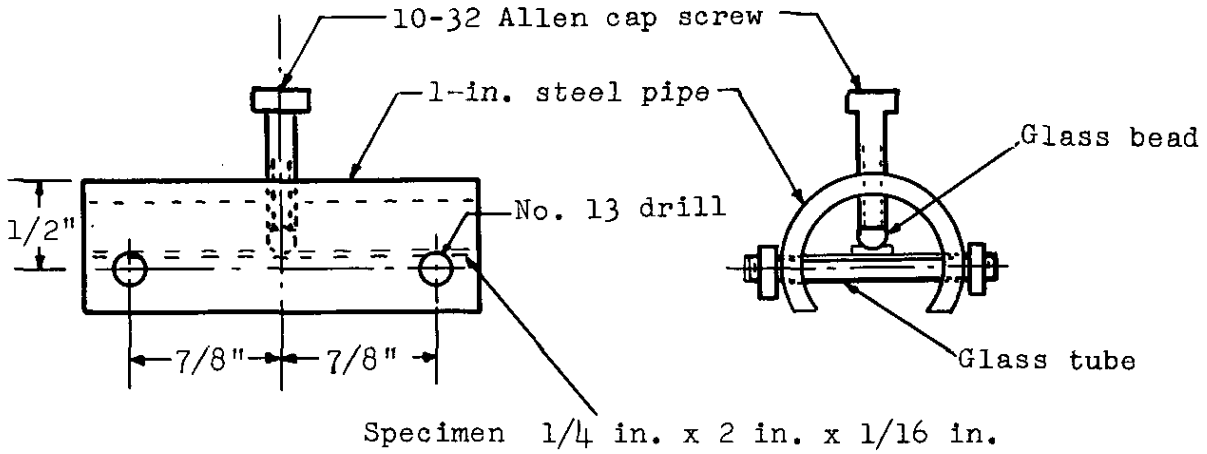

SINGLE POINT LOADING JIG

FIGURE 67

FIGURE 68

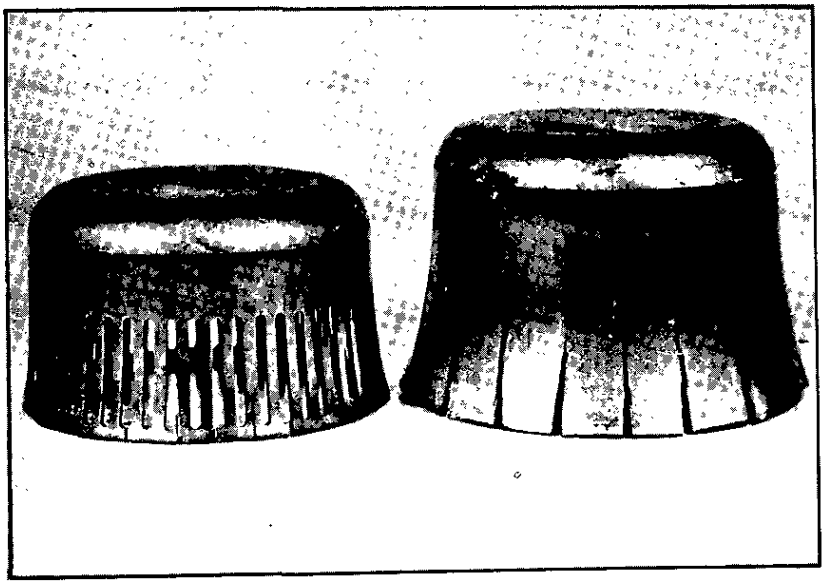

Cracked Type 304 stainless steel bubble cap and blank (cold drawn). Exposed 1850 hr to H_2S-H_2O at 250 lb/sq in. and 40°C.

TABLE I

CHARPY IMPACT TESTS

Embrittlement Resulting from Exposure to H_2S-H_2O

	A212 Trans.	A212 Long.	Rimmed Steel	410
	Impact Valves - ft lb			
A) As machined	64	120 +	60 +	120 +
		119	68	124
	58	128	66	125
	61	124	67	124
B) Exposed to H_2S-H_2O 250 lb at 120°C 160 hr	62	120 +		120 +
	60	111	69	120 +
		129	76	126
	61	120	72	124
C) Exposed to N_2 300 lb at 120°C 740 hr	53	106		138
	64	110	72	154
	62	116	74	141
	60	111	73	143
D) Exposed to H_2S-H_2O 250 lb at 120°C 1700 hr	58	136	71	139
	62	135	72	130
	52	120	76	141
	57	130	73	137
E) Same as D			56	148
	62	140	46	140
	61	146	56	
	62	143	53	144

TABLE II

HYDROGEN EMBRITTLEMENT TESTS OF A212 STEEL BARS

Crosshead speed 0.1 in./mo.

	0.01% Yield Stress psi	0.2% Yield Stress psi	Ultimate Stress psi	Elong. % in 2 in.	Red. of Area %
A) As machined		46,000	74,600	33.5	57.4
		46,500	74,400	33.5	58.7
	35,800	40,200	73,600	30	62
	33,300	39,200	74,400	32	61
B) Tested 1 hr after removal from H_2S		45,100	75,000	31.5	57.4
		45,300	74,600	33	54
C) Stored in air 1000 hr	40,200	44,500	74,400	32	62.5
Cooled in liq. N_2	42,900	45,300	74,500	30	62.5
Tested cold Temp. at break ca. 10°C					
D) Same as C, but heated to 25°C before tensile test	32,600	37,900	73,800	30	62
	31,700	39,000	74,200	30	62
E) Tested cold. Temp. at break ca. 10°C	39,400	43,700	75,000	23	36.8
	44,700	48,600	75,700	23	35.2
F) Similar to E, but heated to 25°C before tensile test	45,500	48,500	74,300	23	28.4
	45,500	48,000	75,200	21	25.6

Note: Samples B to F exposed to H_2S-H_2O for 500 hr at 250 psi and 120°C

Samples E and F also exposed to H_2S-H_2O for 500 hr at 250 psi and 40°C, removed and chilled in liquid N_2

TABLE III

EFFECT OF INTERRUPTIONS ON CORROSION RATES

Corrosion rates for steel in uninhibited H_2S-H_2O solutions at 120°C and 250 lb /sq in. H_2S pressure

Condition	Total Time	Corrosion Rates mil/year
Continuous Test - 3 wk	440 hr	4.0
Changed water once/wk	440	5.6
Dried specimens once/wk	440	5.9
Continuous Test - 6 wk	1050 hr	1.8
Changed water once/wk	1050	5.2
Dried samples once/wk	1050	4.3

Note: Each rate is the average of 2 specimens

TABLE IV

INTERPLANAR SPACINGS OF POWDER PATTERN OF HYDROTROILITE

Interplanar Spacing	Estimated Intensity
5.020A	100
3.472	2
3.118	1
2.960	80
2.634	1
2.534	2
2.456	5
2.345	60
2.067	1
1.843	40
1.800	70
1.739	5
1.720	20
1.674	5
1.558	20
1.521	10
1.431	1
1.405	15
1.352	30
1.283	1
1.256	30
1.236	10
1.191	5
1.132	50
1.103	15
1.055	90
1.038	40
1.028	5
1.005	5
0.999	15

TABLE V

INHIBITORS SUGGESTED BY TESTS AT COLUMBIA UNIVERSITY

Corrosion Test Notebooks - S.A.M. Lab. - 1942

Corrosion rates determined for steel in H_2S-H_2O
250 psi - 120°C

Inhibitor		Corrosion Rate-mils/yr Time in Test 1 wk	2 wk	3 wk
Base Rate Distilled Water	av. of 20	12.3	7.7	6.0
Deionized Water	av. of 12	11.2	6.5	5.6
Formaldehyde	Conc. 500 ppm	9.8	5.1	7.6
Piperidine	Conc. 500 ppm	4.4	3.8	3.6
Pyridine	Conc. 500 ppm	5.1	2.7	2.9
Quinoline	Conc. 500 ppm	13.2	10.1	5.4
Isoquinoline	Conc. 500 ppm	1.0	0.9	2.6
Phenyl Hydrazine	Conc. 500 ppm	6.8	3.5	2.8
Tannic Acid	Conc. 500 ppm	8.1	-	5.0

TABLE VI

TESTS OF SAMPLE CLEANING PROCEDURES

Rimmed steel samples - 104 sq cm each
10% HCl with inhibitor as indicated

80° to 82°F - (28°C)

Concentration of Barrett No. 53	ppm	Weight Loss, Mg. 5 min	10 min	30 min	1 hr	2 hr	4 hr
2 drops/ 25 ml	3,200	0.3	2.5	2.2	1.4	4.0	8.4
1 drop / 25 ml	1,600	1.0	2.9	2.6	3.8	5.0	9.1
1 drop /100 ml	400	1.8	3.3	4.4	2.6	3.3	10.4
1 drop /200 ml	200	6.0	1.9	5.9	6.7	7.3	12.5
186° to 188°F. - (86°C)							
2 drops/ 25 ml	3,200	6.5	8.0	17.7	36.2	72.1	138.9
1 drop / 25 ml	1,600	6.2	6.8	18.6	38.2	70.4	158.7
1 drop /100 ml	400	18.6	28.6	71.5	164.5	598.8	2,129
1 drop /200 ml	200	93.9	102.9	186.7	2,525	7,582	26,114

Note: Weight loss of 4 mg correspond to a rate of 0.1 mil/yr for a 1-wk test
Single specimens were used for each test

TABLE VII

INHIBITORS MOST EFFECTIVE IN TESTS AT THE ENGINEERING RESEARCH LABORATORY

Corrosion rates in mils/yr for steel in H_2S-H_2O
250 psi at 120°C

Inhibitor	Conc. ppm	Time of Test 1 wk	2 wk	3 wk
Tetraethylenepentamine	500	0.8	0.5	0.4
Dodecylamine	500	1.3	1.3	1.1
Deceresol G-61	500	1.2	0.9	0.8
Quaternary O (Imidazoline chloride)	500	0.8	0.6	0.4
Quaternary S (Imidazoline chloride)	500	2.9	1.5	1.2
Duomeen T	500	0.8	0.7	0.6
Duomeen C	500	0.6	0.6	0.4
Trimethylamine	500	6.0	4.3	4.2
Trimethylamine	2,000	2.0	2.1	2.2
Base rates in distilled water (average of 20 tests		12.3	8.5	5.7

TABLE VIII

SYNERGISTIC EFFECTS OF INHIBITOR COMBINATIONS

Steel in H_2S-H_2O solutions
at 250 psi and 120°C

Additions (ppm) to Deionized Water					Corrosion Rate-mils/yr		
					Time of Test		
TEPA	NaOH	$Ca(OH)_2$	NH_3	Piperidine	1 wk	2 wk	3 wk
Base Rate, no additions					12.3	8.5	5.7
50					2.1	2.5	5.0
500					0.8	0.5	0.4
20	10				4.6	4.8	5.1
20	50				1.8	1.4	3.6
20	200				1.8	2.4	2.4
20		10			4.6	4.8	3.8
20		50			10.0	6.0	4.8
20		200			2.3	2.2	3.4
20			10		4.4	3.3	4.0
20			30		1.3	0.9	0.9
20			50		1.4	0.8	1.0
20			50		1.8	1.2	1.5
20			50		2.0	0.8	2.0
20			100		0.6	1.2	3.0
20			100		1.7	1.0	2.2
20			200		1.4	0.8	0.8
20			200		2.0	1.4	1.9
20			200		1.6	0.8	2.2
20	20		30		4.7	4.1	9.4
20	20		30		1.8	2.2	4.2
20	20		30		3.4	4.4	6.0
40	40		50		1.8	2.2	4.2
100	100		100		1.7	1.0	1.8
	200			10	5.8	4.2	3.8
	200			50	5.4	4.0	3.0
	200			200	3.6	4.0	3.2
	500			500	2.0	3.4	4.2

TABLE IX

SLUDGING EFFECTS OF INHIBITORS

Scaled steel samples with approx. 0.243 lb scale/sq ft
Tested in typical amine solution
250 psi H_2A-H_2O

Inhibitor	None	NH_3	TMA	TMA	TEPA
Concentration, ppm		3,000	500	20,000	500
Exposure Time (hr)	406	406	406	499	406
Tests at 120°C					
% of scale loosened	7.8	30.8	7.1	74.7	29.6
Tests at 38°C					
% of scale loosened	1.2	31.2	18.4	-	20.3

TABLE X

RESULTS OF SLUDGING TESTS IN CIRCULATING SYSTEMS

125 psi H_2S-H_2O at 120°C

	Corrosion Rates-mils/yr		Percentage of Total Sulfides in Sludge
	Steel Test Panels	Steel Rings	
Run 1 - 48 hr			
No inhibitor	33.3	-	0.5 gm *
550 ppm TMA	27.0	-	13.3 gm *
Run 2 - 167 hr			
No inhibitor	5.4	17.8	0.6 gm
2000 ppm TMA	2.8	9.2	14.7 gm
Run 3 - 165 hr			
20 ppm TEPA 50 NH_3	12.2	19.7	1.2 gm
20 ppm TEPA 200 NH_3	7.3	11.9	6.7 gm
500 ppm TEPA	9.0	4.5	56.0 gm *
Run 4 - 108 hr			
20 W oil 15% (108 hr)	4.2 Top 9.2 Bottom	8.3	15.2 gm
20 ppm TEPA 200 NH_3 (61 hr)	5.9	15.8	1.4 gm
Run 5 - 355 hr			
500 ppm Duomeen T	1.5 Top - 0.8 Bottom	1.3	13.9 gm
20 W oil - 15%	1.1 Top - 1.8 Bottom	4.6	12.3 gm
20 ppm TEPA 200 NH_3	1.3 Top - 3.2 Bottom	3.9	5.0 gm

* Pot not pickled before these runs

TABLE XI

CORROSION OF MATERIALS IN LIQUID H_2S

Temperature, 40°C

Test No.	Addition	Time Hr	Corrosion Rate, mil/yr					
			A212	A212 Weld	410	304	316	329
1	None	4000	3.0 3.6	-	0.12	0.013	0.022	0.010
2	None	1000	8.3 8.1 7.2	5.6	0.46	-	0.007	-
3	Duomeen T (Saturated)	6200	0.06 0.04 0.07 0.07	0.27 0.40	0.022	0.006	0.004	0.005
4	FeS (Scale)	5500	7.2 4.3 5.5 1.7	6.4 2.0	17.2	1.7	0.009	0.046
5	5% Cl as NaCl	4900	11.9 8.2 9.7 14.5	4.2 2.0	2.9	0.12	0.012	0.050
6	None	4900	2.7 2.2 2.2	1.4 1.3	0.27	0.032	0.012	-
7	None (0.059% H_2O)	3300	0.08 0.07 0.13 0.12	0.29	0.44	0.023	0.004	-

Note: Rates computed as average for entire specimen, although the lower half was covered with H_2O and the upper half with liquid H_2S as shown in Figure 16

TABLE XII

EFFECT OF PRIOR H_2S EXPOSURE ON STEEL WELDABILITY

Plate samples bevelled and exposed to 250 psi H_2S-H_2O at 40°C as indicated

Sample	Size	H_2S Exposure	Surface Cleaning	Preheat	Time H_2S-Weld	Backup Plate	Type Bend	% Elong. in 2"	Bend Angle °	Remarks
Butt Welds										
6A	4" x 4-1/2" x 1/2"	None	Ground	None	-	Clean	L	34.5	180	Rupture in Weld Metal
6B	"						L	34.5	180	Rupture in Weld Metal
6C	"						T	10.9	52	Rupture Started at Edge Defect
6D	"						T	31.3	165	Rupture at Fusion Line
2A	4" x 4-1/2" x 1/2"	330 hr	Ground	1100°F	3-1/2 hr	Exposed	L	15.6	74	Rupture in Weld Metal
2B	"						L	17.2	75	Rupture in Weld Metal
2C	"						T	7.7	27	Broke at Fusion Line
2D	"						T	31.2	164	Broke at Fusion Line
1A	4" x 4-1/2" x 1/2"	330 hr	Ground	None	1-1/4 hr	Exposed	L	4.7	19	Rupture in Weld Metal
1B	"						L	5.5	24	Rupture in Weld Metal
1C	"						T	11.0	60	Rupture at Fusion Line
1D	"						T	7.9	22	Rupture at Fusion Line
4A	7" x 2" x 5/8"	3045 + 330 hr	Ground	1100°F	4-1/4 hr	Clean	L	-	180	Rupture in Weld Metal
3A	7" x 2" x 5/8"	"		None	2-1/3 hr	Clean	L	-	180	Rupture in Heat-Affected Zone
3B	"	"					T	34.4	180	Rupture in Weld at Scribe Mark
5A	7" x 2" x 5/8"	"		None	3 hr	Clean	L	28.0	140	Rupture in Weld Metal
Bead on Plate Welds										
3C	4" x 3/4" x 5/8"	7045 + 330 hr	Ground	None	2-1/3 hr	None	L	-	180	No Break
3D					1 day	None	L	-	35	Break in Bead
3E					9 days	None	L	-	180	No Break
4B	3" x 1" x 5/8"	7045 + 330 hr	Ground	1100°F	4-1/4 hr	None	L	-	180	No Break
4C							L	-	119	Break at Weld
4D					9 days		L	-	52	Break at Weld
4E	4" x 3" x 5/8"	"	None		4-1/4 hr		L	-	10	Many Cracks in Weld
5B	4" x 1" x 5/8"	"	Wire Brush	None	3 hr		L	-	10	Many Cracks in Weld

TABLE XIII

FIELD REPAIR WELDS

6-Inch Pipe

Lab. No.	Condition	Tensile Test			Bend Test	
		Ultimate Stress psi	R.A. %	Elong. in 1"	To Crack	Load to Rupture
A.	Control - New, Ground, No Preheat	65,400	39.7	31	No crack 180°	Cracked at 60 ton
B.	Exposed, Ground Not Preheated	Too Porous			67°	Broke Fish Eyes
C.	Exposed, Ground Preheated	62,000	35.4	46	95°	Not Broken at 60 Ton
D.	Exposed, Not Ground, Preheated	60,290	35.2	24	43°	22 Ton Fish Eyes
E.	Exposed, Not Ground, Not Preheated	62,200	30.6	30	15°	24 Ton Fish Eyes

TABLE XIV

COMPRESSION TESTS OF O-RING SECTIONS

Properties of O-rings after exposure

H_2S-H_2O at 250 lb /sq in.

Name & Type of Compound	Durometer Hardness (initial)	120°C				100°C				80°C				40°C			
		Time (hr)	Hard.[1] (dur)	Perm.[2] Set	Swelling (mils)	Time (hr)	Hard. (dur.)	Perm. Set	Swelling (mils)	Time (hr)	Hard. (dur.)	Perm. Set	Swelling (mils)	Time (hr)	Hard. (dur.)	Perm. Set	Swelling (mils)
Goshen 933 Neoprene GN	75	161	80	23	18	299	70	3	39	209	70	21	31	161	60	20	32
Goshen 1144-1169 Neoprene W	80	257	75	11	70 B	-	-	-	-	1178	70	6	42	3830	100 +	16	6
Linear KN-80 Neoprene W	90	257	80	3	55 Split	114	70	13	36	209	80	20	31	1002	70	19	32
Linear KCC-70 Neoprene W	70	257	65	none	60	299	70	7	43	608	70	none	48	3830	80	none	25
Linear JAJ-70 Natural rubber	70	257	65	17	20	299	70	none	36	2011	60	17	11	3830	80	12	none
Linear ZM-70 Silicone	70	257	55	1 B	13	1574	60	9	none	2011	60	12	none	3830	70	6	none
Garleck 8990 Buna N	70	161	85	30	5	114	90	29	none	608	90	29	1	1002	80	29	none
Houghton 10-V-70 Buna N	70	161	90	30	5	114	80	26	2	608	90	29	4	1572	90	30	2

[1] Hardness values on Shore Durometer A Scale

[2] Original diameter 0.210 in.
30-mil set indicates no resilience

B Blistered

TABLE XV

DEGRADATION TESTS OF PLUG COCK LUBRICANTS

Approx. 1 in. of grease over polished ball bearing

Hot Conditions - 258 hr 250 psi H_2S-H_2O at 120°C

Name of Grease	Form	Color Change	Corrosion of AISI 52100 Steel Ball	Change in Consistency of Grease
Desco No. 600	Stick	Orange to olive green	Yes	Crust at surface
Desco No. 400	Stick	Pink to dark gray	Slight	None
Nordcoseal 421	Stick	Stayed black	Yes	None
Dow Corning Valve Seal A	Bulk	White to gray	Yes	None
Dow Corning No. 11	Bulk	White to gray	Yes	None
Plastilube No. 2	Bulk	Orange to black	Yes	None
Halocarbon Stopcock Grease	Bulk	White to gray	Yes	None
Nordcoseal 546	Stick	Gray to yellow-green	None	Crust at surface
Nordcoseal 721*	Stick	Ivory to light gray	None	None

Cold Conditions - 258 hr 250 psi H_2S-H_2O at 40°C C

Desco No. 600	Stick	Orange to olive green	None	None
Desco No. 400	Stick	Pink to brown	Yes	None
Desco No. 421	Stick	Still black	Yes	None
Valve Seal A	Bulk	White to gray	Yes	None
Dow Corning No. 11	Bulk	White to gray	Yes	None
Plastilube No. 2	Bulk	Orange darkened	None	None
Halocarbon Stopcock Grease	Bulk	None	None	None
Nordcoseal 546	Stick	Gray to yellow-green	None	None
Nordcoseal 721*	Stick	Ivory to gray	Yes	None

* Exposed 164 hr only

Note: Corrosion judged by visual inspection

TABLE XVI

STRESSED BALL BEARING TESTS OF PLUG COCK GREASES

Greases used to protect stressed S.A.E. 52100 balls bearing

Max. tensile stress ca. 300,000 psi

Tests at 40°C, 250 psi H_2S-H_2O

Grease	Time	Ball Behavior OK	Ball Behavior Broken	Color Change
Steel Bearings				
None	168		x	---
Desco 600	161		x	Yellow to green
Dow Corning No. 11	161	x		White to black
Plastilube No. 2	192	x		Brown to dark green
Desco 400	428		x	Orange to dark green
Nordcaseal 721	162	x		White to black
Nordcaseal 546	346	x		Gray to dark green
Other Ball Bearings				
Stellite	594	x		No grease present
Tungsten Carbide	594	x		No grease present

Note: Test setup shown in Fig. 18

TABLE XVII

CONSTITUTION OF SULFIDE DEPOSITS FROM GS UNITS

Sample Description and Date Taken	Temp.°C Approx.	Chemical Analysis Fe	S	Free S	Constitution by X-Ray Examination Major	Minor	Trace
		Weight Per Cent					
1) Unit 203 - Top layer on stripper bubble caps - 10/25/52	200	42.8	51.6	8.2	marcasite	-	pyrite pyrrhotite
2) Layer next to cap - 10/25/52	200	45.4	50.0	1.0	pyrite	marcasite	-
3) HT 101 D - 40th tray level - 10/30/52	120	-	-	-	pyrite marcasite	-	-
4) SC 201 A - Shell side - 10/30/52	40	-	-	-	sulfide X	pyrrhotite	-
5) SC 201 A - Tube side - 10/30/52	30	-	-	-	Fe_2O_3 Fe_3O_4	-	-
6) LH 201 A - Tube side - Inlet -	40-135	60.1	39.9	1.8	pyrrhotite	pyrite	-
7) Flare line - 10/13/52	40	47.9	39.5	7.4	pyrite	pyrrhotite	-
8) Sludge - Flare line - 10/13/52	40	52.4	41.8 (51.1% CS_2 extractable)	-	pyrrhotite	pyrite	-
9) Sludge - Flare line - 10/13/52	40	49.4	44.6 (52.82% CS_2 extractable)	-	pyrrhotite	pyrite	-
10) SC 101 D - 11/20/52	40	48.8	44.4	3.70	pyrite	pyrrhotite	-
11) SX 201 F - Tube side - 12/19/52	150	-	-	-	pyrite	-	-
12) SX 201 F - Tube side - 12/19/52	155	-	-	-	pyrite	marcasite	-
13) SX 201 F - Tube side - 12/19/52	145	-	-	-	pyrite	marcasite	-
14) SX 201 H - Tube side - 12/18/52	155	-	-	-	pyrite	-	-
15) SX 201 H - Tube side - 12/18/52	180	-	-	-	marcasite	pyrite	-
16) SX 201 H - Tube side - 12/19/52	180	-	-	-	marcasite	-	-
17) LH 203 B - Tube side - Fine crystals - 12/29/52	100	-	-	-	pyrrhotite	-	-
18) LH 203 B - Tube side - Coarse crystals - 12/29/52	100	-	-	-	pyrrhotite	-	-
19) LH 202 A - Tube side - 2/4/53	125	-	-	-	pyrite	pyrrhotite	marcasite
20) LH 301 A - Exit side, top tube sheet - 1/30/53	120	-	-	-	pyrite	pyrrhotite	marcasite
21) LH 202 B - First scale to deposit - 2/2/53	125	-	-	-	pyrrhotite pyrite	-	-
22) LH 202 B - Last scale to deposit - 2/2/53	125	-	-	-	pyrrhotite	pyrite	-
23) SX 301 F - 2/11/53	160	-	-	-	pyrite	troilite	marcasite
24) SX 101 G - 2/18/53	190	-	-	-	marcasite	-	pyrite
25) PC 502 A - First to deposit - 2/18/53	110	-	-	-	pyrite	marcasite	-
26) PC 502 A	110	-	-	-	pyrite	-	-
27) Pipe 3 ft downstream from LH 203 B - Last scale deposited 12/24/53	120	-	-	-	pyrrhotite	pyrite	-
28) Same as 27. First scale deposited	120	-	-	-	pyrite	-	-
29) LH 103 - Tube side - 2/6/53 Samples for dissolving tests.	-	-	-	-	pyrite marcasite	-	-
30) SX 301 G - 2/19/53	-	-	-	-	pyrite	marcasite	pyrrhotite

TABLE XVII (Continued)

Sample Description and Date Taken	Temp. °C Approx.	Chemical Analysis Fe	S	Free S	Constitution by X-Ray Examination Major	Minor	Trace
		Weight Per Cent					
31) LH 103 - Inlet tubes - 2/26/53	-	51.6	35.0	0.7	pyrrhotite	-	-
32) LH 102 - First pass - Tube exit - 2/26/53	-	45.8	50.7	0.1	pyrite	marcasite	-
33) LH 103 - Exit end - Second pass - 2/26/53	-	40.2	45.6	1.0	marcasite	-	-
34) LH 102 - Tube side - Exit end - Second pass - 2/26/53	-	43.6	47.7	1.2	pyrite	pyrrhotite marcasite	-
35) PC 201 F - Bottom - Second pass - 2/26/53	-	45.3	53.6	0.3	pyrite	-	marcasite pyrrhotite
36) SX 301 G - Head - Inlet side - 2/26/53	-	43.0	54.1	3.1	pyrite	-	-
37) SX 301 F - Tubes - 2/11/53	-	45.3	51.5	0.2	pyrite	-	-
38) SX 301 G - Tube rinse - 2/26/53	-	45.0	52.6	0.8	pyrite	-	-
39) SX 301 G - Head, Exit end - 2/26/53	-	35.7	58.8	18.0	marcasite	-	sulfur pyrrhotite
40) LH 102 - Shell side - 2/26/53	-	55.3	41.8	1.3	sulfide X pyrrhotite	-	-
41) 411 - Unit 12 Stripper - Top tray 3/4/53	200	42.8	50.1	0.4	marcasite	-	pyrite
42) Same as 41 - Analyzed 4 mo. later	200	31.2	36.8	2.1	(37.3% water soluble)		
43) LH 202 A - Tube sample - 2/4/53	-	-	-	-	pyrite	-	pyrrhotite
44) LH 202 A - Plate of scale	-	-	-	-	pyrrhotite	marcasite pyrite	sulfur
45) LH 103 - Tube sections nearly plugged - First deposit - 2/6/53	-	-	-	-	pyrite marcasite	-	-
46) Same as 45 - Last layer to deposit	-	-	-	-	pyrrhotite	-	-
47) Scale from pump - 28 c.c.p.-1 4/21/53	85	-	-	-	marcasite	-	-
48) Scale from pump - 21 c.c.p.-1 4/21/53	85	-	-	-	marcasite	-	-
49) Unit 16 Stripper - Top tray 4/1/53	200	-	-	-	marcasite	-	-
50) Unit 16 Stripper - Outboard cap - 4/1/53	200	-	-	-	marcasite	-	-
51) Unit 16 Stripper - Inboard cap - 4/1/53	200	-	-	-	marcasite	-	-
52) 18 PC 1A - Hot end - Shell side - 4/30/53	-	-	-	-	pyrite marcasite	-	-
53) 18 LH 2D - Hot end - Tube side - 4/30/53	-	-	-	-	marcasite pyrite	-	-
54) 17 PC 1B - Shell side - Deposit from bottom tube sheet - 4/30/53	-	-	-	-	pyrite marcasite	-	pyrrhotite
55) 17 SX 1C - Tube side - Hot end - 4/30/53	-	-	-	-	pyrite	marcasite	-
56) 17 SH 2 - Tube side - First pass - 4/30/53	-	-	-	-	marcasite	pyrite	-
57) 31 - c.c.p.-2 - Impeller deposit - 4/30/53	-	-	-	-	marcasite	-	pyrite

NOTE: Samples 1 through 40, plus 43, plus 46 from Dana
41, 42, 47, and 57 from Savannah River Plant

TABLE XVIII

SCALE REMOVAL TREATMENTS

Tests made on scale-plugged stainless steel tube sections
LH 103 - Figure 19

No.	Solution	Temperature	Exposure Time, hr	Remarks
1	10% Duclean No. 1 (Inhibited H_2SO_4)	Room	4	No change
2	" " "	"	24	" "
3	" " "	65°C	4	" "
4	" " "	"	24	" "
5	" " "	Boiling	4	" "
6	" " "	"	24	" "
7	Duclean No. 1 (Inhibited H_2SO_4) + Iron powder	80°C	72	" "
8	F-83 (83% HNO_3, 13% H_2SO_4, 4% H_2O)	Room	24	Slight attack, solution circulated through sample tube.
9	10% KCN + O_2 saturated	Room	24	No change*
10	100% Dimethylformamide	Boiling	24	" "
11	10% Na_2SO_3	Room	4	" " *
12	10% Na_2SO_3	"	24	" " *
13	" "	65°C	4	" " *
14	" "	"	24	" " *
15	" "	Boiling	4	" " *
16	" "	"	24	" " *
17	20% NaOH + Zn Metal in excess	Room	24	" "
18	83% Phenol	"	4	" "
19	" "	"	24	" "
20	" "	Boiling	24	" "
21	10% $K_2S_2O_8$	Room	4	" " *
22	" "	"	24	" " *
23	" "	65°C	4	" " *
24	" "	"	24	" " *
25	" "	Boiling	4	" " *
26	" "	"	24	" " *
27	10% $Na_2S_2O_8$	"	24	" " *
28	10% $FESO_4$ + 10% H_2SO_4	Room	4	" " *
29	" " "	"	24	" " *
30	" " "	65°C	4	" " *
31	" " "	"	24	" " *
32	" " "	Boiling	4	" " *
33	" " "	"	24	" " *
34	100% "Cellosolve"	Room	4	" "
35	" "	"	24	" "
36	" "	65°C	4	" "
37	" "	"	24	" "
38	" "	Boiling	4	" "
39	" "	"	24	" "
40	5% NaOH in "Cellosolve" solution	80°C	24	" "

* Followed by exposure to 10% Duclean No. 1 (inhibited H_2SO_4) at 80°C

TABLE XVIII (Continued)

No.	Solution	Temperature	Exposure Time, hr	Remarks	
76	10% $ZnSO_4$	Boiling	24	No change	
77	10% H_2SO_4	"	24	" "	
78	10% Sulfamic acid	"	24	" "	
79	30% NH_4OH	"	24	" "	
80	10% Calgon + 10% NaOH	"	24	" "	
81	" " "	80°C	24	" "	
82	10% H_2SO_4 + 2.5% Versene	65°C	24	" "	
83	" " " (Fe+++)	Boiling	24	" "	
84	" " " "	65°C	24	" "	
85	Trichloroacetic acid, 10%	65°C	24	" "	
86	10% Oxalic acid	Boiling	24	" "	
87	10% Tartaric acid	Room	24	" "	
88	" "	65°C	24	" "	
89	" "	80°C	24	" "	
90	10% Citric acid	"	24	" "	
91	20% Citric acid	Room	14	" "	
92	" "	Boiling	14	" "	
93	20% $NaNO_2$	"	24	" "	
94	10% $NaNO_3$ + 10% H_2SO_4	"	24	" "	*
95	$NaNO_3$, 50%	"	24	" "	*
96	10% Na_2CO_3	"	24	" "	*
97	Heat transfer salt (Hitec), 50%	"	24	" "	*
98	NO saturated H_2O	Room	24	" "	*
99	100% N_2	250°C	24	" "	
100	10% N_2 + 10% H_2SO_4	Boiling	24	" "	
101	10% NaCNS	"	24	" "	
102	SO_2 saturated H_2O	Room	24	" "	
103	10% $NaBiO_3$	Boiling	24	" "	
104	10% Na_2S	"	24	" "	
105	10% K_2S	"	24	" "	*
106	10% $K_2Cr_2O_7$	"	24	" "	*
107	10% $Na_2S_2O_3$	"	24	" "	*
108	10% $KMnO_4$	"	24	" "	*
109	10% $KMnO_4$	"	22	" "	*
110	10% KNO_3	"	24	" "	*
111	10% H_2SO_4 + 5% $K_2S_2O_8$ + 100 p p m Ag^- as $AgNO_3$	"	24	" "	*
112	10% H_2SO_4 + 1% $K_2S_2O_8$ + 100 p p m Ag^- as $AgNO_3$	"	24	" "	*
113	10% H_2SO_4 + 5% $K_2S_2O_8$ + 100 p p m Ag^- as $AgNO_3$	"	24	" "	*
114	10% CrO_3 + H_2SO_4, 10%	"	24	" "	*
115	5% CrO_3 + 5% H_2SO_4	"	24	" "	*
116	10% Hydroxylamine sulfate + 1% H_2SO_4	"	24	" "	
117	20% NaOH + 1% Versene	65°C	4	" "	

* Followed by exposure to 10% Duclean No. 1 (inhibited H_2SO_4) at 80°C

TABLE XVIII (Continued)

No.	Solution	Temperature	Exposure Time, hr	Remarks
41	5% Anthraquinone sodium sulfonate + 5% NaOH + 5% $Na_2S_2O_8$	Boiling	24	No change
42	100% S_2Cl_2	"	24	" "
43	" "	186°C	73	" "
44	10% Na_2WO_4	Boiling	24	" " *
45	10% Na_2VO_4	"	24	" " *
46	20% $Fe_2(SO_4)_3 \cdot (NH_4)_2SO_4$	"	24	" " *
47	10% " " "	200°C	20	" " * 250 psi
48	10% $FeCl_3$	"	24	No change*
49	10% $Fe_2(SO_4)_3$	"	24	" " *
50	10% $(NH_4)_2S_2O_8$	"	24	" " *
51	3% H_2O_2	Room	24	" " *
52	5% H_2O_2	"	40	" " *
53	10% H_2O_2	"	40	" " *
54	15% H_2O_2	"	24	" " *
55	" "	"	40	" " *
56	20% H_2O_2	"	40	" " *
57	30% H_2O_2	"	15 min	Scale attacked; however, reaction products cause peroxide decomposition in this time with heating to boiling point.*
58	30% H_2O_2	Room	40	Same attack, replenish H_2O_2 every two hours.*
59	20% H_2O_2	0-5°C	116	Very slight attack.*
60	20% $Al_2(SO_4)_3$ + 10% HNO_3	Boiling	24	No change *
61	10% $NaNO_3$	"	24	" " *
62	10% $ZnSO_4$ + 10% H_2SO_4	"	24	" " *
63	" " "	65°C	24	" " *
64	30% $ZnSO_4$ + 30% H_2SO_4	Boiling	24	" " *
65	10% $NaBO_3$.	"	24	" " *
66	10% $FeSO_4$	Room	4	" "
67	"	"	24	" "
68	"	65°C	4	" "
69	"	"	24	" "
70	"	Boiling	4	" "
71	"	"	24	" "
72	20% NaOH	"	24	" "
73	30% NaOH	"	23	" "
74	10% H_2SO_4 + Zn metal	Room	24	" "
75	10% $Fe_2(SO_4)_3$ + 10% H_2SO_4	Boiling	24	" " *

* Followed by exposure to 10% Duclean No. 1 (inhibited H_2SO_4) at 80°C

TABLE XVIII (Continued)

No.	Solution	Temperature	Exposure Time, hr	Remarks
118	3% $AgNO_3$	Boiling	24	No change*
119	20% $AgNO_3$	"	22	" " *
120	" "	"	73	" " *
121	100% H_2O	"	24	" "
122	$Pb(C_2H_3O_2)_2$ saturated	200°C	16	" " * 200 psi
123	10% $CuSO_4$	200°C	21	No change* 250 psi
124	100% SO_2	200°C	43	No change 240 psi
125	SO_2 saturated H_2O	200°C	43	No change 240 psi
126	30% NH_4OH	104°C	46	No change 125 psi
127	100% Benzene	Boiling	24	No change
128	100% Tolulene	"	24	" "
129	10% NO saturated Na_2S	Room	48	" "
130	22.7% $Na_2S_2O_3$ + 2.2% $CuSO_4$ + 5.7% H_3PO_4 + 0.2% KCN + 11.4% KAc + 57.3% H_2O + 2.2% $(NH_4)_2CO_3$			
131	10% $MgSO_4$	Boiling	67	No change
132	20% $NaHSO_4$	"	45	" "
133	H_2O saturated with 90% $Ca_3(PO_4)_2$, 8% $CaCO_3$, and 2% mineral oil	"	44	" "
134	5% H_3PO_4	175°C	.5	" " *
135	SO_2 saturated H_2O plus activated carbon catalyst	60°C	48	" "
136	30% CaS_x	Boiling	14	" " *
137	20% $CuCl_2$	"	12	" " *
138	37% HCl	"	18	Some scale attack completely dissolved stainless tube
139	10% Duclean No. 1 ± 10% $NaClO_3$	80°C	72	No change
140	10% Duclean No. 1 + 10% $SnCl_2$	"	22	" "
141	20% $CaCO_3$	Boiling	22	" "
142	20% $PbCO_3$	"	22	" "
143	10% Duclean No. 1 + 10% $NaNO_3$	80°C	73	" "
144	1% $AgNO_3$ + 5% $K_2S_2O_8$ + 10% H_2SO_4	Boiling	1	Slight attack very corrosive to steel*
145	" " "	80°C	51	" "
146	40% Hydrazine hydrate	Room	144	No change
147	10% Hydrazine sulfate	80°C	23	" "

* Followed by exposure to 10% Duclean No. 1 (inhibited H_2SO_4) at 80°C

TABLE XVIII (Continued)

No.	Solution	Temperature	Exposure Time, hr	Remarks
148	10% Iodine + 90% methyl alcohol	Boiling	1	Very corrosive
149	" " "	80°C	42	Very corrosive no scale attack
150	10% HNO_3	Room	19	Some scale attack steel corrosion sample dissolved
151	100% Acetic anhydride	Room	144	No change
152	Glacial acetic acid	"	144	" "
153	98% Formic acid	"	144	" "
154	100% CS_2	"	144	" "
155	20% $ZnSO_4$ + 20% NH_4OH	"	144	" "
156	30% sulfamic acid	80°C	95	" "
157	" "	80°C	23	" "
158	20% sulfamic acid	Boiling	24	" "
159	10% sulfamic acid	"	24	" "
160	10% sulfamic acid + 3% H_2SO_4	"	24	" "

TABLE XIX

SOLUBILITY OF IRON AS IRON SULFIDE IN H_2S-SATURATED H_2O

100 ml water in contact with Fe source for time indicated
Solutions filtered while under pressure

250 psi H_2S-H_2O 17-hr exposure except as noted

Temp.	Iron Source: Troilite		Pyrrhotite		Pyrite		Steel	
	Fe ppm	Final pH	Fe ppm	Final pH	Fe ppm	Final pH	Fe ppm	Final pH
40°C	6.9*	6.2	4.1*	1.8	1.0	3.3	1.9*	2.2
	1.4	3.3	4.7*	3.2	0.1	3.8	4.2*	2.0
	0.5	7.2	0.7**	--	0.7**	--	7.0*	2.8
	1.4	5.6	2.6**	--	0.2**	--	0.9**	6.2
			8.1**	2.6			1.4**	5.2
							0.6	5.8
80°C	0.3	7.0	1.7	2.3	8.5	4.6	1.1	3.9
			.1	2.9				
100°C	1.5	2.9	1.4	2.6	2.4	6.3	1.4	4.2
			1.0	7.8	0.4	4.0	1.4	8.0
			0.7	7.0			2.8	3.2
120°C	0.1*	7.2	0.1*	2.4	0.9*	7.2	1.6*	2.3
	0.3	8.6	6.7	3.4	0.8	8.2	0.8	3.2
	0.9	2.5	0.4	2.5	0.6	2.4	0.6	8.0
	0.4**	8.8	2.1	2.3	0.7**	--	1.2	2.4
	0.5	8.6	1.0**	--	0.9**	--	0.4*	8.7
			0.3**	--	1.2**	8.0	0.2	8.3
			2.3**	8.6				
150°C	1.1	--	1.7	2.2	0.2*	8.5	4.6	2.2
	2.1*	8.6			0.8	--		
	5.0	7.2						
	0.2	6.9						
	0.1	8.4						
170°C	0.1	8.2	0.3	7.7			0.1	6.4

* Three-day test
** Seven-day test

TABLE XX

EFFECTS OF STARTING pH ON IRON SULFIDE SOLUBILITY

Tests at 250 psi, 40°C and 120°C

Pyrrhotite as the Fe Source	Test Temp. °C	Initial pH	Total Fe-ppm	Final pH
10^{-3} molar acid	40	3	9.1	2.7
			11.0	2.0
	120	3	0.8	8.3
			0.3	2.4
			0.5	2.5
10^{-3} molar base	40	11	0.6	8.1
			1.9	2.7
			2.2	2.1
	120	11	1.1	8.3
			0.8	2.8
			1.1	2.7
			2.5	2.9
Steel as the Fe Source				
10^{-3} molar acid	40	3	17.7	3.0
	120		0.3	6.3
	120		0.9	4.3
10^{-3} molar base	120	11	0.2	8.8
			1.1	8.3
			0.4	7.8

Note: Approx. 3-day tests

TABLE XXI

IRON SULFIDE SOLUBILITY TESTS AT LOW H_2S PRESSURES

H_2S-H_2O at 15 psi - H_2S plus H_2O vapor pressure

17 hr except as noted

	Troilite		Pyrite		Steel	
Temp., °C	Fe ppm	Final pH	Fe ppm	Final pH	Fe ppm	Final pH
40	.54	6.1	0.6	7.2	0.5	7.5
	.47*	5.4	1.0	3.2	1.1*	5.4
	2.18*	8.1			1.0	6.3
	1.00	6.0			2.7**	
	1.39	5.9				
120	3.2	8.1	0.4**		0.8	7.1
	5.47**	7.6			1.2	7.8
	1.08**	7.2			0.4	
	.43**				1.6**	6.3
					0.6**	8.4
150	3.44*	8.8	6.8*	8.6		
	1.47	7.8	0.9	7.4		

* 3-day exposure

** 7-day exposure

TABLE XXII

CORROSION BY DILUTE SODIUM HYDROSULFIDE SOLUTIONS

Tests made at 30°C under 200 psi N_2 pressure

Dana water used was vacuum deaerated to reduce oxygen

		Dana Water	50 ppm NaHS	50 ppm NaHS Aerated	500 ppm NaHS	360 ppm NaOH
Original pH		5.9	8.6	8.7	10.0	11.3
Final pH (160-hr test)		7.0	9.1	9.1	10.0	11.1
	Time, Hr		Corrosion Rates, mils/yr			
90-10 Bronze	16	Nil	6.1, 9.2		14.4,10.7	
	45		3.4		5.6	
	97		0.5		1.6	
	120		1.0		2.2	
	160		1.0	1.5	1.5	0.6
	666		0.3	0.2	1.0	0.1
A212 Steel						
	16	0.7	1.0, 3.2		2.2, 2.7	
	45		1.1		0.9	
	97		0.1, 0.8		0.2, 0.5	
	120		0.8		0.5	
	160		0.7	0.4	0.3	0.7
	666		0.1	0.1	0.1	0.05
Rimmed Steel Sheet						
	16	1.2	1.5, 1.1		1.4, 1.1	
	45		0.6		0.5	
	97		0.2		0.2	
	120		.3		.4	
	160		0.2	0.3	0.4	0.12
	666		0.1	0.1	0.2, 0.2	0.04

TABLE XXIII

EROSION - CORROSION IN DILUTE NaHS SOLUTIONS

Tests at 30°C
50 psi N_2

Erosion - Corrosion Test 40 ft /sec jet	Corrosion Rates, mils/yr			
	Time, Hr	100 ppm NaHS	Time, Hr	100 ppm NaHS
90 - 10 Bronze AISI 1045	47	10.4	169	2.1
Control samples away from jet				
90 - 10 Bronze	47	11.7	169	3.3, 2.9, 5.2
A212 steel	47	3.8	169	0.8, 2.84
Rimmed steel	47	4.3, 5.0	169	0.4, 0.5, 0.8, 0.7

TABLE XXIV

HIGH TEMPERATURE CORROSION TEST DATA

H_2S-H_2O

Samples immersed in liquid

168-hr exposure

Corrosion Rate, mils/yr

Steel Type	Temperature, °C				
	120	175	200	225	250
A212	22	25 43	36 29	42 48	38
304	0.15	0.4 0.5	1.8 1.9	2.4 4.3	4.6
316	0.06	0.21 0.46	2.3	2.3 4.0	5.7
329	1.3	0.13 0.12	0.78	0.59 0.27	0.39
410	1.1	34.8	45 41	29 63	22

TABLE XXV

CORROSION OF SILVER SOLDERS

Tests in H_2O saturated H_2S - 100°C

Samples in covered glass bottles

Corrosion Rates, mils/yr

	Time, hr	Rate	% Copper
Sil-Fos	300	121	80
Easy-Flo 45	300	1.9	15
Easy-Flow 3	300	8.4	16
BT	300	39.8	28
Cu	300	420	100
Ag	300	1.4	
Cd	300	5.0	
Ni	300	4.3	
Fe	300	2.1	
Zn	300	9.2	
93% Cu - 7% Ag	500	500	93
92% Ag - 8% Cu	500	3.2	8

TABLE XXVI

CORROSION RESISTANCE OF MATERIALS IN H_2S-H_2O

At 250 psi

Material	Exposure Water or Gas Phase	Corrosion Rate, Mils Per Year: Period 1 136 Hr *	Period 2 158 Hr *	Period 3 135 Hr *	Period 4 160 Hr *	Period 5 134 Hr *	Period 6 480 Hr **	Period 7 638 Hr **	Period 8 785 Hr **	Period 9 656 Hr **	Period 10 524 Hr **	Period 11 786 Hr **	Period 12 1500 Hr **	Average Rate Mil/Yr.
Steel														
A212-1	G	8.2	13.8	27.8	22.7	37.2	10.2	19.2	11.4	21.4	22.0	4.2	12.5	13.9
A212-2	W	8.8	8.8	5.3	5.2	28.6	10.2	31.2	42.4	9.6	26.0	5.0	9.6	16.4
A212-W-1	G	--	--	--	--	--	--	--	--	--	--	6.4	6.6	6.6
1018-1	G	10.2	13.7	16.9	16.0	34.4	1.3	14.2	13.0	14.5	14.3	5.0	10.6	11.5
1018-2	W	4.1	8.9	1.7	7.0	16.0	1.6	12.5	66.2 +++	4.6	18.7	8.0	8.0	13.3
Rimmed 1	W	--	--	8.0	13.3	31.2	11.0	12.4	--	--	--	--	--	13.3
Rimmed 2	G	--	--	23.6	3.5	34.6	11.8	11.9	9.6	7.3	24.6	3.4	19.1	13.6
Rimmed 13791-1	G	--	--	--	15.1	34.6	5.8	16.0	12.1	14.3	15.7	--	--	13.9
Killed 16105-1	G	--	--	--	22.0	32.5	8.9	15.6	14.2	16.0	14.6	--	--	15.1
13790-1	G	--	--	--	16.2	36.2	13.6	13.4	9.1	18.0	17.3	--	--	15.0
16094-1	G	--	--	--	5.3	38.3	4.8	15.6	12.0	15.1	15.0	--	--	13.5
20040-16	G	--	--	--	--	18.4	13.3	14.4	14.6	18.6	16.3	--	--	15.6
19525-24	G	--	--	--	--	23.0	11.6	13.2	10.9	16.9	17.9	--	--	14.6
Galv. Steel	G	--	--	--	Nil	Nil	0.2	3.8	0.3	9.7	15.0	--	--	5.0
Galv. Steel 2	G	--	--	--	--	--	--	--	--	--	Nil	2.2	--	1.1
405 (5% CR) 1	G	3.7	4.9	14.9	4.3	14.8	5.9	9.5	6.2	8.9	14.5 +++	--	--	8.7
405 (5% CR) 2	W	7.8	5.9	4.1	11.4	33.0	3.2	23.8	36.6	10.4	72.6 +++	--	--	19.3
9% Ni 1	G	5.5	15.6	28.8	50.4	52.8	12.0	22.3	14.8	21.5	18.8	--	--	25.5
9% Ni 2	W	5.5	18.7	11.4	40.8	49.2	27.6	30.0	19.6	16.9	40.3	--	--	25.8
Cast Iron														
Ni-Resist 1	G	--	--	--	--	--	--	--	--	3.3	5.7	3.4	1.7	3.0
Ni-Hard 1	G	--	--	--	--	--	--	--	--	2.9	9.7 +++	8.4	--	6.8
Cast Iron	W	--	--	--	--	--	--	--	--	4.7	72.2 +++	19.2	14.5	16.1
Cast Iron	G	--	--	--	--	--	--	--	--	14.0	26.3	14.2	24.5	26.6
Stainless Steel														
410-1	G	1.6	0.8	Nil	0.1	0.7	3.0	2.8	5.0	2.4	14.9	1.9	1.4	3.1
410-2	W	1.2	1.2	Nil	0.4	0.2	Nil	1.6	0.7	2.5	3.0	1.0	0.7	1.1
316-1	G	0.6	Nil	0.2	Nil	Nil	0.1	0.1	0.3	0.4	0.1	0.06	0.04	0.2
316-2	W	0.5	Nil	Nil	Nil	Nil	Nil	0.1	0.3	0.3	0.1	0.04	0.02	0.1
329-1	G	0.5	Nil	Nil	Nil	--	Nil	0.1	0.5	0.1	0.08	0.3	0.1	0.2
329-2	W	0.2	0.5	--	Nil	Nil	Nil	0.2	0.2	0.04	0.5	0.1	0.1	0.1
304-1	G	--	--	--	--	--	--	--	1.1	0.8	0.6	0.2	0.2	0.5
304-S-2	W	--	--	--	--	--	--	--	0.5	0.1	0.4	0.8	0.5	0.3
347-S-1	G	--	--	--	--	--	--	--	1.2	0.3	0.4	0.2	0.05	0.3
316-S-1	G	--	--	--	--	--	--	Nil	4.6	0.3	0.1	0.5	0.05	0.2
316 Clad	G	--	--	--	--	14.3	4.3	3.5	4.1	11.6	13.3	3.2	7.0	6.7
304 Clad	G	--	--	--	--	11.6	4.6	5.0	3.1	11.3	11.4	3.6	7.2	6.6
Nonferrous Alloys														
Nickel 1	G	--	--	--	Nil	7.8	7.0	5.9	1.2	4.2	7.3	0.6	Nil	2.8
Nickel 2	W	--	--	--	Nil	9.4	11.0	8.2	2.8	2.2	2.4	4.7	Nil	3.5
Monel 1	G	10.8	12.5	9.6	17.5	12.5	11.6	15.0	7.0	4.6	3.4	--	--	9.1
Monel 2	W	33.6	32.4	56.4	28.8	38.4	22.2	6.8	23.2	21.1	15.8	--	--	22.9
Monel 3	G	--	--	--	12.0	9.6	7.6	16.1	5.4	--	--	--	--	9.7
Monel 4	W	--	--	--	19.0	28.1	22.4	30.7	21.4	--	--	--	--	24.5
Monel S-1	G	--	--	--	--	--	--	--	--	3.1	0.5	--	--	2.0
Inconel 1	G	--	--	--	0.1	1.0	0.2	1.1	0.2	0.8	0.2	0.3	0.4	0.5
Inconel 2	W	--	--	--	Nil	1.2	0.6	0.8	1.1	0.6	0.3	0.4	0.6	0.7
Ni Clad	G	--	--	--	--	15.0	7.8	6.1	7.0	11.3	11.2	4.6	6.7	7.8
Inconel Clad	G	--	--	--	--	13.8	4.8	6.5	6.0	9.2	10.2	3.7	7.3	6.8
70-30 Brass	G	--	14.4	20.9	20.9	23.0	5.5	18.0	6.1	5.3	7.1	--	--	6.7
Ampco 8	G	--	2304.0	--	--	--	--	--	--	--	--	--	--	2304.
Admiralty 1	G	--	--	--	--	--	1.0	3.0	2.2	3.5	4.8	--	--	2.9
Al-3S-1	G	--	--	--	1.0	1.0	1.0	1.0	4.2 +	--	--	--	--	2.3
Al-3S-2	W	--	--	--	1.6	1.9	21.2	9.5	117.0 +	--	--	--	--	51.0
Elgiloy	G	--	--	--	--	--	Nil	Nil	Nil ++	Nil	--	--	--	Nil
Fine Silver	G	--	--	--	--	--	50.9	4.3	3.4 ++	--	--	--	--	15.7
Platinum	G	--	--	--	--	--	Nil	Nil	Nil	0.02	--	--	--	0.00
Titanium	G	--	0.06	0.1	0.06	0.1	0.06	Nil	0.06	0.2	0.00	0.02	--	0.05
Illium G1	G	--	--	--	--	--	--	--	--	0.2	0.03	0.01	0.01	0.04
D-20-1	G	--	--	--	--	--	--	--	--	0.08	0.04	0.02	0.01	0.03
Chemical Lead 1	G	--	--	--	--	--	--	--	--	--	0.9	--	--	0.9
Chemical Lead 2	W	--	--	--	--	--	--	--	--	--	0.9	0.07	--	0.9
Hastelloy D	G	--	--	--	--	--	--	--	--	Nil	Nil	0.07	0.48	0.15
Stellite No. 6	G	--	--	--	--	--	--	--	0.029	0.03	Nil	Nil	Nil	0.00
85-5-5-5	G	--	--	--	--	--	--	--	--	--	833.0	--	--	833.
85%Ag.-15%Mg	G	--	--	--	--	--	--	--	--	--	--	--	--	70.0
Magnesium	G	--	--	--	--	--	--	--	--	970.0	--	--	--	970.
Silver Solders														
Silvalov 15	G	--	--	--	--	--	--	--	--	104.0	--	--	--	104.0
Silvalov A25	G	--	--	--	--	--	--	--	--	148.0	--	--	--	148.0
Silvalov 50	G	--	--	--	--	--	--	--	--	2.3	--	--	--	2.3
Silvalov 355	G	--	--	--	--	--	--	--	--	2.5	--	--	--	2.5
Easy Flo	G	--	--	--	--	--	--	--	--	1.3	--	--	--	1.3
Easy Flo No. 45	G	--	--	--	--	--	--	--	--	1.7	--	--	--	1.7

* Specimens cleaned with sand soap and water; stagnant conditions-ie. solution not circulated.
** Specimens cleaned with inhibited acid; solution circulated with the exception of 80 hr in period 6, 230 hr in period 7 and 500 hr in period 12.
\+ Very deep pits
++ Thick, tight scale
+++ Abnormally high single period rate

TABLE XXVII

CORROSION RESISTANCE OF MATERIALS IN H_2S-H_2O AT LOW PRESSURE

Material	Exposure Water or Gas	Corrosion Rate Mils per Year: Period 1 372 hr	Period 2 259 hr	Period 3 306 hr	Period 4 1040 hr	Period 5 168 hr	Period 6 168 hr	Period 7 806 hr	Period 8 1060 hr	Period 9 2600 hr	Over-all Mils/Yr	Over-all Hours
Ferrous												
Carbon Steel												
A212-1	G	5.0	12.7	11.4	15.6	26.2	11.4	6.8	3.7	0.8	6.3	6779
A212-2	G	4.6	15.1	11.5	20.4	24.4	15.1	7.0	4.7	1.0	7.4	6779
1018-1	G	5.2	16.7	8.3	15.4	27.7	19.0	8.0	1.9	1.2	6.5	6779
1018-2	G	3.1	10.3	10.6	14.4	31.3	14.3	7.7	2.5	0.9	6.0	6779
Rimmed												
13791-2	G	--	--	--	17.3	25.8	24.0	7.0	3.8	1.1	6.7	5842
Killed												
13790-2	G	--	--	--	17.6	25.2	21.1	7.9	2.5	1.2	6.5	5842
API-5LX	G	--	--	--	14.4	21.6	17.5	7.1	2.9	0.9	5.6	5842
NL9440	G	--	--	--	4.8	20.0	15.6	5.9	2.3	0.7	3.4	5842
16105-2	G	--	--	--	10.6	24.4	14.5	6.1	3.1	1.0	4.8	5842
16094-2	G	--	--	--	13.2	22.9	15.6	7.2	2.5	0.9	5.3	5842
Stainless Steel												
410-1	G	0.4	0.3	1.0	1.2	2.4	1.7	0.5	0.4	0.2	0.5	6779
410-2	G	0.5	0.5	0.6	1.3	2.5	1.2	0.6	0.5	0.2	0.6	6779
316-1	G	0.1	0.1	0.1	0.2	0.8	0.8	0.05	0.0	0.0	0.1	6779
316-2	G	0.1	0.2	0.1	0.2	0.7	1.0	0.02	0.0	Nil	0.1	6779
329-1	G	0.1	0.05	0.1	0.2	0.4	0.5	0.0	0.0	0.0	0.1	6779
329-2	G	0.2	Nil	Nil	0.1	0.4	0.8	0.02	0.0	0.0	0.0	6779
Nonferrous												
Nickel-3	G	--	--	--	7.7	9.7	2.4	0.5	2.4	0.2	2.3	5842
3S Al-3	G	--	--	--	1.2	0.7	4.9	10.6	0.1	1.0	0.2	5842
50% Au-50% Cu	G	--	--	--	--	--	--	Nil	Nil	Nil	Nil	4466
85% Ag-15% Mg	G	--	--	--	--	--	--	0.2	0.4	0.2	0.2	4466
Inconel	G	--	--	--	2.0	3.5	1.2	0.4	0.0	0.0	0.6	5842
Monel	G	--	--	--	7.6	9.0	3.4	1.4	0.0	1.1	2.4	5842
Lead	G	--	--	--	--	--	--	--	0.5	0.1	0.2	3660
Solders												
Silvaloy A-28	G	--	--	--	--	--	--	0.5	0.2	8.8	6.4	3660
Silvaloy 50	G	--	--	--	--	--	--	0.4	0.4	9.2	6.7	3660
Silvaloy 301	G	--	--	--	--	--	--	1.1	0.7	2.1	1.9	3660
Silvaloy 355	G	--	--	--	--	--	--	0.2	0.4	3.1	2.3	3660
Easy Flo 45	G	--	--	--	--	--	--	0.2	0.4	9.6	7.0	3660
BT	G	--	--	--	--	--	--	1.6	0.4	2.7	2.4	3660

TABLE XXVIII

CORROSION RESISTANCE OF
METALS AND NONMETALS EXPOSED TO H_2S

H_2S-H_2O at 250 psi

Material	Time, hr	Temp, °C	Condition	Corr.Rate mils/yr
High speed steel (18-4-1)	460	40	Liquid	0.84
	460	120	"	17.6
430	4,500	120	"	0.56
304 annealed	8,400	120	Gas	0.12
304 sensitized 1 hr 1250°F	8,400	120	"	0.11
316 annealed	8,400	120	"	0.02
316 sensitized	13,000	120	"	0.08
316 annealed	8,400	120	Liquid	0.07
329	8,400	120	Gas	0.21
329	8,400	120	Liquid	0.22
Carp. No. 20	1,900	120	Gas	0.04
Carp. No. 20	1,900	120	Liquid	0.14
Chrome plated 304	9,300	120	"	0.19
Stellite	12,600	120	"	0.13
Chrome Carbide Grade 608	9,300	120	"	0.04
Tantalum	9,300	120	"	0.003
Zirconium	9,300	120	"	0.001
Nonmetallics				Observations
Orlon	1,000	120	Liquid	Red, stiff
Natural rubber	1,500	120	"	Resilient
Steam sheet	1,500	120	"	Resilient
Teflon enamel on 316	700	120	"	Coating not visibly affected
Epoxy resin on 1020	50	40	Liquid	Coating blistered

Note: All exposures over 1000 hr include 3 or more exposure periods

TABLE XXIX

ANALYSES OF GAS IN H_2S CYLINDERS

Cyl. No.	$H_2S + CO_2 + HCl$ Vol. %	CO_2 Vol. %	O_2 Vol. %	HCl Wt. %	Res. Vol. %
XX306	99.2	Nil	0.09	-	0.67
	99.2	Nil	0.11	-	0.69
1542	99.4	Nil	Nil	-	0.60
	99.4	Nil	Nil	-	0.60
G883	99.3	Nil	Nil	-	0.70
	99.3	0.02	0.01	-	0.67
FF3027	99.5	0.02	Nil	-	0.5
	99.4	Nil	Nil	-	0.6
4654	99.3	0.1	Nil	-	0.6
	99.4	Nil	Nil	-	0.6
4961	97.0	0.03	Nil	-	2.97
	97.7	0.02	Nil	-	2.24
DD423	99.3	Nil	Nil	-	0.7
	99.4	Nil	Nil	-	0.6
XX1683	98.5	0.21	0.05	-	1.2
	98.6	0.25	0.06	-	1.1
XX1301	99.0	Nil	Nil	-	1.0
	99.2	Nil	Nil	-	0.8
XX233	98.02	0.22	0.11	<0.01	1.87*
	98.03	-	0.07	--	1.90
XX276	99.75	0.07	0.15	<0.01	0.10
	99.65	-	0.16	-	0.19
XX966	98.56	<0.05	Nil	<0.01	0.44
	98.61	-	0.06	-	0.34
XX1739	95.52	1.7	Nil	<0.01	4.48
	95.73	-	Nil	-	4.27
	95.90	-	0.02	-	4.10
	96.22	-	0.05	-	3.78
	96.36	-	0.03	-	3.64

* Dissolved

TABLE XXX

CHEMICAL COMPOSITION OF 3/8-INCH ALLEN HEAD CAP SCREWS

0.41%	C
0.87%	Cr
0.12%	Mo
0.80%	Mn
0.20%	Si
0.06%	S
-	P

TABLE XXXI

HARDNESS OF 3/8-INCH ALLEN HEAD CAP SCREWS AS A FUNCTION OF TEMPERING TEMPERATURE

Tempering Temperature*	Average Rockwell C Hardness
As quenched	R_C55
850°F	41
950°F	36
1050°F	31
1150°F	26
1250°F	21

* All bolts were austenitized for 30 min. at 1550°F and oil quenched prior to tempering. Bolts were tempered for 1 hr followed by air cooling.

TABLE XXXII

TYPICAL CHEMICAL ANALYSES OF TWO LARGE STUD BOLTS ORIGINALLY OBTAINED FROM THE DANA PLANT

	5/8 in.	1-1/8 in.	Composition Range AISI 4140
%C	0.29	0.38	0.38 - 0.43
%Cr	0.43	0.83	0.80 - 1.10
%Mo	0.10	0.10	0.15 - 0.25
%Mn	0.99	0.80	0.75 - 1.00
%Si	0.18	0.11	0.20 - 0.35
%S	0.05	0.07	0.040 max.
%P	-	0.01	0.040 max.

TABLE XXXIII

LIST OF ENVIRONMENTS USED FOR SULFIDE CORROSION CRACKING TESTS ON BOLTING MATERIALS

A. H_2S-H_2O Systems at a Pressure of 250 psi

1. 120°C
2. 100°C
3. 80°C
4. 60°C
5. 38°C

B. H_2S-H_2O System at Room Temperature and Atmospheric Pressure

C. Water-Saturated Mixture of 100 ppm H_2S in Air

D. Water-Saturated Mixture of 1% H_2S in Air

E. Water-Saturated Mixture of 3% H_2S in Nitrogen

TABLE XXXIV

SUMMARY OF TEST DATA FOR ANNEALED*
3/8-INCH AISI 4140 BOLTS
EXPOSED IN AN H_2S-H_2O SYSTEM AT 38°C AND 250 psi

Hardness Range (Rockwell C)	Range of Applied Stress psi	Number of Bolts Exposed	Number of Bolts Failed	Total Exposure Time
	35-45,000	19	None	1-1 1/2 yr
R_c 15-21	45-60,000	31	None	"
	60-70,000	40	None	"
	70-80,000	38	None	"

* Microstructure of all bolts consisted of ferrite and pearlite instead of tempered martensite

Note: The yield strength of annealed 3/8-in. bolts having a ferritic-pearlitic microstructure and a hardness of R_c 18-22 varied from 70-83,000 psi

TABLE XXXV

SUMMARY OF TEST DATA FOR LARGE AISI 4140 BOLTS
EXPOSED IN AN H_2S-H_2O SYSTEM AT 120°C AND 250 psi

Bolt Size	Number of Bolts Exposed	Hardness Range (Rockwell C)	Range of Applied Stress psi	Number of Bolts Failed	Total Exposure Time
1/2 in.	4	R_c 25-31	50-80,000	None	8 mo
5/8	2	30-32	55-90,000	None	8
3/4	4	25-31	40-80,000	None	8
7/8	2	31-33	55-100,000	None	8
1-3/8	3	31-36	50-85,000	None	8

TABLE XXXVI

SUMMARY OF TEST DATA FOR 3/8-INCH AISI 4140 BOLTS EXPOSED IN H_2S-H_2O SYSTEMS AT 250 psi AND 60, 80, 100, AND 120°C

Temp. of Exposure	Approximate Hardness (Rockwell C)	Approximate Applied Stress, psi	Number of Bolts Exposed	Number of Bolts Failed	Total Exposure Time*
60°C	R_C 40	100,000	5	5	
	55	50,000	3	3	
80°C	40	100,000	5	0	8 mo
	55	50,000	3	2	8 mo
100°C	40	100,000	5	3	6 mo
	55	50,000	3	3	
120°C	40	100,000	5	4	2 mo
	55	50,000	3	3	

* For unfailed bolts

TABLE XXXVII

SUMMARY OF TEST DATA FOR ALL AISI 4140 BOLTS EXPOSED IN A WATER-SATURATED MIXTURE OF 100 PPM H_2S IN AIR

Bolt Size	Approximate Hardness (Rockwell C)	Range of Applied Stress psi	Number of Bolts Exposed	Number of Bolts Failed	Total Exposure Time
3/8 in.	R_C 35	70-80,000	20	None	9 mo
3/8	40	45-55,000	10	"	9
		60-65,000	13	"	9
		90,000	1	"	9
5/8	30	85,000	1	"	9
3/4	30	75,000	1	"	9
7/8	30	80,000	1	"	9
	30	120,000	1	"	9

TABLE XXXVIII

SUMMARY OF TEST DATA FOR ALL AISI 4140 BOLTS EXPOSED IN A WATER-SATURATED MIXTURE OF 1% H_2S IN AIR

Bolt Size	Approximate Hardness (Rockwell C)	Range of Applied Stress (psi)	Number of Bolts Exposed	Number of Bolts Failed	Total Exposure Time
3/8-in.	R_C 35	50-60,000	10	None	8 mo
	35	75-80,000	20	"	9
3/8	40	20-35,000	10	"	8
	40	45-65,000	24	"	8
5/8	30	80-90,000	3	"	7
7/8	30	40-45,000	2	"	9
	30	75,000	1	"	9
3/4	30	75,000	1	"	9
1-1/4	30	120,000	1	"	9

TABLE XXXIX

EFFECT OF PLASTIC PRESTRAIN ON THE CRACKING SUSCEPTIBILITY OF QUENCHED AND DRAWN 3/8-INCH AISI 4140 BOLTS EXPOSED IN AN H_2S-H_2O SYSTEM AT 38°C AND 250 psi

Degree of Prestressing	Amount of Prestrain Introduced	Range of Applied Stress: 35,000-70,000 psi — Number of Bolts Tested	35,000-70,000 psi — Per Cent Failed	Range of Applied Stress: 100,000 psi - Yield Strength — Number of Bolts Tested	100,000 psi - Yield Strength — Per Cent Failed
None	0	60	8	28	21
Below Ultimate Tensile Strength	0.010-0.030, in./in.	4	0	4	50
At or Near Ultimate Tensile Strength	0.050-0.070	6	33	11	64
Beyond Ultimate Tensile Strength	0.070-0.130	7	14	11	100

Note: Range of hardness for non-prestrained bolts was R_C 27-33 and for prestrained bolts was R_C 24-33. All bolts were quenched and drawn and had a tempered martensitic microstructure.

TABLE XL

EFFECT OF PLASTIC PRESTRAIN ON THE CRACKING SUSCEPTIBILITY OF ANNEALED 3/8-INCH AISI 4140 BOLTS EXPOSED IN AN H_2S-H_2O SYSTEM AT 38°C AND 250 psi

Hardness Range (Rockwell C)	Range of Applied Stress (psi)	Amt. of Prestrain	Number of Bolts Exposed	Number of Bolts Failed	Total Exposure Time
R_c 20-21	45-60,000	None	3	None	13-16 mo
18-21	70-80,000	None	5	None	"
18	70,000	0.060 in./in. (Below ultimate tensile strength)	1	None	8 mo
22	65,000	0.180 in./in. (Beyond ultimate tensile strength)	1	1	45 hr

Note: All bolts were annealed and had a ferritic-pearlitic microstructure.

Average yield strength of annealed 3/8-in. bolts in the hardness range of R_c 18-22 was 75,000 psi (70-83,000 psi)

TABLE XLI

EFFECT OF METALLIC COATINGS ON SUSCEPTIBILITY ON 3/8-INCH AISI 4140 BOLTS TO SULFIDE CORROSION CRACKING

Environment	Type of Coating[1]	Number of Bolts Exposed[2]	Number of Bolts Failed	Average Time to Failure	Exposure Time Unfailed Bolts
H_2S-H_2O at 38°C - 250 psi	No coating	4	4	500 hr	
	Cadmium	2	2	1,100	
	Zinc	2	2	1,100	
	Chromium	2	2	1,400	
	Lead	2	2	1,400	
	Brass	2	0		8,200 hr
H_2S-H_2O at Room Temp.- Atm. Press.	No coating	5	5	250 hr	
	Zinc	2	2	500	
	Brass	2	2	600	
	Aluminum	3	2	1,700	11,000 hr
	Cadmium	2	2	7,600	
	Lead	2	1	8,400	14,000
	Chromium	2	1	14,000	14,000

[1] All coatings were electrodeposits having a minimum thickness of 0.002 in. except the aluminum which was a sprayed paint coating applied in three successive light layers.

[2] All bolts exposed had a hardness of R_c 38-42 and were stressed to 55-65,000 psi

TABLE XLII

EFFECT OF NICKEL PLATING ON THE SULFIDE CORROSION CRACKING SUSCEPTIBILITY OF 5/8-INCH AISI 4140 BOLTS EXPOSED IN AN H_2S-H_2O SYSTEM AT 38°C AND 250 psi

Type of Plating	Hardness Range (Rockwell C)	Range of Applied Stress (psi)	Number of Bolts Exposed	Number of Bolts Failed	Total Exposure Time
None	R_c 35-37	60,000	3	3	-
Nickel[1]	R_c 34-36	60-70,000	4	0	1 yr

[1] Electroplated nickel coating was 0.005 in. thick

TABLE XLIII

SUMMARY OF EXPOSURE DATA FOR TYPE 316 STAINLESS STEEL BOLTS EXPOSED IN AN H_2S-H_2O SYSTEM AT 38°C AND 250 psi

Bolt Size	Bolt Hardness (Rockwell B)	Range of Applied Stress (psi)	Number of Bolts Tested*	Total Exposure Time
3/8 in.	R_b 86	(45-60,000)[1]	11	12 mo
3/8	86	(65-85,000)[1]	8	12

* None of the bolts tested failed

[1] These values of applied stress were calculated on the basis of Hooke's law even though the yield point of the bolts had been exceeded

Physical Properties of Type 316 Stainless Steel (Taken from Literature)

Hardness:	R_b 86
Yield Strength (0.2% offset):	35,000 psi
Ultimate Tensile Strength:	90,000 psi

TABLE XLIV

SUMMARY OF EXPOSURE DATA FOR INCONEL BOLTS EXPOSED IN A NUMBER OF H_2S-H_2O SYSTEMS

Environment	Bolt Size	Bolt Hardness (Rockwell C)	Range of Applied Stress (psi)	Number of Bolts Tested*	Total Exposure Time
H_2S-H_2O at 38°C and 250 psi	3/8 in.	R_c 26-27	90-110,000	5	11 mo
	1/2	28-30	100-110,000	3	10
H_2S-H_2O at Room Temp.-Atm. Press.	3/8	26-27	80-110,000	5	22
	1/2	28-30	95-100,000	3	20
100 ppm H_2S in air (water-saturated)	3/8	26-27	85-110,000	5	6
1% H_2S in air (water-saturated)	3/8	26-27	85-110,000	5	6

* None of the bolts tested failed

Average Physical Properties of 3/8-in. Inconel Bolts

Hardness:	R_c 26-27
Yield Point:	110,000 psi
Yield Strength (0.2% offset):	130,000 psi
Ultimate Tensile Strength:	140,000 psi

TABLE XLV

SUMMARY OF EXPOSURE DATA FOR INCONEL-X BOLTS EXPOSED IN A NUMBER OF H_2S-H_2O SYSTEMS

Environment	Bolt Size	Bolt Hardness (Rockwell C)	Range of Applied Stress (psi)	Number of Bolts Tested*	Total Exposure Time
H_2S-H_2O at	3/8 in.	R_c 34-36	100-110,000	4	9 mo
38°C and 250 psi	1/2	19-21	100,000	1	12
H_2S-H_2O at Room Temp.- Atm. Press.	3/8	34-36	100-125,000[1]	4	18
	1/2	19-21	90- 95,000	2	18
1% H_2S in air (water-saturated)	3/8	34-36	100-135,000[1]	4	3
	1/2	19-21	95-100,000	2	6

* None of the bolts tested failed

[1] One bolt out of four was prestressed to its ultimate tensile strength before stressing to the level indicated

Average Physical Properties of Inconel-X Bolts

	3/8 in.	1/2 in.
Hardness	R_c 34-36	R_c 19-21
Yield Strength (0.2% offset)	135,000 psi	100,000 psi
Ultimate tensile strength	180,000 psi	110,000 psi

TABLE XLVI

SUMMARY OF EXPOSURE DATA FOR MONEL BOLTS EXPOSED IN A WATER-SATURATED MIXTURE OF 1% H_2S IN AIR[1]

Bolt Size	Bolt Hardness (Rockwell C)	Range of Applied Stress (psi)	Number of Bolts Tested*	Total Exposure Time
3/8 in.	R_C 23-24	65-90,000	5	6 mo

* None of the bolts tested failed.

[1] This was the only environment tested.

Physical Properties of Monel (Taken from Literature)

Hardness:	R_C 23
Yield Strength (0.2% offset):	105,000 psi
Ultimate Tensile Strength:	115,000 psi

TABLE XLVII

SUMMARY OF EXPOSURE DATA FOR K-MONEL BOLTS EXPOSED IN A NUMBER OF H_2S-H_2O SYSTEMS

Environment	Bolt Size	Bolt Hardness (Rockwell C)	Range of Applied Stress (psi)	Number of Bolts Tested*	Total Exposure Time
H_2S-H_2O at 38°C and 250 psi	3/8 in.	R_C 21-24	65- 90,000	5	11 mo
	3/8	32-34	100-125,000	2	4
H_2S-H_2O at Room Temp.-Atm.Press.	3/8	21-24	70- 90,000	5	22
	3/8	32-34	105-125,000	2	12
100 ppm H_2S in air (water-saturated)	3/8	21-24	70- 90,000	5	6
1% H_2S in air (water-saturated)	3/8	21-24	60- 70,000	6	8

* None of the bolts tested failed.

Average Physical Properties of K-Monel Bolts

	R_C 21-24	R_C 32-34
Yield Strength (0.01% offset)	90,000 psi	120,000 psi
Yield Strength (0.2% offset)		135,000 psi
Ultimate Tensile Strength	125,000 psi	160,000 psi

TABLE XLVIII

SUMMARY OF EXPOSURE DATA FOR DURONZE (5% ALUMINUM BRONZE) BOLTS EXPOSED IN A NUMBER OF H_2S-H_2O SYSTEMS

Test Environment	Bolt Size	Bolt Hardness (Rockwell B)	Range of Applied Stress (psi)	Number of Bolts Exposed	Number of Bolts Failed	Total Exposure Time
H_2S-H_2O at	3/8 in.	R_b 90	50,000	3	None	11 months
38°C and	3/8	90	(60,000)[1]	2	None	11
250 psi	1/2	90	(95,000)[1]	1	None	11
H_2S-H_2O at	3/8	90	50,000	3	None	21
room tem-	3/8	90	(60,000)[1]	2	1	21
perature	1/2	90	(65 - 75,000)[1]	2	None	21
and atmos- pheric pressure						
100 ppm	3/8	90	50,000	3	None	6
H_2S in air	3/8	90	(60,000)[1]	2	None	6
(water- saturated)						
1% H_2S in	3/8	90	50,000	3	None	6
air (water-	3/8	90	(60,000)[1]	2	None	6
saturated)	1/2	90	(65 - 75,000)[1]	2	None	6

[1] These values of applied stress were calculated on the basis of Hooke's Law even though the yield point of the bolts had been exceeded

Average Physical Properties of Duronze Bolts

Hardness	R_b 90
Yield Strength (0.01% offset)	50,000 psi
Yield Strength (0.2% offset)	65,000 psi
Ultimate tensile strength	95,000 psi

TABLE XLIX

SUMMARY OF EXPOSURE DATA FOR 75ST
ALUMINUM BOLTS EXPOSED IN TWO H_2S-H_2O SYSTEMS

Test Environment	Bolt Size	Bolt Hardness (Rockwell B)	Range of Applied Stress (psi)	Number of Bolts Exposed	Number of Bolts Failed	Total Exposure Time
H_2S-H_2O at	1/2 in.	R_b 89-90	60 - 70,000	2	1	19 mo
room temperature and atmospheric pressure	1/2	89-90	(110,000)[1]	1	None	19
1% H_2S in air (water-saturated)	1/2	89-90	(80 - 90,000)[1]	2	None	8

[1] These values of applied stress were calculated on the basis of Hooke's law even though the yield point of the bolts had been exceeded

Physical Properties of 75ST Aluminum (Taken from Literature)

Hardness:	R_b 89-90
Yield Strength (0.2% Offset):	80,000 psi
Ultimate Tensile Strength:	90,000 psi

TABLE L

SUMMARY OF CORROSION RATES FOR AISI 4140 STEEL EXPOSED IN VARIOUS H_2S-H_2O SYSTEMS

H_2S-H_2O Environment[2]	Corrosion Rate in Mil /Yr [1] Short Time Exposure (100-400 hr) Vapor Phase	Short Time Exposure (100-400 hr) Liquid Phase	Long Time Exposure (800-1800 hr) Vapor Phase	Long Time Exposure (800-1800 hr) Liquid Phase
Room Temp. and Atm. Press.	3	8	2	6
38°C. and 250 psi	3	9	2	5
100 p p m H_2S in air (water-saturated)	0.2	3	0.2	2
1% H_2S in air (water-saturated)	8[3]	1.0	4[3]	1.0
3% H_2S in nitrogen (water-saturated)	1.5	4	-	-
38°C. and 250 psi with 500 ppm of Duomeen T[4] added to the liquid phase	-	1.5	-	-
38°C and 250 psi with 500 ppm of TEPA[4] added to the liquid phase	-	1.5	-	-

[1] Corrosion samples were rounds of 3/4 in. diameter and 3/4 in. length. The same samples were used throughout each test with the sulfide scale being removed by pickling in inhibited HCl at the end of each test period. All corrosion rates listed are the average of two or more tests for the period of time indicated.

[2] No corrosion specimenswere exposed in the 120°C and 250 psi environment.

[3] The much higher corrosion rates for the vapor phase in this environment as compared to the liquid phase are believed to be related to the accelerating effect of air on the sulfide corrosion process.

[4] No vapor-phase rates are listed because these inhibitors are low vapor pressure amines with little effect on corrosion occurring in the vapor phase.

TABLE LI

QUALITATIVE EVALUATION OF CONDITION OF METALLIC COATED AISI 4140 BOLTS AFTER EXPOSURE TO VARIOUS H_2S-H_2O SYSTEMS

Type of Metallic Coating[1]	Surface Condition of Bolts After Exposure to the H_2S-H_2O Systems Listed*			
	Room Temperature and Atmospheric Pressure	38°C and 250 psi	100 ppm of H_2S in air (water-saturated)	1% H_2S in air (water-saturated)
Cd	Yellow sulfide coating	Yellow sulfide coating was blistered near fracture	Yellow sulfide coating	Yellow sulfide coating
Cr	Dull appearance	Slightly corroded	Bright appearance	Badly corroded
Pb	Light sulfide coating	Moderately corroded with some blistering	Very light sulfide coating	Very light sulfide coating
Zn	Light sulfide coating	Light sulfide coating	Very light sulfide coating	Very light sulfide coating
Brass	Blue sulfide coating	Heavy blue sulfide coating	Light blue sulfide coating	Blue sulfide coating
Ni	Coating still intact under light sulfide scale	Coating still intact under light sulfide scale	--	--
Al paint	Bright appearance	--	--	--

* No coated bolts were exposed in the 120°C - 250 psi system

[1] All coatings were electroplated with the exception of the Al paint which was sprayed on in three light coats

TABLE LII

QUALITATIVE EVALUATION OF CONDITION OF NONFERROUS BOLTS AFTER EXPOSURE TO VARIOUS H_2S-H_2O SYSTEMS

Surface Condition of Bolts After Exposure to the H_2S-H_2O Systems Listed*

Bolting Material	Room Temperature and Atmospheric Pressure	38°C and 250 psi	100 ppm of H_2S in air (water-saturated)	1% H_2S in air (water-saturated)
Monel and K-Monel	Slightly corroded	Slightly corroded	Not corroded	Moderately corroded
Duronze	Severely corroded	Severely corroded	Not corroded	Severely corroded
75ST Aluminum	Severely corroded[1]	--	--	Not corroded
Type 316 Stainless	--	Not corroded	--	--
Inconel and Inconel-X	Not corroded	Not corroded	Not corroded	Not corroded

* No nonferrous bolts were exposed in the 120°C - 250 psi system. The observations for the 3% H_2S in nitrogen (water-saturated) system were not listed because they were obscured by the corrosion that had occurred during a prior exposure of the same bolts in the 1% H_2S in air (water-saturated) system.

[1] Severe corrosion of aluminum bolts was probably due to iron sulfide scale coming into contact with the bolts.

TABLE LIII

SULFIDE STRESS CORROSION TESTS

Samples dead weight loaded as indicated
250 psi H_2S-H_2O at 40° and 120°C.

Material	Type Specimen	Hardness	Stress	% Yield	Time 120°C.	Time 40°C.	Time Total	Result
A 212	Round - Weld	Rc 15	70,000	140	1,500	-	1,500	Broke
	Round - Weld	Rc 15	70,000	140	-	1,850	1,850	Broke
	Round	Rc 15	69,300	139	909	-	909	Broke
	Round	Rc 15	69,300	139	2,332	-	2,332	Broke
	Round	Rc 15	62,400	125	2,490	-	2,490	Broke
	Round	Rc 15	60,900	122	4,456	-	4,456	Broke
	Round - Notched	Rc 15	60,000	120	785	-	785	Broke
	Round	Rc 15	60,000	120	3,466	-	3,466	Broke
	Round	Rc 15	60,000	120	2,996	2,266	5,262	Broke
	Round	Rc 15	50,000	100	7,045	2,809	9,854	Broke
	Round - Notched	Rc 15	60,000	120	453	-	453	O.K.
	Round - Notched	Rc 15	59,800	120	453	-	453	O.K.
	Round	Rc 15	57,000	114	-	1,270	1,270	O.K.
	Round - Notched	Rc 15	51,400	103	3,224	1,980	5,204	O.K.
	Round	Rc 15	50,000	100	2,626	-	2,626	O.K.
	Round	Rc 15	50,000	100	3,466	-	3,466	O.K.
	Square - Notched	Rc 15	48,900	100	136	-	136	O.K.
	Square - Notched	Rc 15	48,600	99	136	-	136	O.K.
	Round	Rc 15	40,800	81	294	-	294	O.K.
	Round	Rc 15	40,300	81	294	-	294	O.K.
	Round	Rc 15	30,200	64	136	-	136	O.K.
	Round	Rc 15	29,600	60	136	-	136	O.K.
ASTM A193-49T B7 4140-4145)	Round	Rc 30	120,000	91	-	1,270	1,270	Broke
	Round	Rc 35	120,000	80	1,192	796	1,988	Broke
	Round - Prestrain	Rc 34	118,000	80	-	1,716	1,716	Broke
	Round	Rc 29	110,000	86	543	493	1,036	Broke
	Round	Rc 38	100,000	62	161	-	161	Broke
	Round	Rc 39	92,000	54	20	-	20	Broke
	Round	Rc 31	90,000	53	2,862	1,343	4,205	Broke
	Round - Notched	Rc 29	86,000	67	2,306	3,006	5,312	Broke
	Round	Rc 40	80,000	46	328	-	328	Broke
	Round	Rc 40	50,000	29	-	360	360	Broke
	Round - Prestrain	Rc 34	50,000	37	-	806	806	Broke
	Round	Rc 36	50,000	31	-	360	360	Broke
	Round	Rc 44	50,000	20	161	-	161	Broke
	Round	Rc 38	50,000	30	-	1,343	1,343	Broke
	Round	Rc 32	50,000	36	-	1,008	1,008	Broke
	Round	Rc 32	50,000	36	2,085	-	2,085	Broke

TABLE LIII (Continued)

Material	Type Specimen	Hardness	Stress	% Yield	Time 120°C.	Time 40°C.	Time Total	Result
ASTM A193-49T B7 4140-4145)	Round	Rc 47	50,000	20	232	-	232	Broke
	Round	Rc 40	30,000	23	1,033	-	1,033	Broke
	Round	Rc 28	90,000		331	-	331	O.K.
	Round	Rc 31	88,600	67	1,989	2,640	4,629	O.K.
	Round	Rc 29	87,600	68	2,575	330	2,905	O.K.
	Round - Notched	Rc 28	80,000	64	2,174	3,757	5,931	O.K.
	Round	Rc 30	79,000	61	1,865	-	1,865	O.K.
	Round	Rc 12	70,000	100	331	-	331	O.K.
	Round	Rc 27	61,900	51	1,863	-	1,863	O.K.
	Round	Rc 30	61,600	47	810	330	1,140	O.K.
	Round - Notched	Rc 29	60,000	48	2,174	3,767	5,931	O.K.
	Round	Rc 38	50,000	30	1,151	1,343	2,494	O.K.
	Round	Rc 32	50,000	36	970	1,343	2,313	O.K.
	Round - Prestrained	Rc 29	49,300	38	2,002	1,126	3,128	O.K.
	Round	Rc 31	39,400	29	162	-	162	O.K.
	Round	Rc 25	30,000	26	1,192	796	1,988	O.K.
	Round	Rc 36	29,700	25	331	-	331	O.K.
	Round	Rc 33	20,000	14	-	1,270	1,270	O.K.
	Round	Rc 24	80,000	80	-	1,404	1,404	Broke
410	Round	Rc 15	80,000	100	-	1,850	1,850	Broke
	Round	Rc 29	71,000	64	-	1,850	1,850	Broke
	Round	Rc 24	70,000	70	-	1,850	1,850	Broke
	Round	Rc 15	70,000	88	3,224	1,022	4,246	Broke
	Round - Notched	Rc 19	60,000	75	2,037	-	2,037	Broke
	Round - Notched	Rc 18	60,000	75	1,252	-	1,252	Broke
	Round	Rc 12	70,000	100	4,460	3,757	8,223	O.K.
	Round	Rc 24	60,000	60	3,224	633	3,857	O.K.
	Round	Rc 18	60,000	75	3,244	-	3,244	O.K.
	Round	Rc 18	60,000	75	3,244	-	3,244	O.K.
	Round	Rc -	50,200	63	589	-	589	O.K.
	Round	Rc -	47,200	59	589	-	589	O.K.
17-4 P.H.	Round	Rc 30	100,000	110	-	1,850	1,850	Broke
	Round	Rc 30	82,000	90	641	-	641	Broke
	Round	Rc 42	80,500	41	641	-	641	Broke
	Round	Rc 31	60,400	65	641	-	641	Broke
329	Round	Rc 22	70,000	87	524	-	524	Broke
	Round - Notched	Rc 21	70,000	87	1,966	-	1,966	Broke
	Round	Rc 19	70,000	87	4,419	-	4,419	O.K.
	Round	Rc 21	60,000	75	4,419	-	4,419	O.K.
	Round - Notched	Rc 21	60,000	75	656	-	656	O.K.

TABLE LIII (Continued)

Material	Type Specimen	Hardness	Stress	% Yield	Time 120°C.	Time 40°C.	Time Total	Result
304 Annealed	Round		70,000	230	524	-	524	Broke
304 Sensitized 1 hr 1200°F	Round		65,000	215	492	806	1,298	Broke
304 Annealed	Round		65,000	215	-	806	806	Broke
304 Sensitized 1 hr 1200°F	Round		60,300	200	1,124	2,076	3,200	Broke
304 Annealed	Round		60,000	200	1,124	2,076	3,200	Broke
304 Annealed	Round - Prestrained		80,000	-	2,978	1,008	3,986	O.K.
304 Annealed	Round		50,000	165	1,124	1,270	2,394	O.K.
316 Annealed	Round		70,000	200	524	-	524	Broke
316 Sensitized 1 hr 1200°F	Round		70,000	200	3,858	1,343	5,201	Broke
316 Annealed	Round		70,000	200	3,858	1,343	5,201	O.K.
316 Annealed	Round		65,000	185	817	335	1,152	O.K.
316 Sensitized 1 hr 1200°F	Round		65,000	185	817	335	1,152	O.K.
316 Annealed	Round		60,000	170	817	1,141	1,958	O.K.
316 Sensitized 1 hr 1200°F	Round		60,000	170	817	1,141	1,958	
Rimmed Steel	Round - Notched		50,000	150	2,693	-	2,693	Broke
Rimmed Steel	Round - Notched		50,000	150	2,693	-	2,693	O.K.
J 55	Round - Notched		70,000	127	638	-	638	Broke
H 40	Round - Notched		70,000	174	785	-	785	Broke
Inconel	Round	Rc 3	70,000	175	486	-	486	Broke
Inconel X	Round	Rc 45	150,000	100	1,731	-	1,731	Broke
Inconel X	Round	Rc 43	100,000	63	3,433	1,008	4,441	O.K.
K Monel	Round	Rc 40	100,000	101	3,433	1,008	4,441	O.K.

TABLE LIV

SULFIDE STRESS CRACKING OF AUSTENITIC STAINLESS STEEL

All specimens exposed to H_2S-H_2O at 250 psi for times and temperatures as indicated.

Sample Number	Material	Stress, (psi)	Temp., °C	Time, hr	Condition	Type of Failure	Nitric Acid Corrosion Rate, in./pen./mo
Tension Specimens - Dead Weight Loaded							
39	304	70,000	120	524	Broken	Transgranular	0.00054
40	316	70,000	120	524	Broken	Transgranular	0.00056
61	304	60,000	40	2076	Broken	Transgranular	0.00060
62	304	60,000	40	1270	O.K.	Transgranular	0.00057
62	304	65,000	40	806	Broken	Transgranular	0.00057
63	304	60,000	40	2076	Broken	Transgranular	0.00089
71	304	65,000	40	806	Broken	Irregular	0.00078
72	304	60,000	120 40	817) 1141)	O.K.	No cracks	0.00057
74	316	60,000	40 120	1141) 817)	O.K.	Shallow Trans.	0.00062
80	316	65,000	120 40	817) 335)	O.K.	Shallow Trans.	0.00060
81	316	65,000	120 40	817) 335)	O.K.	Shallow Trans.	0.00071
Weld Plates							
48	304	Weld Stress	40	12,000	Cracked	Intergranular	0.012
49	304	Weld Stress	40	12,000	Cracked	Intergranular	0.0033
50	316	Weld Stress	40	12,000	O.K.	No cracks	0.0012
51	316	Weld Stress	40	12,000	O.K.	No cracks	0.0015
Strongbacks - S R P Design							
1	304		40	570	Cracked	Intergranular	0.0019
2	304		40	1500	Cracked	Intergranular	0.0057
3	304		40	3500	Cracked	Intergranular	0.0069
4	304		40	4000	Cracked	Intergranular	0.0046

TABLE LV

BEAM DEFLECTION TESTS OF AISI 4140

Samples 2" x 1/4" x 1/16"
Supports 1.750" apart. Single point loading.
Exposed to 250 psi wet H_2S

V.H.N.	Stress psi	Temperature	Time (hr)	Result
570	100,000	80°C	20	Broke
570	100,000	80°C	203	Broke
563	50,000	30°C	26	Broke
563	50,000	30°C	72	Broke
563	50,000	30°C	184	Broke
563	90,000	120°C	568	O.K.
604	50,000	120°C	512	O.K.
570	50,000	120°C	512	O.K.
570	50,000	120°C	512	O.K.
570	50,000	120°C	512	O.K.
563	50,000	120°C	120	O.K.
563	39,000	30°C	76	O.K.
563	25,000	30°C	780	O.K.
563	25,000	30°C	506	O.K.

TABLE LVI

STRESS ON UNFAILED NONFERROUS BOLTS BEFORE AND AFTER EXPOSURE IN H_2S-H_2O SYSTEMS

Bolting Material	Bolt Size (in.)	Number of Bolts	Yield Strength (0.2% offset) (psi)	Bolting Stress (psi) Original[1]	Bolting Stress (psi) Final[2]	Length of Exposure at 20°-40°C (mo.)
Duronze	1/2	2	65,000	65-70,000	60-70,000	8
75ST Aluminum	1/2	1	80,000	(105,000)[3]	45,000	20
Inconel	1/2	3	130,000	110-120,000	95-100,000	7
	1/2	2	130,000	125-130,000	100-105,000	7
Inconel-X	3/8	4	135,000	120-125,000	100-110,000	6
	3/8	2	135,000	130-135,000	105-110,000	6
	3/8	4	135,000	(155-170,000)[3]	105-115,000	6
	3/8	1	135,000	135,000(235,000)[4]	130,000	6
	3/8	1	135,000	125,000(185,000)[4]	120,000	6
	1/2	2	100,000	105-120,000	90-95,000	8

[1]Stress originally applied to bolts.

[2]Stress on bolt after exposure to H_2S-H_2O systems at temperatures of 20°-40°C. This final stress was determined from the decrease in bolt length which occurred when the bolt was detorqued and the load thereby removed.

[3]These values of applied stress were calculated on the basis of Hooke's law even though the yield point of the bolts had been exceeded.

[4]These bolts were first prestressed to the values given in parentheses, detorqued, and then restressed to the lower values shown ahead of the parentheses.

TABLE LVII

STRESS RELAXATION DATA FOR 5/8-INCH AISI 4140 BOLTS AT ROOM TEMPERATURE AND AT 120°C

Length of Exposure Period	Bolting Stress (psi) As a Function of Time Under Load[1]							
	Room Temperature Exposure				120°C. Exposure			
	Bolt No. 1[2]		Bolt No. 2[3]		Bolt No. 3[2]		Bolt No. 4[3]	
	Original	Final	Original	Final	Original	Final	Original	Final
Zero	108,000	106,000	158,000	123,000	110,000	106,000	193,000	123,000
1 hr.	106,000	106,000	117,000	115,000	107,000	99,000	123,000	106,000
24 hr.	106,000	105,000	115,000	112,000	100,000	95,000	109,000	101,000
1 wk.	103,000	103,000	114,000	111,000	95,000	94,000	102,000	98,000
1 mo.	104,000	102,000	111,000	107,000	94,000	90,000	97,000	95,000
6 mo	102,000	99,000	109,000	104,000	94,000	88,000	103,000	97,000

[1] Known stresses were applied to the bolts and maintained for the periods of time indicated. The final stress on a bolt was determined from the decrease in bolt length which occurred when the bolt was detorqued.

[2] The initial stresses on these two bolts were below the yield strength of the bolts (140,000 psi).

[3] The initial stresses on these two bolts were above the yield strength of the bolts (140,000 psi).

TABLE LVIII

STRESS RELAXATION DATA FOR VARIOUS NONFERROUS BOLTING MATERIALS AT TEMPERATURES OF 20°-30°C

Bolting Material and Yield Strength (psi)[2]		Bolting Stress (psi) As A Function Of Time Under Load[1]									
		Zero		1 hr		24 hr		1 wk		1 mo	
		Original	Final	Original	Final	Original	Final	Original	Final	Original	Final
Inconel X (135,000)	(1)	126,000	113,000	109,000	109,000	109,000	109,000	107,000	107,000	105,000	105,000
	(2)	117,000	100,000	98,000	98,000	102,000	102,000	98,000	98,000	98,000	98,000
	(3)	86,000	86,000	86,000	86,000	78,000	78,000	82,000	82,000	82,000	82,000
Inconel (130,000)	(1)	110,000	87,000	122,000	102,000	108,000	98,000	98,000	98,000	91,000	91,000
K-Monel (105,000)	(1)	87,000	80,000	80,000	80,000	80,000	80,000	82,000	79,000	80,000	80,000
	(2)	59,000	59,000	56,000	56,000	59,000	59,000	56,000	56,000	54,000	54,000
	(3)	67,000	67,000	66,000	66,000	65,000	65,000	75,000	75,000	74,000	74,000
K-Monel (135,000)	(1)	132,000	113,000	112,000	109,000	109,000	109,000	109,000	109,000	110,000	110,000
	(2)	98,000	95,000	94,000	92,000	90,000	90,000	88,000	88,000	90,000	90,000
Duronze (65,000)	(1)	70,000	56,000	68,000	62,000	62,000	58,000	53,000	53,000	58,000	58,000

[1]Known stresses were applied to the bolts and maintained for the periods of time indicated. The final stress on a bolt was determined from the decrease in bolt length which occurred when the bolt was detorqued.

[2]The numbers in parentheses are used to designate individual bolts of the same material. Each bolt was used throughout the entire test period of one month. All bolts were 3/8 in. studs. Yield strength was determined by 0.2% offset method.

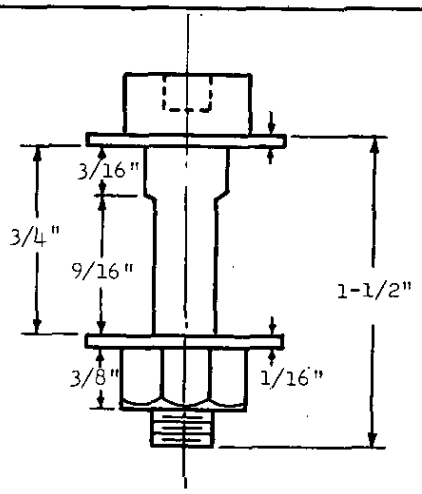

Hooke's Law: $E = \frac{\text{Stress}}{\text{Strain}} = \frac{P/A}{e/l}$ (1)

where P = load, A = area, e = elongation, l = gage length over which elongation occurs, and E = modulus of elasticity.

Solving Equation (1) for e: $e = \frac{Pl}{EA}$ (2)

Let: e_u = elongation of unthreaded shank of bolt

e_t = elongation of threaded region within gage length of bolt (gage length included one-half of the nut thickness).

e = total elongation of bolt

Then: $e = e_u + e_t$ (3)

Substituting Equation (2) in Equation (3):

$$e = \frac{Pl_u}{EA_u} + \frac{Pl_t}{EA_t} = \frac{P}{E}\left(\frac{l_u}{A_u} + \frac{l_t}{A_t}\right) \quad (4)$$

where l_u = length of unthreaded shank = 0.250 in.

l_t = length of threaded region = 0.812 in.

A_u = area of unthreaded shank = 0.111 sq. in.

A_t = minimum area of threaded region = 0.0701 sq. in.

Substituting Numerical Values in Equation (4):

$$e = \frac{P}{30 \times 10^6}\left(\frac{0.250}{0.111} + \frac{0.812}{0.0701}\right) = 4.62 \times 10^{-7}P \quad (5)$$

$$P = 2.16 \times 10^6 e \quad (6)$$

Maximum stress in bolt: $S_{max.} = \frac{P}{A_{min.}} = \frac{P}{0.0701}$ (7)

Substituting Equation (6) in Equation (7):

$$S_{max.} = \frac{2.16 \times 10^6}{0.0701} e = 3.08 \times 10^7 e \quad (8)$$

Maximum stress in bolt = (3.08×10^7)(measured elongation)

DERIVATION OF FORMULA USED FOR CALCULATING STRESS ON 3/8-INCH ALLEN HEAD CAP SCREWS FROM MEASURED VALUES OF ELONGATION

EXHIBIT B

RELAXATION OF BOLT LOADS

INTRODUCTION

The relaxation of bolting stresses during the course of testing in H_2S-H_2O environments was of primary interest because of the effect of applied stress on the susceptibility to sulfide corrosion cracking. Any severe relaxation of bolting stresses that occurred during testing would greatly lessen the cracking susceptibility. This was of most concern in the 120°C environment, where the higher testing temperature might be expected to lead to greater relaxation of bolt loads. Since little or no information was available in the literature about the creep of ferrous materials under load at temperatures below 900°F, steps were taken to obtain the desired information as a corollary to the bolting investigation.

EXPERIMENTAL DETAILS

Laboratory data on the relaxation of bolt loads were obtained in two ways. The first method consisted of measuring the stress still present on unfailed bolts at the end of their test exposure in the H_2S environments. This involved measuring the change in length of the bolt that occurred when the load was removed. The decrease in bolt length was then translated into bolting stress by means of the following formula:

$$S = E\left(\frac{e}{l}\right) \qquad (1)$$

where S is the final or recovered stress on the bolt, e is the decrease in length upon load removal, and l is the gage length of the bolt. A comparison of the final stress with the original stress applied to the bolt then provided a measure of the relaxation that had occurred.

The second method used to study relaxation of bolt loads was the exposure of bolts loaded to known values of applied stress in air, rather than in H_2S environments. Exposures were made at both room temperature and at 120°C. At periodic intervals the bolt loads were removed to determine the existing stresses and then reapplied to provide similar values of stress. In this way it was possible to follow the relaxation of bolting stresses with time under load and in the absence of any corrosion.

DISCUSSION OF RESULTS

The maintenance of bolt loads by AISI 4140 steel stud bolts during test exposures in the three main H_2S-H_2O systems is illustrated in Figure 60. All of the data shown are for bolts stressed below their yield strength, which ranged from 120,000 - 160,000 psi. Figure 60 shows that the relaxation of bolting stresses increased with increasing exposure temperature and with increasing original applied stress. The maximum stress relaxation which occurred among these bolts was around 20%.

The results of stress measurements on a number of nonferrous bolts before and after exposure to H_2S environments are given in Table LVI. In general, the nonferrous bolts behaved similarly to the ferrous bolts if the differences in yield strength were taken into consideration. When the original stress levels on the nonferrous bolts were of the order of their yield strengths, stress relaxations of about 15-20% occurred. The stress measurement data presented in Figure 60 and Table LVI were in error by as much as 5000 psi in extreme cases. This is demonstrated by those points in Figure 60 which are located above the line of "no stress relaxation" and which, therefore, are obviously in error.

The results of the stress-relaxation studies run on both ferrous and nonferrous bolts are presented in Tables LVII and LVIII. The data in Table LVII show that AISI 4140 steel bolts stressed to below their yield strength for a total of six months underwent a stress relaxation of the order of 3% at room temperature and 6% at 120°C. For the same bolts the cumulative decrease in stress, which included the six loading and unloading operations, was about 6% at room temperature and 20% at 120°C. Similar results were obtained for the two bolts originally stressed beyond their yield strengths, except that the initial unloading was accompanied by a much larger decrease in the recovered stress. The data in Table LVII for bolts that were tightened and then immediately loosened suggest that the bulk of the relaxation in stress occurred during the initial torquing-up or loading of the bolt.

The greater amount of stress relaxation at 120°C is believed to be due to the lower yield strength of the material at that temperature. Gunnert[12] has shown that steel specimens stressed at room temperature and then heated to some higher temperature in the range of 100-300°C will undergo stress relief if the original value of applied stress is greater than the yield strength of the steel at the elevated temperature. Thus, a bolt stressed at or near its room-temperature yield strength would be expected to undergo a greater stress relaxation upon exposure at 120°C than it would at room temperature.

The stress-relaxation data in Table LVIII for nonferrous bolts reinforce two earlier conclusions. First, the amount of stress relaxation is greater for the higher values of initial applied stress. Secondly, the bulk of the stress relaxation seems to have occurred during the initial stressing of the bolt. Compare, for example, the values of bolting stress for tightening followed by immediate loosening.

CONCLUSIONS

1. The degree of stress relaxation in loaded bolts increased with increasing applied stress and increasing temperature of exposure.

2. The maximum stress relaxation that occurred among ferrous and nonferrous bolts exposed to H_2S-H_2O systems was of the order of 15-20%. These high values of stress relaxation were for bolts stressed close to their yield strength.

3. The bulk of the stress relaxation occurred during the initial stressing operation in the case of the bolts exposed at room temperature. Where bolts were exposed at 120°C, the greater part of the stress relaxation took place upon heating to 120°C.

EXHIBIT C

ACKNOWLEDGMENTS

Since the laboratory work mentioned in this report was done by many individuals, the authors want to acknowledge their efforts.

M. H. Brown and W. B. De Long were in charge of the general direction of the work. T. N. Rhodin, Jr., made a study of the knowledge of H_2S corrosion problems with emphasis on the petroleum-industry experience at the time this project was started. J. M. Stone made a survey of other industrial experience with H_2S. E. A. Kachik and R. C. McMillen studied equipment for inspecting steel to locate laminar defects. Effects of H_2S corrosion on fatigue were studied by J. T. Ransom. H. C. Barber studied hydrogen transfer and high-temperature corrosion. G. P. Monet checked the feasibility of ion exchange for inhibitor recovery. E. A. Kachik and A. Pocalyko made a metallographic study of the fragmented Type 410 stainless steel bubble caps. G. W. Beckman made the studies of corrosion in liquid H_2S, clad-plate inspection, repair welding, a major portion of the bolt testing, and much of the work on general corrosion.

The bolting materials study was completed and that portion of the report written by D. Warren. J. A. Snyder was responsible for the other laboratory work and the balance of the report.